

For Reference

NOT TO BE TAKEN FROM THIS ROOM

Ex LIBRIS
UNIVERSITATIS
ALBERTAENSIS



T H E U N I V E R S I T Y O F A L B E R T A

RELEASE FORM

NAME OF AUTHOR GORDON DONALD FONSTAD
TITLE OF THESIS..... THE EXPLOSIVE DEMOLITION
..... OF ICE SHEETS
.....
DEGREE FOR WHICH THESIS WAS GRANTED..... Master of Science
YEAR THIS DEGREE GRANTED..... 1981

Permission is hereby granted to THE UNIVERSITY
OF ALBERTA LIBRARY to reproduce single copies of this
thesis and to lend or sell such copies for private,
scholarly or scientific research purposes only.

The author reserves other publication rights,
and neither the thesis nor extensive extracts from it
may be printed or otherwise reproduced without the
author's written permission.



Digitized by the Internet Archive
in 2019 with funding from
University of Alberta Libraries

<https://archive.org/details/Fonstad1981>

THE UNIVERSITY OF ALBERTA

THE EXPLOSIVE DEMOLITION OF ICE SHEETS

by



Gordon Donald Fonstad

A Thesis

Submitted to the Faculty of Graduate Studies and Research
In Partial Fulfilment of the Requirements for the Degree
of Master of Science

Department of Civil Engineering

Edmonton, Alberta

Spring, 1981

81-2

THE UNIVERSITY OF ALBERTA
FACULTY OF GRADUATE STUDIES AND RESEARCH

The undersigned certify that they have read, and recommend to the Faculty of Graduate Studies and Research, for acceptance, a thesis entitled THE EXPLOSIVE DEMOLITION OF ICE SHEETS submitted by Gordon Donald Fonstad in partial fulfilment of the requirements for the degree of Master of Science.

Date / /

DEDICATION

To the advancement of Military Science,
in the hopes that the knowledge thereby gained
can also serve man in peace.

ABSTRACT

The available literature on the use of explosives in demolishing a floating ice sheet is reviewed to present the variety of factors which have been considered and the number of approaches used. As most of these sources are obscure, the data from them has been appended to this thesis.

While the majority of the previous studies considered the explosive charge weight and the depth of placement of the charges below the ice as the primary controlling variables, only one study considered the effect of ice thickness on the overall relationship. As well, the majority of the previous studies made only passing reference to the dynamic scaling relationships for blast effects, and presented their findings in dimensional form. Only the one previously mentioned study analysed the ice demolition data in light of the nondimensional scaling parameters.

The results of the previous analysis, which incorporated the dynamic scaling relationships and ice thickness into the formulation of 'optimum' ice demolition criteria, were confirmed independantly in this investigation. Recommendations are made, in the form of simple formulae, to determine the optimum charge weight, depth of placement and resulting crater size, as a function of ice thickness.

An investigation into the effect of the charge placement hole showed that the craters resulting from an explosion beneath an open hole were perceptibly smaller than

ABSTRACT
(Continued)

those for which the placement hole had been allowed to re-freeze. However, where the placement hole had been left open, there was no discernable effect caused by the size of that hole, for the range of hole sizes tested.

It was determined that the gravitational term in the general nondimensional ice demolition relationship had negligible influence on the resulting crater dimensions.

An investigation was conducted into whether the type of explosive used had an effect on the results. The investigation showed there seemed to be such an effect. A simple set of equations are presented to give the charge weight, placement depth and the resulting crater radius as a function of the ice thickness, where the explosive is specifically TNT. Energy-equivalent amounts of other explosives may then be determined from the 'Effectiveness as an External Charge', which is shown herein to be an indicator of specific energy.

It was shown that charges detonated below an ice sheet were more effective than an equal amount the same explosive detonated as an unconfined charge placed on the surface of the ice. A preliminary relationship was derived, excluding the effects of ice thickness and explosive type, which gives the crater radius as a function of the weight of an unconfined surface charge.

The use of individual optimum charges placed in a row

ABSTRACT
(Continued)

to obtain a continuous gap or lead was investigated. It is shown that an increase in the resulting cratered area can be obtained. The cratered area was found to increase by some 100% for charges placed two optimum crater radii apart. However, charges set three optimum crater radii apart do not connect to form a continuous lead.

The use of military prepackaged linear explosives, such as the Bangalore Torpedo, was investigated as well. The tests showed that for ice of the thickness encountered, approximately 0.35 m, these charges could be used to create a gap in the ice. Generally, a row of individual point charges detonated below the ice was more efficient than the linear charges. It was found that a single tube of Bangalore suspended vertically below the ice formed a crater that was equivalent to one formed by the detonation of a point charge of the same energy equivalent weight. The vertically placed Bangalore, however, cleared more ice from the crater.

It was shown that shaped charges could be used to create placement holes quickly in the ice to accept larger ice demolition charges. However, the ultimate depth of cratering by the shaped charges used could not be ascertained with the thickness of ice encountered, as the charges, detonated with different standoff distances, all caused craters which extended fully through the ice sheet encountered.

Finally, a technique known as 'directed blasting',

ABSTRACT
(Concluded)

which is designed to increase the amount of ice ejected from a crater, was tested. It was determined that the desired directed effect could be achieved with certain combinations of an auxiliary charge weight and detonation delay between the auxiliary charge and the optimum main charge, but it was shown that the method is sensitive to the detonation delay. Generally the required delay is less than 30 m sec, and, as commercial delay detonators are generally longer than 30 m sec, the desired delay has to be achieved using different lengths of det cord (primacord) between the charges.

Recommendations for further research are made.

PREFACE

The investigation for this thesis was carried out under contract with the Canadian Department of National Defence. As the problem addressed was military, much of the discussion herein is therefore related to military applications, although there are civilian applications of the results of this investigation.

Due to the military nature of the original investigation, some of the references used during the study carry a security classification. While the writer, being an Officer in the Canadian Armed Forces Reserves, could access this information, Security Orders for the Department of National Defence, pursuant to the Official Secrets Act, prohibits divulging classified material. Therefore, some of the reference material used cannot be cited in this thesis.

ACKNOWLEDGEMENTS

The writer wishes to sincerely thank his advisor, Dr. R. Gerard, for his valued assistance, continual support, guidance and patience throughout this investigation. Without his help, this investigation may not have reached completion.

Many other individuals, too numerous to cite, contributed willingly of their talents and expertise. The following are but a few who are deserving of special note.

Dr. J.H.B. Anderson and Mr. G.K. Briosi of the Canadian Defence Research Establishment - Suffield, provided the research contract administration as well as welcomed guidance and assistance in the early stages of the investigation. Mr. Briosi also assisted in data collection during the field experiments. Their assistance is appreciated.

The investigation was made possible through the financial support of the Defence Research Establishment - Suffield, under Contract No. 8SU79-00159 to Dr. N. Morgenstern of the University of Alberta. Dr. Morgenstern is thanked for his assistance in establishing and administering this contract.

ACKNOWLEDGEMENTS

(Continued)

Dr. B. Stimpson is gratefully acknowledged for his efforts in the formulation and conduct of the experimental program.

The author sincerely thanks the Commanding Officer, Major (now Lieutenant Colonel) M. Lougher-Goodey, his Officers, and the men of 1 Combat Engineer Regiment, Canadian Armed Forces, who worked under freezing conditions to carry out the experimental program.

The writer would also like to extend special thanks to both the Officer Commanding, and the men, of the U.S. Navy 'Seals' Diving Team; as well as the Officer Commanding, and the Canadian Forces Shallow Water Divers, of 1 Combat Engineer Regiment. These groups undertook the placement, beneath the ice, of some of the charges fired. Their good humour while emerging from the water into -35°C temperatures was heartening.

The statistical analysis for this thesis was carried out using the Biomedical Computer Programs P-Series, revised 1979. The programs were developed at the Health Sciences Computing Facility, University of California at Los Angeles, sponsored by the U.S. National Institutes of Health Special

ACKNOWLEDGEMENTS

(Continued)

Research Resources Grant RR-3.

Dr. M. Mellor, of the U.S. Army Corps of Engineers' Cold Regions Research and Engineering Laboratory (CRREL) graciously provided the writer with a copy of the notes he had made in 1972 while conducting an analysis similar to that contained herein. Dr. Mellor's notes provided information on the manner in which his analysis had been conducted, which had not previously been published, and enabled the writer to replicate that analysis.

The writer is indebted to his employers, Alberta Environment, who gave the writer leave of absence in order to complete his studies and to carry out the field work for this thesis.

The text was produced with the kind permission of Miss C.M. Brodsky, Barrister and Solicitor, on a word processor leased by her firm. Drafting of the many figures was carried out by Mrs. S. Notton, for which the writer is grateful.

TABLE OF CONTENTS

CHAPTER		PAGE
	Title Page	ii
	Approval Sheet	iii
	Dedication	iv
	Abstract	v
	Preface	ix
	Acknowledgements	x
	Table of Contents	xiii
	List of Tables	xvii
	List of Figures	xviii
	List of Plates	xxi
	List of Appendicies	xxiii
	Nomenclature	xxv
1	INTRODUCTION	
	1.1 General	1
	1.2 Canadian Experience	2
	1.2.1 Canadian Armed Forces Experience in Alberta	3
	1.2.2 Civil Experience in Alberta	5
	1.2.3 Civil Experience in Manitoba	6
	1.3 Background to the Problem	6
	1.4 The Problem	11
	1.5 Scope of the Study	11
2	PRELIMINARY CONSIDERATIONS	
	2.1 General	13
	2.2 Factors Affecting the Problem	13
	2.3 Dimensional Analysis	16
3	SURVEY OF THE LITERATURE	
	3.1 General	20
	3.2 Reported Studies of Blasting Floating Ice Sheets	22
	3.2.1 Van Der Kley (1965)	22
	3.2.2 Purple (1965)	23
	3.2.3 Barash (1966)	24
	3.2.4 Wade (1966)	30
	3.2.5 Kurtz, Benfer, Christopher, Frankenstein, Van Wyhe and Roguski (1966)	34
	3.2.6 Frankenstein and Smith (1966, 1970 a, 1970 b)	50
	3.2.7 Nikolayev (1970, 1971)	51
	3.2.8 Moor and Watson (1971)	59
	3.2.9 Mellor and Kovacs (1972)	60
	3.2.10 Mellor (1972)	61

TABLE OF CONTENTS

CHAPTER		PAGE
3	SURVEY OF THE LITERATURE (Cont'd)	
3.3	Reported Study of Penetrating Floating Ice Sheets With Shaped Charges	67
3.3.1	Introduction	67
3.3.2	Description and Action of Shaped Charges	68
3.3.3	Benert (1957)	72
4	SOME ASPECTS OF EXPLOSIVES	
4.1	General	75
4.2	Definition and Types of Explosives	76
4.3	Strengths of Explosives	80
4.3.1	Grade Strength	85
4.3.2	Weight Strength	86
4.3.3	Bulk Strength	87
4.3.4	Relative Weight and Bulk Strengths ...	88
4.3.5	Effectiveness as an External Charge ..	89
4.3.6	Heats of Detonation	89
4.3.7	Specific Energy	90
4.4	Properties of Some Explosives	95
5	EXPERIMENTAL PROGRAM	
5.1	Experimental Objectives	97
5.2	Experiment Descriptions	98
5.2.1	Experiment 1	99
5.2.2	Experiment 2	99
5.2.3	Experiment 3	100
5.2.4	Experiment 4	100
5.2.5	Experiment 5	101
5.2.6	Experiment 6	102
5.2.7	Experiment 7	103
5.3	Field Additions to the Program	105
5.4	Conduct of the Program	109
5.4.1	Charge Preparation	112
5.4.2	General Conduct of the Experiments ..	116
5.4.3	Measurement Techniques	124
6	EFFECTS OF POINT CHARGES	
6.1	The Chilcotin Data	131
6.2	Analysis of Optimum Conditions	137
6.2.1	Retrieval of Mellor's 1972 Regression Analysis	137
6.2.2	Regression with Additional Terms in the Model	147

TABLE OF CONTENTS

CHAPTER	PAGE
6	EFFECTS OF POINT CHARGES (Cont'd)
6.2.3	Regression with Extended Data 149
6.2.4	Analysis with 'Normalized' Explosive Weights 153
6.3	The Effects of Gas Venting 168
6.4	Charges Placed at the Ice Surface 172
6.4.1	Chilcotin Data 172
6.4.2	Analysis of All Surface Charge Data . 176
6.5	Findings 179
7	THE EFFECTS OF ROW CHARGES
7.1	The Chilcotin Data 187
7.2	Analysis of Experiment 1 187
7.2.1	Single Charge Comparative Data 187
7.2.2	Row Charge with 1 CER's SOP 193
7.3	Analysis of the Additional 'Row' 195
7.4	Analysis of All Row Charge Data 196
7.5	Findings 203
8	MULTIPLE CHARGES
8.1	Introduction 205
8.2	Decked Charges 205
8.3	Directed Blasting 207
8.3.1	Experiments of Nikolayev 209
8.3.2	Discrepancies in Nikolayev's Observations 221
8.4	The Chilcotin Data 224
8.4.1	Design of the Directed Shots 225
8.4.2	Observations from Experiment 4 230
8.5	Findings 241
9	LINEAR CHARGES
9.1	Introduction 244
9.2	Dimensional Analysis 245
9.3	Experiment 5 248
9.3.1	Linear Charge Description 248
9.3.2	Experiment Description 251
9.3.3	Discussion of Results; Det Cord Charges 255
9.3.4	Discussion of Results; Bangalore Torpedos 260
9.4	Analysis of the Linear Charges 268
9.5	Findings 274

CHAPTER	PAGE
10	SHAPED CHARGES
10.1	Introduction 278
10.2	Description of Charges 279
10.3	Analysis of Experiment 6 280
10.4	Findings 286
11	CONCLUSIONS
11.1	General 289
11.2	Point Charges 289
11.3	Row Charges 291
11.4	Multiple Charges 292
11.5	Linear Charges 294
11.6	Shaped Charges 295
12	RECOMMENDATIONS FOR FURTHER RESEARCH
12.1	Introduction 296
12.2	Recommendations Regarding Point Charges .. 296
12.2.1	Extension of Tests to Thicker Ice . 296
12.2.2	Confirmation of the Recommenda- tions With Respect to Energy Equivalent Charges 297
12.2.3	Investigation of the Influence of the Gas Bubble 298
12.2.4	Investigation of Simpler Regres- sion Models 299
12.2.5	Extension to Other Ice Forms 300
12.2.6	Methods of Determining the Ice Debris Content 300
12.3	Recommendations Regarding Row Charges 301
12.4	Recommendations Regarding Linear Charges . 302
12.5	Recommendations Regarding Shaped Charges . 304
12.6	Recommendations Regarding Directed Blasting 304
	BIBLIOGRAPHY 306
	APPENDIX A : 'Data on Ice Blasting from the Literature' 313
	APPENDIX B : 'Characteristics and Properties of Explosives' 332
	APPENDIX C : 'Investigation of the Gas Bubble Radius R_0 ' 347

LIST OF TABLES

Table	Description	Page
1	Chilcotin Data - Point Charges	132
2	Summary of Explosives used in Ice Demolition	154
3	Calculation of Specific Energy Ratios	157
4	Summary of Surface Charge Data; Chilcotin Experiment 3	173
5	Surface Charge Data from the Literature	177
6	Chilcotin Row Charge Data	188
7	Single Shot Data for 1 CER's Placement Criteria	190
8	Row Charge Analysis with Equivalent TNT Charges	199
9	Determination of C	227
10	Directed Blasting; Chilcotin Data	231
11	Cratered Area; Chilcotin Directed Blasting	233
12	Linear Crater Data; Det Cord Charges	260
13	Linear Crater Data; Bangalore Torpedos	262
14	Scaled Parameters for the Linear Charges	269
15	Comparison of Linear and Row Charge Craters	272
16	Chilcotin Shaped Charge Data	282

LIST OF FIGURES

Figure	Description	Page
1	Factors Affecting the Problem	15
2	Crater Radius as a Function of Charge Weight and Depth of Placement (After Barash, 1966)	28
3	Wade's Data (1966)	32
4	Kurtz et.al.'s Data (1966)	38
5	Data of Frankenstein and Smith (1966)	52
6	Scaled Curves for Ice Blasting (After Mellor, 1972)	65
7	Scaled Curves for Ice Blasting (After Mellor, 1972)	66
8	Shaped Charges	69
9	Cross Section of a Typical Hole from a Cone-Shaped Charge	71
10	Half-Sections of the Shaped Charges Tested by Benert (1957)	73
11	Distinction between High and Low Explosives in terms of Rate of Chemical Reaction	78
12	Some Aspects of the Ballistic Mortar	83
13	Relation Between Relative Weight Strength, Specific Energy and Lead Block Test Excavation Values (After Meyer, 1977)	94
14	Site Map	110
15	Schematic Ring Main	122
16	Measurement Devices	126
17	Half Section of Debris Isolation Device ..	130
18	Predicted and Observed Scaled Radius; Mellor's Data	142

LIST OF FIGURES

(Continued)

Figure	Description	Page
19	Calculated and Observed Crater Radius; Mellor's Data	143
20	Calculated and Observed Scaled Crater Radius; Chilcotin Data	145
21	Calculated and Observed Crater Radius; Chilcotin Data	146
22	Calculated and Observed Crater Radius; All Data, Explosives as Originally Reported	151
23	'Effectiveness as an External Charge' as a Specific Energy Indicator	159
24	Calculated and Observed Crater Radius; All Explosives Converted to Equivalent TNT Charges	166
25	Effect of Placement Holes (Gas Venting) ..	170
26	Surface Charge Results	175
27	Crater Radius For Surface Charges (All Data)	178
28	Chilcotin Row Craters	189
29	Area Demolished per Unit Weight	192
30	Row Craters; After Kurtz et.al.(1966)	197
31	Row Charge Crater Area for Various Charge Spacings; Data Converted to Equivalent TNT Charges	202
32	Effect of Decked Charges	208
33	Factors Affecting Directed Blasting	210
34	Effect of Detonation Delay in Directed Blasting	212
35	Effect of Directing Angle in Directed Blasting	214

LIST OF FIGURES

(Continued)

Figure	Description	Page
36	Effect of Auxiliary Charge Weight in Directed Blasting	216
37	Effect of the Main Charge Placement Depth in Directed Blasting	218
38	Nikolayev's Directed Data Analysed as Single TNT Charges	222
39	Directed Blasting; Chilcotin Shots D1-D6 .	232
40	Directed Blasting; Chilcotin Shots D7-D9 .	239
41	Factors Affecting Linear Explosions	246
42	Linear Charge Craters for Det Cord Charges	258
43	Linear Charge Craters for Bangalore Torpedos	261
44	Scaled Parameters for Linear Charges	270
45	Cratered Area; Linear and Row Charges	273
46	Crater Radius for Shaped Charges	283
47	Crater Depth for Shaped Charges	287

APPENDIX FIGURES

C1	Gas Bubble Radius for TNT Charges	351
----	---	-----

LIST OF PLATES

Photograph	Description	Page
1	Field Camp at Drummond Lake	111
2	A Block of DM 12 Explosive	114
3	Charge Preparation	115
4	Two Prepared Charges and Two Rolls of Det Cord	115
5	4.51 kg - 40% Forcite Charge (30 Cartridges)	116
6	4.54 kg (10 lb) Amex II Charge	116
7	Augering a Placement Hole	117
8	Placing an Explosive Charge	118
9	Detonation of First Four Charges	120
10	Typical Charge Connection to Det Cord Ring Main	121
11	Method of Taking Vertical Photographs of a Crater	127
12	Typical Vertical Photograph of a Crater (Crater from Shot 30 of Table 1)	127
13	Profiling the Ice Debris Thickness Across a Crater	128
14	Test Area on Drummond Lake	131
15	Crater for 9 kg Surface Charge	174
16	Crater for 18 kg Surface Charge	176
17	Ice Debris for Single Shot; 1 CER Placement Criteria	194
18	Ice Debris; Experiment 1	194
19	Ice Debris; Experiment 1	195
20	Venting Plume from Directed Blasting; Shots D1 through D3	235

LIST OF PLATES

(Continued)

Photograph	Description	Page
21	Directed Blasting Craters D4 through D9 ..	237
22	Directed Blasting Craters D4 through D9 ..	238
23	Venting Plume from Directed Blasting; Shots D7 through D9	240
24	A Bangalore Torpedo	249
25	Surface-laid Bangalore Torpedo	252
26	Placement of Vertical Bangalore Tube	252
27	Divers at Entry Hole	253
28	3 Strand Det Cord Charge on Surface	254
29	Detonation of Surface Bangalore, Surface Det Cord and Vertical Bangalore Tube	255
30	3 Strand Det Cord Results	256
31	Subsurface 5 Strand Det Cord Results	259
32	Subsurface 10 Strand Det Cord Results	259
33	Vertical Bangalore Crater	263
34	Ice Debris; Vertical Bangalore Crater	264
35	Surface Bangalore Crater	265
36	Subsurface Bangalore Crater	266
37	Ice Debris; Surface Bangalore Crater	267
38	Charge Demolition No 14 Mk1 11 lb 'Hayrick' with Zero Standoff	279
39	Hayrick Charge with 1.22 m Standoff	280
40	Detonation of Shaped Charges	281
41	Crater for Hayrick with 0.305 m Standoff .	285
42	Crater for Hayrick with 1.219 m Standoff .	285

LIST OF APPENDICIES

APPENDIX A - Data on Ice Blasting from the Literature.

Table	Description	Page
A-1	Data From Van Der Kley (1965) - Single charges	314
A-2	Data From Van Der Kley (1965) - Decked charges	316
A-3	Data From Purple (1965)	317
A-4	Data From Barash (1966)	318
A-5	Data From Wade (1966)	320
A-6	Data From Kurtz et.al. (1966) - Single charges	321
A-7	Data From Kurtz et.al. (1966) - Row charges	322
A-8	Data From Kurtz et.al. (1966) - Scaled Single charge data	324
A-9	Data From Frankenstein and Smith (1966)	325
A-10	Data From Nikolayev (1970) - Single charges	326
A-11	Data From Nikolayev (1970) - Decked charges	327
A-12	Data From Nikolayev (1971) - Directed Blasting	328
A-13	Data From Mellor and Kovacs (1972)	330
A-14	Data From Benert (1957) - Shaped charges	331

LIST OF APPENDICIES

(Continued)

APPENDIX B - Characteristics and Properties of Explosives.

Table	Description	Page
B-1	Characteristics of Shaped Charges Used by Benert (1957)	333
B-2	The Explosives Family (After Meyer) ...	334
B-3	Common Explosives and Ingredients Used In the U.S. Explosives Industry	335
B-4	Some Characteristics of Principal U.S. Explosives	336
B-5	Properties of Some Explosives	338
B-6	Strengths of Explosives Compared to ANFO	344
B-7	Properties of CIL Explosives	345

APPENDIX C - Investigation of the Gas Bubble Radius R_0 348

NOMENCLATURE

- a = regression intercept
- A_C = calculated crater area (m^2)
- A_O = observed crater area (m^2)
- b_n = regression coefficients ($n = 1, 2, 3, \dots, 9$)
- c = velocity of propagation of the
shock wave ($m\ s^{-1}$)
- C = a constant
- d_O = diameter of the placement hole (m)
- d = depth of placement of the charge
below the ice (m)
- d' = diameter of linear explosive tube (m)
- D = depth of water below the ice; diameter of
crater (m)
- E = energy released upon detonation (J)
- E' = energy released upon detonation per unit
length of linear charge ($J\ m^{-1}$)
- f = specific energy (J)
- g = gravitational constant ($m\ s^{-2}$)
- h = placement height of surface charges above
the upper ice surface; standoff distance for
shaped charges (m)
- l = horizontal distance between main and
auxiliary charges in directed blasting (m)

NOMENCLATURE

(Continued)

- L = length of crater for row and linear craters (m)
- n = number of moles of gases generated per unit mass of explosive; weighting factor for repeated tests in Mellor's regression analysis
- P = pressure of gases (m or ft of water; atmospheres)
- P_0 = atmospheric pressure, pressure at the detonation depth (m or ft of water; atmospheres)
- Q = heat of detonation (cal gm^{-1})
- r = multiple correlation coefficient
- R = resulting crater radius (m); Ideal Gas constant
- R' = half width of linear crater (m)
- R_{av} = average calculated crater radius (m)
- R_c = calculated crater radius (m)
- R_0 = radius of the gas bubble (m)
- S = charge spacing in a row (m)
- t_d = delay time between detonations (sec)
- t_i = ice thickness (m)
- t_s = snow thickness (m)

NOMENCLATURE

(Concluded)

T = temperature; the absolute temperature of the explosion ($^{\circ}\text{K}$)

v_g = specific volume of detonation gases (volume per unit weight) (l kg^{-1} ; $\text{m}^3 \text{kg}^{-1}$)

V = volume of gases (m^3)

W = mass of explosive charge (kg ; lb)

W' = mass of linear explosive charge (kg m^{-1})

X_1 = scaled placement depth ($d/W^{1/3}$)

X_2 = scaled ice thickness ($t_i/W^{1/3}$)

Y = scaled crater radius ($R/W^{1/3}$); total energy associated with the radial flow of fluid during the expansion of the gas bubble (J)

Z = depth of placement from top of ice (m)

α = directing angle for directed blasting (degrees)

ρ = density of water (kg m^{-3}),

ρ_i = ice density (kg m^{-3}),

ρ_s = snow density (kg m^{-3}),

CHAPTER 1

INTRODUCTION

1.1 General

Natural ice covers are used extensively as winter transportation routes and construction platforms in cold regions. Where the natural ice thickness is insufficient to carry the imposed loads of such activities, procedures have been developed to increase the ice thickness. Depending on the final geometry, the thickened portions are known as ice bridges or ice islands.

In the event of warfare in northern latitudes, ice covers could be an aid to both sides of the conflict. For military purposes it is therefore desirable to be able to prevent the use of covers as transportation routes by hostile forces should the need arise.

An obvious method of preventing the use of an ice cover is to demolish it, mechanically or with explosives. Explosive methods include bombing, shellfire or the use of conventional chemical explosives. This thesis is concerned with the latter approach.

There is a comprehensive (Military) literature on conventional demolition tasks carried out during warfare. However, although there have been a few ad-hoc investigations by various units of the Canadian Armed Forces (CAF)

of procedures for the explosive demolition of ice sheets, little seems to have been recorded.

Civilian requirements for ice removal have been in the fields of clearing shipping lanes, the construction of temporary port facilities in the Arctic and Antarctic, the clearing of ice (including ice bridges) from inland waterways prior to breakup in order to prevent ice jams, and the destruction of ice jams once they have formed. Much of the quantitative and/or qualitative data in the literature are from these sources.

1.2 Canadian Experience

Before delving too deeply into the details of ice demolition, it is of interest to consider some of the experience gained in this field by Canadians.

The earliest published Canadian work in ice demolition was that of Barnes (1928). Barnes conducted experiments during the 1920s using Thermite, a low or deflagrating explosive (now considered more of a pyrotechnic than an explosive) to clear ice from some of the rivers of Eastern Canada, and to remove an ice jam from the Allegheny River in the United States (Bolsenga, 1968). Thermite is a 25/75 mixture of aluminum and iron oxide, components which have a strong exothermic reaction producing aluminum oxide and iron. The uses of thermite are in welding railway tracks, and, during the Second World War, as a filler for incendiary

bombs (Meyer, 1977). The force of the 'explosion' produced by the thermite, according to Barnes, "resulted from the heated metal [of the iron produced in the reaction] in contact with the ice and water." (Bolsenga, 1968). The effectiveness of this 'explosive', and Barnes' work in this field in general is apparently "controversial" (Bolsenga, 1968).

Except for Barnes' work, and one other study which will be seen later which used compressed gas, explosive demolition of ice has been carried out using conventional (chemical) explosives.

The following examples of military and civilian experiences in ice blasting serve to illustrate both the magnitude of the problem and, to some degree, the expense involved in blasting ice with no background information from which to formulate a plan of attack. The examples cited are all from Western Canada as the information was more readily available.

1.2.1 Canadian Armed Forces' Experience in Alberta

The CAF has had some experience, outside of training, in the use of explosives for removing ice, particularly ice jams.

In 1951 the Royal Canadian Air Force (RCAF) was called upon to bomb an ice sheet which had caused an ice jam and subsequent flooding of the South Saskatchewan River at Medicine Hat:

"Altogether, the RCAF dumped five and one-half tons of explosive on the ice."

(Calgary Herald, 2 April 1951)

The explosives shattered the ice sheet but did not release the ice jam. The reason for the failure of the bombs to release the jam was attributed to the delay fuses being too long, with the result that the bombs exploded in the river bed where much of the shock was absorbed by the soft mud (Edmonton Journal, 30 March 1951). Subsequently, men of the Royal Canadian Engineers (RCE) were called in to work on the ice, as they could work in close contact and thus could place their charges more advantageously. They first detonated a series of TNT (Trinitrotoluene) charges, totalling one ton in weight, and later a second series which totalled a ton and a quarter (Edmonton Journal, 4 April 1951), which finally dislodged the ice jam.

In 1963 an ice jam formed at the confluence of the McLeod and Athabasca Rivers at Whitecourt. Two RCE Officers and a dozen men of the Pioneer Platoon, 2nd Battalion Princess Patricia's Canadian Light Infantry, later augmented by five additional Pioneers, spent six days and used 6220 pounds of explosive (Polar Forcite) to clear the jam (Buckley, 1963).

A similar service was carried out by members of an Army Reserve (Militia) Regiment on the Oldman River at Fort Macleod in 1972 (Lethbridge Herald, 31 March 1972).

Because of the nature of these operations no quantitative data was collected on the effects of the charges used. Buckley's (1963) account of the operation at Whitecourt however is interesting from the viewpoint of the conduct of the operation and the problems encountered.

1.2.2 Civil Experience in Alberta

As the phenomenon of ice jamming in the Province of Alberta has become better documented, the Provincial Government has undertaken both blasting operations and 'pre-blasting' (blasting of the ice sheet in advance of breakup) operations to clear the ice from certain rivers in areas where it is known that ice jams form.

Blasting and pre-blasting operations have been carried out regularly in Alberta since 1974. The Province has spent an average of \$17,000 per year on ice blasting since 1975, with \$35,950 having been spent in 1978 alone. These operations have been carried out on the Peace, Athabasca, Bow and Milk Rivers (Personal Communication, Alberta Environment, 1980).

Again, because of the emergency nature of the operations, no quantitative information was collected. Reports, written individually or collectively by Alberta Environment and the Alberta Research Council for each specific operation, are held by Alberta Environment, and include Nuttall (1974); Andres (1975); Szabon (1976); Davies, Deepprose and Hunt (1976); Doyle (1977); Doyle and Andres (1978) and

Doyle and Andres (1979).

1.2.3 Civil Experience in Manitoba

Quantitative information for other Canadian applications of the ice demolition problem were not readily available, again due to the nature of the operations conducted.

The Manitoba Department of Transportation, Bridge Division, reports an annual expenditure of between \$10,000 and \$200,000 in clearing ice (Personal Communication, 1979). Their 'method' involves aerial observation to locate ice jams in rivers in the springtime. When a jam is located, explosives are dropped onto/into it from a helicopter hovering above the river. Explosives are delivered in this manner until the ice jam moves out, and no data is collected at all (Personal Communication, 1979). During the winter of 1968-1969, however, the Province of Manitoba spent \$34,600 on ice removal with an estimated \$90,000 benefit accruing from the expenditure (Acres, 1971)

1.3 Background to the Problem

Van Der Kley (1965) reported that attempts were made in Europe over 220 years ago to use explosives for clearing ice. These were not for any military purpose, but rather were to remove the ice obstructing rivers and causing flooding (ice jams), or to assist the icebreaking ships of the period in removing ice from the vital shipping lanes. It ap-

pears that the first attempts to clear ice using explosives were made in Germany in 1758, when "Bombs were affixed below the ice and exploded" (Van Der Kley, 1965). Between that time and the beginning of the present century a number of experiments were carried out using dynamite, gunpowder and 'other' explosives. Little is known of the results of these early attempts. By the end of the last century, scientists had determined how to express the effect of explosives on solids; however, this had not been extended to the effect on a floating ice sheet.

The use of explosives to demolish ice sheets continued through the first half of this century, although again little is known of the results achieved. It was not until the early 1960s that serious study of the effect of explosives on ice was undertaken in the Western world.

Although the Soviets had been carrying out such investigations since 1948 (Sinotin et.al., 1970), information on the results of these studies was very restricted. The information and data contained in the Russian literature was not generally available in the west until the publication of translations by the U.S. Army Corps of Engineers' Cold Regions Research and Engineering Laboratory (CRREL) in the early 1970's.

A summary of the use of explosives in the Western world, with limited Soviet experiences included, for both surface- and aerial-delivered explosives on ice sheets and ice jams was presented by Bolsenga (1968) in his literature

review of ice jams. The information contained in Bolsenga's investigation however did not "...appear to cater to the constraints of the [present Canadian] military requirement" (Dr. J. Anderson, Defence Research Establishment, Personal Communication, 1979).

Current CAF publications refer to the use of explosives for ice demolition (Classified Reference), however, due to the incompatibility noted by Anderson, only general guidelines are available in the Forces' publications. As a result, Units of the CAF have had to develop their own Standard Operating Procedures (SOPs) for the demolition of ice. As an example, 1 Combat Engineer Regiment (1 CER) has developed the SOP of placing 2.25 kg (5 lbs) of explosive at a depth of 1.5 m (5 ft) below the ice, and spaces the charges 1.5 m (5 ft) apart. During discussion at the time of the fieldwork for this thesis, a member of 1 CER reported that while he was serving in 2 CER, that Unit had conducted ice demolition experiments of its own, and, presumably, had developed their own SOP for ice demolition.

The usual ice thicknesses in North America and Europe range from about 0.2 to 2.0 m. It is therefore doubtful that fixed procedures such as those currently used by 1 CER would use an 'optimum' explosive mass over the entire range of possible thicknesses.

When deciding on an optimum procedure, consideration must be given to both charge size and placement. All previous tests (Chapter 3) have shown that an explosive charge

has its greatest effect on a floating ice sheet when the charge is suspended in the water below the ice. To place an explosive charge beneath a floating ice sheet, some form of placement hole must be made in the ice. This can be effected mechanically or through the use of explosives detonated on the surface of the ice. The existence of the placement hole, however, may affect the results of the suspended main charge detonation in that the gaseous products of detonation may escape or 'vent' through the placement hole before all of the useful work derived from the expansion of those gases can be obtained.

As has been noted, it is generally accepted that best effects are obtained from charges placed under the ice. However, if the available time is limited, particularly during warfare, the use of surface-laid charges becomes advantageous. Such charges may be a row of single (or point) charges, a pre-packaged linear charge (such as the military Bangalore Torpedo or one of the 'Viper' class of charges), or, finally, the military Rapid Demolition Device (RDD) for concrete. The efficacy of such charges and placement has not been evaluated.

Another consideration in the preparation of the demolition is the length of time the explosives must be suspended in the water during tactical operations before firing. The effects of water on the explosive used may restrict its use because of the water resistance (or lack thereof) of the particular explosive and the length of time certain 'water

resistant' explosives can remain submerged. Some civilian explosives have no water resistance, hence requiring extensive waterproofing of the charges during field fabrication, whereas others can be immersed for short periods with little effect, providing the depth of placement and duration of immersion are within the manufacturer's prescribed limits. The use of military explosives and accessories, which are more highly plasticised and hence water resistant, reduces this problem significantly.

Of further concern to the CAF is the obstacle created by the demolished ice, and the life of this obstacle.

In conventional route denial operations the length of the gap (obstacle) created should exceed the spanning capability of an enemy's tactical bridging equipment if the gap is to be viable. In the denial of the use of an ice sheet, the gap may not have to be quite as extensive as the foregoing, because the load bearing capacity of a semi-infinite ice sheet is significantly reduced from that of an infinite ice sheet due to the discontinuity at the edge of the ice.

The duration of the obstacle created is also of importance. After a portion of the ice sheet is destroyed, it will commence to 'heal' itself by refreezing at a rate governed by the prevailing atmospheric conditions. Thus, a period ranging from a few hours to a few of days may be all that is required to allow the ice to thicken sufficiently to permit a man to cross the refrozen gap. A significantly longer time would be necessary before heavy vehicular loads

could cross the refrozen ice.

Hence, although the explosive demolition of ice has been carried out for over 200 years, there is little quantitative data available from experiments conducted prior to 1960. Within the CAF, only guidelines exist, with the result that SOPs for the explosive demolition of ice have had to be developed by each unit based on its own experiments and experience.

There was therefore a need for a systematic review and assessment of the available information on the explosive demolition of ice sheets, to provide the necessary background for the development of an SOP for use throughout the CAF.

1.4 The Problem

The problem was to determine the optimum ice demolition procedure to achieve the largest area of demolished ice for a given mass of explosive, and to develop the background for an SOP that provides a close approximation to the optimum for the range of ice thicknesses likely to be encountered by the CAF.

1.5 Scope of the Study

The scope of this study included the investigation of the optimization of charge mass (or weight) and placement

with respect to the ice and its thickness, based on the data available in the literature and field experiments on a limited range of ice thicknesses. The effect of placement technique (ie, surface placement versus sub-surface placement), and the effect of the placement hole were included. Emphasis was placed on point charges, but other aspects, such as the effectiveness of linear charges, were investigated to a limited extent in order to better define the remaining problems to be solved.

The study consisted of collecting and reviewing the available literature, planning a series of experiments to verify and extend the findings from the literature review, conducting the experiments and analysing the results.

CHAPTER 2

PRELIMINARY CONSIDERATIONS

2.1 General

As a means of introducing those aspects of ice demolition which are discussed in the review of the literature (Chapter 3), this chapter will present:

- a. the factors which affect the problem, and
- b. a dimensional analysis of these factors.

2.2 Factors Affecting the Problem

Consider, in the general case, an ice sheet of thickness t_i , overlain by some depth of snow t_s , which is floating on water of depth D . The ice, snow and water have densities of ρ_i , ρ_s and ρ respectively.

The intention is to create a hole in the ice by detonating an explosive charge. Upon detonation, a certain amount of energy E is released, the amount depending upon the chemical composition of the explosive. At the same time, the mass of the explosive is instantaneously converted to the gaseous products of detonation, which initially occupy the same volume as the original explosive, but at a much higher temperature and pressure. The gases expand, creating a gaseous sphere or bubble of radius R_0 , and in doing so

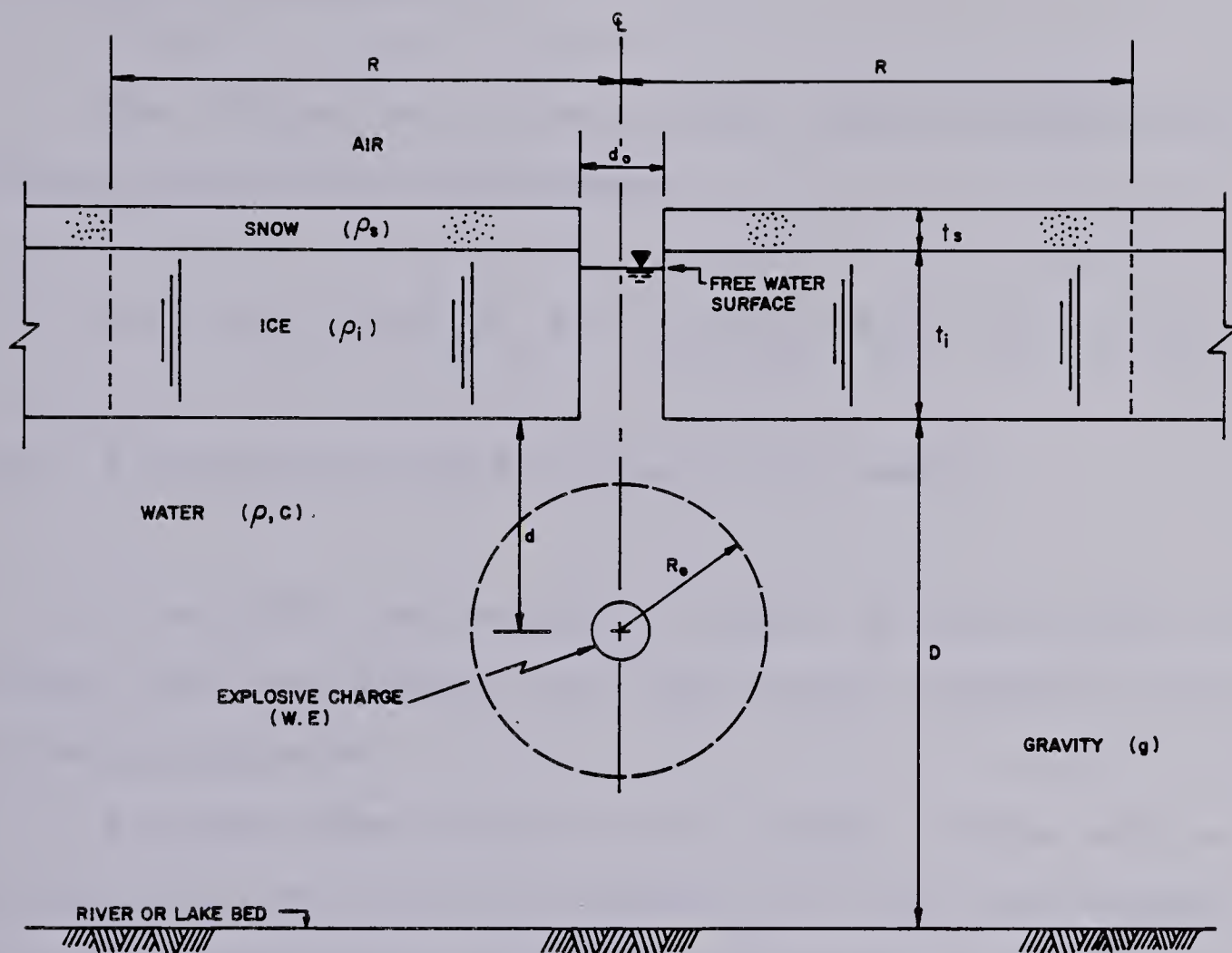
utilize some of the energy. The size of the gas bubble is determined by the volume of gas produced per unit mass upon detonation, for which the term "bubble effectiveness" has been used by Kurtz et.al. (1966). The sudden expansion of the gas bubble creates a stress or shock wave which propagates at a velocity c through the medium in which the explosion occurred.

As will be seen in the review of the literature, it has been found through experience that the best results in cratering a floating ice sheet are obtained when the charge is placed and detonated in the water under the ice. To make this placement, a hole of diameter d_0 must be made in the ice, and the charge lowered and placed a distance d below the bottom of the ice sheet. The convention that d is measured positive down from the bottom of the ice sheet will be adopted for this thesis.

As a result of the detonation of the explosive charge a hole or crater of radius R will be created in the floating ice sheet. To create the crater the water and ice sheet must be displaced upward against gravity g .

The parameters discussed above are shown in Figure 1.

The properties of ice, such as compressive and tensile strength, Young's Modulus, etc., are not considered in this thesis. Other investigations found in the literature have not included these parameters, and, it is considered that these properties will be nearly constant for situations which may be encountered.



LEGEND:

t_s = SNOW THICKNESS (mm)	d = DEPTH OF CHARGE PLACEMENT (m)
ρ_s = DENSITY OF SNOW (kg m^{-3})	D = DEPTH OF WATER BELOW ICE (m)
t_i = ICE THICKNESS (mm)	R = RESULTING CRATER RADIUS (m)
ρ_i = DENSITY OF ICE (kg m^{-3})	C = VELOCITY OF SHOCK WAVE (m s^{-1})
ρ = DENSITY OF WATER (kg m^{-3})	W = WEIGHT OF EXPLOSIVE CHARGE (kg)
g = GRAVITATIONAL CONSTANT (m s^{-2})	E = ENERGY OF DETONATION (J)
d_o = DIAMETER OF PLACEMENT HOLE (m)	R_g = RADIUS OF GAS BUBBLE (m)

FIGURE 1

FACTORS AFFECTING THE PROBLEM

2.3 Dimensional Analysis

The discussion in the previous section implies the following functional relationship:

$$f_1(t_i, t_s, D, \rho_i, \rho_s, \rho, E, R_o, c, d_o, d, R, g) = 0 \quad \dots (1)$$

where f_1 represents the functional relationship.

To simplify the analysis, a number of factors can be removed from consideration for the reasons outlined in the following paragraphs.

A simple force balance of the weight of snow and ice against the buoyant force of the ice will show that a depth of snow of approximately half the ice thickness will be sufficient to depress the top of the ice below the static water level. The ice, being weak in tension, will crack, causing water seepage onto the ice surface. This water will combine with the snow to form a slush, which freezes, creating a form of ice known as snow-ice that will become part of the ice thickness. It is therefore reasonable to expect that the thickness of snow will be something less than half of the ice thickness. Given that the density of snow ρ_s is in the order of 0.1 gm cm^{-3} , whereas that of ice is 0.92 gm cm^{-3} , it is not unreasonable to expect that the mass of snow present will be much less than that of ice. The depth and density of snow (t_s and ρ_s) on the ice can therefore be omitted

from the analysis.

Previous studies (Kurtz et.al., 1966) have shown that the depth of water D has no effect on the resulting crater dimensions and can be neglected. This was ascertained from a series of tests to determine if reflection of the shock wave from the bed of the water body would enhance the cratering effect of a detonated explosive charge.

Equation 1 therefore reduces to:

$$f_2 (t_i, \rho_i, \rho, E, R_o, c, d_o, d, R, g) = 0 \quad \dots (2)$$

As each of t_i, ρ_i, d_o, d and R are readily measurable as data, g is a constant, and the size of the gas bubble and its effect are unknown, ρ, E and c were chosen as repeating variables. A simple dimensional analysis yields:

$$f_3 \left(\frac{t_i}{(E/\rho c^2)^{1/3}}, \frac{d_o}{(E/\rho c^2)^{1/3}}, \frac{d}{(E/\rho c^2)^{1/3}}, \frac{R}{(E/\rho c^2)^{1/3}}, \frac{R_o}{(E/\rho c^2)^{1/3}}, \frac{\rho_i}{\rho}, \frac{c^2}{g(E/\rho c^2)^{1/3}} \right) = 0 \quad \dots (3)$$

If it is considered that ρ, ρ_i and c are constant for situations to be encountered, they can be incorporated in the constants implicit in such a function. While this last elimination makes each of the 'nondimensional' groups or terms dimensional in a strict sense, the dimensional groups do continue to represent the nondimensional ones:

"... a model analysis will show that the parameters are indeed identified by dimensionless groups. [and] ... the dimensionless products determine functional forms of certain dimensional groups, given specific restrictions on a model-prototype comparison." (Baker et.al., 1973)

The 'specific restrictions' mentioned are that the model and prototype experiments must be conducted under identical atmospheric conditions. This restriction is met in the previous ice demolition studies as well as the experiments carried out for this thesis, in that most of the detonations occur with the charge immersed in water at relatively shallow depth. Those experiments where the charge was detonated above the lower surface of the ice sheet do not meet this restriction, and were not included in the subsequent analysis.

It has been shown (Baker et.al., 1973) that for a given type of chemical explosive, the energy released upon detonation is proportional to the weight of the explosive charge. The weight W , which is readily measured, can be substituted for the energy E in Equation 3. Thus the implied functional relationship is further reduced to:

$$f_4 \left(\frac{t_i}{W^{1/3}}, \frac{d_o}{W^{1/3}}, \frac{d}{W^{1/3}}, \frac{R}{W^{1/3}}, \frac{R_o}{W^{1/3}}, \frac{1}{g W^{1/3}} \right) = 0 \quad \dots (4)$$

In normal blasting operations the placement hole is effectively stemmed (filled or packed with some material) so that gas venting, and hence d_o , is not a concern. However,

this has not been shown to be the case for ice demolition. For now, the effect of gas venting will be considered negligible. An investigation into this effect is conducted later in this thesis, which shows, in fact, that the size of placement hole has no discernable effect on the resulting crater radius. Furthermore it is often considered that the gravity effects are small. If the explosives used are considered to be identical with regard to the proportions of the released energy associated with the shock wave and gas bubble, the parameter R_0 can be eliminated. The function then reduces to:

$$f_5 \left(\frac{t_i}{W^{1/3}}, \frac{d}{W^{1/3}}, \frac{R}{W^{1/3}} \right) = 0 \quad \dots (5)$$

This final relationship is precisely the Hopkinson or 'cube root' scaling for blast effects. Hopkinson, states (Baker et.al., 1973):

"... that self-similar blast [shock] waves are produced at identically scaled distances when two explosive charges of similar geometry and the same explosive but of different sizes are detonated in the same atmosphere."

CHAPTER 3

SURVEY OF THE LITERATURE

3.1 General

This chapter presents a summary of previous work carried out on ice demolition. The data from the references is collected herein because, as Mellor (1972) states: "Most of [the] sources are obscure." Bolsenga (1968) has summarized the studies available to 1968 in a literature review on the subject of ice jams.

Three basic types of study are available in the literature. These are:

- a. blasting of floating ice sheets.
- b. ice blasting carried out on solid, glacial-type ice, such as reported by Livingston (1960), and,
- c. studies of the effects of 'shaped charges' on floating ice and frozen ground, such as Benert's (1957) investigation.

Of these, the blasting of glacial ice is not applicable to the present study as the mechanics of the blast effect in solid ice is different from that for floating ice.

The use of shaped charges is also a different type of blast than is being considered herein. Nevertheless a short

investigation of the use of shaped charges for making placement holes in the ice for the main charges is included.

The most applicable type of literature to the present study is that concerned with the demolition of floating ice sheets. In this literature the majority of the experiments which have been conducted have utilized a single (or 'point') charge. The charges have been placed below, within, on top of, and suspended above, the ice. A second category of charge used in these experiments has been the multiple charge, where two charges are placed in close proximity to enhance one-another. Two types of multiple charge have been reported, the 'decked' charge, where a small auxiliary charge is placed above a main charge, and what is herein termed the 'directed' charge, where the auxiliary is placed above and to the side of the main charge. The final category of experiments has been the use of a series of point charges placed in a row, with various spacings between the charges, all detonated simultaneously. These last will be referred to herein as 'row charges'.

The blasting of ice has been reported in the literature for two types of floating ice. The first is solid ice sheets, typical of frozen-over lakes, streams, estuaries and seas. The second type is ice jams, where floes of ice in varying sizes are jammed into a porous mass. The ice jam is generally thicker than the ice forming it.

3.2 Reported Studies of Blasting Floating Ice Sheets

3.2.1 Van Der Kley (1965)

Van Der Kley, (1965) reported the results of a series of experiments carried out by the Dutch Rijkswaterstaat, with the assistance of the Dutch Army, between 1961 and 1963. The experiments were to determine the effects of explosions on floating ice, primarily to evaluate if explosions of this sort assist ice-breakers in their task of clearing shipping lanes.

A series of experiments were carried out on Lake IJssel (IJsselmeer), and on the River Waal, using both low and high explosives: gunpowder, guncotton, Ammonal, Dutch Dynamite, Dutch TNT, American TNT, and an unspecified 'plastic' explosive. The ice thicknesses encountered varied from 0.090 m (3.54 in) to 1.900 m (74.8 in). In all, 72 data 'sets', consisting of the charge weight (W), ice thickness (t_i), depth of placement below the bottom of the ice (d) and resulting crater radius (R) were presented for single charges. However, some of these tests were repeated many times (up to 30). A total of 235 test shots were fired in the experiments. If a single test was repeated only average values of R were reported (Mellor, 1972). The results of these tests are reproduced herein in Table A-1 of Appendix A.

Van Der Kley also reports the results of 18 tests using multiple 'decked' charges, though he terms these 'percussion' charges. The charges consisted of a small auxili-

ary (percussion) charge and a main charge. Both were suspended below the ice, with the auxilliary charge vertically above the main. Both charges were detonated simultaneously. The data for these tests are reproduced in Table A-2 of Appendix A.

The main points brought out by Van Der Kley that are of concern to this thesis were:

- a. The individual explosions made large circular holes in the ice. The ice outside the cratered area had few cracks in it, and was apparently still so strong that it did not "become detached from the main sheet";
- b. Explosions are most effective when the charges are placed "immediately" under the ice; and
- c. Placing the charges and detonating them is time consuming, requiring a large labour force.

There is no discussion of the efficacy of the decked charges in Van Der Kley's report.

3.2.2 Purple (1965)

Major R.A. Purple of the U.S. Army Corps of Engineers conducted experiments in Korea on methods of combining parts of the various types of the Army 'equipment' bridging (pre-

fabricated bridges which can be constructed readily in the field) with a natural ice sheet to produce a bridge which could carry more than the ice alone, but which did not require a complete bridge set to be utilized. As an aside to those tests, experiments were conducted to determine the most effective method of clearing the ice with explosives if construction of a floating equipment bridge was necessary.

Explosive charges consisting of 2.27 kg (5 lb) of the plastic explosive Composition-4 (C-4) were placed at depths between "just below" to 3.05 m (10 ft) below the ice. In addition, one charge was placed on the ice surface and tamped or 'stemmed' with sandbags. Ice thickness varied from 0.102 m (4 in) to 0.152 m (6 in).

Purple's data are reproduced in Table A-3 of Appendix A. An average ice thickness of 0.127 m (5 in) is given in the table, as the ice thickness where each charge was placed was not published.

Purple did not discuss the ice demolition tests. However, it can be seen from his data that the premise that 'best effects' are obtained from charges placed immediately below the ice appears true, at least for the ice thickness he encountered.

3.2.3 Barash (1966)

Barash (1966) reported a series of tests conducted January through March 1960 by the U.S. Naval Ordnance Laboratory. Originally the work was published under the title

'Underwater Explosions Beneath Ice', but the report was security-classified and not made public. Due to the interest in explosions beneath ice that developed in the mid 1960s, the unclassified aspects of the original report were published in 1966.

The results of 45 explosions (or shots) were reported. Charge weights varied from 19.05 kg (42 lb) to 0.454 kg (1 lb). These charges were cast TNT spheres, except for five charges of the explosive HBX-3. The charges were placed at various positions with respect to the ice sheet, ranging from 0.61 m (2 ft) above the ice, through placement within the ice, to placement 6.10 m (20 ft) below it. Ice thicknesses varied from 0.508 m (20 in) to 0.762 m (30 in) during the course of the experiments.

The features of these experiments of interest to this thesis were:

- a. As the shock wave pulse reaches the ice sheet, it initially causes the ice to rise in the shape of a dome;
- b. The gas bubble, which migrates toward the surface from its point of formation, first appears at the surface either before or after the ice dome begins to fall back, depending on the depth of the explosion;
- c. As the gas bubble vents through the ice to the atmosphere, pieces of ice are thrown out,

either mostly upward or mostly radially, depending on the 'phase' of the gas bubble at the time it vents.

- d. The result of the explosion is an area, more or less circular in shape, containing pieces of ice, varying from zero to 100 percent of the ice originally in the area. The broken up area may contain a smaller area free of ice (open water). In some cases a "serious" circumferential crack may exist at some distance beyond the edge of the crater.

The 'phases' of the gas bubble are described by Cole (1948) as a pulsing (expansion and contraction) effect which is caused by changes in pressure within the bubble.

Initially the volume of the gaseous products of detonation occupies the same volume as the original explosive, but at much higher pressure than the surrounding water. The bubble therefore expands, pushing the water away, until the gas pressure equals the hydrostatic pressure of the water. As the water is moving away from the point of detonation, fluid momentum keeps it moving in that direction, causing the gas bubble to expand further, and the pressure within it to fall below the surrounding hydrostatic pressure.

At this time the fluid pressure exerts its influence and the bubble begins to collapse. As the bubble collapses, the gas pressure is once again built up until it equals the

surrounding hydrostatic pressure. Fluid momentum keeps the bubble contracting, to the point where the pressure inside is great enough to cause it to begin to expand again, and the cycle is repeated.

This pulsing motion is accompanied by a migration of the bubble toward the surface due to the density difference between the gas and the water.

Thus the gas bubble can be in one of four phases as it vents through the ice into the atmosphere:

1. expanding,
2. stationary - expanded,
3. contracting, and
4. stationary - contracted.

Though not substantiated during the review of the literature, it is thought that maximum ejection of ice from the crater would occur if the gas bubble were still expanding when it vented through the ice sheet. Momentum of the fluid set in motion by the expansion of the gas bubble would also assist in lifting ice out of the crater.

The results of these tests are reproduced in Table A-4. The measurements of crater radius, charge weight and placement depth are plotted in Figure 2. From the figure it is apparent that there is an 'optimum' placement depth for a charge of given weight.

With regard to this optimum placement depth, Barash

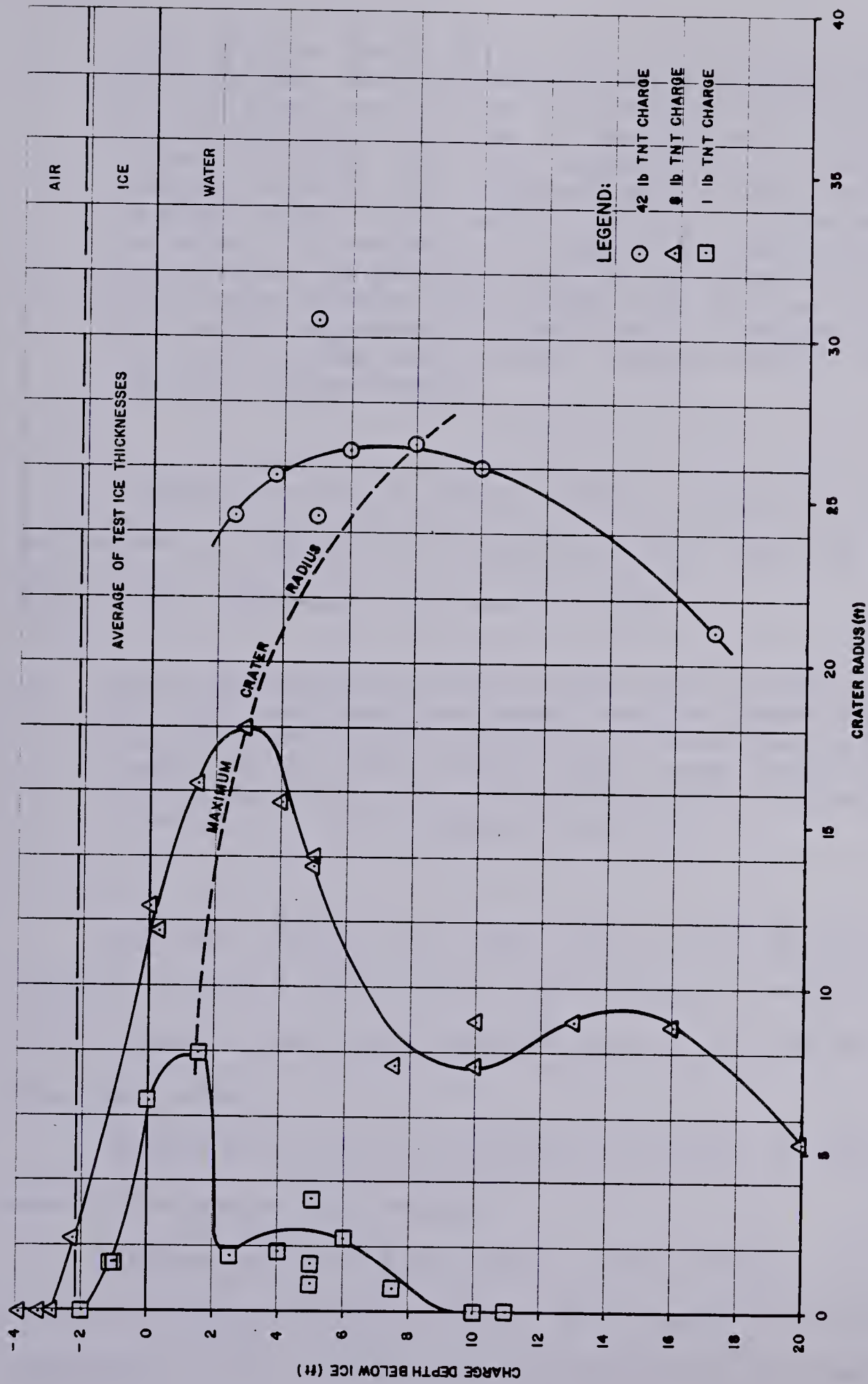


FIGURE 2
CRATER RADIUS IN ICE FOR CHARGE DEPTH AND WEIGHT
(AFTER BARASH , 1966)

states:

"The optimum charge depth, and the corresponding hole radius, are both approximately proportional to the cube root of the charge weight. This is not surprising, in view of the two well established scaling laws for geometrically similar configurations, one relating to the shock wave and the other to the bubble. First, the distance at which a given value of peak shock wave pressure occurs is proportional to the cube root of the charge weight; and second, the maximum bubble radius expected in free water is proportional to the cube root of the charge weight, for shallow charge depths."

Barash goes on to argue that the peculiar shape of the curves of Figure 2 is related to the size and dynamic state of the bubble at the time it vents:

"This suggests that the bubble plays a more important role than the shock wave in determining the size of the hole [crater]. This finding is supported by the greater hole sizes generally resulting from the use of HBX-3, an explosive producing a larger bubble than TNT."

Although Barash felt that "water depth may be a significant variable because of its effect on bubble migration", like Van Der Kley (Section 3.2.1), he did not evaluate that effect.

Barash also did not consider the effect of the thickness of the ice on his results.

Though Barash did consider to some extent the 'scale' effects of charge weight (through his comment on the proportionality of his results to the cube root of the charge

weight), he presented his data in dimensional form.

3.2.4 Wade (1966)

Wade (1966) reported the results of seven shots conducted during 'Operation Peggy' in February of 1966 by the U.S. Army Alaska (USARAL) under the direction of the U.S. Army Corps of Engineers, Alaska District.

The explosive used was Ammonium Nitrate and Fuel Oil (ANFO), primed with booster charges of C-4. The first six tests were conducted using 36.29 kg (80 lb) charges placed at various depths beneath an ice cover. The thickness of the ice varied between 0.483 m (19 in) and 0.610 m (24 in), and there was a snow cover "about" 0.305 m (12 in) deep. The snow density was reported to be 20 percent. The seventh shot was included to test whether ANFO would "deteriorate over a period of time". A "double" charge of 72.57 kg (160 lb) of ANFO was prepared using year-old fertilizer, and fired on the surface of the ice.

The specific objectives of the experiments were:

- a. To determine the optimum depth the explosives should be placed below an ice sheet to obtain maximum cracking [rather than cratering] from the explosions,
- b. To give operational personnel first-hand training, and

c. To support and supplement studies of the Nuclear Cratering Group, Livermore California.

(See Kurtz et.al., 1966)

Each 80 lb charge of ANFO was placed in a 16 gallon, plastic-lined can, with 30 to 40 lbs of sand ballast, a 2.5 lb block of C-4 as an interior booster charge, and two 2.5 lb blocks of C-4 as exterior booster charges. The charges were placed and allowed to 'cure' (soaking of the ammonium nitrate fertilizer with the fuel oil to ensure saturation) for 24 hours, during which the placement holes, which had been filled with snow and ice chips from the holes, were allowed to freeze over.

The data from Operation Peggy are reproduced in Table A-5 of Appendix A, and has been plotted in Figure 3. Because of the few tests fired, and the choice of placement depths, the crater radius curve of Figure 3 shows a trend opposite to that found by Barash. However, if the 7.5 lbs of C-4 booster charge is considered in terms of its energy producing ability and equated to an equivalent weight of ANFO, and allowance made for the fact that the specific energy release of ANFO (energy per unit weight) is less than half that of the TNT which Barash used, it can be shown that Wade's data is consistent with the form of the curves found by Barash.

Wade's data shows that the optimum depth of placement for cracking the ice sheet is greater than for cratering it.

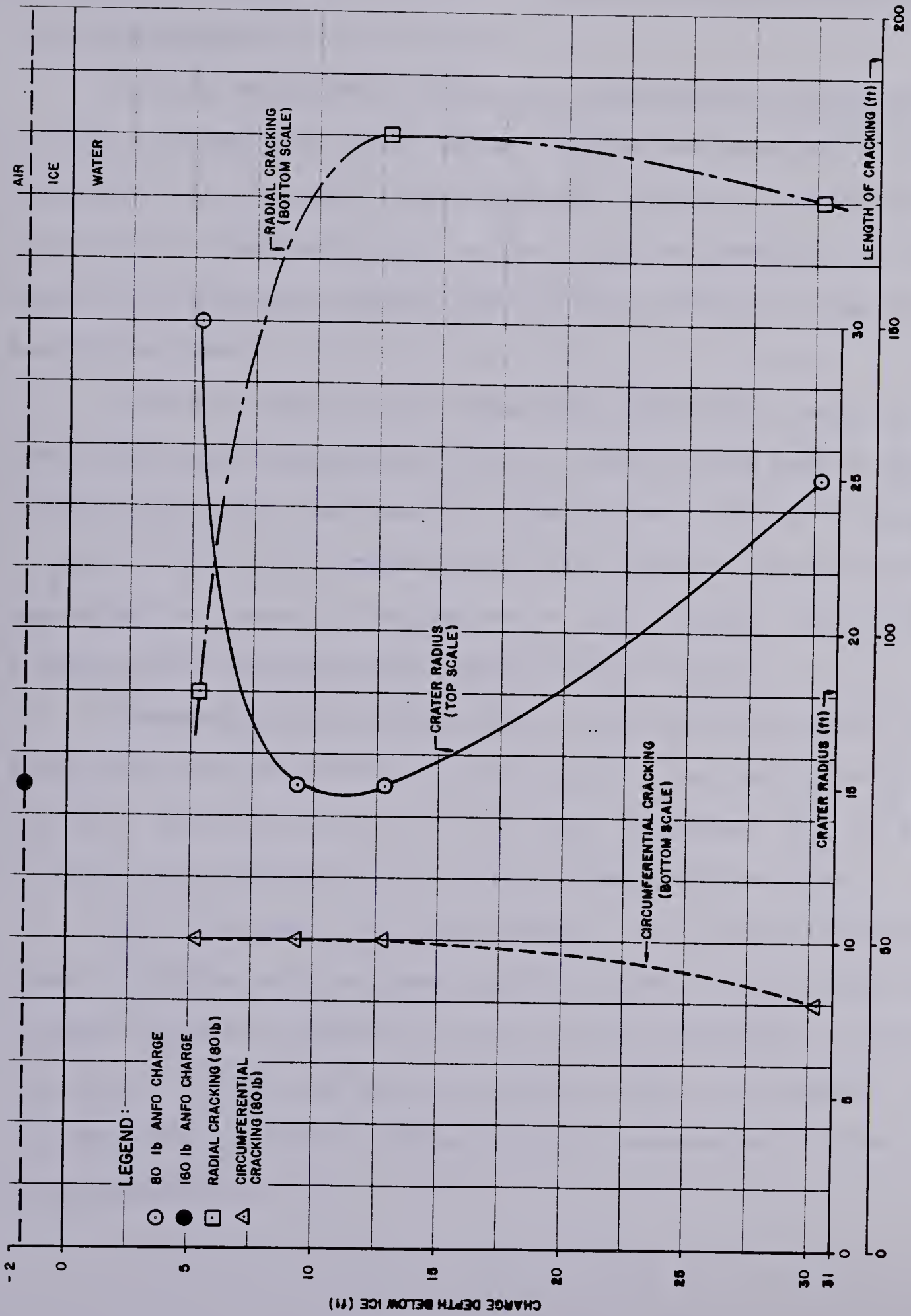


FIGURE 3 DATA FROM WADE, (1966)

However, the efficacy of these cracks in weakening the ice is not documented in any detail.

In his experiments, Wade did not consider the effects of ice thickness or water depth, though he does note that reflection of the shock wave from the bed of the water body remained an "indeterminate factor". In the deepest of his tests, the explosive charge was in fact resting on the bottom of the lake.

A final note on the data from Operation Peggy concerns the ice thicknesses given in Table A-5. Wade's data indicate that the ice was not homogeneous, but had a layer of water in it. The presence of this layer of water can be explained in terms of depression of the original ice due to a snow load as described earlier (Section 2.3).

Generally there was 0.305 to 0.381 m (12 to 15 in) of snow over 0.051 to 0.076 m (2 to 3 in) of ice, which in turn was over 0.076 to 0.102 m (3 to 4 in) of water, all on top of 0.356 to 0.432 m (14 to 17 in) of the main ice sheet.

For purposes of this thesis, the ice thicknesses given in Table A-5 includes the two layers of ice and the included layer of water, as the density difference between the two is small, and it is considered that the inertia of the combined ice-water system would be comparable to that of homogeneous ice.

3.2.5 Kurtz, Benfer, Christopher, Frankenstein, Van Wyhe and Roguski (1966)

As stated in the previous section, the experiments of Operation Peggy (Wade, 1966) were conducted to support and supplement the experiments of the U.S. Army Nuclear Cratering Group (NCG). These latter experiments were conducted two weeks later during 'Operation Breakup'. Operation Breakup entailed a fairly comprehensive experimental program, the most comprehensive to date in the literature, though only 18 single charges and three row charges (of five point charges each) were fired.

The objectives of Operation Breakup were (Kurtz et. al., 1966):

- a. To determine the relationship between depth of detonation and the size of the water gap produced in an ice cover by underwater explosions,
- b. To determine the effects of boundary reflection of the explosive shock wave on this relationship,
- c. To determine the effect of charge spacing on the size and shape of the water gap resulting from the detonation of a row of charges,
- d. To determine the effect of charge yield and placement depth on crack propagation, and
- e. To support theoretical studies of row cratering by observing surface motion phenomena,

crack propagation and bubble coalescence.

Kurtz et.al. noted that in almost every previous study an attempt was made to identify the optimum depth of burst. For instance, the curves due to Barash (Figure 2) indicated a maximum 'optimum' crater radius for bursts "slightly below" the ice (Kurtz et.al., 1966); an abrupt decrease in crater radius with an increase in the depth of burst; and, a slight increase over the minimum radius achieved at placement depths "equivalent to the bubble radius or greater". Similarly for "relatively thin" ice and small charges, Van Der Kley (1965) and Purple (1965) indicated optimum results from charges placed "just below" the ice. Wade (1966) in Operation Peggy and "previous (unavailable) studies", noted some advantage to be gained in placing larger charges deeper than just below the bottom of the ice. The authors of Operation Breakup noted:

"These previous experiments indicated a wide range of 'optimum depths of burst because of varying ice thicknesses and strengths, and the uncertainties in the comparative effectiveness of various explosives." (writer's emphasis)

The experimental program of Operation Breakup consisted of:

- a. Single Charge - Deep Water Calibration Series, to satisfy the requirements of objec-

- tive a. (This series was also called simply the 'Calibration Series'),
- b. Row Charge Detonation, to satisfy the requirements of objectives c. and e.,
 - c. Bottom Reflection Series, to satisfy the requirements of objective b., and
 - d. Yield Scaling Shot, for objective d.

Added to the program were two 'field fabricated' charges, one each of ANFO and TNT, to provide "comparative effects information" (Kurtz et.al., 1966) to supplement the data from the planned program.

High speed photography was included as part of the data collection.

The charges were C-4, (except for the two mentioned above), varying from 57.8 kg (127.5 lb) to 64.6 kg (142.5 lb), with one test, the Yield Scaling Shot, using a charge of 426.4 kg (940 lb). The two 'field fabricated' charges were 68 kg (150 lb) of TNT and 72.6 kg (160 lb) of ANFO. The thickness of the ice cover varied from 0.737 m (29 in) to 0.917 m (36.1 in). Placement depths ranged from zero to 10.67 m (35 ft). The depths of water encountered below the ice ranged from 3.05 m (10 ft) to 15.75 m (51.67 ft). The resulting data are reproduced for the single and row charges in Tables A-6 and A-7 of Appendix A respectively.

The charges were pre-packaged in aluminum spheres, complete with two high-energy exploding-bridge-wire detona-

tors, with Tetryl (a different explosive) pellets as a booster charge on each detonator. The use of the high-energy electrical detonators (requiring 3000 volts to initiate them) enabled the charges to be prepackaged and transported 'armed', because:

"...high voltage detonators are inherently safer than low voltage or non-electric detonators."

The Single Charge - Deep Water Calibration Series, or Calibration Series, was used to determine the 'optimum' placement depth. The charges were initially intended to be a constant 41.45 kg (136 lb), however, the loading density of the aluminum spheres varied during packing, so that the final weight of explosive varied somewhat. Table A-8 of Appendix A reproduces the data as converted, through scaling laws, by Kurtz et.al. to a standard 41.45 kg (136 lb) charge weight. This data is plotted in Figure 4. The trend is obviously similar to that found by Barash (Figure 2).

The optimum depth of burst for the given (converted) charge weight was determined as 3.05 m (10 ft) from Figure 4, yielding a crater radius of 11.26 m (36.95 ft). This figure was used for the spacing of charges within a row for the Row Charge Detonation series.

The Bottom Reflection Series was included to study the effect of the depth of water for "shallow water" shots, or the effect of the proximity of the detonation to the bottom of the water body for "deep water" shots, as Wade (1966)

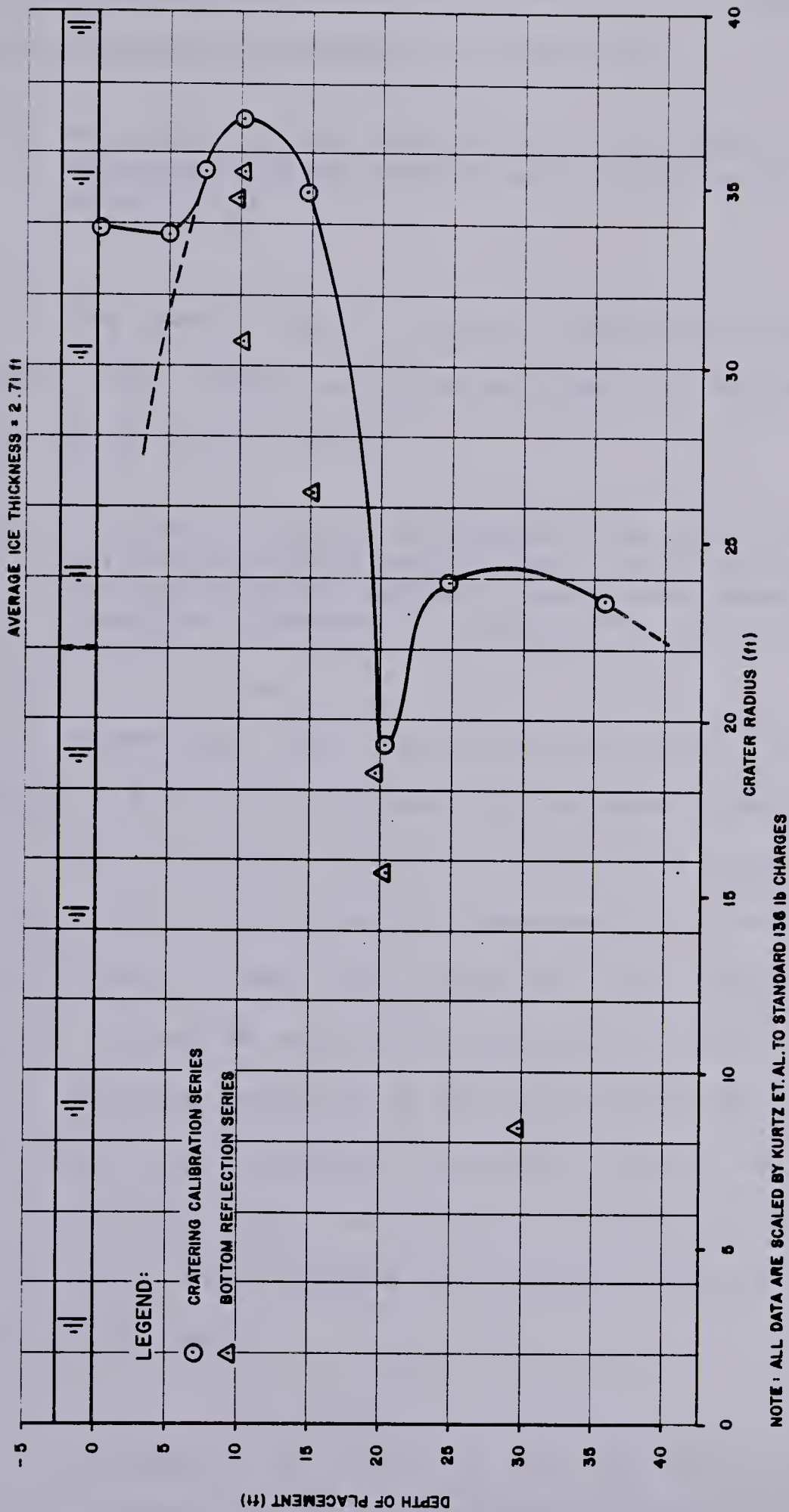


FIGURE 4
DATA FROM KURTZ ET. AL. (1966)

had indicated that there might be such an effect. The authors of Operation Breakup believed that:

"...under proper conditions, the shock wave reflected from the bottom could enhance the crater dimensions".

The results of the Bottom Reflection Series showed, however, that there was no enhancement of crater radius. In fact, Kurtz et.al. stated:

"...for all shots detonated, the radii [of crater] were significantly less..[than optimum from the Calibration Series]...and there were no reflection phenomena or mechanisms visible to the eye."

Presumably, the "visible to the eye" included their analysis of the high speed photography taken during each shot. This reduction in crater radius is evident in Figure 4. Kurtz et.al concluded that because the crater radii were "significantly less" than those for the crater calibration series, the matter might warrant further investigation.

From the analysis of the high speed film taken during each test, three 'phases' of surface motion were noted (not to be confused with the phases of bubble motion), plus a fourth which was observed only during shallow water tests. These phases were:

- a. Phase 1, a rising of the surface of the ice sheet due to the expansion of the gas bubble

(note that Barash attributed this to the shock wave while Kurtz et.al. attributed the motion to the expansion of the gas bubble).

- b. Phase 2, high velocity venting of the gases contained in the bubble through the ice sheet,
- c. Phase 3, low angled venting of water caused by the rapid rush of water into the cavity vacated by the gas when it vented during Phase 2, and
- d. Phase 4, (for shallow water shots) a "mud surge", which is a second surge of water, similar to that of Phase 3, but weaker, and always very muddy.

Phase 1 motion was ascribed to the expansion of the gas bubble before it vented through the ice, as there was "no indication that the motion was due to the 'spall' phenomenon associated with the passage of the shock wave through the ice". This phase had "radically" different durations, depending on the depth of burst (depth of charge placement). For charges placed at less than the optimum depth (determined from the calibration series), the gas bubble vented "immediately", and Phase 1 motion was barely detectable. For the two deepest shots, Phase 1 lasted over 1200 m sec. It was noted in fact that for these deeper shots the ice was moving downward before the advent of Phase 2.

Kurtz et.al. therefore concluded that for these deeper shots, the ice was not broken up by Phase 1 movement, but rebounded elastically, and was broken up by the Phase 2 motion.

Phase 2 motion was the venting of the gas bubble through the ice sheet. The timing for this phase varied from "immediately" following detonation for the 'shallow' placement depths, to more than 1200 m sec for the deeper shots. The venting gas carried water, ice and snow with it. The base of the vent through the ice was typically from 6.1 m (20 ft) to 9.1 m (30 ft) wide (at its maximum dimension), and its height varied from "about" 12.2 m (40 ft) for the deep shots, to 39.6 m (130 ft) for the zero placement depth shot. The velocity of the Phase 2 gas vent varied with the depth of burst, being higher for the shallower shots. It was reported that the advent of Phase 2 motion was difficult to determine for shots fired with a depth of burst less than 6.1 m (20 ft), because Phase 2 motion began while the ice was still accelerating during Phase 1.

Phase 3 motion was described as:

"... a low-angle vent of water and vapour caused by the rush of water into the cavity vacated by the gas bubble as it vented."

The motion occurred at a "relatively late" time, being in the order of 1 second following detonation. It was noted that this surge ejected additional ice from the crater. For

the shallowest (zero) depth of burst, no Phase 3 motion was noted, presumably because the Phase 2 motion was immediate and complete upon detonation, hence creating a very small gas cavity (if any) in the water.

The final phase of motion, Phase 4, or the "mud surge", was noted for deep placement depths in "relatively shallow" water. The motion was again "late", occurring 1.5 to 2 seconds after detonation. The water apparently "boiled up violently" at the surface, usually surging outside the crater. As noted, the water was "always very muddy", and "it appeared to be a second water surge, similar to Phase 3, but having much less force". No explanation was given for the cause of this mud surge.

Kurtz et.al. summed up their observations of the surface motion phenomena as follows:

"The ice sheet is bulged upwards by the expanding gas cavity, and is broken and partially ejected by the venting of the gas bubble. A 'bonus' effect [in terms of clearing debris from the crater] is gained by water rushing into the cavity vacated by the venting gas. This water surge ejects additional ice from the crater."

Kurtz et.al. suggested that the shape of their optimum curve (Figure 4) could be explained by variations in the dynamics of the gas bubble. For single shots they argued that the proximity of the bubble to the ice surface and the water body (lake) bottom could be important, because "blow-out", or the venting of gases, imparts additional velocity

to the ejecta. They also felt that the size and location of the gas cavity would affect the path of the shock wave(s) reflected from either the bottom or from the ice itself.

Explosions in water generate gas bubbles that had been well defined by Cole (1948) for the explosive TNT. The gas bubble pulsates rapidly while it migrates to the surface as outlined earlier. Kurtz et.al. assumed that the "bubble effectiveness" (ability to generate a certain volume of gas per unit weight of explosive) of their explosive was equivalent to TNT, and used the following relationship, which they indicated was due to Cole (1948), to estimate the bubble radius:

$$R_0 = 12.8 \left[\frac{W}{Z + 34} \right]^{1/3} \quad \dots (6)$$

where: R_0 = gas bubble radius (ft)
 W = yield (explosive weight (lb), and
 Z = depth of burst below the top of
the ice (ft)

It was found that the optimum depth of placement corresponded "approximately" to half the bubble radius. From previous discussion, for shallow depths of burst, Phase 2 motion (gas venting) was almost indistinguishable from Phase 1, hence Kurtz et.al. concluded that the size of the crater was due, at least in part, to the gas bubble and its dynamic state when it vented through the ice.

For a placement depth approximately equal to the bubble radius, or twice optimum depth, the gas bubble would have collapsed to a compressed, higher pressure state (Section 3.2.3) just prior to venting. The crater radius in this case would be minimal, and would explain the minimum in the curve of Figure 4.

For deeper placement depths, the bubble would have begun to expand again as it neared the surface, resulting in an increase in crater radius from the minimum, which was also observed in their data as shown on Figure 4.

Two observations were made by Kurtz et.al. concerning the combined effects of surface and bubble motion. First, if the proximity of the lake bottom had any effect on the optimum crater size, it could not be easily detected. Second, the optimum placement depth will give best results in shallow water, which seems to contradict their first observation. It was observed that:

"...bottom variations do appear to change the relative importance of shock waves and bubble venting in the cratering mechanism."

and under certain circumstances:

"...that the various crater mechanisms [shock wave, gas vent and water surge] work against each other."

Finally it was noted that the larger crater radii produced from depths of burst greater than the bubble radius

could not be:

"...explained by early surface motion, but rather must be connected with bubble pulsations and blowout at a later time."

The next area considered by the authors of Operation Breakup was that of row charges. Three rows, A, B and C, of five charges each were fired. The spacings between each of the five charges were, for rows A, B and C respectively, 1.0, 1.5 and 2.0 times the previously determined optimum crater radius from the crater calibration series (36 ft), for the thickness of ice encountered.

Each charge in the row "appeared to act independently". Phase 1 motion could "not be differentiated" from Phase 2 as the placement depths were "shallow". There were:

"...five distinct [gas venting] plumes in each row, and five distinct third phases of motion. The third phase of motion did overlap on adjacent charges, but only after venting [third phase vent] through the ice sheet."

Since each gas bubble vented sometime "prior to 50 m sec, and the ice surface between adjacent charges was "in place long after" this time, the authors concluded that:

"...there was obviously no coalescence of gas bubbles of adjacent charges beneath the ice."

For the spacings used between the charges there were no cusps formed around the final crater (to indicate five

separate craters), hence the authors concluded that Phase 2 and 3 motions were responsible for any crater enhancement for row charges, not coalescence of the gas bubble beneath the ice.

All of the craters from the tests, except the Yield Scaling Shot, were "completely covered with debris consisting of ice fragments and snow". The larger shot left a "significant" area of open water.

The size of the largest ice blocks found in the single charge craters "seldom exceeded 3 ft [0.91 m] or 4 ft [1.22 m] in diameter". However, for the row charges and the Yield Scaling Shot, the maximum size was in the order of 20 x 40 ft (6.1 x 12.2 m). The presence of these larger blocks was attributed by the authors to the fact that:

"The larger yields may, for instance, generate a water wave large enough to separate large slabs [of ice] along planes of weakness."

The presence of these large ice fragments in the crater suggests that the ice is fractured in bending, beyond the eventual radius of the crater caused by the venting of the gas bubble. Subsequent surging during the third phase of motion could then dislodge the larger ice floes along these fracture planes.

The presence of the larger ice floes is of importance in military 'denial' operations, because Kurtz et. al. stated that a man was able to traverse the water gap created by

one of their explosions by using a large floe as a raft.

The presence of these large floes in each of the row shots also had an effect on the enhancement of the crater dimensions perceived by the original authors. Initially, comparing a row crater half-width to the crater radius of a similar point charge indicated increases of 57, 58 and 82 percent over the point charge crater radius for rows A, B and C respectively (Table A-7). However, if the width of the large ice floes remaining in the crater is deducted from the row crater half-widths, presuming that their presence is due to the fracture and surge action rather than to the action of the gas vent, the crater 'enhancements' are reduced to 3, 4 and 28 percent respectively.

Kurtz et.al. also considered the effects of the detonation in forming cracks in the ice outside of the cratered area. The two types of crack noted in the previous studies, ie, radial and circumferential, were also found here. The "main" type of crack found was the circumferential. These cracks circled the crater, "in whole or in part", at different distances from the crater's edge. Radial cracks, forming "spokes of a wheel" around the craters were considered by Kurtz et.al. to be minor. Although the collected crack data was limited, the cracks "...did not appear to affect vehicular mobility over the thick, uncratered ice". The authors postulated that had these cracks formed in river ice, where the ice is subjected to shear stresses imposed on it by the river flow, the cracks would facilitate downstream displace-

ment of large floes of ice (providing of course that the floes had somewhere to displace to).

Refreezing of the craters was also studied, but the data on the refreezing aspect were sparse. However, it did show that, under the influence of the air temperatures experienced (0°F to -30°F), a man could stand in the centre of a crater the day after it had been made.

The length of time required before vehicle loads could safely be applied to a refrozen crater would obviously be much greater as it would take longer to grow the required ice thickness. Of further interest, for the consideration of vehicles crossing a refrozen crater, is the debris on the surface of the intact ice. Ice debris thrown just clear of the crater during Phase 3 motion freezes to the intact ice sheet and hampers vehicular traffic.

A parameter that has an important influence on the refreezing rate is the amount of debris left in the crater. This is important as the debris acts as a filler material, hence lessening the amount of new ice which has to be formed to achieve a given thickness. Thus a crater free of debris will take longer to freeze to some thickness than will a crater choked with ice debris. Presumably then, the refreezing rate is dependant not only upon the air temperature, but the volume of ice debris left in the crater as well.

Kurtz et.al. noted that the bearing capacity of ice in a refrozen, debris-filled hole, should be "approximately" the same as that in a refrozen hole without debris. The de-

termination of loads which can be applied to either type of refrozen crater can thus be found from existing tables of ice bearing capacity as a function of thickness.

To summarize the findings of Kurtz et.al., in addition to defining the optimum curve for 41.45 kg (136 lb) charges of C-4, and obtaining some dimensions for row charges, the following general conclusions were reached:

1. The reflection of the shock wave from the lake bottom did not appear to enhance crater dimensions;
2. Cracks appeared to propagate better from larger yield explosions;
3. There did not appear to be any evidence of gas bubble coalescence under the ice in row charge detonations;
4. "Commonly used" scaling laws may be used to estimate the effects of higher yield ice cratering experiments; and
5. Maintenance of open water gaps created by ice cratering explosions in still water in the Arctic is limited to a few hours because rapid refreezing occurs; however, in a river or stream, the broken ice may be moved out by the current, thus facilitating the maintenance of a clear channel.

It is of interest to note that while Kurtz et.al. made mention of 'scaled ice thicknesses', they did not include the effect of ice thickness in their analysis.

As part of the overall study, it is also worth mentioning that tests were carried out on captive fish to determine the effect on them of explosions at different distances. While certain of the captive fish died from the tests, one point which the authors mentioned was that no fish, other than the captive ones placed quite close to the charges, were found dead following the tests.

3.2.6 Frankenstein and Smith (1966, 1970a, 1970b)

In three publications (1966, 1970a, 1970b), Frankenstein and Smith present and discuss the results of Operation Breakup (Kurtz et.al., 1966). However, their first (1966) publication includes three additional data sets (shots) collected from tests on the Mississippi River near Elk River Minnesota. The additional data are shown in Table A-9 of Appendix A.

The Mississippi River explosions were intended to weaken a solid ice sheet near the toe of an ice jam. The ice was thinner than that encountered during Operation Breakup, and was described as being "partially deteriorated". The explosive used was not reported, however, as the data were presented in conjunction with the data from Kurtz et.al., it is presumed that the explosive used by Frankenstein and Smith was also C-4.

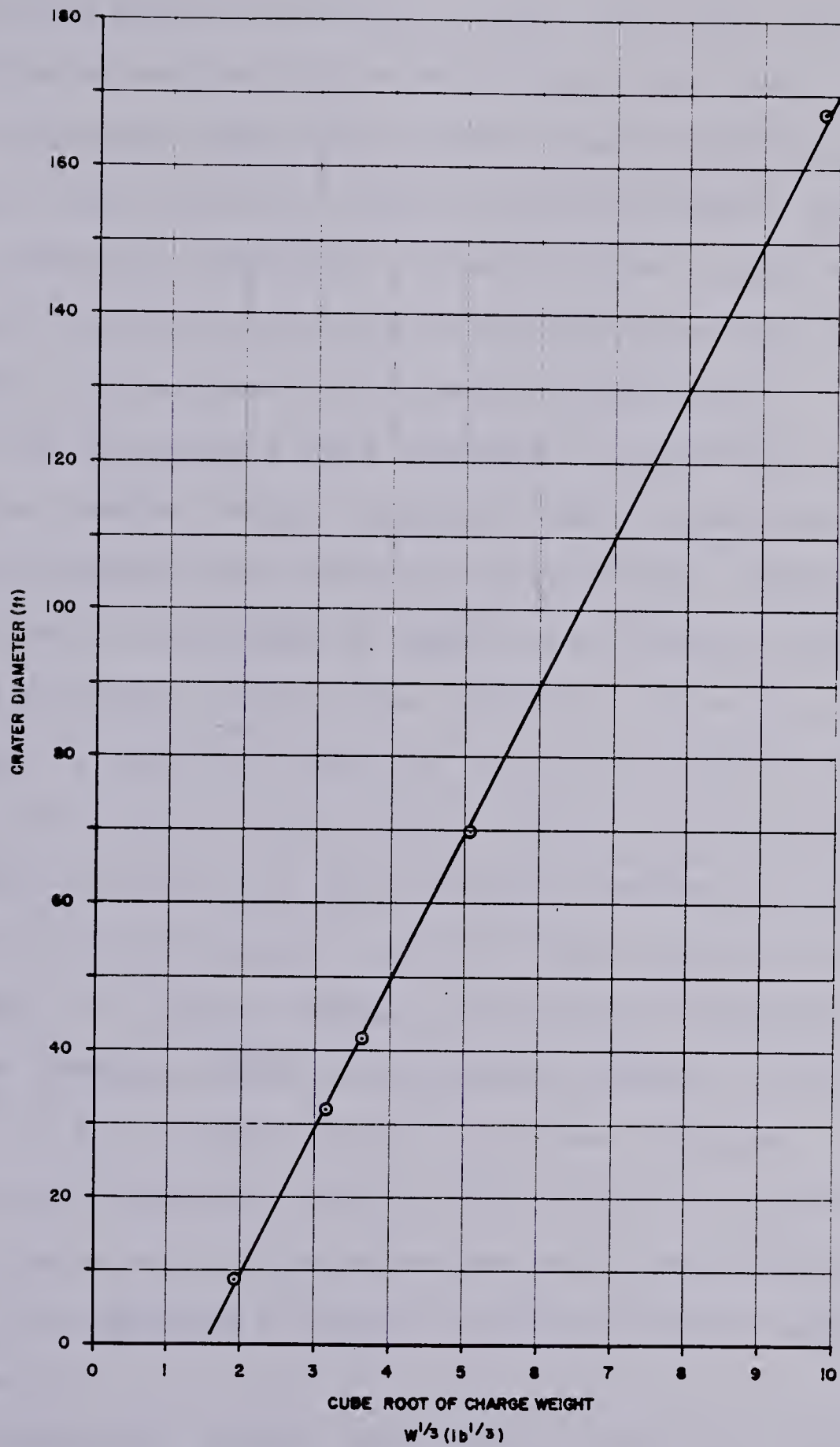
This data is plotted in Figure 5 in the form used by Frankenstein and Smith (1966). This presentation is noteworthy in that it was the first use of 'scaled' data. It was stated (1970a) that the figure was "...used universally in the United States, including Alaska, for obtaining the charge weight for the desired crater size". The figure must be used in conjunction with a depth of burst equation, this being that the depth of placement should be "twice the cube root of the charge weight" (1966).

Noting the "linearity and consistency" (1970b) of the results, Frankenstein and Smith indicated "...that the ice thickness and strength may not have the effect on crater size [that] one would imagine" (1966).

3.2.7 Nikolayev (1970,1971)

Nikolayev reported (1970,1971) the results of Soviet experiments on blasting sea ice in the Antarctic. The experiments were conducted in 1969 to investigate the use of explosive demolition of ice sheets for assisting ship passage. The techniques developed have apparently gained usage in the USSR for the clearance of ice jams as well. The data given by Nikolayev was for floating ice sheets, and hence is applicable to this thesis.

In the 1970 publication Nikolayev mentioned that "a" technique for blasting ice in rivers, lakes and northern seas had already been developed, and was "widely" used in the USSR. It is not known if this technique is the one he



NOTE: 1. AFTER FRANKENSTEIN AND SMITH

FIGURE 5
SCALED CHARGE WEIGHT vs CRATER DIAMETER⁽¹⁾

used in his first (reported in 1970) Antarctic experiments, or whether he was working on developing a new one.

Nikolayev also noted (1970) that Antarctic sea ice "differs from the ice of other bodies of water" in that it has a "somewhat different structure" due to its salinity, and has a "greater plasticity". He noted therefore that the Antarctic ice may react differently to blasting.

The experiments were conducted to determine the most effective charge weight, optimum charge placement depth, zones of cracking and "total ice destruction" (crater dimensions), and to find ways to improve ice blasting efficiency. The ice thickness ranged from 1.050 to 1.100 m (41.3 to 43.3 in), over a depth of water of 45 to 60 m (148 to 197 ft). Charges of a Soviet explosive (Trotyl) weighing between 25 and 30 kg (55 to 66 lb) were detonated between 2.4 and 4.5 m (7.8 to 14.7 ft) beneath the top of the ice. The experiments consisted of single charges, and what Nikolayev termed "paired" charges, which are 'decked' charges in the terminology of this thesis. With the decked charges, the main charge was detonated first, and the auxiliary 25 m sec later. The data given by Nikolayev are given in Tables A-10 and A-11 of Appendix A for the single and decked charges respectively.

Nikolayev noted that using "blasting experience [from] other bodies of water" it had been determined that the 25 to 30 kg charges were required for ice in the order of 1.1 m thick. The experiments, then, were to confirm this

procedure on Antarctic ice. The tests showed that the optimum placement depth was 3.2 m from the top of the ice (2.1 m or 6.84 ft below the bottom of the ice), whereas in "other" bodies of water the placement depth ranged 2.9 to 3.0 m below the top of the ice (1.8 to 1.9 m below the bottom of the ice). The "area of total destruction" (crater) was noted to be slightly smaller for the Antarctic ice than for the same charges in the ice of "other bodies of water". Nikolayev reasoned that the higher plasticity of the saline ice was responsible for this phenomenon.

Nikolayev noted that (1970):

"In an under-ice explosion, ice is destroyed by the shockwave and by the energy of water masses set in motion by the explosion products [gases].

As a shockwave travels toward the surface... ..through water and ice, it compresses them, thereby crushing the ice and separating it from the pack. At distances remote from the explosion site, the force of the shockwave decreases and it is only able to crack the ice. Under the effect of gases and hydrodynamic pressure, the water with the crushed ice gushes up to a height that depends on the depth of the charge and its weight."

The other type of experiments conducted were those using the decked charges. The theory behind these charges was given by Nikolayev (1970) as:

"The main charge was detonated first and the booster [auxiliary] charge 0.025 sec later. As it spread and rose to the surface, the gas bubble from the main charge was flattened, as it were, by the explosion of the booster charge, increased in diameter [the gas bubble of the main charge] and encircled the gas bubble of the

latter."

Nikolayev stated that previous experimental data had shown that the use of paired charges increased the total ice destruction area by "about" 20 percent, an increase of 9.5 percent in the radius of the crater. The data from the Antarctic experiments showed a similar increase according to Nikolayev.

Nikolayev felt that for assisting lane clearing for shipping, the area of crack formation was more important than the size of the crater produced, as (1970) ice:

"...riddled with large and small cracks is much weaker, and can be easily forced by an icebreaker or by other vessels of the ice-breaking class..."

Nikolayev's second set of experiments (reported in 1972) investigated a modified decked charge technique: the auxiliary charge was now placed above and to the side of the main charge, and detonated first. The technique was called "directed blasting" by Nikolayev, as the intent was to direct the ejecta from the explosion away from the crater. Previous studies had shown that upwards of 90 percent of the fractured ice fell back into the crater from the vertical plume sent up by the venting gas from a normal point charge explosion. Directed blasting was aimed at redirecting this plume to some angle to the vertical.

To quote Nikolayev (1971):

"The principle of directed blasting is based on the rule which states that the main ejection of material within which an explosion occurs, is directed along the least line of resistance, ie along the shortest distance from the charge to the free surface. The free surface may be other than a natural one. This could be the surface of some hollow or cavity artificially created in the material being blasted..."

"...such a cavity can be formed [in water] with the aid of a preliminary blasting of an auxiliary charge.

...the [main charge] should be exploded at that instant when the gaseous cavity of the auxiliary charge reaches its maximal proportions, the pressure of gases within it manages to decrease sufficiently, but the cavity itself has not yet collapsed."

The experiments were again conducted on Antarctic sea ice, of thickness 1.100 m (43.3 in), with a depth of 40 to 50 m (131 to 164 ft) of water beneath it. TNT was the explosive used in these experiments. For this ice thickness, Nikolayev determined that to obtain optimum results, a charge weight of "around" 31 kg (68 lb) was required as a single charge. For the directed technique, this total charge weight was broken down into a main charge of 25.2 kg (55.6 lb), which was "one case" of TNT, and a 4.8 kg (10.6 lb) auxiliary charge. The amount of explosive in the auxiliary charge was varied for three of the four experiments carried out, and ranged from 3.2 to 8.4 kg (7 to 18.5 lb), the main charge being kept at 25.2 kg. Other factors in the experiments which were varied were the relative positions of the charges, which determined the angle to the vertical, and the time delay between detonations of the charges.

The craters formed by this technique were elliptical rather than circular. The data are reproduced in Table A-12 of Appendix A, with depths of placement recomputed to be 'below the bottom of ice' instead of Nikolayev's measurement from the top of the ice sheet. Nikolayev measured the ice ejected from the crater by approximate volume, in order to determine the amount of ice cleared from the crater. This data is also included in Table A-12.

As mentioned above, Nikolayev expected that the optimum time delay between detonations should be the time of increase of the radius of the gas bubble formed by the auxiliary charge to its maximum dimension. This time, according to Nikolayev, is dependant upon the energy and size of the auxiliary charge and its depth of placement. It was found that the optimum delay between the main and auxiliary charges used was 0.025 seconds. The resulting craters were generally larger than craters formed in ice by a single charge of the same total weight.

Nikolayev found that between 5 and 50 percent of the ice could be ejected from the crater with directed blasting, compared to less than 10 percent from single charge detonations. The optimum ejection angle was found to be 45 degrees from the vertical. Observation showed that (1971):

"...around 60% of the ejected ice lies along the direction of throwing, roughly 15% is thrown to either side, and only 10% is thrown in a direction to the rear of the [throwing] direction."

Notwithstanding the relative efficiency of directed blasting in clearing ice from the crater, zones (craters) completely free of ice debris were not obtained. Nikolayev indicated that the nature of ice ejection, or the "explosion processes on breakdown of ice", is a more complex phenomenon than directed blasting of soils or rock (from whence the idea had come), and attributed the difference to the forces of ice adhesion to the water, viscosity, incompressibility, and the forces of the water's "internal friction".

From the experiments Nikolayev concluded (1971) that:

- a. directed blasting can be successfully utilized,
- b. the resulting craters are approximately 1.5 times larger than those formed by single charges of the same charge weight, and up to 50 percent ejection of ice can be achieved,
- c. the placement of the main charge should be in accordance with previously determined optimal placement for single charges,
- d. the auxiliary charge should be 1/6th of the weight of the main charge,
- e. the optimum angle of blast is 45 degrees to the vertical, and
- f. for the charges Nikolayev used, the optimum delay between detonations was 0.025 seconds.

Nikolayev's experiments are discussed in greater detail in Chapter 8.

3.2.8 Moor and Watson (1971)

Moor and Watson (1971) were concerned more with the field application procedures of ice jam and ice cover removal than the strictly experimental aspects of ice cover demolition. They placed small charges in river ice, along a line which, when detonated, would produce a "perforated line" (of craters) which the forces acting on the ice sheet could easily shear at spring breakup. Two sticks of "ditching powder" were placed at the bottom of 0.762 m (30 in) deep holes in 0.914 m (36 in) thick ice. Thus, the detonations occurred within the ice, rather than below it as has been the usual case. It was found that this method would yield a 1.68m (5.5 ft) diameter crater in the ice. Rows of charges with spacings between charges of 1.68 m (5 ft), 2.44 m (8 ft) and 3.05 m (10 ft) were detonated, all charges detonated simultaneously. It was found that the 1.68 m spacing gave a complete (connected) crater, while the others yielded a row of individual craters.

Minor radial cracking was noted around the craters, as well as "shattering and cracks" between craters in a row.

They concluded that the method held promise as an economical method of creating shear lines in ice sheets.

Information on the explosive used by Moor and Watson is minimal:

"Ditching powder is manufactured as 1-1/4 in x 8 in sticks, averaging 0.459 lb per stick, with velocity [of detonation] of about 15,000 ft/sec"

The exact nature of the explosive is not known, as, for example, Canadian Industries Limited (CIL) (1968) manufactures a number of explosives in cartridges of the size indicated by Moor and Watson, with approximately the same velocity of detonation. These explosives range from straight dynamite through ammonia and gelatin dynamites, of various grade strengths. Furthermore, CIL used to manufacture a 'ditching dynamite', though not any longer (Personal communication, CIL, 1980).

3.2.9 Mellor and Kovacs (1972)

Mellor and Kovacs (1972) investigated the use of compressed gas 'blasting' for ice demolition. Experiments were conducted on lake ice in New Hampshire and Alaska, using compressed carbon dioxide and compressed air, with a few shots using chemical explosives during each series of tests for comparative purposes.

Mellor and Kovacs indicated that compressed gas had a number of advantages as a blasting agent, these being:

- a. much lower pressures than chemical explosives, allowing compressed gas use in close proximity to structures or ships,
- b. blasting action is such that the ice will tend to break by widespread heaving rather

- than localized shattering,
- c. with compressed air systems, repetitive blasting can be carried out without need for direct access to recharge the discharge ports,
 - d. minimizes possibility of harming aquatic life, and
 - e. no pollution from blast products.

The use of compressed gas as a means of demolishing an ice sheet appears to have more applications to civilian than military uses. Mellor and Kovacs noted, however, that on an equivalent energy basis, the use of compressed gas was comparable to the use of explosives.

The data from the chemical explosive shots made by Mellor and Kovacs for comparative purposes to the gas shots are reproduced in Table A-13 of Appendix A.

3.2.10 Mellor (1972)

In this technical note, Mellor compiled and analysed, by regression, the data on point charges reported in the literature up to that date. The data analysed included that due to Van Der Kley (1965), Purple (1965), Barash (1966), Wade (1966), Kurtz et.al. (1966), Frankenstein and Smith (1966), and Mellor and Kovacs (1972).

Mellor noted that the blasting of floating ice sheets had not been studied theoretically, though Cole (1948) had

outlined the fundamental considerations. While Van Der Kley (1965) had developed a geometric analysis, the essential constants were empirically derived from his tests. Mellor further noted that although many U.S. investigations had applied cube root scaling to damage radius and charge depth, the scaling requirement for ice thickness had been ignored.

Mellor used a multiple linear regression analysis to determine empirical relationships between crater radius, ice thickness, charge depth and charge weight. He noted that the chief difficulty in deriving the relationship was that the data were "too sparse and ill-conditioned". This resulted from the fact that past experiments had usually been aimed at determining the optimum conditions, so that most combinations of variables which gave poor results were avoided. As Mellor states:

"This practice produces data that are unsuitable for defining relationships by regression analysis or by any other sort of empiricism."

The problem was simplified by the expedient of specifying the charge weight relationship on the basis of similitude considerations. Noting that it is not possible to satisfy all similitude requirements simultaneously, cube root scaling was selected, as "experience had shown" that it gave satisfactory results. Cube root scaling was applied to all linear dimensions, and the multiple regression analysis was carried out using the scaled variables.

Mellor obtained 171 sets of data from the literature. There were a few points he omitted from his analysis, these being data sets where the charge placement was above the bottom of the ice sheet. In the case of Van Der Kley's (1965) data, where repetitive tests had been carried out, but only average results reported, Mellor felt that the data had to be weighted in some manner. He weighted it by including a single data set "'n' times, where 'n' is the square root of the number of times the test was repeated". Mellor's regression equation had the form (1972):

$$Y = a + b_1X_1 + b_2X_2 + b_3X_1^2 + b_4X_1X_2 + b_5X_2^2 + b_6X_1^3 + b_7X_1^2X_2 + b_8X_1X_2^2 + b_9X_2^3 \quad \dots(7)$$

where: $Y = \text{scaled crater radius } (R/W^{1/3})$,
 $X_1 = \text{scaled placement depth } (d/W^{1/3})$,
 $X_2 = \text{scaled ice thickness } (t_i/W^{1/3})$,
 $a = \text{regression intercept, and}$
 $b_n = \text{regression coefficients.}$

Two independent regression analyses were conducted on the data, using separate regression programs developed at CRREL, which "gave similar results". Two of the terms of the equation, with coefficients b_1 and b_4 , were dropped from the final analysis, as they had shown little significance.

Mellor cited the results of his analysis as (1972):

"The standard error of estimate [of scaled crater radius] was 1.377 and the multiple correlation coefficient was 0.6945. The F-test value was 21.69 with 163 degrees of freedom and 7 parameters."

The results of this regression analysis were presented in graphical form as reproduced in Figures 6 and 7.

Mellor indicated that the curves should be used with caution, especially at the extremes of depth and ice thickness scales, presumably due to the lack of data in these ranges and the "ill-conditioning" of the entire data set. The figures, however, give a (1972):

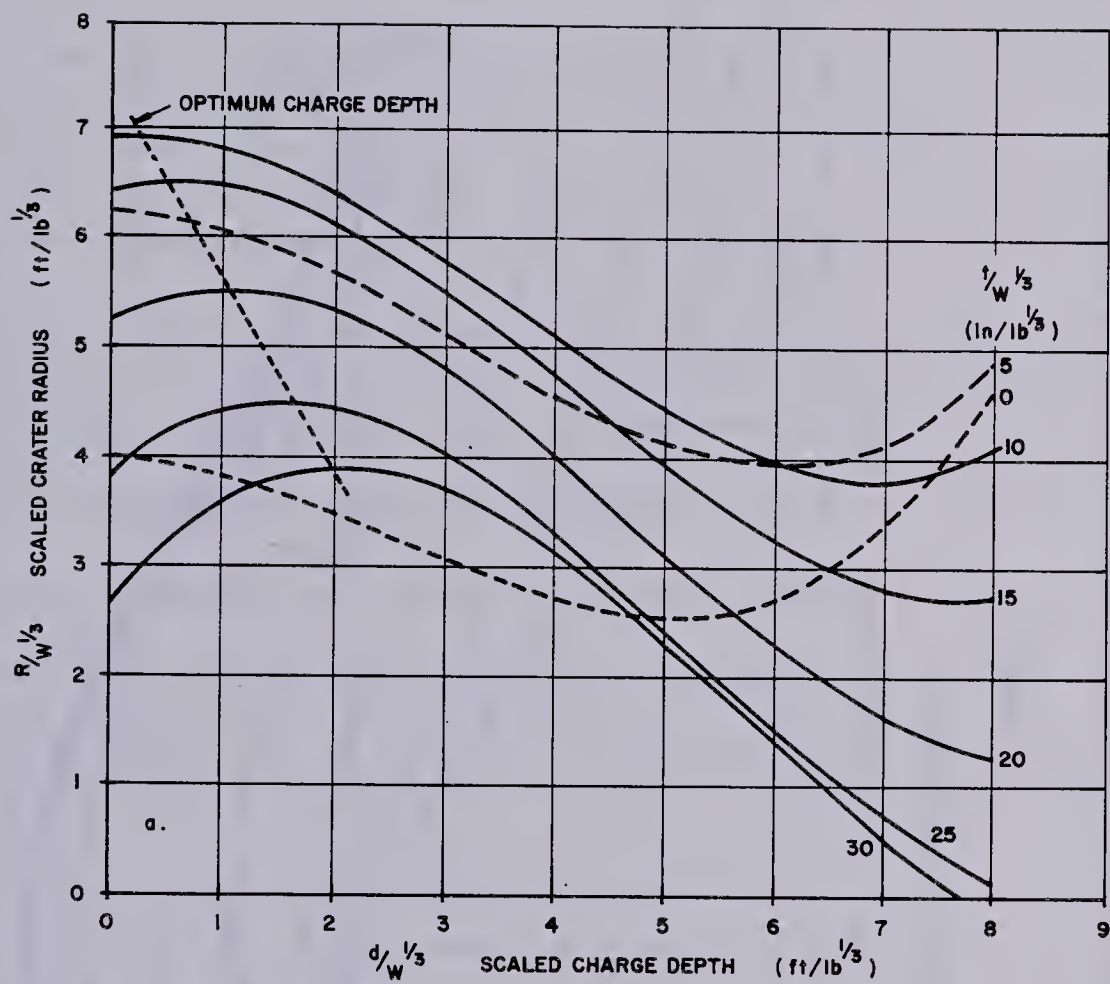
"...clear indication of optimum performance at a particular value of scaled ice thicknesses for given scaled depths, and ...the scaled optimum charge depth varies with scaled ice thickness."

Mellor suggested a rational procedure for designing optimum performance blasts in ice of specified thickness based on his curves. To obtain maximum crater radius the curves indicate that the scaled ice thickness "is about $10^{1/3}$ in/lb", and scaled optimum charge depth "is about $0.3^{1/3}$ ft/lb". Measuring a maximum scaled crater radius of $6.9^{1/3}$ ft/lb from Figure 7, the optimum ice thickness and scaled depths of placement were used to determine the following:

$$W = (t_i/10)^3 \quad \dots (8a)$$

$$d = 0.03(t_i) \quad \dots (8b)$$

$$\text{to give } R = 0.69(t_i) \quad \dots (8c)$$

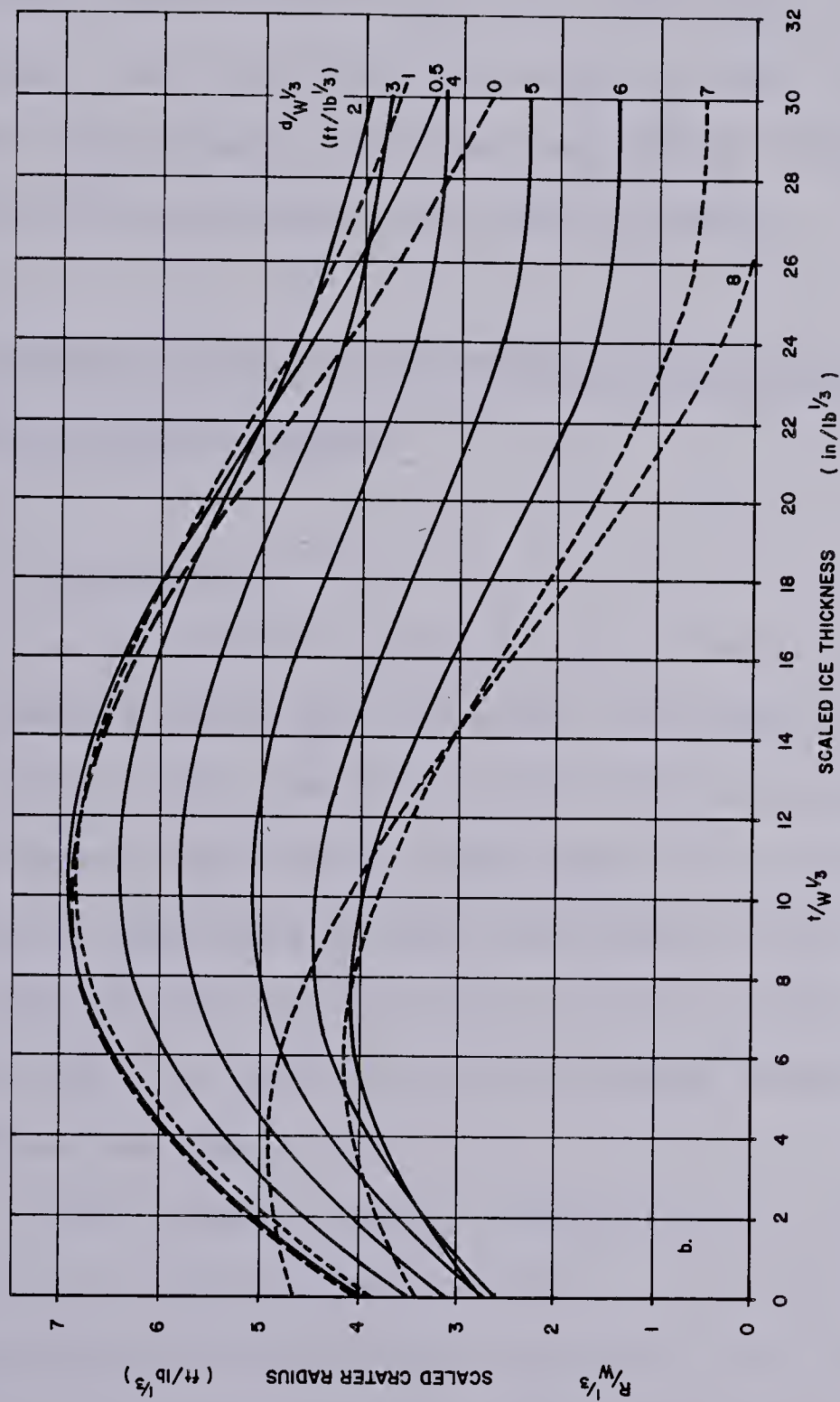


NOTE: CURVES ARE DERIVED FROM MULTIPLE REGRESSION ANALYSSIS.

FIGURE 6

SCALED RELATIONSHIP FOR BLASTING FLOATING ICE SHEETS

AFTER MELLOR (1972)



NOTE: CURVES ARE DERIVED FROM MULTIPLE REGRESSION ANALYSIS.

FIGURE 7

SCALED RELATIONSHIP FOR BLASTING FLOATING ICE SHEETS
AFTER MELLOR (1972)

where W is in pounds, d and R are in feet, and t_i is in inches. These are referred to herein as Mellor's preliminary ice demolition relationships.

Mellor's results are interesting in that although previous studies had either not considered the target (ice) thickness, or had vaguely alluded to some thickness-charge weight relationship, none had determined a dependence of the demolition effectiveness on ice thickness.

3.3 Reported Study of Penetrating Floating Ice Sheets with Shaped Charges

3.3.1 Introduction

As indicated in Chapter 1, in order to place explosive charges below the ice sheet, some form of hole must be made in the ice. These may be made mechanically (eg with power augers, chainsaws, hand augers or ice chisels) or with the use of explosive charges detonated on the surface of the ice. The charges may be either point charges calculated to breach the ice, or they can be shaped charges designed to penetrate the ice.

While shaped charge penetration of normal military demolition targets such as steel, concrete etc., is well documented in the military literature, the same cannot be said for the penetration of ice, either glacial or floating.

Before presenting the study carried out on shaped charge penetration of ice, a brief discussion of shaped

1. The first part of the document discusses the importance of maintaining accurate records of all transactions and activities. It emphasizes that proper record-keeping is essential for transparency and accountability, particularly in financial matters. The text suggests that organizations should implement robust systems to track income, expenses, and assets, ensuring that all data is up-to-date and easily accessible.

2. The second section focuses on the role of internal controls in preventing fraud and errors. It outlines various measures that can be put in place, such as segregation of duties, regular audits, and the use of standardized procedures. The document stresses that these controls are not just for compliance but are also vital for the long-term health and stability of the organization.

3. The third part of the document addresses the challenges of managing a large and diverse workforce. It discusses the importance of clear communication, effective leadership, and the ability to adapt to changing circumstances. The text provides practical advice on how to foster a positive work environment, encourage innovation, and ensure that all team members are aligned with the organization's goals.

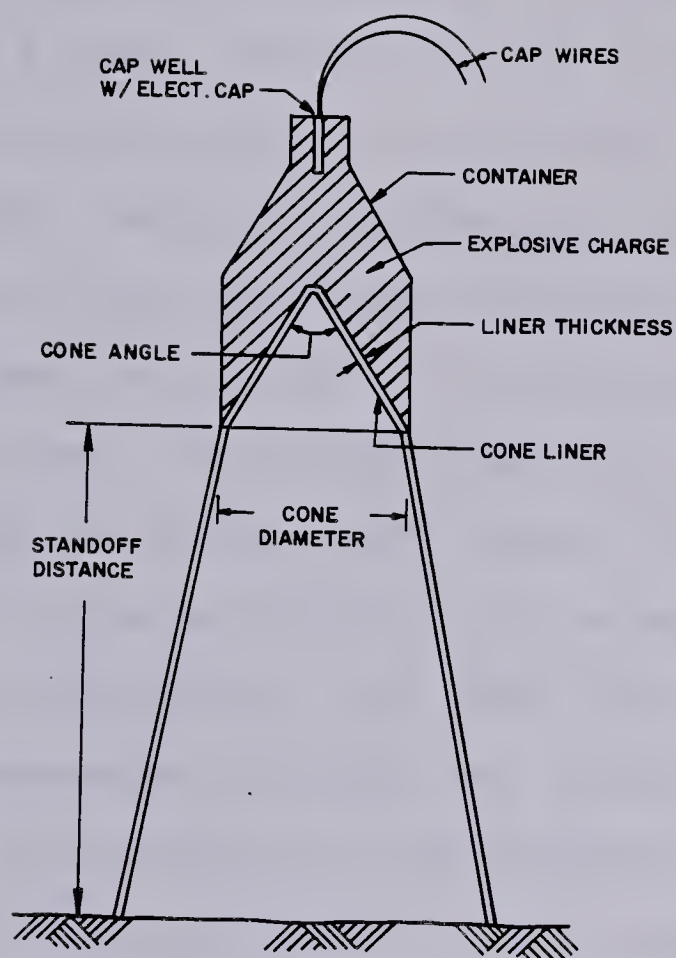
4. The final section of the document discusses the importance of staying current with industry trends and regulations. It highlights the need for continuous learning and professional development for all employees. The text also touches on the importance of maintaining strong relationships with external stakeholders, including customers, suppliers, and regulatory bodies.

charges is in order.

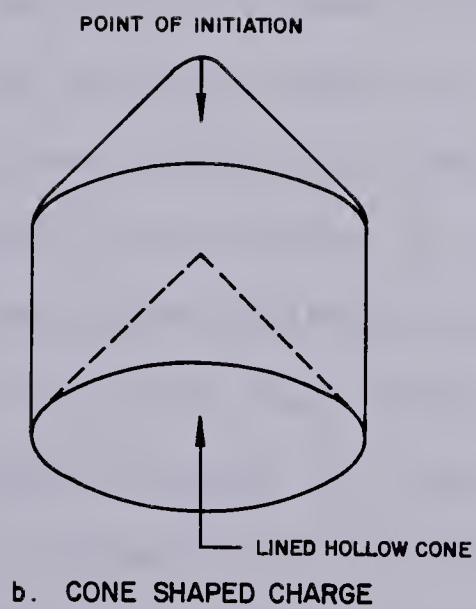
3.3.2 Description and Action of Shaped Charges

A shaped charge is a pre-packaged charge designed to concentrate its explosive effect at a point to obtain penetration of the target, or to concentrate its effect along a line to cut the target cleanly. A cutaway view of a shaped charge, the U.S. M3 (40 lb), is shown in Figure 8a. The penetrating (or cone shaped) charge is circular in plan, while the cutting (or wedge shaped) charge is an elongation of the section, as shown in Figure 8b and 8c respectively. As can be seen, there is a recession or 'hollow' at the bottom of the charges; for this reason they are sometimes referred to as 'hollow charges'. Discussion of these charges will be restricted to the circular or penetrating charge.

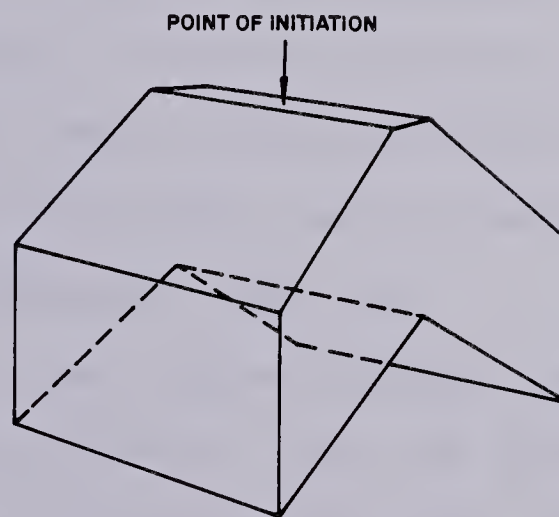
The charge hollow is conical. The liner of the cone is usually made of some different material than the container of the explosive. When the charge is detonated, the recessed cone collapses downward from the apex, and the heat of the explosion causes the cone material to form into two distinct parts that move toward the target, both concentrating at a focal point defined by the angle of the cone before firing. The line from the apex of the cone to this focal point is called the 'axis' of the charge. Part of the cone material combines with the gaseous products of detonation from the charge's explosive filler to form a gas jet. The remainder of the material forms a molten carrot-shaped mass



a. SHAPED CHARGE DEFINITIONS



b. CONE SHAPED CHARGE



c. WEDGE SHAPED CHARGE

FIGURE 8
SHAPED CHARGES

called the 'slug'. The jet travels at a much higher velocity, 1829 to 9144 m sec⁻¹ (6000 to 30,000 ft/sec) than the slug, which travels between 457 to 914 m sec⁻¹ (1500 to 3000 ft/sec) (Cook, 1958). When the superheated jet concentrates at the focal point of the charge and impinges upon a target, it "produces pressures greatly in excess of the yield strength of the target, forcing the [material] to flow plastically out of the way of the jet" (Benert, 1957; Riddoch, 1979), and causes the penetration of the target.

Experiment and analysis have shown that the depth of penetration is independent of both the velocity of the jet and the velocity of detonation of the explosive filler, but is proportional to the length of the jet. It has been determined that the leading end of the jet travels faster than the trailing end, causing the jet to lengthen as it travels. Thus the depth of penetration increases with 'standoff' , which is a height above the target at which the charge is placed (See Figure 8a). The upper limit to this increase occurs when the standoff is large enough that the jet becomes elongated to the point where it begins to break up.

A typical hole formed by cone shaped charges fired into frozen ground is shown in Figure 9. All the points shown in Figure 9 are of interest to this study: the total penetration depth; the diameter of the penetration hole for placement of charges through it; as well as the crater depth, if the ice is thinner than this depth; and the crater diameter for venting effects of the gases from the main

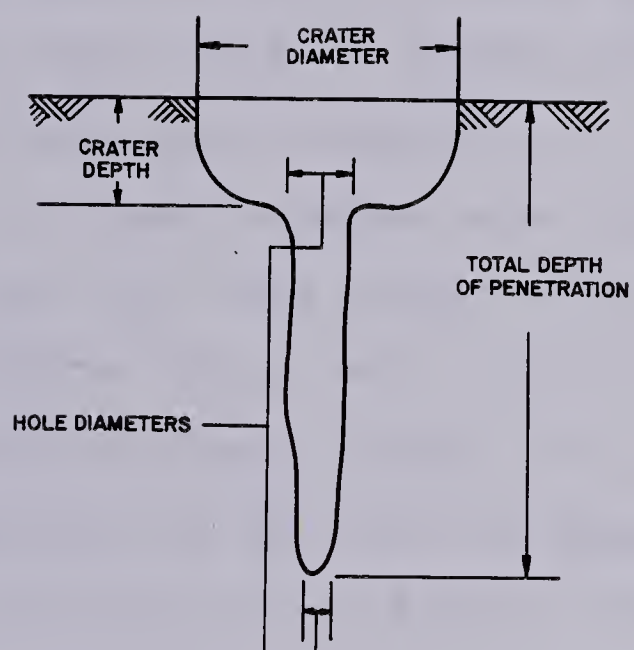


FIGURE 9

CROSS SECTION OF A TYPICAL HOLE FROM A SHAPED CHARGE

charge.

Only one study of the penetration of shaped charges into ice and frozen ground was found in the literature.

3.3.3 Benert (1957)

Benert (1957), published the results of experiments on the penetration of frozen ground by shaped charges, conducted at Fort Churchill, Manitoba, during the early spring of 1955 and 1956. Eight tests of shaped charge penetration of a floating ice sheet were included.

In all, six shaped charges were tested in frozen ground, however, only four were tested on ice, these being: U.S. Army Shaped Charge M2 and M2A3, a 5 lb "experimental" charge, and a small "Jet Tapper Charge". The charge characteristics are summarized in Table B-1 of Appendix B.

Sectional views of all of the six charges used are shown in Figure 10.

Six charges were fired above fresh water ice (Stygge Lake), and the other two were fired above the "brackish water" ice of the Churchill River estuary. The holes formed had similar characteristics to those shown in Figure 9. The results of the detonations are shown in Table A-14 of Appendix A.

On the basis of these tests Benert concluded that ice could be penetrated by shaped charges to a greater depth than frozen ground (his data for frozen ground penetration have not been included). By measurement and inspection,

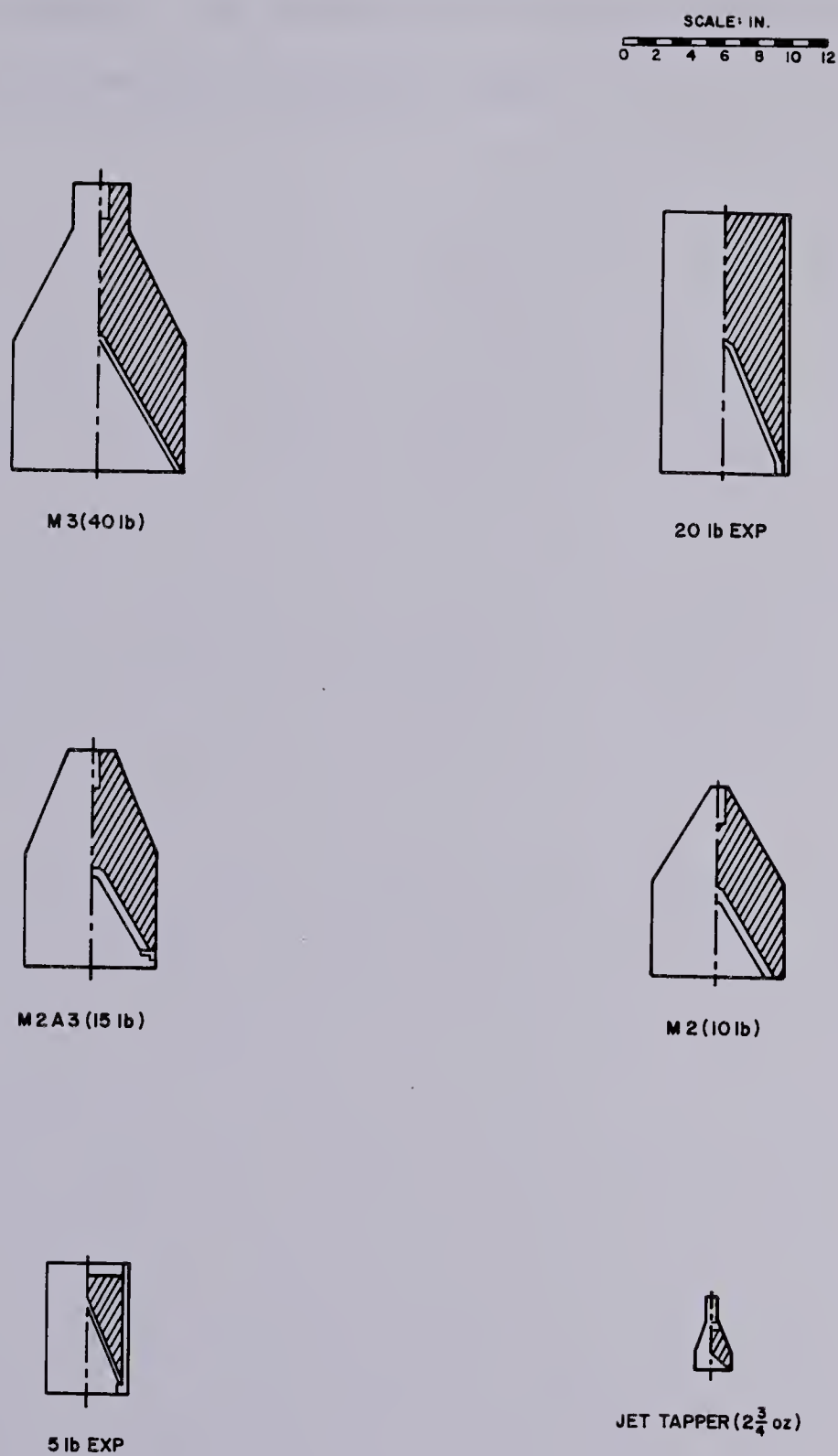


FIGURE 10
HALF SECTIONS OF SHAPED CHARGES TESTED BY BENERT (1957)

Benert concluded that there was no discernable difference between the craters and penetration holes formed in fresh water ice and "brackish" (saline) ice.

CHAPTER 4

SOME ASPECTS OF EXPLOSIVES

4.1 General

The subject of explosives is vast, incorporating the fields of chemistry, thermodynamics and mechanics. In the review of the literature in the previous chapter there were a wide variety of explosives used in the experiments. Certain aspects of explosives and explosive technology utilized in the analysis for this thesis are discussed in this Chapter.

Since the end of the Second World War, the available literature on explosives has been one of two types. The first is the field of general research and development, for which the published material is scientifically oriented. The second is the 'technical' publications and handbooks developed and published by explosives manufacturers for civil applications of the technology. While this literature is more readily available, the information contained therein tends not to be as scientific as the first source. As a result, there is a disparity of information on certain aspects of explosives which are required to carry out any form of comparative analysis.

4.2 Definition and Types of Explosives

In a general sense, an explosive is any substance or device which will produce, upon release of its potential energy, a sudden outburst of gas and other detonation products, thereby exerting high pressures on its surroundings (Cook, 1958). Under this general definition, Cook identified three fundamental types of explosives:

- a. mechanical,
- b. chemical, and
- c. atomic.

Of these the present concern is with chemical explosives. As was noted above, quite a wide variety of these explosives were used in the experiments reported herein. In the analyses reviewed in Chapter 3, no attempt seems to have been made to consider the properties of the explosives used. For example, Mellor's (1972) analysis, which was the most comprehensive treatment of the reported data which could be found, used the reported weight of the explosive for scaling the data, without attempting to 'normalize' the data to some standard explosive (Mellor, Personal Communication, 1980).

Chemical explosives are so common that the term 'explosives' has come to be synonymous. This will be accepted herein. The following definition of chemical explosives is a composite of definitions suggested by Cook (1958), Canadian

Industries Limited (CIL) (1968) and Meyer (1977):

An explosive is a solid, liquid or gaseous material, which, either alone or combined with others, forms a metastable compound. Because of this metastable state, when properly initiated, the compound undergoes a rapid and violent chemical decomposition reaction without participation of external reactants. The decomposition produces large volumes of gases and other minor detonation products at high temperature, which cause high pressures to be exerted on any surrounding medium.

Such explosives can be divided into two types (Cook, 1958):

- a. detonating or 'high' explosives, and
- b. deflagrating or 'low' explosives.

The division between the two types is based on the detonation velocity (propagation rate of the chemical decomposition front within the explosive mass). If this is less than the velocity of sound, it is a 'low' explosive; if it is higher, it is a 'high' explosive (Meyer, 1977). Figure 11 illustrates the distinction between low and high explosives in terms of the rate of chemical reaction.

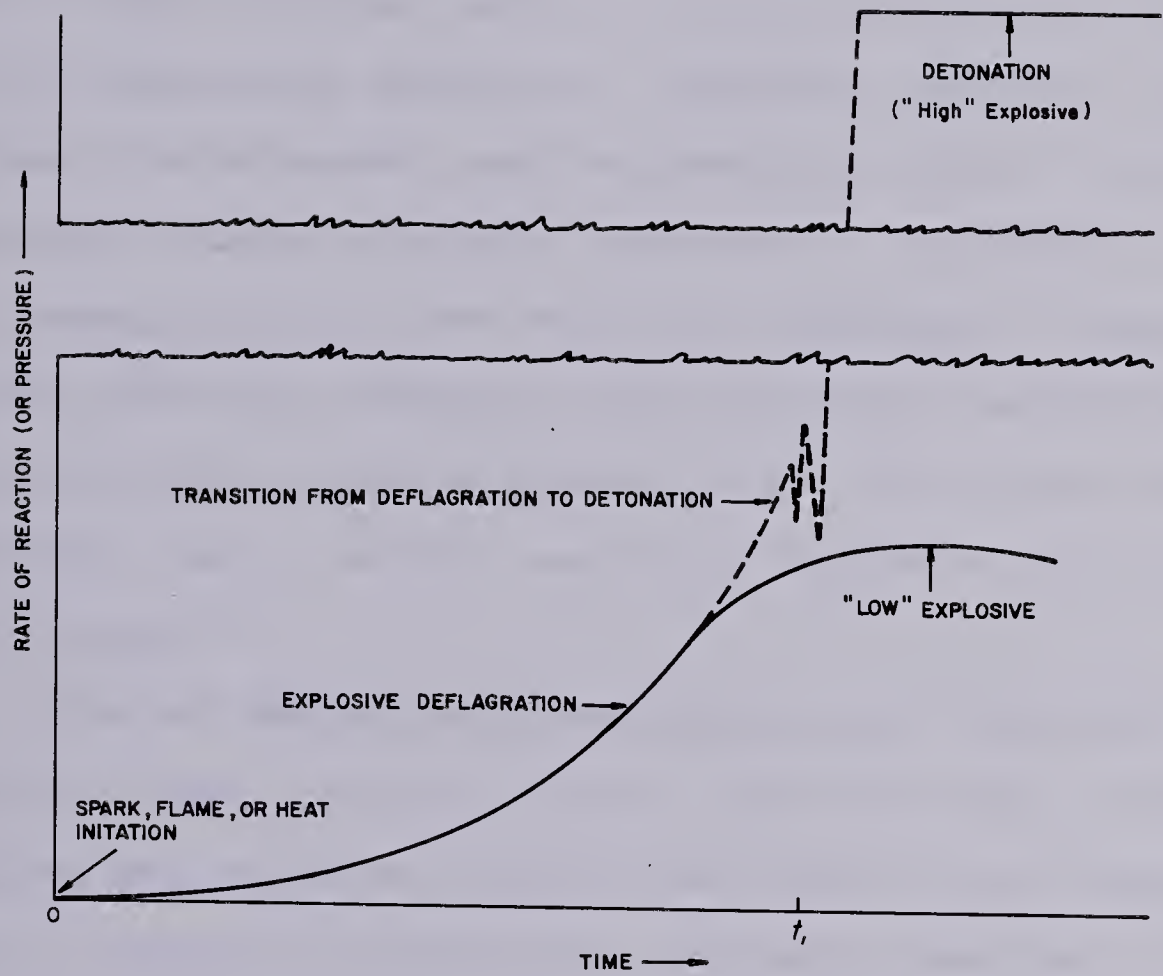


FIGURE II
EXPLOSIVE DEFLAGRATION VERSUS DETONATION AND TRANSITION
FROM DEFLAGRATION TO DETONATION
AFTER COOK (1958)

20

Date		Description	
1890	Jan 1	Balance	100.00
1890	Feb 1	Received	50.00
1890	Mar 1	Received	25.00
1890	Apr 1	Received	10.00
1890	May 1	Received	5.00
1890	Jun 1	Received	2.50
1890	Jul 1	Received	1.25
1890	Aug 1	Received	.62
1890	Sep 1	Received	.31
1890	Oct 1	Received	.16
1890	Nov 1	Received	.08
1890	Dec 1	Received	.04
1890	Total		200.00

By the Cashier
J. H. Smith

Detonating explosives can be further sub-categorized into 'primary' and 'secondary' explosives. The distinction between these two lies in the method of initiation of the detonation reaction. Primary explosives detonate by simple ignition. This simple ignition can be provided by a spark, flame, impact or other heat source of appropriate magnitude for the particular explosive. Secondary explosives require the use of a detonator, and frequently a 'booster' charge. A detonator contains a primary explosive to initiate the chemical decomposition of the secondary explosive. A booster is a more sensitive secondary explosive which reinforces the detonation wave of the detonator to deliver a more powerful detonation wave to the secondary explosive main charge (Cook, 1958).

Low or deflagrating explosives are initiated by an igniter, flame, spark or similar ignition agent. Rates of reaction are seldom more than a few tenths of one percent of that in detonating explosives, and peak pressures attained are seldom more than a few percent of that resulting from detonation. Low explosives react quickly enough for their energy to be fully utilized when the reaction is adequately confined by some external means (Cook, 1958).

Because of the high sensitivity of primary explosives their major use is as detonators. Secondary explosives form the bulk of high explosives used by the military and private industry. Tables B-2 and B-3, of Appendix B, indicate the divisions of the explosives family, and some of the more

common explosives in each group.

4.3 Strengths of Explosives

In spite of the fact that explosives are often compared to one another in terms of their performance for a given task, the most ambiguous and misused term in the explosives field is 'strength'. The comparative strength of explosives have been reported in a variety of ways.

According to Canadian Industries Limited (CIL), the term strength refers to the energy content of the explosive, which, in turn, is a measure of its ability to do work (CIL, 1968). They note, however, that even though two explosives may be equivalent in energy rating, they may not produce the same blasting action. This is attributed to the fact that properties other than strength have a bearing on overall performance. Thus there is a difference between explosive strength and its ultimate performance.

Meyer (1977) agrees with this observation, stating:

"The performance potential of an explosive can not be described by a single parameter. It is determined by the amount of gas liberated per unit weight [gas effectiveness], the energy involved in the process and by the propagation rate [detonation velocity] of the explosive"

Thus the desirable 'strength' properties of an explosive are highly dependant upon the task. If an explosive is to be set in a borehole, as in underground mining opera-

The first part of the course will focus on the ancient Greek philosophers, starting with the Pre-Socratics and moving through Plato and Aristotle. We will then turn to the medieval period, covering the work of Augustine, Aquinas, and others. The modern period will be covered in the second half of the course, with a focus on Descartes, Locke, and Kant. The course will conclude with a look at contemporary philosophy, including the work of Wittgenstein and Heidegger. Throughout the course, we will explore the central themes of philosophy, such as the nature of reality, the self, and the good life. We will also examine the methods of philosophy, including logical analysis and phenomenology. The course is designed to provide a comprehensive introduction to the history of philosophy, and to develop the critical thinking skills necessary for philosophical inquiry.



tions, the "relevant parameter is strength" (Meyer, 1977), with the important features being high gas yield and heat of explosion. When a strong disintegration (shattering) effect is required in the near vicinity, the most important parameters are the detonation rate and explosive density (Meyer, 1977). This shattering effect of explosives is called 'brisance', for which a brisance "value" is determined as the product of the loading density, specific energy of the explosive and detonation rate (Meyer, 1977). Two of these properties, density and detonation rate, can be determined in a laboratory. Specific energy, however, is calculated from the thermodynamics of the chemical decomposition reaction.

To compare performance of different explosives a number of standard tests have been developed. These include the ballistic mortar; lead (Trauzel) block; jumping mortar; vessel mortar; large lead block; crater and aquarium tests. The tests, however, give relative rather than absolute performance data, the results for a given explosive being compared to that of a chosen, standard explosive.

Of these tests, only the ballistic mortar and lead block tests will be described herein, as an indication of the comparative nature of all of the tests. The description of the remainder may be found elsewhere (Cook, 1958; Meyer, 1977).

The ballistic mortar consists of a heavy pendulum fitted with a mortar at the free end. The mortar is provided

The first of these is the fact that the
the second is the fact that the
the third is the fact that the
the fourth is the fact that the
the fifth is the fact that the
the sixth is the fact that the
the seventh is the fact that the
the eighth is the fact that the
the ninth is the fact that the
the tenth is the fact that the
the eleventh is the fact that the
the twelfth is the fact that the
the thirteenth is the fact that the
the fourteenth is the fact that the
the fifteenth is the fact that the
the sixteenth is the fact that the
the seventeenth is the fact that the
the eighteenth is the fact that the
the nineteenth is the fact that the
the twentieth is the fact that the
the twenty-first is the fact that the
the twenty-second is the fact that the
the twenty-third is the fact that the
the twenty-fourth is the fact that the
the twenty-fifth is the fact that the
the twenty-sixth is the fact that the
the twenty-seventh is the fact that the
the twenty-eighth is the fact that the
the twenty-ninth is the fact that the
the thirtieth is the fact that the
the thirty-first is the fact that the
the thirty-second is the fact that the
the thirty-third is the fact that the
the thirty-fourth is the fact that the
the thirty-fifth is the fact that the
the thirty-sixth is the fact that the
the thirty-seventh is the fact that the
the thirty-eighth is the fact that the
the thirty-ninth is the fact that the
the fortieth is the fact that the
the forty-first is the fact that the
the forty-second is the fact that the
the forty-third is the fact that the
the forty-fourth is the fact that the
the forty-fifth is the fact that the
the forty-sixth is the fact that the
the forty-seventh is the fact that the
the forty-eighth is the fact that the
the forty-ninth is the fact that the
the fiftieth is the fact that the
the fifty-first is the fact that the
the fifty-second is the fact that the
the fifty-third is the fact that the
the fifty-fourth is the fact that the
the fifty-fifth is the fact that the
the fifty-sixth is the fact that the
the fifty-seventh is the fact that the
the fifty-eighth is the fact that the
the fifty-ninth is the fact that the
the sixtieth is the fact that the
the sixty-first is the fact that the
the sixty-second is the fact that the
the sixty-third is the fact that the
the sixty-fourth is the fact that the
the sixty-fifth is the fact that the
the sixty-sixth is the fact that the
the sixty-seventh is the fact that the
the sixty-eighth is the fact that the
the sixty-ninth is the fact that the
the seventieth is the fact that the
the seventy-first is the fact that the
the seventy-second is the fact that the
the seventy-third is the fact that the
the seventy-fourth is the fact that the
the seventy-fifth is the fact that the
the seventy-sixth is the fact that the
the seventy-seventh is the fact that the
the seventy-eighth is the fact that the
the seventy-ninth is the fact that the
the eightieth is the fact that the
the eighty-first is the fact that the
the eighty-second is the fact that the
the eighty-third is the fact that the
the eighty-fourth is the fact that the
the eighty-fifth is the fact that the
the eighty-sixth is the fact that the
the eighty-seventh is the fact that the
the eighty-eighth is the fact that the
the eighty-ninth is the fact that the
the ninetieth is the fact that the
the ninety-first is the fact that the
the ninety-second is the fact that the
the ninety-third is the fact that the
the ninety-fourth is the fact that the
the ninety-fifth is the fact that the
the ninety-sixth is the fact that the
the ninety-seventh is the fact that the
the ninety-eighth is the fact that the
the ninety-ninth is the fact that the
the hundredth is the fact that the

with a borehole, into which a heavy (approximately 16 kg) solid steel projectile is snugly fitted. A few grams, (usually 10) of explosive are fired in the chamber. The projectile is driven out of the mortar by the gases produced by the detonation, and the recoil of the mortar is a measure of the energy of the projectile, the magnitude being determined from the deflection of the pendulum. The deflection is measured as a percent of that produced by detonating 10 grams of blasting gelatin (Meyer, 1977), or 10 grams of TNT (Cook, 1958). Figure 12 shows the pertinent aspects of the ballistic mortar.

The ballistic mortar is apparently a reliable instrument with respect to reproducibility of test results (Cook, 1958).

The Trauzl lead block test, named after its inventor, involves detonating a 10 gram sample of explosive in a cavity within a massive soft-lead cylinder. The detonation excavates the cavity to a larger size than existed originally. The volume of the cavity is determined by filling it with water, after which the initial cavity volume is deducted to yield the explosively-excavated volume. The results of this test are reported as the number of cubic centimetres excavated by the 10 gram sample: $\text{cm}^3/10 \text{ gm}$ (Meyer, 1977).

Although the first international standardization of this test occurred in 1904, the test is no longer standard. According to Meyer:



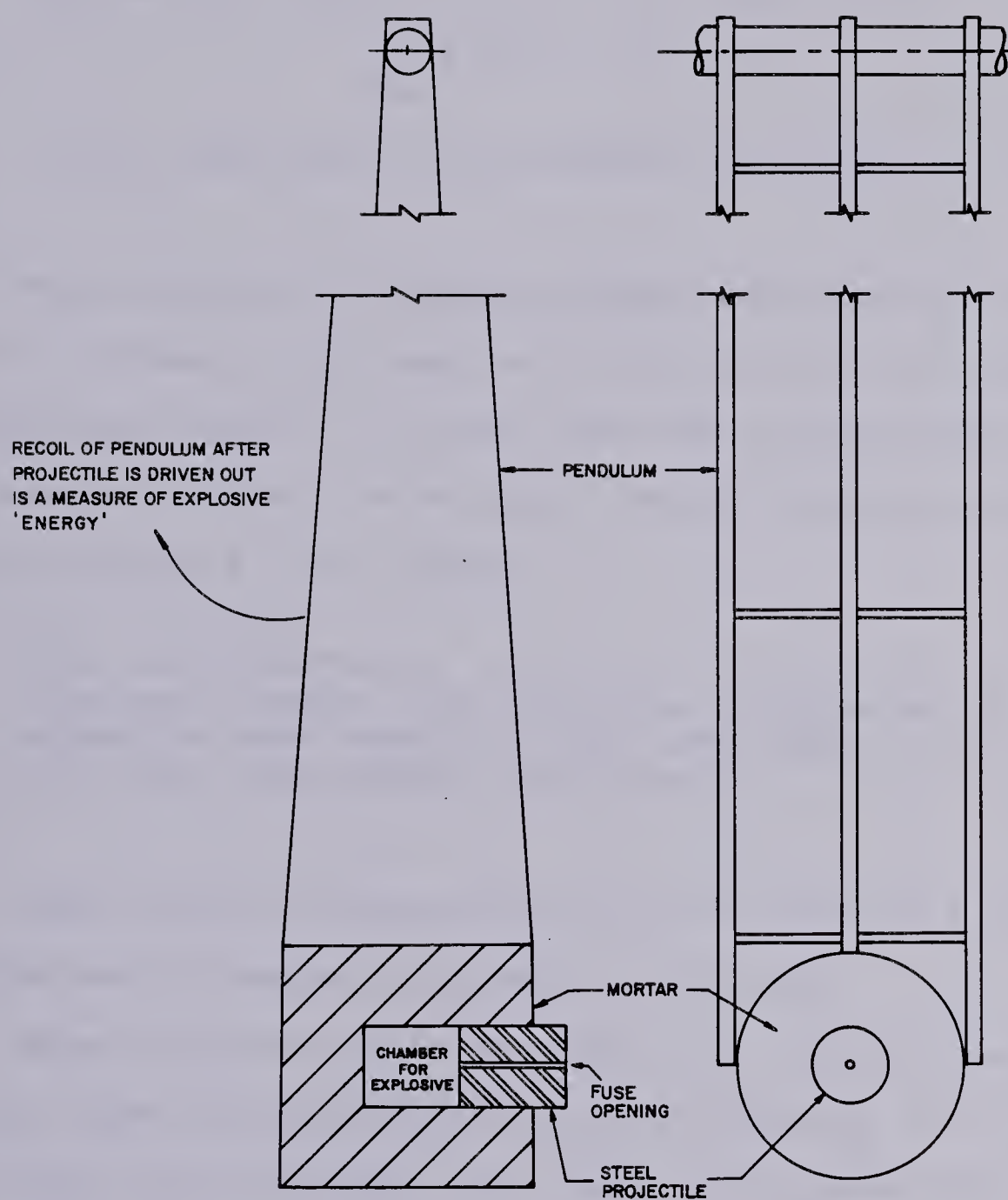


FIGURE 12

ASPECTS OF THE BALLISTIC MORTAR

SKETCH FROM PHOTOGRAPH IN CIL (1968)

"In France the lead block performance value is given by the 'coefficient d'utilisation pratique (c.u.p.)': if m_x is the mass of the tested explosive, which gives exactly the same excavation as 15 g [gm] of Picric Acid, the ratio:

$$\frac{15}{m_x} \times 100 = \% \text{ c.u.p.} \quad \dots (9)$$

is the coefficient d'utilisation pratique."

Meyer goes on to discuss another modification recommended in Germany which uses an 11 millilitre (ml) sample, the excavation results of which are then recalculated to a 10 gm sample. Further, he reports a "recent" European standardization using a 10 ml sample:

"The reported value refers to a mixture of Nitropenta [PETN] with potassium chloride which gives the same result as the test sample under identical experimental conditions."

Meyer reports lead block excavation data for a number of explosives in the original form ($\text{cm}^3/10 \text{ gm}$).

Meyer indicates that for both the ballistic mortar and lead block tests the explosive is detonated in a confined space, such that for "all practical purposes" the parameter measured is the "work of decomposition of an explosive in a borehole", and further:

"The disadvantage of both [ballistic mortar and lead block] methods consists in the fact that the quantity of the sample used in the tests (exactly or approximately 10g) is quite small, and for this reason accurate comparative data can be obtained only with more sensitive explosives; less sensitive materials require a longer detonation development distance, within which a



considerable portion of the 10g sample does not fully react."

This leads to the consideration of the various comparative descriptors used in the technical literature. Besides the lead block excavation values mentioned earlier, these include: Grade Strength, Weight Strength, Bulk Strength, Relative Weight and Bulk Strengths, an 'Effectiveness as an External Charge', Heats of Detonation and Specific Energy. These will be described individually and briefly.

4.3.1 Grade Strength

Grade strength is given for nitroglycerine (or straight) dynamites. It is defined as the percentage by weight of nitroglycerine contained in the particular dynamite. Thus a 60% straight dynamite contains 60% nitroglycerine by weight (CIL, 1968).

As often pointed out in the literature, the grade strength number is not a linear indicator of the performance of the explosive, because nitroglycerine is not the only energy producing ingredient in the composition of the dynamite. Dynamites usually contain either ungelatinized nitroglycerine or gelatinized nitroglycerine, in different proportions, as well as sodium nitrate and wood or vegetable meal (Meyer, 1977). More recently, nitroglycerine has been replaced with ammonium nitrate-based ammongelites, containing nitroglycol, to improve the handling safety characteris-

The first of these is the question of the origin of the human race. It is generally admitted that the human race is of African origin, and that it has spread from Africa to all other parts of the world. The second question is the question of the development of the human race. It is generally admitted that the human race has developed from a lower to a higher state, and that it has done so in a regular and orderly manner. The third question is the question of the influence of the environment on the human race. It is generally admitted that the environment has a great influence on the human race, and that it has done so in a regular and orderly manner.

The fourth question is the question of the influence of the human race on the environment. It is generally admitted that the human race has a great influence on the environment, and that it has done so in a regular and orderly manner. The fifth question is the question of the future of the human race. It is generally admitted that the human race has a bright future, and that it will continue to develop and progress in a regular and orderly manner.

The sixth question is the question of the relationship between the human race and the other races of the world. It is generally admitted that the human race is related to the other races of the world, and that it has done so in a regular and orderly manner. The seventh question is the question of the relationship between the human race and the other animals of the world. It is generally admitted that the human race is related to the other animals of the world, and that it has done so in a regular and orderly manner.

tics. These fuel-oxidizer ingredients also contribute to the gas and heat generation of the explosive reaction. Thus if the percentage of nitroglycerine or nitroglycol is changed, the percentage of other ingredients must change correspondingly. Because of the addition to the net reaction by the other ingredients, the nonlinearity of the explosive's performance, with respect to the grade strength number, results. For example, a 60% straight dynamite is only "about" one and one-third times as strong as a 30% grade strength (CIL, 1968).

4.3.2 Weight strength

The weight strength of an explosive is determined using the ballistic mortar test described earlier. The deflection of the mortar caused by detonation of a 10 gram sample of Blasting Gelatin (92 - 94% nitroglycerine, gelatinized with 8 - 6% soluble guncotton) is arbitrarily taken as a weight strength of 100. The percent of this deflection caused by a 10 gram sample of the explosive being tested is its weight strength (Meyer, 1977).

Hemphill (1981) points out:

"In non-straight-nitroglycerine explosives the percentage rating is a comparison to an equal weight of nitroglycerine dynamite. That is, 40% ammonia dynamite can produce the same energy as 40% straight [nitroglycerine] dynamite."

CIL (1968) agrees with this observation, with the ex-

1. The first part of the document discusses the importance of maintaining accurate records of all transactions. It emphasizes that proper record-keeping is essential for the transparency and accountability of the organization. The text outlines the various methods used to collect and analyze data, ensuring that the information is reliable and up-to-date.

2. The second part of the document focuses on the implementation of the proposed changes. It details the steps involved in the process, from the initial planning stage to the final execution. The document highlights the challenges faced during the implementation and provides solutions to overcome them. It also discusses the role of each department in ensuring the successful completion of the project.

3. The third part of the document provides a summary of the findings and conclusions. It reiterates the key points discussed in the previous sections and emphasizes the importance of continuous monitoring and evaluation. The document concludes by stating that the proposed changes are expected to improve the overall efficiency and effectiveness of the organization.

4. The fourth part of the document contains a list of references and a bibliography. It includes citations from various sources, including books, articles, and reports. The references are used to support the arguments made in the document and to provide a basis for further research. The bibliography is organized alphabetically by the author's name.

5. The fifth part of the document is a conclusion. It summarizes the main findings of the study and provides a final statement on the importance of the research. The conclusion states that the proposed changes are feasible and will lead to significant improvements in the organization's performance. It also expresses the hope that the findings of the study will be useful to other organizations facing similar challenges.

6. The sixth part of the document is an appendix. It contains additional information that is not included in the main body of the document. This includes a list of abbreviations, a glossary of terms, and a list of figures and tables. The appendix is organized into sections corresponding to the different types of information it contains.

7. The seventh part of the document is a list of figures and tables. It includes a list of all the figures and tables used in the document, along with a brief description of each. The list is organized by the order in which the figures and tables appear in the document. This section is useful for readers who want to locate specific information quickly and easily.

8. The eighth part of the document is a list of figures and tables. It includes a list of all the figures and tables used in the document, along with a brief description of each. The list is organized by the order in which the figures and tables appear in the document. This section is useful for readers who want to locate specific information quickly and easily.

9. The ninth part of the document is a list of figures and tables. It includes a list of all the figures and tables used in the document, along with a brief description of each. The list is organized by the order in which the figures and tables appear in the document. This section is useful for readers who want to locate specific information quickly and easily.

10. The tenth part of the document is a list of figures and tables. It includes a list of all the figures and tables used in the document, along with a brief description of each. The list is organized by the order in which the figures and tables appear in the document. This section is useful for readers who want to locate specific information quickly and easily.

ception that they indicate the ammonia dynamite will only develop:

"...about the same amount of energy [as the straight dynamite] even though it [the ammonia dynamite] contains an appreciable lower percentage of nitroglycerine. The percent strength markings for [grades of non-straight dynamite] are on the basis of weight strength..." (writer's emphasis)

As the non-straight dynamites are graded by weight strength, which may, or may not (depending on the reference) produce the same energy as an explosive with the equivalent grade strength, no direct comparison between weight strength and grade strength can be made.

4.3.3 Bulk Strength

Commercial explosives are sometimes compared on a bulk or volume strength basis. In the literature this refers to the strength per cartridge or per unit volume of the explosive (CIL, 1968). Presumably the strength comparison is based on one of the standard tests such as the ballistic mortar, though the reference does not discuss this.

In explosives which are designated by bulk strength, the strength or energy content of a given size of cartridge of any particular grade is compared with the bulk strength of the same cartridge size of straight dynamite. This method is also employed for 'blasting agents' (CIL, 1968). The grade strength of the straight dynamite used in the compar-



THE JOURNAL OF THE AMERICAN MEDICAL ASSOCIATION
PUBLISHED WEEKLY
CHICAGO, ILL., MAY 1, 1919
VOLUME 21, NO. 19

CONTENTS
ORIGINAL ARTICLES
The Medical Profession and the Public Health
The Medical Profession and the Public Health
The Medical Profession and the Public Health
The Medical Profession and the Public Health

DEPARTMENTS
The Medical Profession and the Public Health
The Medical Profession and the Public Health
The Medical Profession and the Public Health
The Medical Profession and the Public Health

ison is not mentioned in the reference, and, as discussed, the energy produced by various grade strengths of dynamite varies with the nitroglycerine content. Thus no comparison can be made between grade and bulk strengths.

4.3.4 Relative Weight and Bulk Strengths

In the previous discussion of weight and bulk strengths, it was shown that the resulting strength values are, in reality, 'relative' strengths, as they are compared to either blasting gelatin or TNT, in the case of weight strength, or to some grade strength of dynamite in the case of bulk strength. Meyer (1977), in fact refers to the weight strength as "relative" weight strength.

The attempt to define "relative" strength comparisons is confused because at least one manufacturer, CIL (1980), presents entirely different 'relative' weight strength (RWS) and 'relative' bulk strength (RBS). These are "related to AN/FO [ammonium nitrate and fuel oil, usually ANFO] which has an assigned RWS and RBS value of 100" (CIL, 1980). Again the method of comparison is presumably from a standard test such as the ballistic mortar, except that ANFO is used instead of the two previously quoted explosives as the base explosive. The use of ANFO as the base for CIL's reported RWS and RBS precludes a direct comparison to the weight and bulk strengths discussed earlier, as the datum for comparison is different in each case.



4.3.5 Effectiveness as an External Charge

Elsewhere in the literature concerning the use of explosives for clearing ice (Bolsenga, 1968), a factor called the "relative effectiveness as an external charge" is cited. This term is attributed to the U.S. Department of the Army.

This factor is given for a number of explosives used in the ice blasting experiments that Bolsenga summarized. The comparison is the effectiveness of the particular explosive as an external charge, related to the effectiveness of TNT as an external charge. The term 'external charge' implies the charge is an unconfined breaching charge, this being the manner that explosives are generally deployed in military demolition activities, therefore the comparison is based on brisance, or something similar, rather than 'strength' as discussed herein. The amount of a particular explosive required for a demolition task, as an amount of TNT required, is simply determined from the ratio of the effectiveness of each explosive type.

A summary of the 'effectiveness as an external charge' values for various explosives is reproduced from the U.S. Army Field Manual FM 5-34, 1969, (Unclassified), in Table B-4 of Appendix B. The values quoted by Bolsenga (1968) were taken from an earlier version of this table.

4.3.6 Heats of Detonation

A further means of comparing explosives was used by Kurtz et.al. (1966). In their study of relative ice crater-

ing effectiveness of three explosives; C-4, ANFO and TNT, they used the "approximate experimental heats of detonation" of the explosives as the basis of comparison. These were given, along with that of Nitromethane (Kurtz et.al., 1966) as:

Explosive	Experimental Heat of Detonation (kcal/gm)
Composition C-4	1.20
ANFO	0.94
TNT	1.10
Nitromethane	1.18

Note that the heats of detonation given by Meyer (1977) for TNT (1.21 kcal/gm) and Nitromethane (1.08 kcal/gm) are close to the values given above.

The equivalent weights of explosive are determined from the ratio of the heats of detonation.

4.3.7 Specific Energy

A number of methods for the comparison of explosive effectiveness have been discussed thus far. However, all of these require comparison to some standard explosive, and none have been determined for all explosives. As well, none of the preceeding methods can be used in a direct comparison to a strength given by another method. Because the effectiveness of each explosive depends on several parameters that can vary from one situation to another, and the blasting action is not necessarily synonymous with strength, these single parameter effectiveness measures are of little value



for research purposes. For this purpose, a much more suitable parameter has been described by Meyer (1977):

"When we imagine the reaction of an explosion to proceed without volume expansion and without heat evolution, it is possible to calculate a theoretical thermodynamic value of the pressure [of the gases occupying the original volume of the explosive before detonation], which is different from the shock wave pressure; if this [the compressed gas] pressure is now multiplied by the volume of the [original] explosive, we obtain an energy value, the specific energy."

and further:

"As far as the strength of propellants and explosives is concerned, the most relevant thermodynamically calculable parameter is the specific energy. This is the amount of energy which is released when the gases in the body of the explosive (which are imagined to be compressed in their initial state) are allowed to expand at the explosion temperature while performing useful work. In order to illustrate the working performance obtainable from explosive materials, this magnitude is conventionally reported in metre-tons per kilogram or in Joules [per kilogram]."

The specific energy, according to Meyer, is therefore calculated from the general equation of state for gases:

$$f = PV = nRT \quad \dots (10)$$

where: f = specific energy,

P = pressure of gases in compressed state,

V = Volume of gases in compressed state,



n = number of moles of gases generated per
unit mass of explosive,

R = Ideal Gas constant, and

T = the absolute explosion temperature.

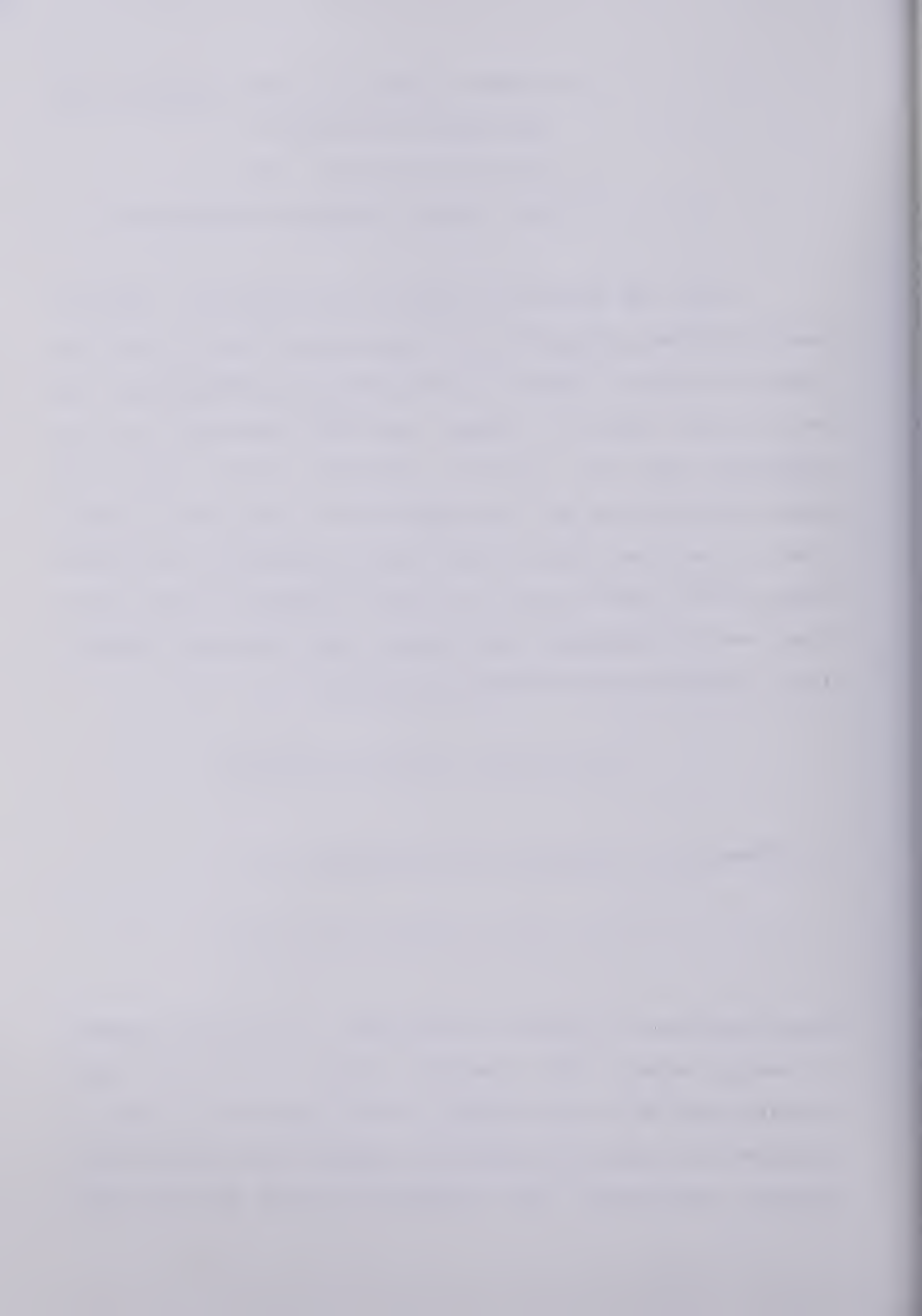
Given the molecular formula of an explosive, chemical reaction/process equations and calculations will yield the number of gaseous moles (n) of detonation gas-products, as well as the amount of 'other' residual by-products of the reaction, which are usually considered minor. Given the heats of formation of the compounds in the initial explosive, as well as those of the reaction products, for which Meyer (1977) gives tables, the heat liberated by the reaction can be determined, and hence, the explosion temperature. Equation 10 can then be used with:

$$R = 8.478 \times 10^{-4} \text{ m T } ^\circ\text{K}^{-1} \text{ mol}^{-1}$$

if dimensions of metre-tons are required, or:

$$R = 8.313 \times 10^{-3} \text{ kJ } ^\circ\text{K}^{-1} \text{ mol}^{-1}$$

when dimensions of Joules are required, to calculate specific energy (Meyer, 1977). Specific energy results from these calculations if a unit weight of the explosive is used to calculate the moles of explosive compound for the reaction/process calculation. For a detailed account of the proce-



dure, see Meyer (1977).

Specific energy is sometimes reported with the dimensions of pressure, ie atmospheres. This requires that the pressure be that generated from a unit volume of the explosive rather than unit weight. The dimensions of pressure follow readily from Equation 10, for with volume set to unity, the equation becomes:

$$f = P \quad \dots (11)$$

Strictly speaking, however, f is an energy value and should be reported as such (Meyer, 1977).

Contrary to the expectation that no single-parameter measure of effectiveness will be adequate in all circumstances, Meyer states that specific energy values are "very consistantly parallel to the performance data obtained by conventional tests". This is particularly true for tests of large samples of explosives. For example, Figure 13 shows the relationship between weight strength (Section 4.3.2), specific energy and the lead block excavation volumes described earlier.

Comparison of explosives on the basis of specific energy is carried out in the same manner as before, that is, through the ratio of specific energies.

Measures such as the heats of detonation used by Kurtz et.al., or specific energy, have the advantage of being a basic property of the explosive, and hence do not re-

The first of these is the question of the origin of the human race. It is generally admitted that the human race is descended from a common ancestor, but the question of the origin of this ancestor is still a matter of dispute. Some authorities believe that the human race originated in Africa, while others believe that it originated in Asia. The question is still open, and it is one of the most important questions in the history of the human race.

The second question is the question of the development of the human race. It is generally admitted that the human race has developed from a lower state to a higher state, but the question of the nature of this development is still a matter of dispute. Some authorities believe that the human race has developed from a lower state to a higher state, while others believe that it has developed from a higher state to a lower state. The question is still open, and it is one of the most important questions in the history of the human race.

The third question is the question of the future of the human race. It is generally admitted that the human race will continue to develop, but the question of the nature of this development is still a matter of dispute. Some authorities believe that the human race will continue to develop from a lower state to a higher state, while others believe that it will continue to develop from a higher state to a lower state. The question is still open, and it is one of the most important questions in the history of the human race.

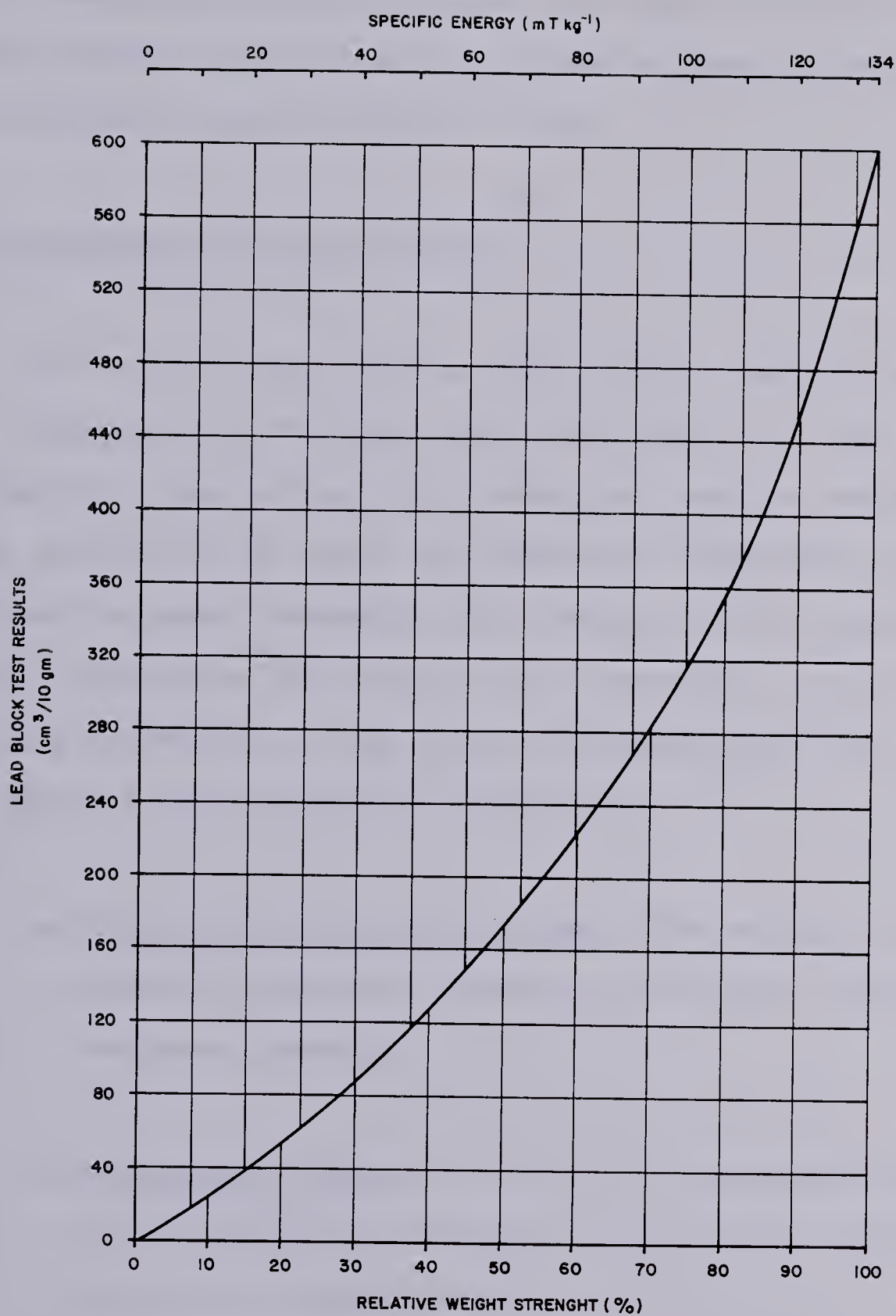
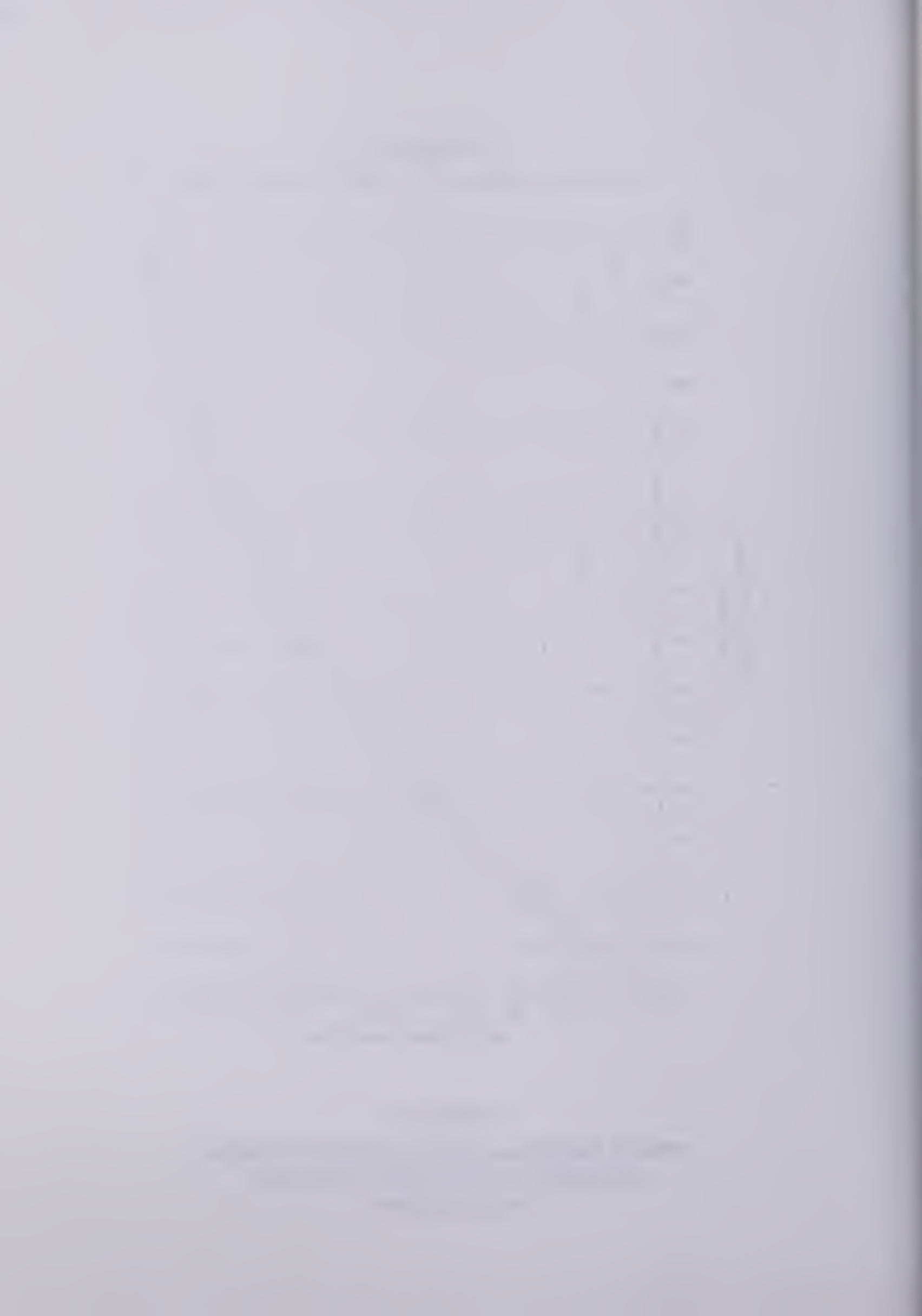


FIGURE 13
SPECIFIC ENERGY AND RELATIVE WEIGHT STRENGTH
IN RELATION TO LEAD BLOCK TEST VALUE
AFTER MEYER (1977)



quire reference to some other explosive. Specific energy and heat of detonation have a further advantage in that a comparison between explosives can be made without reference to some arbitrary, albeit standard, test.

4.4 Properties of Some Explosives

In the previous section the various comparisons between explosive 'strengths' were discussed. It was found that measures such as specific energy or heat of detonation showed promise as a means of comparing explosives without reference to some standard test. Meyer (1977) summarizes various properties of primary and secondary explosives. These are reproduced in Table B-5 of Appendix B. This table lists the following explosive properties:

- a. Volume of Detonation Gases: the volume of gaseous detonation products at 0°C and 1 Atmosphere pressure,
- b. Detonation Velocity: the rate of propagation of the chemical decomposition reaction front through the explosive,
- c. Heat of Explosion: the difference between the energy of formation of the explosive compound and the energy of formation of the reaction

products is given off during the decomposition as the heat of explosion, which in turn raises the reaction products to the detonation temperature,

d. Specific Energy: discussed previously in Section 4.3.7, and

e. Lead Block Excavation Values: discussed previously in Section 4.3.

The summary by Meyer was for explosive types by their chemical compound designation. Meyer did give limited data on mixtures of explosive compounds by their manufacturer's trade names, however, these data were limited to Weight Strength, Density and Lead Block excavation or c.u.p. value (Equation 9). As the explosives, cited by trade name, were all of European manufacture, their properties have not been included in the Table.

For completeness, the Relative Weight Strength, Relative Bulk Strength and Specific Gravity of some common North American explosives (by trade name), are Given in Table B-6 of Appendix B. The data has been adapted from the ICI Handbook of Blasting Tables. Table B-7 of Appendix B is also included to give the same data, plus water resistance and velocity of detonation for common CIL explosives (CIL, 1980).

THE UNIVERSITY OF CHICAGO
DEPARTMENT OF THE HISTORY OF ARTS
AND ARCHITECTURE
1100 EAST 58TH STREET
CHICAGO, ILLINOIS 60637

OFFICE OF THE DEAN
1100 EAST 58TH STREET
CHICAGO, ILLINOIS 60637
TEL: 773-936-5000
FAX: 773-936-5001
WWW.CHICAGOEDU.EDU

THE UNIVERSITY OF CHICAGO
DEPARTMENT OF THE HISTORY OF ARTS
AND ARCHITECTURE
1100 EAST 58TH STREET
CHICAGO, ILLINOIS 60637
TEL: 773-936-5000
FAX: 773-936-5001
WWW.CHICAGOEDU.EDU

THE UNIVERSITY OF CHICAGO
DEPARTMENT OF THE HISTORY OF ARTS
AND ARCHITECTURE
1100 EAST 58TH STREET
CHICAGO, ILLINOIS 60637
TEL: 773-936-5000
FAX: 773-936-5001
WWW.CHICAGOEDU.EDU

CHAPTER 5

EXPERIMENTAL PROGRAM

5.1 Experimental Objectives

Information gained from the literature review, and discussion with the study coordinators from DRES, suggested the following primary objectives for the field investigation:

- a. Determine the optimum point charge for a range of ice thicknesses,
- b. Determine the optimum depth of placement of those charges, and
- c. Determine the optimum spacing of individual, optimum charges in a row charge.

A number of secondary objectives were set for preliminary investigation of the factors involved, these being:

- a. To determine the efficacy of standard, pre-packaged linear charges in ice demolition,
- b. To determine the effects of charge placement, ie the effect on the resulting crater of gas venting through the placement hole,

- c. To document the efficacy of placement of charges on the surface of the ice, and
- d. To test methods of increasing the fraction of ice ejected from the crater using the direct-ed blasting technique.

Most attention was paid to obtaining data for the primary objectives and secondary objective b. The experiments for the remainder of the secondary objectives were designed to outline investigation needs and methods.

5.2 Experiment Descriptions

The program consisted of seven experiments to encompass the objectives outlined above. Ultimately, one experiment was dropped from the program, Experiment 7, for reasons to be outlined.

All of the experiments were to be carried out using the standard Military explosive C-4. However, a supply problem had developed at the explosive manufacturer, so a substitute was made. The substitute used was a NATO standard explosive, a PETN based explosive called DM-12 which is manufactured in Germany. All experiments, except where noted, used DM-12 as the explosive.

The following is a brief description of each experiment.

5.2.1 Experiment 1

Experiment 1 was designed to document the effects of placing charges in accordance with 1 CER's SOP, as outlined in Section 1.3. To this end, a row of six charges, each weighing 2.25 kg (5 lb) were set at a depth of 1.5 m (5 ft) below the top of the ice, and were spaced 1.5 m (5 ft) apart. The charges were detonated virtually simultaneously through the use of a 'ring main' (circuit of detonating cord or 'primacord') connecting all of the charges. The results of this Experiment are discussed in Chapter 7.

5.2.2 Experiment 2

Experiment 2 was by far the largest portion of the experimental program. The experiment was designed to fulfill the requirements of the first two primary objectives; optimizing the charge weight and placement, as well as to fulfill the secondary objective of documenting the effects of placement hole diameter on venting of the gaseous products of detonation before all useful work could be obtained from them. The experiment initially consisted of 44 separate detonations, but was increased to 86 through field additions to the program (Section 5.3).

For this experiment four charge weights; 0.5, 1.0, 2.25 and 4.5 kg, were selected, based on initial ice thickness measurements, to bracket the optimum crater producing condition described by Mellor (1972) based on ice thickness (Figure 7). Five different placement depths were selected to

set the charges at, again based on Mellor's analysis. These depths were: inside a shallow hole at the surface of the ice (and tamped with snow), at the ice/water interface, at 'optimum depth' as described by Mellor, and at 3 and 5.5 times the optimum depth for the measured ice thickness. For the charges at the ice/water interface and at optimum placement depth, four different placement hole conditions existed for each charge weight. Three hole diameters were used: 0.152, 0.305 and 0.457 m (6, 12 and 18 in), with the hole being left open. The fourth condition was a 0.152 m hole left to refreeze overnight with the charge in place.

The results of Experiment 2 are discussed in Chapter 6.

5.2.3 Experiment 3

Experiment 3 was designed to document the effects of large explosive charges set on the surface of the ice. This was included to give an indication of how effective a series of charges set in this manner, as a 'hasty' demolition technique by the CAF, would be. The experiment consisted of setting one charge each of 9 kg (19.8 lb) and 18 kg (39.7 lb) on the ice surface, detonating them, and recording the results. The results are given in Chapter 6.

5.2.4 Experiment 4

Experiment 4 was designed to test methods of increasing the fraction of ice ejected from the crater, a secondary

objective, through the use of the directed blasting technique described by Nikolayev (1971). Charge weights of 4 and 12 kg were used for the main charges, with 0.125, 0.75 and 2.50 kg auxiliary charges. The auxiliary charges were detonated first, with time delays for detonating the main charge of between 1.92 and 46.15 m sec. The 'directing angle' to the vertical was maintained at 45° for each of the nine shots fired.

Commercial delay detonators had been provided by the CAF. However, these provided too long a delay for the intended purpose, so expedient delays had to be arranged. Delays between detonations were achieved by providing various lengths of military det-cord (primacord) from the ring main to the main charge. Thus, when the explosive train was fired in the ring main, the detonation wave had a longer distance to travel in the line to the main charge than to the auxiliary, hence providing a delay. The velocity of detonation of the det-cord was taken as published in the CAF handbooks, 7925 m sec^{-1} (26,000 ft/sec). Using this velocity the length of det-cord required to produce a desired delay could be calculated.

Experiment 4 is discussed further in Chapter 8.

5.2.5 Experiment 5

Experiment 5 was designed to document the efficacy of standard military linear charges in ice demolition. The experiment consisted of placing both single and multiple (10)

strands of det-cord, as well as a length of 'Bangalore Torpedo', both above and below the ice, and detonating them. Originally it had been intended to test both sizes of the 'Viper' class of linear charge instead of the det-cord. However, the expense and availability of the Vipers prohibited this. Placement of the charges under the ice was effected by both the CAF Shallow Water Divers of 1 CER, and by divers of the U.S. Navy 'Seals' diving team, who were on the exercise with 1 CER to conduct their own annual under-ice diving classification training.

A second part of this experiment consisted of setting one section of Bangalore Torpedo through a placement hole, so the Bangalore was vertical, with its top at the bottom of the ice sheet.

The explosive filler of Bangalore Torpedos can be one of Composition B, Amatol 80/20 (80% Ammonium Nitrate, 20% TNT), (U.S. Department of the Army, 1969), or a 50/50 Pento-lite (50% TNT, 50% RDX), (Hemphill, 1981) depending on the year of manufacture and 'Mark' of the charge.

Experiment 5 is discussed further in Chapter 9.

5.2.6 Experiment 6

Experiment 6 was included to test the effectiveness of using shaped charges to create placement holes in the ice sheet. Five shaped charges were set with standoffs of 0 (zero) m (ie on the ice) to 1.22 m (4 ft). Again, it had been planned to use the standard military cone-shaped (Sec-

tion 3.3.2) 'Beehive' charge such as shown in Figure 8, which are designed for penetration. However, these were not available, so wedge-shaped 'Hayrick' charges were substituted.

Experiment 6 is discussed further in Chapter 10.

5.2.7 Experiment 7

A final experiment was included in the program, though it did not cover one of the objectives of the program. The experiment was designed to evaluate the effects of a sequence of explosions detonated with delays calculated to match the natural frequency of the ice-water system. In this manner it was thought that the exitation of the natural frequency of the ice-water system would cause resonance in that system, with the result that more widespread destruction of the ice could be achieved than with a series of charges of the same total weight, set in the conventional manner described earlier.

The experiment was dropped from the program. The intent of the experiment and the reason it was deleted were as follows.

Calculations showed that the critical frequency for the ice thickness and depth of water present below the ice was approximately 0.1 Hz. To excite this frequency, a pulse from any source, but in this case from an underwater explosion, would be required every 10 seconds. Although timed detonations with this delay is a relatively simple arrange-

ment, it was judged that the pulse would have to be delivered to the same point of the ice sheet. This required placing charges virtually on top of one another. To locate armed charges (detonators inserted if firing electrically, or hooked into a ring main with delay detonators using nonelectric initiation techniques) close enough to each other to provide a pulse at the same location leads to two possible complications.

The first is sympathetic detonation of all of the charges upon detonation of the first. Some explosives are very 'sensitive' to shock (for example, grades of 'ditching dynamite' were manufactured to take advantage of this sensitivity, such that initiation of charges could be achieved by the shock wave travelling through the soil rather than having to hook all charges up to a ring main), the gap sensitivity of the DM-12 (which is the measure of how far apart charges have to be to prevent sympathetic detonation) was not known, hence it was not known if sympathetic detonation would occur from the shock of the first detonation. Further, to achieve the delay required to excite the frequency of the ice-water system, it had been decided to initiate the explosion through electrical detonators, as nonelectric detonators with multiples of a 10 second delay were not available. Each charge was to have its own detonator, and the series of charges were to be hooked into a 'ripple board', which is a firing board having a number of terminals. Each charge is connected to a central, 'hot' terminal, and to its own

'cold' terminal, but the circuit is not complete. Completion of the circuit, and hence initiation of the detonator, is accomplished by touching the 'cold' terminal with a lead wire from the 'hot' terminal. This connection is manual, and could be timed. The presence of the electrical detonators, which are filled with a sensitive primary explosive, could also have led to sympathetic detonation, by the detonators themselves going off.

The second potential problem, considered the most important by the Forces' personnel conducting the experiments, was the possibility of the detonation of the first charge destroying the remaining charges. In this case, if sympathetic detonation did not occur, the result would have been that pieces of the explosives destroyed by the blast would have been scattered through the water under the ice. Forces' regulations prohibit leaving unexpended ammunition or explosives lying around (for safety reasons), yet the retrieval of the explosives and detonators from under the ice would have been virtually impossible for the divers, considering the light available under the ice, not to mention dangerous.

After discussion of these problems with the Forces personnel, it was decided to drop Experiment 7 from the program. It will not be discussed further herein.

5.3 Field Additions to the Program

A number of additional test shots were added to the

program after it had started. These were to fill a perceived inadequacy of data in certain areas, or to include data that was convenient to determine.

The first addition was the results of two shots fired at DRES, at Canadian Forces Base Suffield, Alberta. The two shots were fired before the commencement of the main program, and were intended to see how the program would proceed, as well as allow organization and practice of the data gathering methods (Section 5.4.3) by the University personnel, who were responsible for data collection. After the main program started it was noted that the results of the two explosions were consistent with what was being observed, hence it was decided to incorporate the crater dimensions into the final data. The shots were assigned their own experiment number, 0 (Zero), and the data was added to that from Experiment 2. These were the only data added as a matter of convenience.

Two additional shots were fired before the commencement of the main testing program. These were for purposes of confirming charge placement calculation procedures, which would have to be carried out quickly once the general activity of the main program commenced, and still be sufficiently accurate to obtain the data desired. The data from these two shots were added to the data of Experiment 0.

The SOP of 1 CER was tested in Experiment 1. However, it was noted in the field that there would be no single charge data with which to compare the results of the row

charge specified by the SOP. Therefore, two single 2.25 kg (5 lb) charges were placed and fired in accordance with the criteria of the SOP. The data from these shots were to be used to assess the efficacy of the row shot, and were added to the single charge data for Experiment 2.

During the experimental program calculations showed that the planned tests were indeed 'bracketing' the optimum condition given by Mellor's curves (Figure 7), as had been intended. The data however tended to be grouped about this optimum, which had led Mellor to be concerned that the data he used in his regression analysis (which showed a similar trait) were too "ill conditioned" (Mellor, 1972). Mellor had also indicated (1972) that:

"The curves [of Figures 6 and 7] should be used with caution, especially at the extremes of depth and thickness scales."

This was presumed to be due to a deficiency of data in these ranges, hence additional tests were incorporated into the experiments to give data at the extremes of the thickness scales. Two 'large' charges, of 20 and 25 kg (44 and 55 lb) were detonated at a depth of 1.83 m (6 ft), which was calculated to be well in excess of the optimum depth for the charge weight and ice thickness encountered. These would yield data for the 'small' scaled ice thickness range of Figure 7. To obtain data at the other end of the scaled thickness range, a series of four 0.25 kg (0.55 lb) and four

1.0 kg (2.20 lb) charges were placed at depths of between 0.91 and 1.83 m (3 to 6 ft), again calculated to be in excess of the optimum scaled depth. The results of these tests were also added to the data of Experiment 2.

In times of war, the supply of standard military explosives may be taxed to the point where it becomes necessary to use whatever is available. Supplies of industrial (civilian) explosives would be the first logical choice; however, expedients such as making ANFO in the field for certain tasks may be advantageous. In order to test the efficacy of explosives other than military, and to obtain data of a comparative nature to the remainder of the tests, as well as the data reported in the literature, a series of eight charges of each of the three types of industrial explosives: 40% Forcite, Amex II and Hydromex T3, were included in Experiment 2. Each of these are trade names of explosives manufactured by CIL. Of the three, Forcite is reported by CIL (CIL, 1968) to be a gelatin (and ammonia gelatin) dynamite, Amex is an ANFO 'blasting agent', and the form of Hydromex used was a bulk, ANFO-based 'slurry' explosive (CIL, 1980). The charges of these three explosives were placed at the same depths as the two series of Experiment 2 where the placement depth was 3 and 5.5 times the computed optimum. The data was added to that of Experiment 2.

Of the experiments reported in the literature, only Kurtz et.al. (1966) reported results from detonating row charges (Section 3.2.5). The spacings between the charges in

their rows had been set at 1.0, 1.5 and 2.0 times the optimum crater radius they had determined previously. The only tests that had been made with the charge spacing greater than one crater diameter were those of Moor and Watson (1971), and as discussed, their data is not suited to the analysis conducted herein. Therefore a final addition to the experimental program for this thesis was made. A series of six charges, calculated from Mellor's curves to produce an optimum crater, were placed with a spacing of 3 times the calculated crater radius and fired. The results of this test are discussed further in Chapter 7.

5.4 Conduct of the Program

The experiments were conducted at Drummond Lake in the CAF 'Chilcotin' training area in central British Columbia, January 21 through 24, 1980 shown in Figure 14. The Chilcotin training area is located just north of the hamlet of Riske Creek, which is itself 30 km due southwest of the Town of Williams Lake. 1 CER had been tasked by DRES to conduct the experiments as a military exercise under the "technical guidance" (1 CER Trials Directive, January 1980, Classified) of the University of Alberta and DRES personnel.

A base camp was established at the east end of Drummond Lake from which 1 CER conducted both its own winter training and the experimental program. A temporary firing range was established, in accordance with CAF procedures and



safety regulations, at the southeast corner of Drummond Lake, within which all testing was to be conducted.

Accommodation and meals, under canvas, were provided within the base camp for the personnel from the University of Alberta and DRES (Photo 1).



Photo 1: Field Camp at Drummond Lake

Two Field Troops of 11 Field Squadron, 1 CER, each consisting of one Officer and 25 to 30 enlisted ranks, carried out the mechanics of the testing. Number 1 Troop was assigned Experiments 1, 2 and 3, as well as the additional shots using the commercial explosives and the two single shots using the placement criteria of 1 CER's SOP. These experiments were conducted during the first two days of testing. Number 3 Troop was assigned the balance of the experiments and additions, which were completed during the final two days allotted for the testing.

Before describing the general conduct of the experiments, it must be noted that as the testing was being carried out as a military exercise, once the charge placement criteria was given to the Troop Commander responsible for the particular tests, that Officer had complete control of the operation. He was responsible for the logistics, charge preparation, charge placement, detonation and personnel safety. The order in which the tests were fired was determined by his assessment of the optimal use of the available manpower and equipment, and was not necessarily synchronous with the order in which the tests were planned.

5.4.1 Charge preparation

The charges were prepared in an area on the shore of the lake adjacent to the base camp, and brought forward when required. The charges were not prepared closer to the site as the vehicle containing all of the explosive stores drawn from the temporary ammunition dump was an Armoured Personnel Carrier, which was too heavy to sit on the ice sheet for the duration of the day's testing.

As mentioned, four explosive types were used during the experiments. These were a military PETN based plastic explosive (DM-12) and three commercial explosives: 40% Forcite (dynamite), Amex II (ANFO blasting agent) and Hydromex (ANFO blasting slurry). The DM-12 came packaged in rectangular blocks measuring 95 x 58 x 62 mm, each block wrapped in a waterproof paper and containing 0.5 kg of explosive. The

Forcite came in cylindrical cartridges (1 in x 8 in) wrapped in a waterproof paper, there being "approximately" (CIL, 1968) 0.34 lb of explosive per cartridge (Note: for the Chilcotin tests 166 cartridges of Forcite were counted in a 55 lb lot, or 0.33 lb (0.15 kg) per stick). Both the Amex and Hydromex came in bulk, the Amex in one 50 lb (22.68 kg) polyethelene bag, and the Hydromex in two 25 lb (11.34 kg) polyethelene bags.

The charges to be made up were, for the most part, 0.5, 1.0, 2.25 and 4.5 kg. For the DM-12 even numbers of 0.5 kg blocks could be used except for the 2.25 kg charges, where a block of explosive was carefully measured and cut in half. The smallest DM-12 charges made up were 0.25 kg, for which a block of the explosive was again carefully cut in half. It is considered that the experimental error introduced by cutting the charges in this manner is negligible. Charges larger than 4.5 kg could be made up with a number of whole blocks of the explosive. A length of det cord was doubled up and had an overhand knot (thumbknot) tied at the doubled over end. This knot was to be placed in the centre of the charge, and would ultimately transfer the detonation wave to the explosive. The required number of blocks of explosive to make up a charge were unwrapped (Photo 2) and taped together around the knot in the det cord.

The whole charge was inserted into a plastic bag, with the free ends of the doubled up det cord protruding, and securly taped to make the charge waterproof. The two



Photo 2: A Block of DM 12 Explosive

ends of the det cord protruding from the charge were the leads with which the charge was to be connected to the ring main (firing circuit) as described in the next section. Finally the charges were tied with string, a length of which was left to suspend the charge below the ice. Two of the larger charges are shown in preparation, and with rolls of det cord ready to be brought forward in Photos 3 and 4.

The Forcite charges were made up in similar fashion, with the exception that the thumbknot in the doubled up det cord was inserted into one of the sticks of Forcite split open for this purpose. The split stick was subsequently taped up to ensure good contact between the explosive and the det cord. The Forcite charges were made up with whole sticks to approximately the same weight as the main DM-12 charges. Charges were made up with 4, 8, 15 and 30 sticks,



Photo 3: Charge Preparation



Photo 4: Two Prepared Charges
and Two Rolls of
Det Cord

giving charge weights of 0.60, 1.20, 2.25 and 4.51 kg respectively. A 4.51 kg Forcite charge is shown in Photo 5.

Charges of Amex and Hydromex were made up by slowly pouring the explosive into a plastic bag (which then formed the waterproof casing) attached to a calibrated spring balance, weighing the charge to the nearest 0.25 lb (0.11 kg). The charge weights made up were 1.25, 2.5, 5.0 and 10.0 lbs (0.57, 1.13, 2.27 and 4.54 kg respectively). Both of the explosives are secondary explosives (Section 4.2) being too

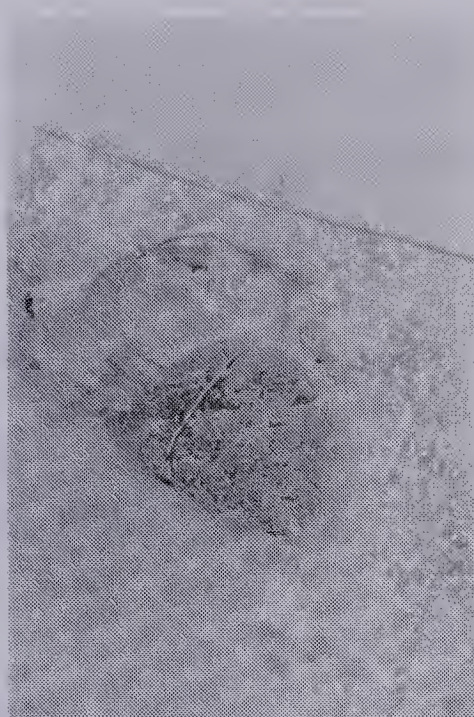


Photo 5: 40% Forcrite Charge
4.51 kg (30 Cartridges)

Photo 6: Amex II Charge
4.54 kg (10 lb)

insensitive to be detonated using only the det cord (CIL, 1968), therefore a half-stick of Forcrite, with the knotted det cord inserted, was incorporated into the charge as a booster, to initiate the detonation. A 4.54 kg Amex charge is shown in Photo 6.

5.4.2 General Conduct of the Experiments

While the charges were being made up, placement holes were cut in the ice. These holes were made with a 6 inch (15.24 cm) powered ice auger (Photo 7), or, for those shots of Experiment 2 requiring a larger placement hole, or those charges which were too large to fit through the 15 cm hole, with a chain saw. Ice thickness measurements were taken at each placement hole and recorded on data sheets, of which

there was one per hole. The ice thickness measurements were used to determine the appropriate depth of placement, using the preliminary relationships given by Mellor (Section 3.2.10), which were also recorded on the data sheets.



Photo 7: Augering a Placement Hole

The charges were set at the appropriate placement depth by suspending them from a stick placed across the placement hole (Photo 8). A length of string remaining from packaging the charges was used for this purpose, such that the approximate centre of mass of the charge was at the required depth. The two det cord leads incorporated into the

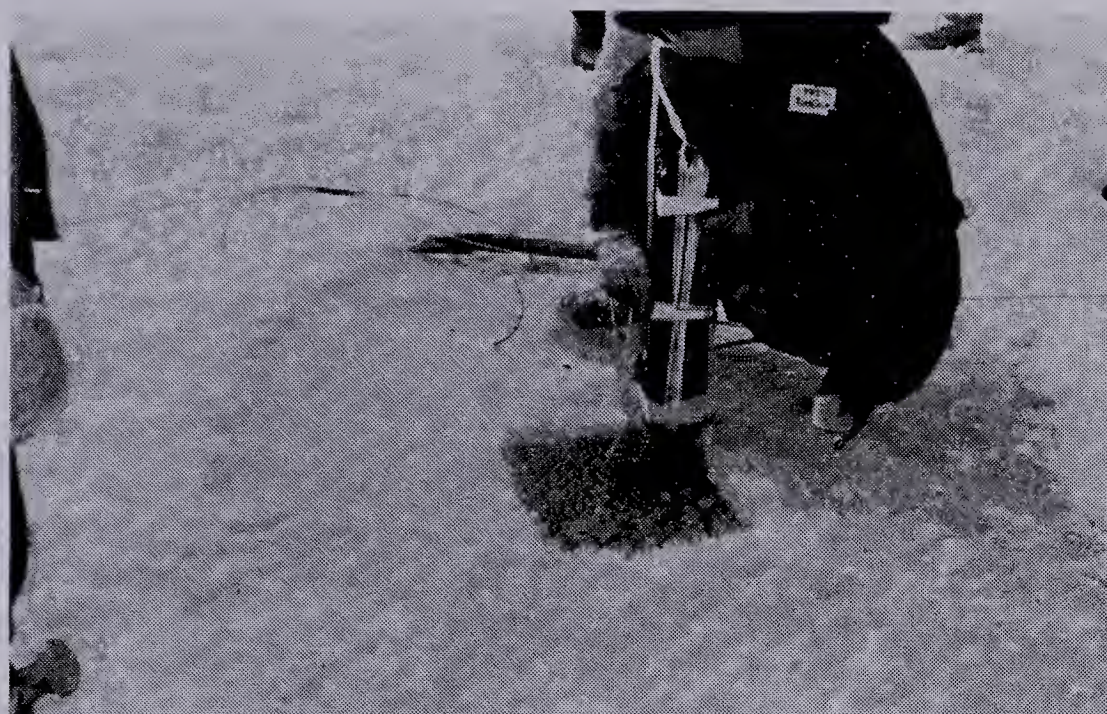


Photo 8: Placing an Explosive Charge

basic charge were left sticking out of the hole.

Concerning the charge placement, one series of tests was designed to have the charges detonated 'at' the lower ice surface, while others were designed to have the charges placed at 'optimum depth' and deeper. Considering the small placement depths for the 'zero' and 'optimum' conditions (optimum depth averaged 13 cm), and the physical size of the charges, errors could be introduced into the placement depth setting. The charge sizes for these shots were from 9.5 x 5.8 x 6.2 cm (one block of DM-12) for the 0.5 kg charges, to 19.0 x 11.6 x 11.6 cm (approximately) for the 4.5 kg charges. A small measurement error when tying off the charge (as shown in Photo 8) would have been sufficient to alter the scaled depth of placement. For charges placed deeper than optimum depth, this error would not have as great an effect

on scaled placement depth as for the shallower-placed charges.

Prior to the first tests being carried out it had been determined from random ice thickness measurements that the charges could be placed and detonated on a 50 ft (15.24 m) square grid, with no overlap between the largest (computed) resulting craters. Between detonations, the Troop Commander in charge would have to inspect the cratered area to ensure that all charges had detonated and that there was no potentially hazardous material (pieces of explosive blown clear by partial detonations, unexploded charges thrown up onto the ice, etc.) in the area. As this would cause a delay before work could continue, it was decided to fire a number of shots simultaneously to expedite the testing. The first four shots of Experiment 2, incorporating all four of the main charge weights, were fired from a ring main (to be described) using a single detonator. It was observed that four separate and distinct venting plumes occurred (Photo 9), and there was no overlap of the craters. The next four shots were fired with separate detonators, and delayed by using different lengths of fuse to each. Charge weights for the second four were the same as the first, and placement depths were the same (placement hole diameter varied). Inspection and measurement of the second four craters indicated that they were essentially the same size as the first four. This indicated that a series of charges fired from a single ring main (simultaneous detonation), with the calculated 15 m

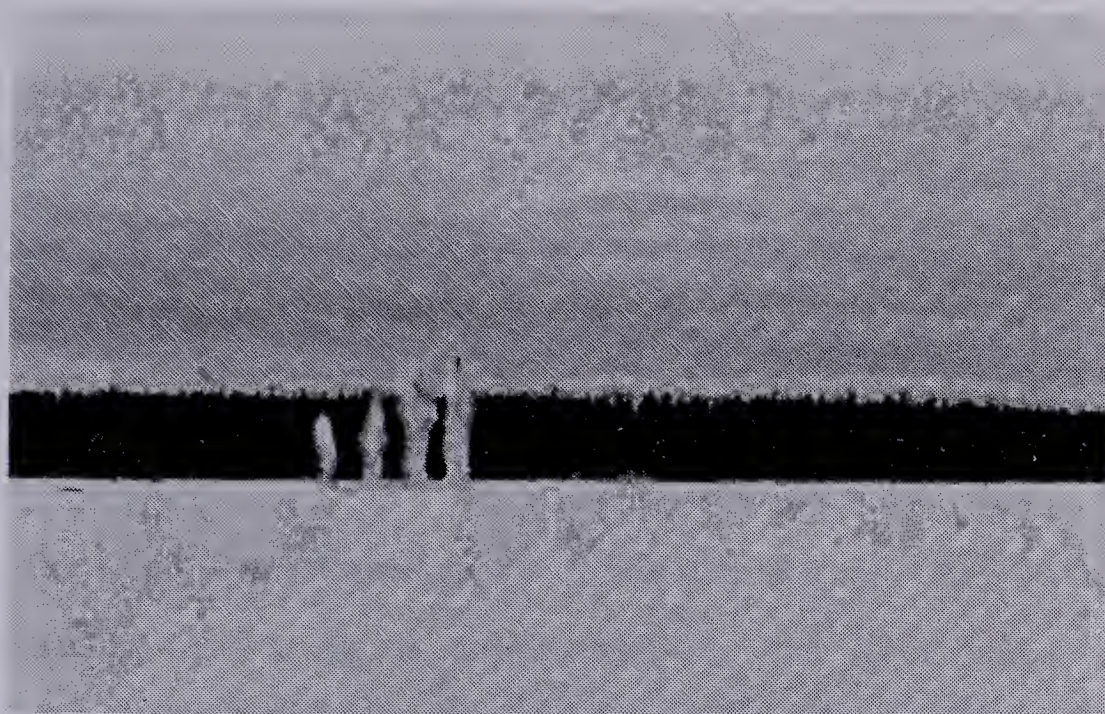


Photo 9: Detonation of the first four charges

spacing between them would not interact and affect the resulting craters. It was therefore decided to detonate eight charges in a row from a single ring main to speed up the testing.

As the shots fired would not necessarily be in the order planned, some record had to be kept to associate the resulting crater with a particular shot. With eight charges to be detonated simultaneously in a row, a numbering system was established to identify the crater by row and 'column' of the grid matrix established.

Following the verification that rows of charges could be detonated without affecting the resulting craters, the remainder of the experiments proceeded. When all charges in a row were in place, the det cord leads from the charges were connected to a ring main in the following manner. A line of det cord was laid down one side of the placement

holes, turned around, and brought back along the other side to the starting point. The det cord leads were attached with tape to the ring main on both sides of the placement hole, with the leads pointing toward the open end of the U formed by the ring main to keep continuity of direction of the detonation front. The leads were attached such that a minimum of three inches of lead were in close contact with the ring main. When all charges were connected in this manner the open ends of the U were connected to the detonator to close the 'ring'. A schematic drawing of the final detonation circuit (ring main and charge leads) is shown in Figure 15, and a typical charge hookup is shown in Photo 10.



Photo 10: Typical charge connection
to Det Cord Ring Main

Use of a detonating circuit as shown increases the probability of all charges firing, because when the detona-

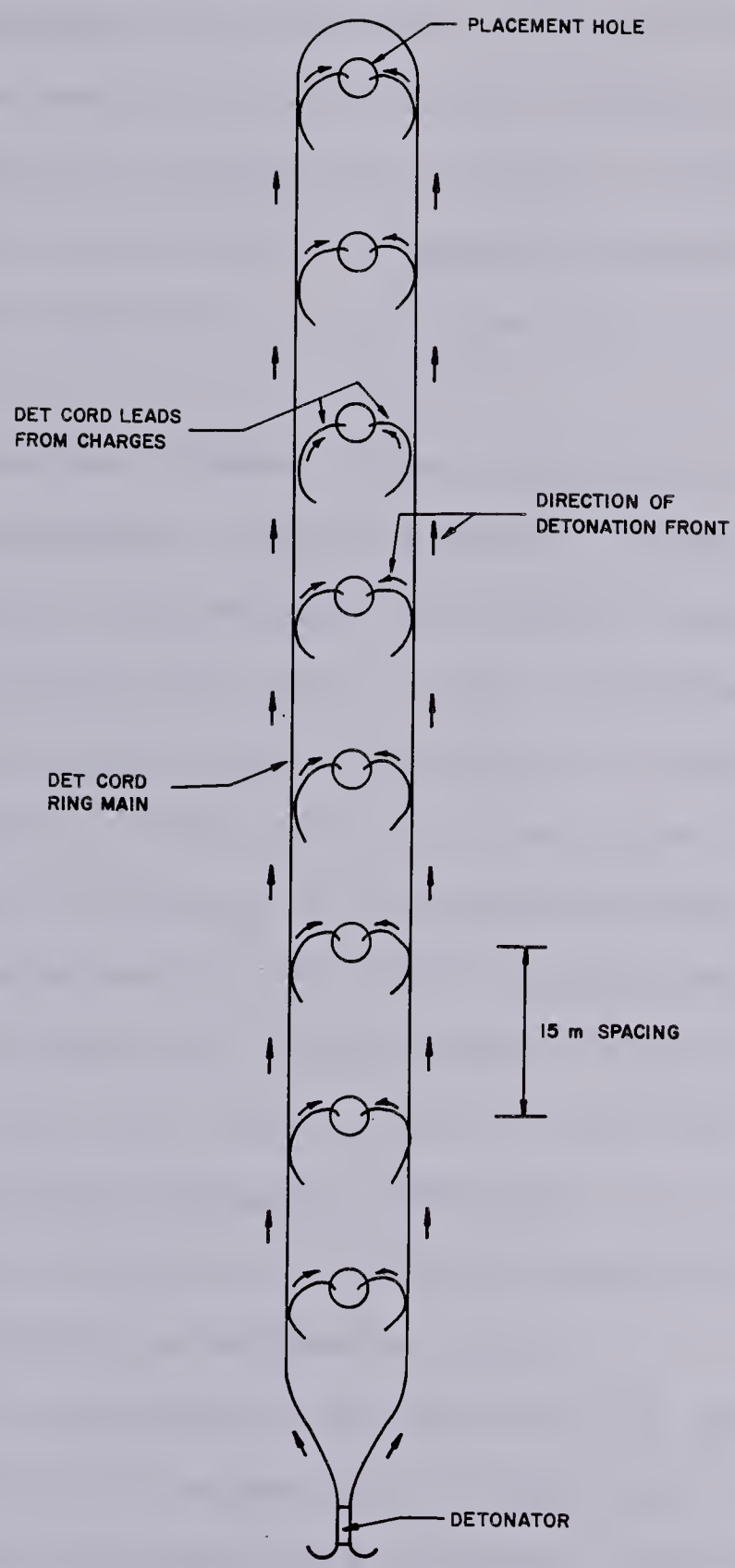


FIGURE 15
SCHEMATIC RING MAIN

tor is exploded, the det cord on both sides of the placement hole also detonates, and therefore detonates both leads to the charges, a condition known to the military as 'dual initiation' (not to be confused with 'double initiation' where two detonators are connected to separate strands of det cord which are then attached to one or the other of the leads to the charges).

The area was cleared of all personnel prior to attaching the detonator, except the Safety Officer and the man who would attach the detonator to complete the firing circuit and then ignite the fuse. In most instances the initiation 'set' for the ring main consisted of a nonelectric detonator, a length of fuse sufficient to allow the firer and Safety Officer to withdraw to a safe observation point (approximately 300 m away), and a fuse igniter consisting of a spring loaded firing pin which struck a 0.22 calibre blank cartridge to light the fuse. A few of the tests were fired using an electrical detonator connected to an Armed Forces pattern blasting machine to give the troops practice in this method of initiating an explosive train.

Once the detonation had occurred the Safety Officer inspected the site to ensure all charges had detonated and that there was no potentially hazardous material lying on the surface of the ice. Once the 'all clear' was given, personnel were allowed to go forward, inspect the results, commence crater measurements and continue the preparation of the next row of charges.

The experiments were conducted in this manner for all of the tests.

5.4.3 Measurement Techniques

A. Ice Thickness

Ice thicknesses were measured at placement holes, and occasionally at the lip of a crater, using a 0.75 m length of 6.4 mm (0.25 in) diameter reinforcing steel with a 90° bend in one end. The measurements are considered accurate to + 2 mm.

B Crater Radius

The crater radius for the single charges of Experiments 0, 2 and 3 was determined from the average of three diameter measurements taken at roughly equal intervals around the perimeter of the crater. All crater measurements were taken to the nearest centimetre.

The crater radius for the 'row charge' of Experiment 1 was measured for its length (along the line of the row) and at three equidistant points along the length for its width.

The craters formed by the directed blasting of Experiment 4 had diameter measurements taken at four locations. These were: in line with the main and auxiliary charges, perpendicular to that line, and the bisectors of the first two measurements.

The measurements of crater size for the linear charges of Experiment 5, when a crater was formed, were the length of the crater and its width at four equidistant spacings along the length.

Crater measurements for the shaped charges of Experiment 6 were made as for a single charge.

C Ice Debris

The ice debris remaining in the crater was measured to determine the efficiency of the techniques in removing ice from the crater. The debris remaining was measured in three ways.

First, for every crater, one or more photographs of the surface of the crater were taken from above it. This was carried out by attaching a camera with a wide angle lens to a mount fixed at a 45° angle to the end of a sectioned tubular pole (Figure 16 a), and, after setting the timing device on the camera, holding the pole at a 45° angle over the crater (Photo 11) to take the photograph.

The combinations of 45° angles ensured that the camera was directly above the crater and pointing vertically down. A typical photograph taken in this manner is shown as Photo 12. In each photograph a metric survey rod was laid across the crater for scale, and, the crater number from the 'row and column' numbering system described earlier was written on a piece of paper and laid on the surface of the crater for identification.

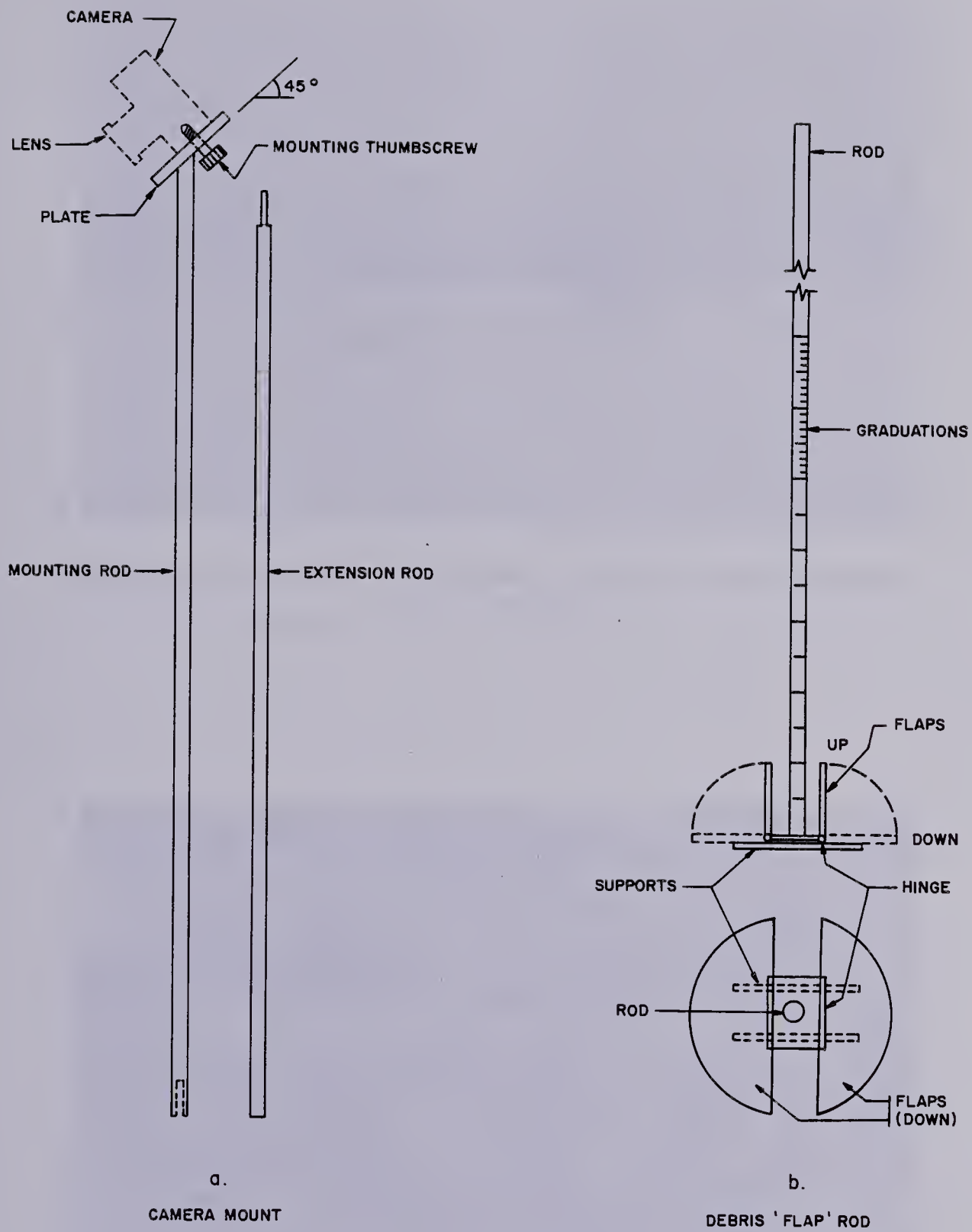


FIGURE 16
MEASUREMENT DEVICES



Photo 11: Method of taking Vertical Photographs
of a crater

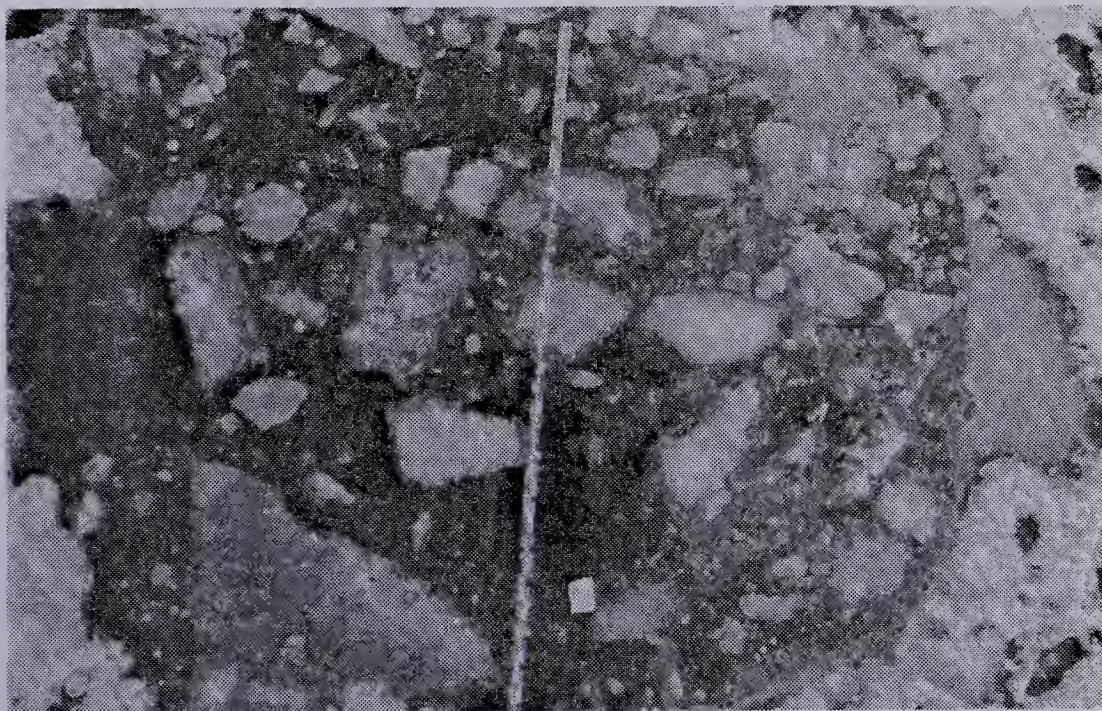


Photo 12: Typical Vertical Photograph of a Crater
(Shot 30, Experiment 2, Table 1)

The second ice debris measurement was the debris thickness. Using a rod with hinged flaps at one end and a graduated scale on the rod itself, (Figure 16 b) the debris thickness at a number of random locations around the perimeter of the crater was measured. Random measurements were made as the debris was not of uniform thickness, nor was it uniform in its spatial distribution within the crater. The flaps of the rod folded up while being inserted through the debris, in order to cause as little displacement as possible. Once immersed, a sharp tug on the rod caused the flaps to fold down (or open) because of fluid drag. The rod was raised until it could be felt that contact was made with the underside of the debris. For some craters, a profile of the debris thickness across the crater was taken from an aluminum boat dragged across the crater (Photo 13).



Photo 13: Profiling the Ice Debris Thickness
across a crater

The final debris measurement was for purposes of determining the porosity of the debris/water complex remaining in the crater. For selected craters, a 45 gallon drum with top and bottom removed and a urethane foam floatation collar attached (Figure 17) was inserted into the crater. This device was used to isolate a certain amount of debris, which was then removed, and weighed in a plastic pail 'tare' on a spring balance.

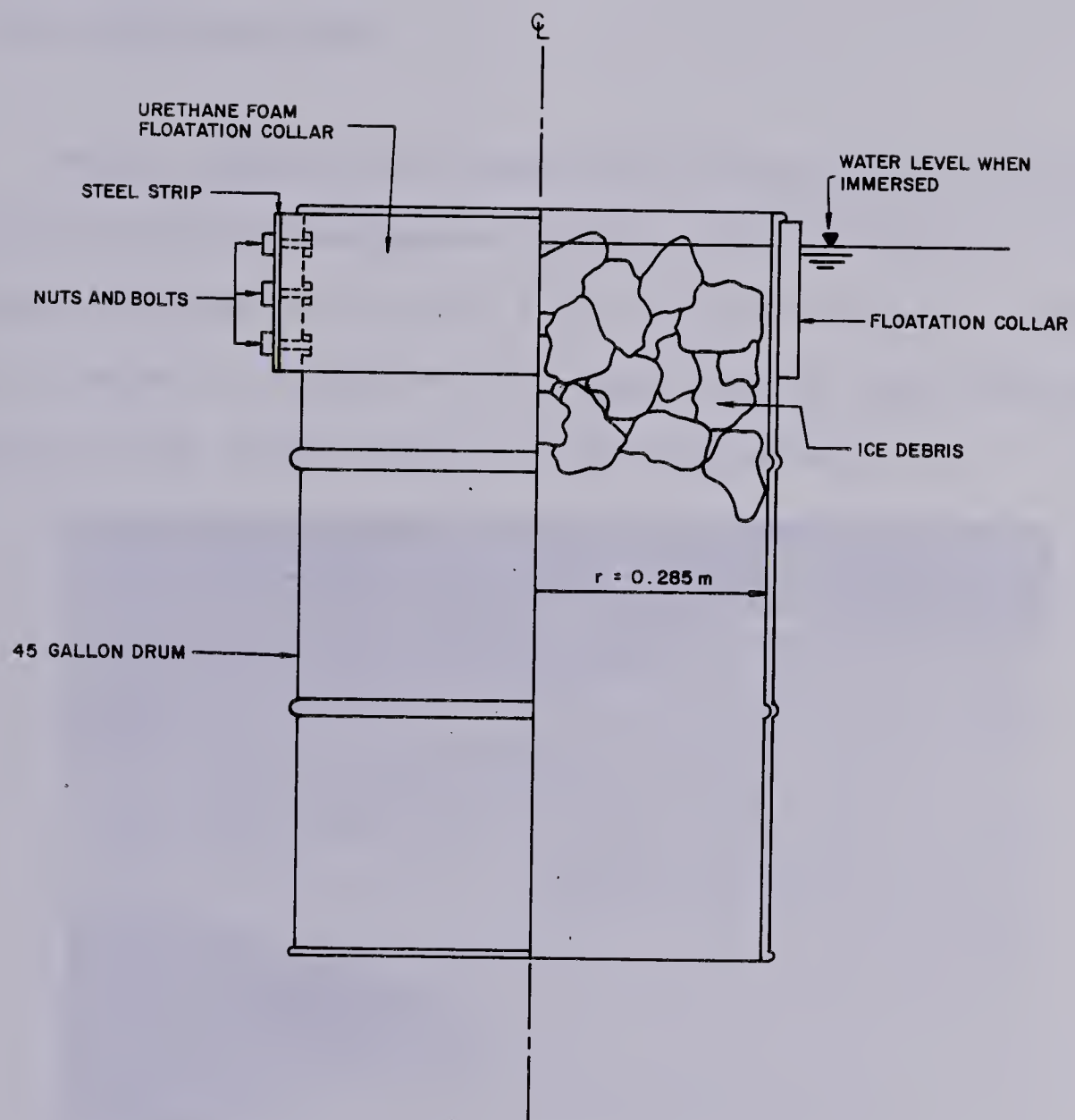


FIGURE 17
HALF SECTION OF DEBRIS
INSULATION DEVICE

CHAPTER 6

EFFECTS OF POINT CHARGES

6.1 The Chilcotin Data

Point charge data from the Chilcotin tests included the results from Experiments 0 and 2, plus additions to the program outlined in Section 5.3. The test area on Drummond Lake is shown in Photo 14, with the craters from Experiment 2 shown in the right-centre of the photograph.

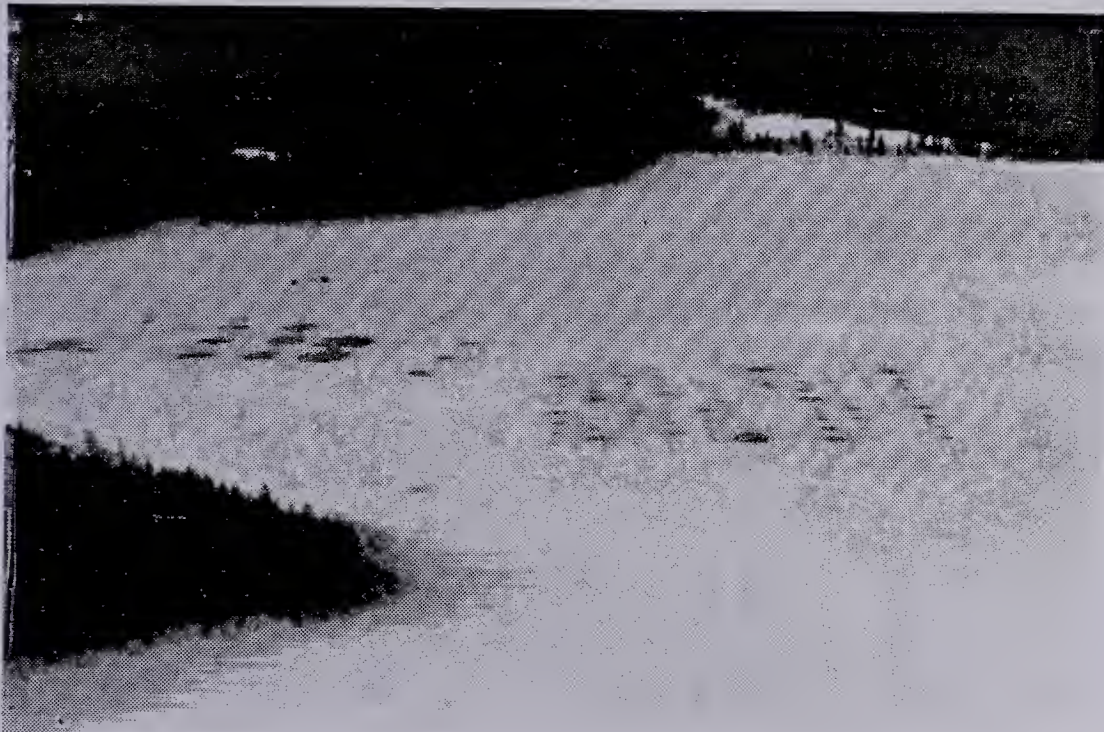


Photo 14: Test Area on Drummond Lake

The Chilcotin data are presented in Table 1 following.

TABLE 1
The Chilcotin Data
(For Point Charges)

Shot No	Expt No	Explosive	Placement Condition	Placement Hole Diameter (mm)	Charge Weight (kg)	Ice Thickness (m)	Placement Depth (m)	Water Depth (m)	Crater Radius (m)
1	0	DM 12	Optimum	152.4	1.00	0.439	0.19	-	3.12
2					2.00	0.439	0.15	-	4.06
3	0	DM 12	Optimum	152.4	1.25	0.340	0.12	2.28	2.79
4					1.25	0.355	0.13	3.45	2.95
5	2	DM 12	At Surface 1	-	0.50	0.368	-0.29	-	0.55
6				-	1.00	0.387	-0.31	-	0.74
7				-	2.25	0.343	-0.27	-	1.26
8				-	4.50	0.381	-0.30	-	2.14
9	2	DM 12	Bottom of Ice 2	152.4	0.50	0.318	0.0	4.33	2.20
10					1.00	0.305	0.0	4.34	2.31
11					2.25	0.343	0.0	4.41	3.26
12					4.50	0.356	0.0	4.50	4.19
13	2	DM 12	Bottom of Ice	304.8	0.50	0.330	0.0	4.98	2.36
14					1.00	0.381	0.0	4.55	2.61
15					2.25	0.305	0.0	4.50	2.99
16					4.50	0.305	0.0	4.50	4.22
17	2	DM 12	Bottom of Ice	457.2	0.50	0.324	0.0	4.83	1.58
18					1.00	0.381	0.0	4.67	2.20
19					2.25	0.362	0.0	4.72	3.19
20					4.50	0.375	0.0	4.83	4.52

TABLE 1

(Continued)

Shot No	Expt No	Explosive	Placement Condition	Placement Hole Diameter (mm)	Charge Weight (kg)	Ice Thickness (m)	Placement Depth (m)	Water Depth (m)	Crater Radius (m)
21	2	DM 12	Bottom of Ice	152.4	0.50	0.381	0.0	5.05	2.10
22				Refrozen	1.00	0.381	0.0	4.88	2.60
23					2.25	0.356	0.0	4.83	3.77
24					4.50	0.381	0.0	4.93	4.53
25	2	DM 12	Optimum	152.4	0.50	0.381	0.14	4.85	1.78
26					1.00	0.318	0.11	4.74	2.31
27					2.25	0.343	0.12	4.23	3.44
28					4.50	0.330	0.12	4.17	3.84
29	2	DM 12	Optimum	304.8	0.50	0.318	0.11	4.10	1.92
30					1.00	0.305	0.11	4.24	2.58
31					2.25	0.406	0.15	4.52	3.37
32					4.50	0.381	0.14	5.11	4.27
33	2	DM 12	Optimum	457.2	0.50	0.368	0.13	4.99	1.91
34					1.00	0.381	0.14	4.60	2.40
35					2.25	0.381	0.14	4.27	3.26
36					4.50	0.387	0.14	4.29	3.96
37	2	DM 12	Optimum	152.4	0.50	0.381	0.14	4.14	1.80
38				Refrozen	1.00	0.381	0.14	4.19	2.98
39					2.25	0.381	0.14	4.37	3.51
40					4.50	0.356	0.13	4.70	4.65
41	2	DM 12	3 x Optimum	152.4	0.50	0.337	0.70	4.79	1.83
42					1.00	0.330	0.69	5.11	2.63

TABLE 1

(Continued)

Shot No	Expt No	Explosive	Placement Condition	Placement Hole Diameter (mm)	Charge Weight (kg)	Ice Thickness (m)	Placement Depth (m)	Water Depth (m)	Crater Radius (m)
43	2	DM 12	3 x Optimum	152.4	2.25	0.394	0.82	-	3.32
44					4.50	0.368	0.77	-	4.24
45	2	DM 12	5.5 x Optimum	152.4	0.50	0.394	0.78	4.71	1.75
46					1.00	0.394	0.78	4.64	2.42
47					2.25	0.387	0.77	4.74	3.45
48					4.50	0.394	0.78	4.59	4.16
49	3	DM 12	1 CER SOP	152.4	2.25	0.406	1.50	-	3.53
50					2.25	0.394	1.54	-	3.33
51	4	DM 12	'Deep'	304.8	20.00	0.334	1.83	8.81	6.26
52					25.00	0.367	1.83	8.78	7.40
53	5	DM 12	'Deep'	152.4	0.25	0.368	0.61	8.17	1.90
54					0.25	0.368	0.91	8.17	1.11
55					0.25	0.356	1.22	8.18	0.56
56					0.25	0.356	1.83	8.18	0.79
57	5	DM 12	'Deep'	152.4	1.00	0.356	0.91	8.18	2.57
58					1.00	0.356	1.22	8.18	2.26
59					1.00	0.356	1.52	8.18	1.28
60					1.00	0.356	1.83	8.18	1.01
61	6	DM 12	Optimum	152.4	1.50	0.356	0.14	4.22	3.23
62					1.50	0.356	0.14	4.22	2.70
63					1.50	0.356	0.14	3.99	3.24
64					1.50	0.356	0.14	3.91	3.27

TABLE 1

(Continued)

Shot No	Expt No	Explosive	Placement Condition	Placement Hole Diameter (mm)	Charge Weight (kg)	Ice Thickness (m)	Placement Depth (m)	Water Depth (m)	Crater Radius (m)
65	Add 6	DM 12	Optimum	152.4	1.50	0.356	0.14	3.61	2.89
66					1.50	0.356	0.14	3.45	2.97
67	Add 7	40% Forcite	3 x Optimum	152.4	0.60	0.346	0.47	4.25	1.82
68					1.20	0.349	0.73	4.32	2.70
69					2.25	0.356	0.74	4.32	3.50
70					4.51	0.330	0.70	4.34	4.02
71	Add 7	40% Forcite	5.5 x Optimum	152.4	0.60	0.356	0.69	4.27	2.11
72					1.20	0.349	0.73	4.48	2.42
73					2.25	0.356	0.70	3.99	2.88
74					4.51	0.375	0.74	3.84	4.42
75	Add 7	Amex II	3 x Optimum	152.4	0.57	0.381	0.79	4.45	1.03
76					1.13	0.387	0.82	4.39	2.72
77					2.27	0.394	0.82	4.38	3.60
78					4.54	0.394	0.82	4.38	3.75
79	Add 7	Amex II	5.5 x Opt	152.4	2.27	0.387	0.53	4.34	3.35
80	Add 7	Hydromex	3 x Optimum	152.4	0.57	0.356	0.74	4.27	1.09
81					1.13	0.387	0.73	4.19	1.71
82					2.27	0.356	0.74	4.75	1.12
83					4.54	0.387	0.81	4.74	1.11
84	Add 7	Hydromex	5.5 x Opt	152.4	4.54	0.343	0.77	4.25	1.15

TABLE 1

(Concluded)

Shot No	Expt No	Explosive	Placement Condition	Placement Hole Diameter (mm)	Charge Weight (kg)	Ice Thickness (m)	Placement Depth (m)	Water Depth (m)	Crater Radius (m)
85	3	DM 12	Surface	-	9.00	0.395	-0.39	-	1.86
86					18.00	0.395	-0.39	-	2.99

All placement depths and depths of water measured from ice/water interface.

- Notes:
1. Charge placed in 76 mm (3 in) hole in surface of the ice and tamped with snow.
 2. Charge placed at ice/water interface.
 3. Single shots using 1 CER's SOP for comparison to results of Experiment 1.
 4. Additional shots for 'large scaled ice thickness'.
 5. Additional shots for 'small scaled ice thickness'.
 6. Single shots from 'row charge' where craters did not connect.
 7. Additional shots using commercial explosives.
 8. Crater radius large. Ice bordering crater 'bent up', suspect crater measurement taken to outside of raised lip rather than inside of true crater.
 9. Crater radius small. Suspect partial detonation of charge due to water seepage or insufficient loading density.

6.2 Analysis of Optimum Conditions

The placement of single charges for Experiment 2 and the related additional single charges had been determined from Mellor's preliminary relationships for blasting floating ice sheets (Equations 8a, 8b and 8c). It was planned to compare the results of the Chilcotin experiments with the calculated crater radii from Mellor's analysis to see how well that analysis predicted the independent data. However, the coefficients for Mellor's regression analysis had not been published, and had since been lost (Mellor, 1980, Personal Communication). It was therefore necessary to try and replicate the original analysis. Mellor had indicated (Personal Communication) that those data where the charges had been placed above the lower ice surface were omitted from his analysis. Presumably this was due to the similitude restriction mentioned in Chapter 2 regarding detonations in the same atmosphere. Therefore that same data was omitted from the analysis contained herein.

6.2.1 Retrieval of Mellor's 1972 Regression Analysis

With metrification in Canada, the Chilcotin data had been collected using the System International (SI) units. Therefore the retrieval of the regression analysis was carried out with the original data converted to SI as well. The original data: Van Der Kley (1965), Purple (1965), Barash (1966), Wade (1966), Kurtz et.al. (1966), Frankenstein and

Smith (1966) and Mellor and Kovacs (1972) are given in Appendix A. Where Mellor had included a certain number of data sets 'n' times in his analysis to weight reported average values of repeated tests (where 'n' was the square root of the number of tests the reported averages were for), this was carried out for the analysis contained herein.

The regression was carried out using the "Biomedical Computer Programs P-Series - BMDP" (Dixon and Brown, 1979).

The initial analysis undertaken was a straight multiple linear regression of the scaled crater radius as a function of nine terms involving the independant scaled ice thickness and charge placement depth, ie:

$$Y = a + b_1X_1 + b_2X_2 + b_3X_1^2 + b_4X_1X_2 + b_5X_2^2 + b_6X_1^3 \\ + b_7X_1^2X_2 + b_8X_1X_2^2 + b_9X_2^3 \quad \dots(7)$$

The straight multiple linear regression model would not, however, retain all nine of the terms in the above equation, as a built-in tolerance limit caused the program to reject some of them. The 'tolerance limit' is described elsewhere (Dixon and Brown, 1979). Because of this tolerance limit a term (variable) would be rejected if it was too highly correlated with another independant term ($r^2 > 0.99$ between the two), or, if its entry would cause the r^2 value between two independant terms already accepted into the equation, to exceed the tolerance limit.

This straight multiple linear regression program

omitted the terms with coefficients b_2 , b_3 and b_7 from the final regression equation because of the tolerance limit. This was contrary to Mellor's findings, in that he had omitted the terms with coefficients b_1 and b_4 from his final analysis because of their insignificance. Because of the tolerance restriction, Mellor's analysis could not be replicated with this simple regression program.

A second regression analysis was attempted using a forward stepping, stepwise multiple linear regression program. The program selected variables (terms) of Equation 7 for entry in a manner designed to maximize the F-ratio, which is a test of the significance of the coefficients of the independent variables in the regression equation. Using this treatment only four of the nine terms were entered into the regression equation because of the tolerance limit. The terms entered were those with coefficients b_1 , b_4 , b_8 and b_9 , giving a multiple correlation coefficient of 0.623. The inclusion of terms with coefficients b_1 and b_4 was contrary to Mellor's findings, and somewhat surprising, as the only two terms omitted by Mellor were included in the regression equation using this treatment.

Mellor's regression analysis was finally replicated using a third regression treatment. This third program (BMDP - P9R) analyses all possible subsets of the data entered, and, allows the suppression of the tolerance limit to an extremely low value. With this model, one possible explanation of why Mellor omitted the particular terms he did (in con-

trast to the above regression which retained these terms) was discovered. In the first program run, the multiple correlation coefficient (r) was 0.692 (cf Mellor's 0.695), but the contribution to the multiple r^2 by the term with coefficient b_1 was only 0.0005, the smallest contribution of any of the terms, and which is negligible. The contribution from the term with coefficient b_4 was 0.0013 for the first run. Leaving the term with coefficient b_1 out of a second run resulted in a multiple correlation coefficient of 0.691, with the contribution of the term with coefficient b_4 to the multiple r^2 being only 0.0035, the lowest contribution of the remaining terms. Omitting this second term from a third run resulted in a multiple correlation coefficient of 0.689.

The following summarizes the statistical parameters reported by Mellor (1972) for the regression analysis, as well as that produced from the last analysis described above:

	Mellor (English Units)	Mellor (SI)	This Analysis (SI)
Mean (of predicted)	-	-	2.102
Standard Error of Estimate	1.377	0.546	0.550
Multiple Correlation			
Coefficient (r)	0.6945	-	0.6889
Multiple r^2	0.4823	-	0.4745
F Statistic	21.69	-	21.03
Degrees of Freedom	163	-	163
Number of Parameters	7	-	7

From the above statistical parameters it can be seen that the regression analysis carried out on the original data is comparable to Mellor's. The regression equation obtained from this analysis was:

$$\begin{aligned}
 Y = & 1.547 + 7.728(X_2) - 0.419(X_1^2) - 14.828(X_2^2) \\
 & + 0.141(X_1^3) - 0.551(X_1^2X_2) + 1.317(X_1X_2^2) \\
 & + 6.593(X_2^3) \quad \dots (12)
 \end{aligned}$$

The comparison between predicted and observed scaled crater radius for Mellor's data is shown in Figure 18. The skew of the data about the theoretical line of best fit shows that Equation 12 underpredicts the larger values of scaled crater radius, and overpredicts the smaller ones. Thus, either the terms of the regression model used by Mellor (Equation 7) do not fully account for all of the phenomena involving the three nondimensional parameters included in it, or, one or more of the terms of the general nondimensional relationship of Equation 2 (Chapter 2) need to be included in a regression analysis to more fully explain the phenomena. As this first analysis was only to replicate Mellor's original analysis, no attempt was made to include more variables than he had used.

The comparison between crater radius calculated using Equation 12 and observed crater radius for Mellor's data is shown in Figure 19. From this it can be seen that although there is a marked skew in the scaled data (Figure 18), Equa-

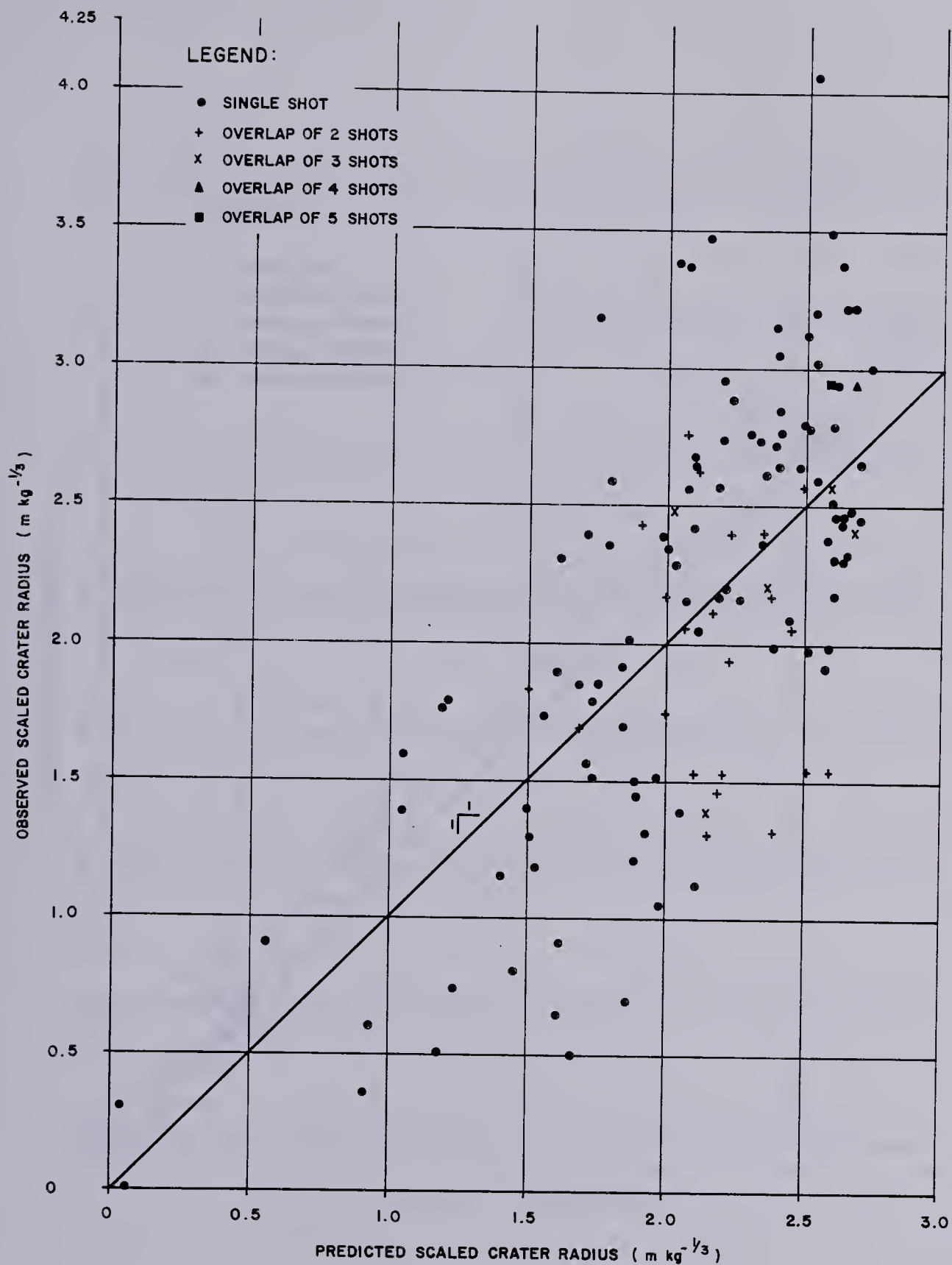


FIGURE 18
 PREDICTED AND OBSERVED SCALED CRATER RADIUS
 MELLOR'S DATA

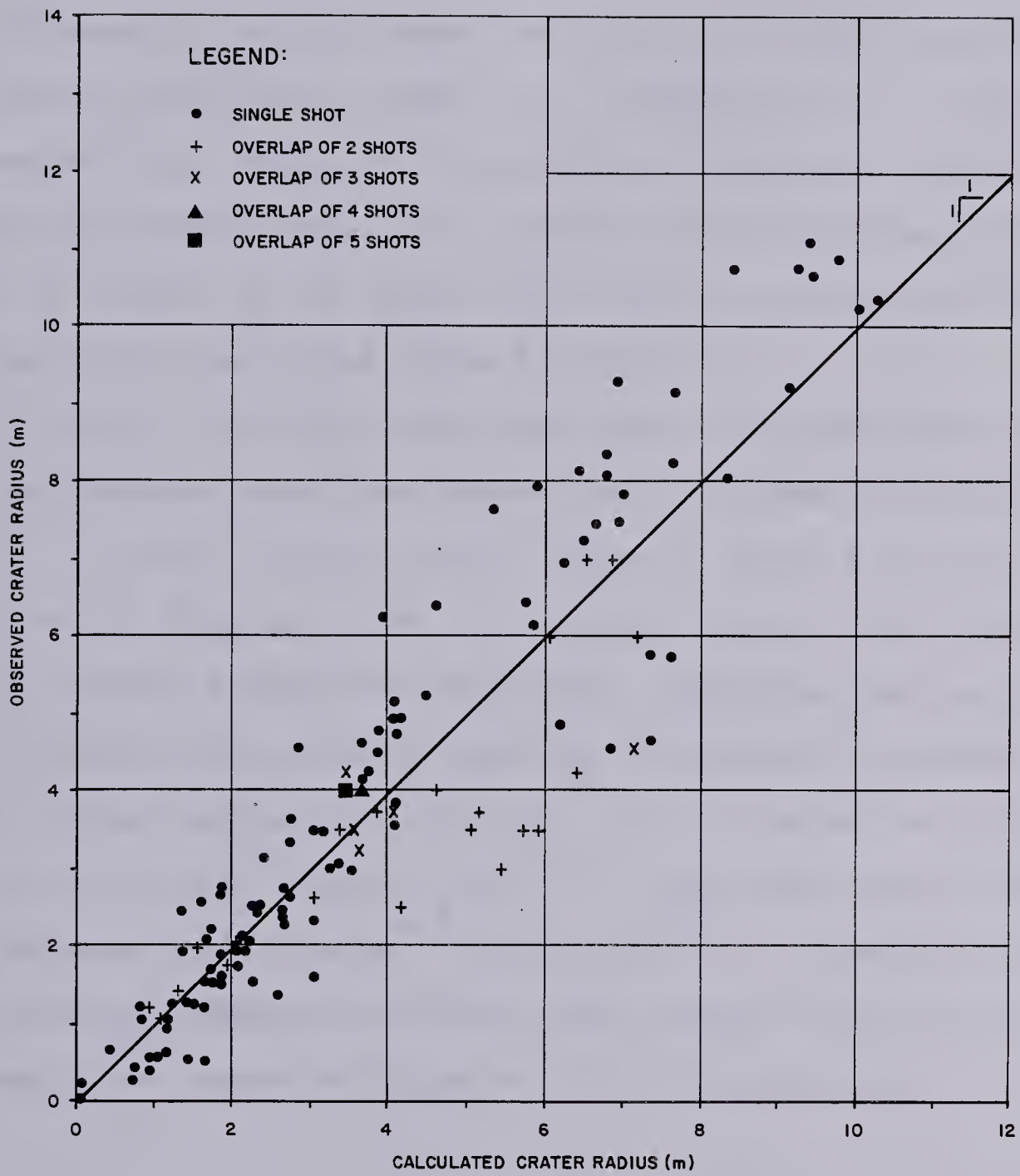


FIGURE 19
CALCULATED AND OBSERVED CRATER RADIUS
MELLOR'S DATA

tion 12 provides a reasonable means of predicting the crater radius.

The Chilcotin data were analysed in a similar fashion. Figures 20 and 21 show the results of this analysis, and confirm that while there is a suggestion of a skew in the scaled data, Equation 12 provides a reasonable method of predicting crater radius. The three outlying Hydromex shots shown in Figure 21 are those which were considered to have only partially detonated (Note 9 of Table 1).

Mellor (1972) had indicated that "maximum crater radius is achieved when the scaled ice thickness is about $10^{1/3}$ in/lb ...[and]...scaled charge depth is about $0.3 \text{ ft/lb}^{1/3}$ " which could then be used to design optimum performance blasts in ice of specified thickness. Computing the maximum of the surface described by Equation 11 yielded a maximum scaled crater radius of $2.73 \text{ m/kg}^{1/3}$ for a scaled ice thickness of $0.34 \text{ m/kg}^{1/3}$ ($10.4 \text{ in/lb}^{1/3}$), when the scaled depth of placement is $0.13 \text{ m/kg}^{1/3}$ ($0.34 \text{ ft/lb}^{1/3}$). Therefore with ice thickness measured in metres, the optimum conditions for ice demolition based on Equation 12 are described by:

$$W = 25 t_i^3 \quad \dots (13a)$$

$$d = 0.4 t_i \quad \dots (13b)$$

$$\text{to give: } R = 8 t_i \quad \dots (13c)$$

where W is in kilograms, d and R are in metres.

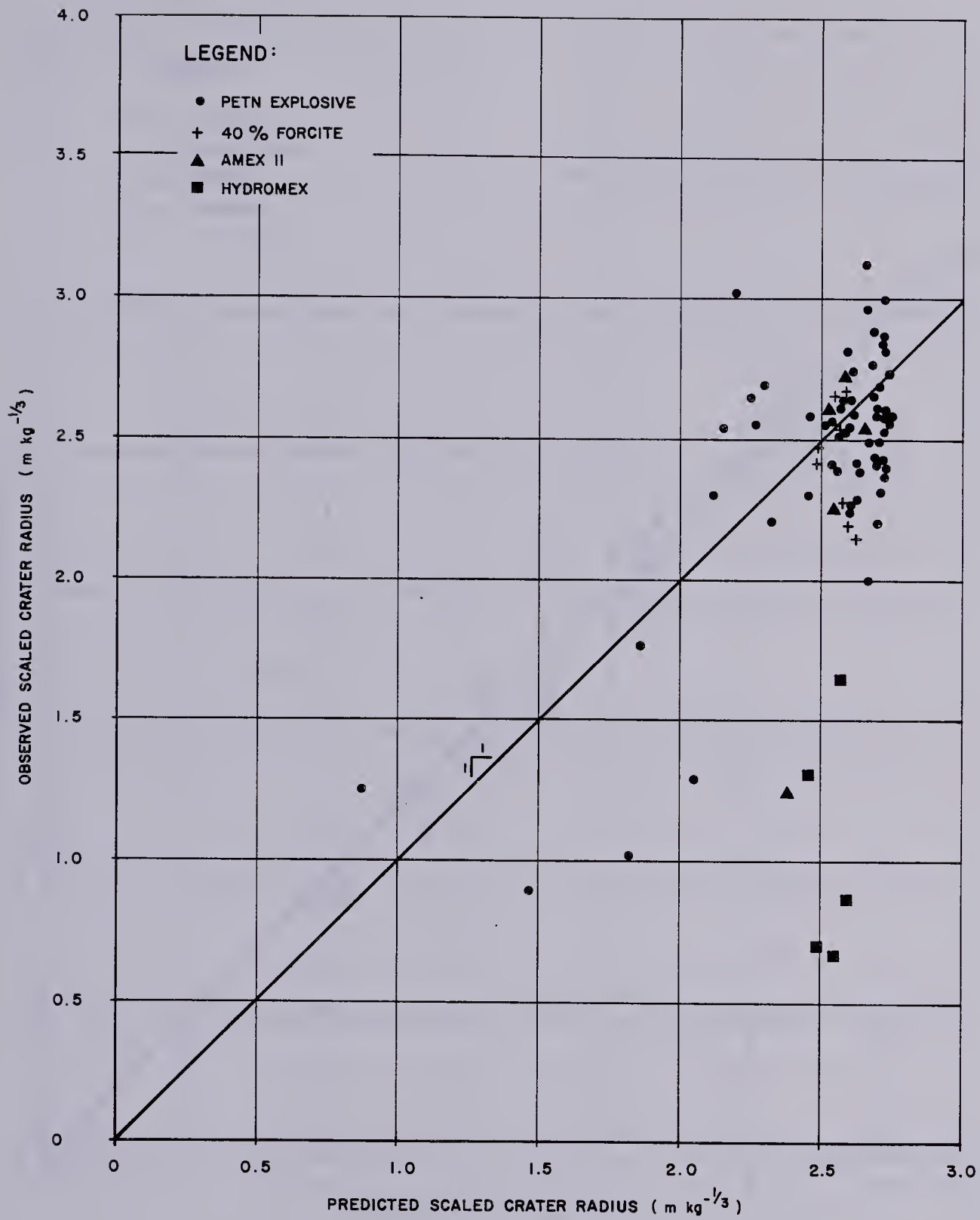
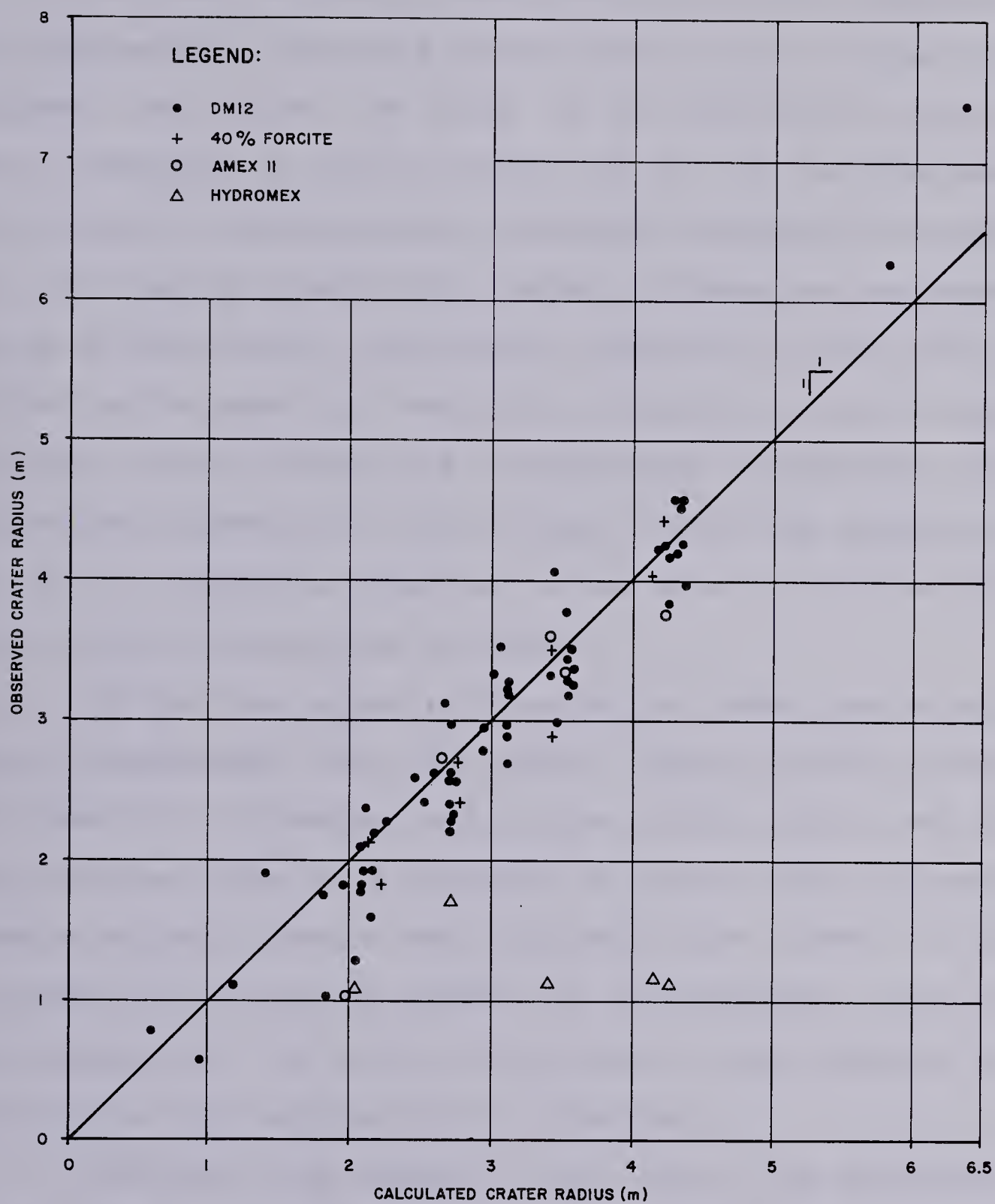


FIGURE 20
CALCULATED AND OBSERVED SCALED CRATER RADIUS
CHILCOTIN DATA



6.2.2 Regression with Additional Terms in the Model

As there had been a pronounced skew in the comparison of observed and calculated scaled crater radius, it was considered that either the terms of the regression equation were inadequate to fully account for all of the phenomena involving the nondimensional parameters included in the model, or, that an insufficient number of dimensionless parameters of the general relationship (Equation 2) had been included in the model to begin with. Equation 4 was the most complete of the simplified dimensionless functional relationships, therefore it was decided to try and improve the fit of the regression equation to the data by incorporating more of the terms of that equation.

Of the six terms in Equation 4, three had already been incorporated into the model, leaving scaled charge placement hole diameter, scaled gas bubble radius and the gravitational term to be included. Of these, only the experiments reported herein had considered the effect of the placement hole, thus the effects of this parameter could not be assessed for the whole of the data, as the required dimension was not reported in the literature.

Similarly, the effect of the size of the gas bubble could not be assessed. Although Cole (1948) had documented the gas bubble produced by the underwater detonation of TNT charges, and had presented an equation for the determination of the radius of the gas bubble in terms of the energy of detonation and the pressure at the detonation depth, there

was insufficient information for the explosives reported in the ice demolition literature to determine the gas bubble size for each of the shots in the data set analysed by Mellor.

A number of equations describing the size of the gas bubble have been reported in the literature since Cole's equation (Kurtz et.al, 1966; Jordaan, 1969 and Nikolayev, 1971), which have been summarized in Appendix C. These again relate the resulting gas bubble radius to either the energy or heat of detonation and the pressure at the explosion depth. Meyer (1977) had given the volume of detonation gases, as well as other properties (Table B-5), for a number of pure explosive compounds. A comparison of the volume of detonation gases and the explosive specific energy reported by Meyer shows that the two are not necessarily directly related. Most of the explosives reported in the ice demolition literature were not pure explosive compounds, but were mixtures of these. As it was not known exactly how the properties of explosives which affect the production of gases would combine in the explosive mixtures, the determination of the gas bubble radius for each of the shots in Mellor's data set was not possible. Therefore, the effect of gas bubble radius on the overall ice demolition relationship could not be included in the analysis being considered.

Therefore, to assess the effect on scaled crater radius of other parameters from the general nondimensional ice demolition relationship, only the gravitational term could

be included into the regression model. The parameter was included as a first order term in the regression model. A second analysis of the data analyzed by Mellor, including this new term, showed a very slight improvement in the multiple correlation coefficient and standard error of estimate for the resulting regression equation. The improvement, however, was only in the order of 0.1%.

As this analysis had shown that the effects of gravity on the resulting scaled crater radius relationship were negligible, and as there was insufficient data to incorporate either of the other two terms of Equation 4 remaining, subsequent regression analyses were carried out using only the regression model formulated by Mellor.

6.2.3 Regression with Extended Data

Until the experiments conducted for this thesis, only one data set could be found which was published since Mellor conducted his analysis. This was Nikolayev's (1970) data for single charges, the reference for which was not translated until 1973.

The data compiled by Mellor, and that given by Nikolayev and this thesis were combined and analysed by regression in the same manner as previously described. In all, 264 data sets were included in the analysis. In this analysis it was found that the terms of Equation 7 with coefficients b_1 and b_4 could again be omitted from the final regression equation due to their low contribution to the

multiple r^2 .

The statistical parameters associated with this analysis are given below with those obtained previously using only Mellor's original data.

	Mellor's Data Only	Extended Data
Mean	2.102	2.195
Standard Error of Estimate	0.550	0.518
Multiple Correlation Coefficient	0.6889	0.6551
Multiple r^2	0.4745	0.4136
F Statistic	21.03	27.50
Degrees of Freedom	163	256
Number of Parameters	7	7

As can be seen from the above, the regression equation obtained with the extended data has a slightly lower multiple correlation coefficient. The regression equation obtained was:

$$\begin{aligned}
 Y = & 1.768 + 5.473(X_2) - 0.395(X_1^2) - 10.559(X_2^2) \\
 & + 0.130(X_1^3) - 0.462(X_1^2X_2) + 0.951(X_1X_2^2) \\
 & + 4.462(X_2^3) \quad \dots (14)
 \end{aligned}$$

The comparison between crater radius calculated with Equation 14 and that observed in the field, for all data sets, is shown in Figure 22. Note that not all of the DM-12

LEGEND:

- | | |
|------------------|--------------------------|
| □ ANFO | ◇ 40 % GELATINE DYNAMITE |
| • C-4 | ▽ MILITARY DYNAMITE |
| △ TNT | ◆ HBX-3 |
| X GUNCOTTON | ▼ TROTYL |
| ■ GUNPOWDER | ○ DM 12 |
| ● DUTCH DYNAMITE | ▼ 40 % FORCITE |
| + DUTCH TNT | ■ AMEX |
| | ▲ HYDROMEX |

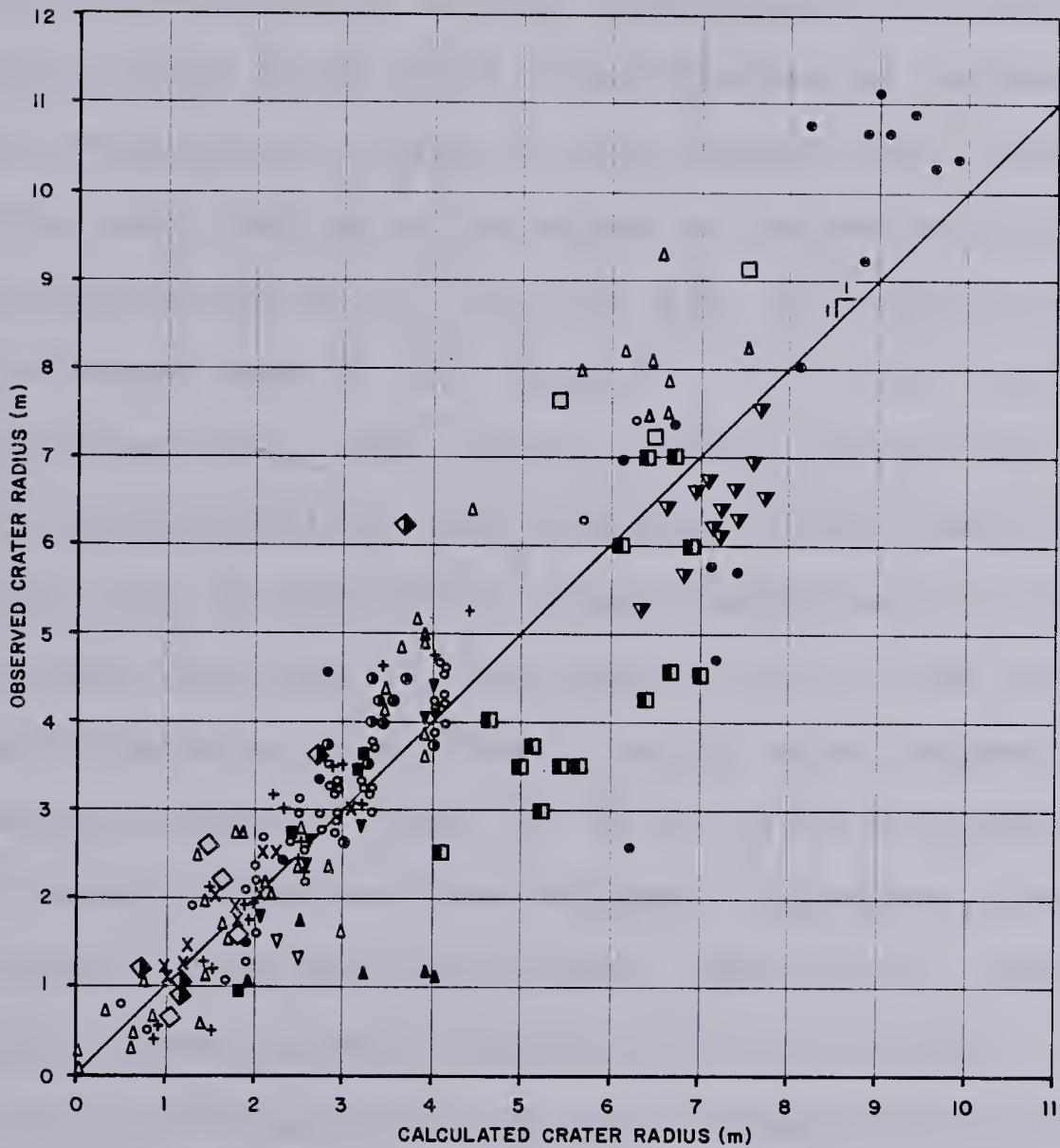


FIGURE 22
 CALCULATED AND OBSERVED CRATER RADIUS
 ALL DATA
 EXPLOSIVES AS ORIGINALLY REPORTED

shots from the Chilcotin tests are shown in the figure, as the density of plotted points in the range $1.0 < R < 3.0$ was too great. The figure shows that Equation 14 tends to under-predict the crater radius for larger craters, as was noted in the previous section with Equation 12.

Kurtz et.al. (Section 3.2.5) had encountered some difficulty in determining optimum conditions due to the "uncertainties in the comparative effectiveness of various explosives". Therefore, Figure 22 was plotted with different symbols for each explosive in order to determine if there was any stratification of the data due to explosive type. The figure shows that in the range $R > 2.0$, the more brisant explosives (C-4, TNT, Dutch Dynamite, Dutch TNT) tend to produce larger craters than calculated. The less brisant explosives, such as gunpowder, which should have a greater lifting effect than the brisant explosives, do not produce as large a crater as their charge weight alone suggests. It is noteworthy, however, that two shots using gunpowder and three of ANFO, which are not brisant explosives, created larger craters than was calculated. These shots were for substantial charge weights, ranging from 25 to 68 kg.

The stratification of the more brisant explosives is particularly noticeable, over the whole range of crater radii, for the TNT shots. Only a few, and those for smaller charges, produced craters smaller than calculated, whereas four shots of the explosive C-4 produced smaller craters, in the mid-range, than calculated. Comparison of the scaled



data for these four indicated that the scaled depth of placement for each had been large, which would account for the smaller craters (See Figure 7).

The replication of Mellor's analysis, and this last analysis using the extended data, had used the charge weight as reported in the literature for each type of explosive. In order to assess the finding that brisant explosives were producing larger craters than the regression equation predicted, based on charge weight, it was necessary to convert or 'normalize' the charge weights reported to some common explosive base.

6.2.4 Analysis with 'Normalized' Explosive Weights

In the discussion of explosives in Chapter 4, it was noted that a variety of means were available to compute equivalent weights of different explosives. What was not clear from the literature, however, was which blasting performance criteria is invoked in an equivalency calculation using the various means available. That is, given that there are at least two performance criteria, being a lifting or 'strength', and a shattering or 'brisance' (Section 4.3), the literature does not elucidate which of these is invoked if, say, Grade Strength or Relative Bulk Strength are used in the determination of equivalent weights of different explosives.

Table 2 lists the explosives reported in the ice demolition literature, along with those used in the Chilco-

the first of these is the fact that the
the second is the fact that the
the third is the fact that the
the fourth is the fact that the
the fifth is the fact that the
the sixth is the fact that the
the seventh is the fact that the
the eighth is the fact that the
the ninth is the fact that the
the tenth is the fact that the
the eleventh is the fact that the
the twelfth is the fact that the
the thirteenth is the fact that the
the fourteenth is the fact that the
the fifteenth is the fact that the
the sixteenth is the fact that the
the seventeenth is the fact that the
the eighteenth is the fact that the
the nineteenth is the fact that the
the twentieth is the fact that the
the twenty-first is the fact that the
the twenty-second is the fact that the
the twenty-third is the fact that the
the twenty-fourth is the fact that the
the twenty-fifth is the fact that the
the twenty-sixth is the fact that the
the twenty-seventh is the fact that the
the twenty-eighth is the fact that the
the twenty-ninth is the fact that the
the thirtieth is the fact that the
the thirty-first is the fact that the
the thirty-second is the fact that the
the thirty-third is the fact that the
the thirty-fourth is the fact that the
the thirty-fifth is the fact that the
the thirty-sixth is the fact that the
the thirty-seventh is the fact that the
the thirty-eighth is the fact that the
the thirty-ninth is the fact that the
the fortieth is the fact that the
the forty-first is the fact that the
the forty-second is the fact that the
the forty-third is the fact that the
the forty-fourth is the fact that the
the forty-fifth is the fact that the
the forty-sixth is the fact that the
the forty-seventh is the fact that the
the forty-eighth is the fact that the
the forty-ninth is the fact that the
the fiftieth is the fact that the
the fifty-first is the fact that the
the fifty-second is the fact that the
the fifty-third is the fact that the
the fifty-fourth is the fact that the
the fifty-fifth is the fact that the
the fifty-sixth is the fact that the
the fifty-seventh is the fact that the
the fifty-eighth is the fact that the
the fifty-ninth is the fact that the
the sixtieth is the fact that the
the sixty-first is the fact that the
the sixty-second is the fact that the
the sixty-third is the fact that the
the sixty-fourth is the fact that the
the sixty-fifth is the fact that the
the sixty-sixth is the fact that the
the sixty-seventh is the fact that the
the sixty-eighth is the fact that the
the sixty-ninth is the fact that the
the seventieth is the fact that the
the seventy-first is the fact that the
the seventy-second is the fact that the
the seventy-third is the fact that the
the seventy-fourth is the fact that the
the seventy-fifth is the fact that the
the seventy-sixth is the fact that the
the seventy-seventh is the fact that the
the seventy-eighth is the fact that the
the seventy-ninth is the fact that the
the eightieth is the fact that the
the eighty-first is the fact that the
the eighty-second is the fact that the
the eighty-third is the fact that the
the eighty-fourth is the fact that the
the eighty-fifth is the fact that the
the eighty-sixth is the fact that the
the eighty-seventh is the fact that the
the eighty-eighth is the fact that the
the eighty-ninth is the fact that the
the ninetieth is the fact that the
the ninety-first is the fact that the
the ninety-second is the fact that the
the ninety-third is the fact that the
the ninety-fourth is the fact that the
the ninety-fifth is the fact that the
the ninety-sixth is the fact that the
the ninety-seventh is the fact that the
the ninety-eighth is the fact that the
the ninety-ninth is the fact that the
the hundredth is the fact that the

TABLE 2Summary of Explosives Used in Ice Demolition

Reference	Explosives	Comments
Van Der Kley	Gunpowder Dynamite Guncotton American TNT Dutch TNT Plastic Explosive	Type not Specified Nitrocellulose Not Specified
Purple	C-4	
Barash	TNT HBX-3	Not Identified
Wade	ANFO	
Kurtz et.al.	C-4 TNT ANFO	
Frankenstein and Smith	-	Not Specified
Nikolayev	Trotyl	Soviet Explosive (Tetryl, Tetrytol ?)
Mellor and Kovacs	40% Gelatin Dynamite Military Dynamite	
This Thesis	DM-12 40% Forcite Amex II Hydromex	PETN Explosive Gelatin Dynamite ANFO Blasting Agent ANFO Blasting Slurry

tin experiments.

The primary and secondary explosives' properties listed in Table B-5 of Appendix B are for individual or pure explosive compounds, not for mixtures of compounds, which is what the majority of the explosives listed in Table 2 are. Therefore methods other than those listed in Table B-5 had to be found as a means of determining equivalent weights of explosives. Fortunately, the equivalency method used by the CAF and the U.S. Forces - the Effectiveness as an External Charge (hereafter referred to as 'effectiveness') - is listed in Table B-4 for most of the explosives shown in Table 2.

It was not known precisely what this 'effectiveness' measured. However, as outlined in Section 4.3.5, the comparison is as an external breaching charge, as most military demolition tasks are concerned with shattering the target. It was therefore presumed that 'effectiveness' was a measure comparable to brisance. Further, it had been noted (Section 4.3) that a brisance "value" (Meyer, 1977) is determined as the product of loading density, specific energy of the explosive and detonation rate. Thus there should be a relationship between 'effectiveness' and specific energy. The 'effectiveness' values given in Table B-4 are those for the particular explosives relative to that of TNT. Therefore the relationship postulated between 'effectiveness' and specific energy should really be between 'effectiveness' and the ratio of the explosive's specific energy to that of TNT.

A comparison of the properties given in Tables B-4

and B-5 reveals that both 'effectiveness' and specific energies are given for only three explosives: TNT, Tetryl and PETN. This is because Meyer only listed data for single compounds, not mixtures. In his discussion of thermodynamic calculation of decomposition reactions, Meyer (1977) stated "The chemical formula of mixtures may be obtained by [percent] addition of the atom numbers of the components...". Throughout his example calculation, Meyer continued to utilize percent addition of thermodynamic properties (volume of detonation gases, energies of formation, enthalpies of formation, etc.) to arrive at final values for his example explosive. Therefore, as the percent composition of a good number of the explosive mixtures listed in Table B-4 could be found in the literature (Meyer, 1977 ; Hemphill, 1981), it was decided to use this method to determine the specific energies of the explosive mixtures. The calculated specific energies would be somewhat inaccurate because, as was indicated in Chapter 4, the primary constituents of an explosive are not the only energy producing ingredients. Therefore the energy producing ability of the secondary ingredients in the mixtures may not be fully accounted for in this type of analysis.

Table 3 lists explosives and 'effectiveness' ratios from Table B-4 for a number of explosives, the percent composition of the explosive mixtures in the group, and gives the calculated ratio of specific energy to that of TNT. These results are plotted in Figure 23. Except for the cal-

TABLE 3

Calculation of Specific Energy Ratios

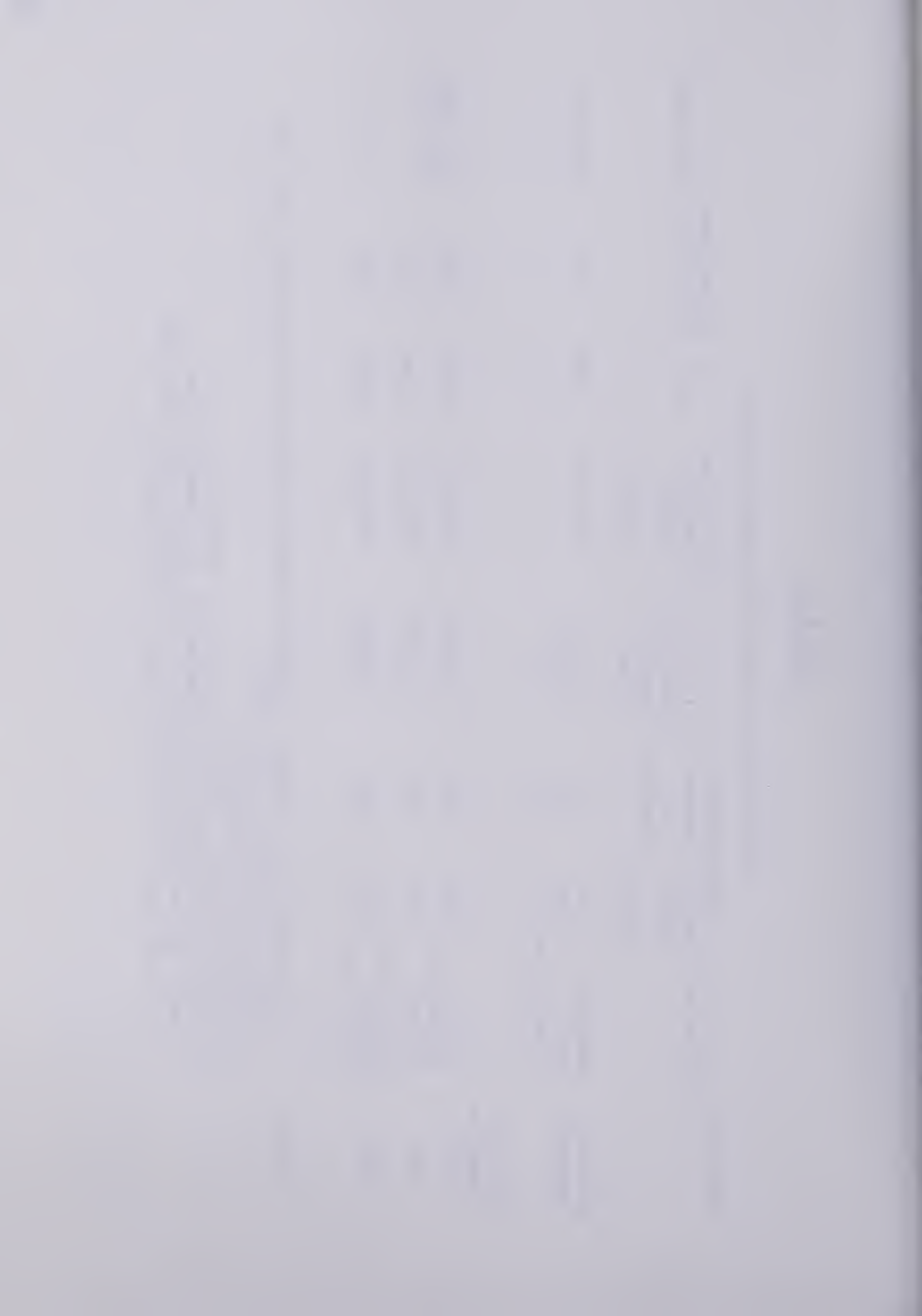
Explosive	Explosive	Specific Energy f _f (kJ/kg)	Constituents Percent of Mixture	Contribution to Specific Energy (kJ/kg)	Calculated Specific Energy f _c (kJ/kg)	f _c /f	Effective- ness Ratio	Referencel
TNT	TNT	838	100	838.		1.000	1.00	Meyer
Tetryl PETN	Tetryl	1069	100	1069.		1.276	1.25	Meyer
	PETN	1338	100	1338.		1.597	1.66	Meyer
Tetrytol	Tetryl	1069	75	801.75	1011.25	1.207	1.20	Hemphill
	TNT	838	25	209.50				
Tetrytol	Tetryl	1069	70	748.30	999.70	1.193	1.20	Meyer
	TNT	838	30	251.40				
Composition B	Hexogen	1354	60	812.40	1139.22	1.359	1.35	Hemphill
	TNT	838	39	326.82				
Composition B	Wax	-	1	-				
	Hexogen	1354	60	812.40	1147.60	1.369	1.35	Meyer
Composition C-3	TNT	838	40	335.20				
	Hexogen	1354	79	1069.66	1069.66	1.276	1.34	Hemphill
Composition C-3	Plasticiser ²	-	21	-				
	Hexogen	1354	78	1056.12	1056.12	1.260	1.34	Meyer
Composition C-4	Plasticiser ³	-	22	-				
	Hexogen	1354	91	1232.14	1232.14	1.470	1.34	Hemphill
Composition C-4	Plasticiser ⁴	-	9	-				
	Hexogen	1354	90	1218.60	1218.60	1.454	1.34	Meyer
Composition C-4	Poyliso-	-						
	butylene ⁵	-	10	-				

TABLE 3
(Continued)

Calculation of Specific Energy Ratios						
Explosive	Explosive Specific Energy f (kJ/kg)	Constituents Percent of Mixture	Contribution to Specific Energy (kJ/kg)	Calculated Specific Energy f _C (kJ/kg)	f _C /f	Effective-ness Ratio Reference ¹
Military Dynamite	Hexogen	1354	75	1015.50	1.362	0.92
	TNT	838	15	125.70		
	Plasticiser ²	-	10	-		
Straight Dynamite 40%	Nitro-glycerine	1318	40	527.20	0.629	0.65
	50%	1318	50	659.00		
	60%	1318	60	798.80		
	Nitro-glycerine				0.944	0.83

U.S. Army
FM 5-34

- Notes:
1. References cited report slightly different percent compositions for the explosives given in this table
 2. Unspecified plasticiser.
 3. Meyer indicates this plasticiser is explosive.
 4. Hemphill indicates this plasticiser is nonexplosive.
 5. Meyer gives polyisobutylene as the plasticiser, but does not indicate if it is explosive or nonexplosive.



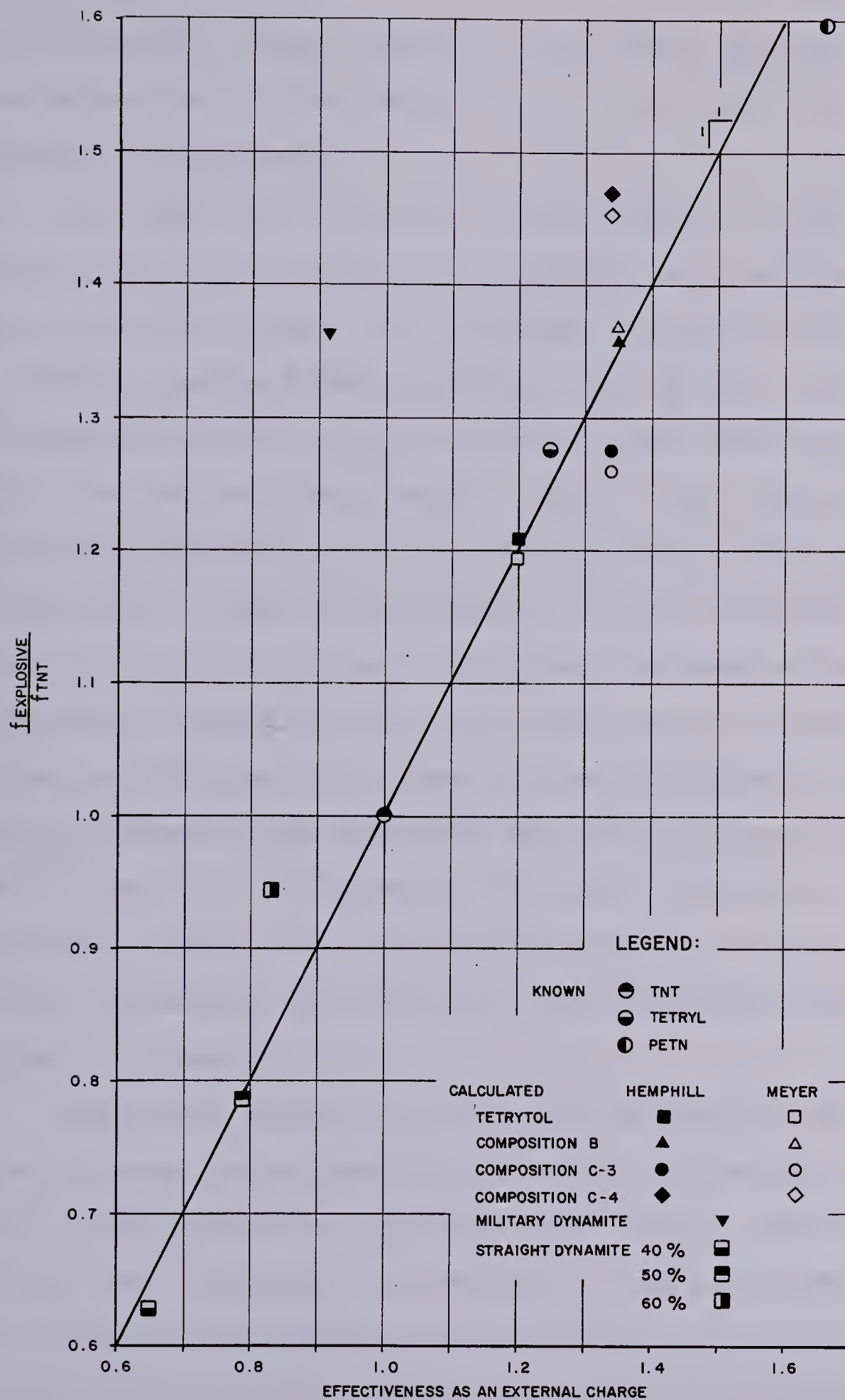


FIGURE 23

'EFFECTIVENESS AS AN EXTERNAL CHARGE' AS A SPECIFIC ENERGY INDICATOR

culated specific energy ratio for Military Dynamite, the figure shows that 'effectiveness' is a fairly good indicator of specific energy ratio.

The data for which an 'effectiveness' ratio was available was: Van Der Kley, for Gunpowder and American TNT; Purple, for C-4; Barash, for TNT; Wade, for ANFO; Kurtz et. al. for C-4, ANFO and TNT; and Mellor and Kovacs, for Military Dynamite and 40% Gelatin Dynamite. The remaining data, mostly from Van Der Kley, was not used in the following analysis as either there was no 'effectiveness' ratio, or it was uncertain if the 'effectiveness' ratios available were applicable to the particular explosive. For example the 'effectiveness' of Dutch TNT may not be the same as for American TNT due to different additives in the explosive mixture. Finally, the particular explosive may not have been described sufficiently in the reference to permit assigning an 'effectiveness' ratio, for example Dutch Dynamite" was not sufficient to determine the dynamite type (straight, gelatin or ammonia), or grade.

The charge weights for the data originally analysed by Mellor were normalized to an energy equivalent charge weight of TNT using the 'effectiveness' ratio. The normalized data were analysed by regression in the manner described previously. The appropriate statistical properties of the analysis are given below for both (i) using all of the terms of Equation 7, and (ii) omitting those terms with coefficients b_1 and b_4 .

	All Terms	Reduced Terms
Mean	2.0856	2.0856
Standard Error of Estimate	0.6531	0.6471
Multiple Correlation Coefficient	0.6847	0.6830
Multiple r^2	0.4688	0.4665
F Statistic	8.53	11.12
Degrees of Freedom	87	89
Number of Parameters	9	7

The resulting regression equation, for the case of omitting the two terms, was:

$$\begin{aligned}
 Y = & 2.191 + 1.875(X_2) - 0.497(X_1^2) + 1.461(X_2^2) \\
 & + 0.174(X_1^3) - 0.836(X_1^2X_2) + 2.475(X_1X_2^2) \\
 & - 5.701(X_2^3) \quad \dots (15)
 \end{aligned}$$

As shown by the multiple correlation coefficient, Equation 15 fits the data almost as well as the replication of Mellor's analysis, for which Equation 12 was derived with a multiple correlation coefficient of 0.6889.

In order to incorporate the Chilcotin single charge data into the analysis, it too had to be converted to an energy equivalent weight of TNT. For the DM-12 charges an assumption had to be made. Table B-4 of Appendix B shows an 'effectiveness' ratio for PETN as 1.66. In the context in which this was given in the reference (U.S. Army FM 5-34, 1969), it must be assumed that the ratio is for pure PETN.

DM-12 however is an explosive mixture, only a percentage of which is PETN (Classified Reference). Therefore, making the assumption that the 'effectiveness' of DM 12 can be calculated as its PETN-content percentage of the 'effectiveness' of pure PETN, an 'effectiveness' ratio of 1.43 resulted. This was then used to determine the equivalent charge weight of TNT to give the same energy yield.

The conversion of the CIL explosives - 40% Forcite, Amex II and Hydromex - was not as simple. As indicated in Section 4.3.4, CIL does not report its explosives' strength parameters in the same manner as anyone else. Their 'Relative Weight Strength' (RWS) and 'Relative Bulk Strength' (RBS) are related to ANFO, hence no direct comparison could be made using the parameters they published and those given in Table B-4. The RWS and RBS for the explosives used in the Chilcotin experiments are given in Table B-7 (CIL,1980) as:

Explosive	Relative Weight Strength	Relative Bulk Strength
40% Forcite	79	135
Amex II (gravity loaded)	99	99
Hydromex (T3)	88	155

For Forcite CIL (1968) states: "In this gelatin [dynamite] a portion of the nitroglycerine is replaced by ammonium nitrate, thus it is sometimes referred to as an ammonia gelatin". Knowing from Table B-4 what the 'effectiveness' of gelatin and ammonia dynamites are, the 'effectiveness' of

Forcite can be selected if it can be determined with any finality exactly what Forcite is. As the difference between the 'effectiveness' of gelatin and ammonia dynamites is small, and as there is a certain percentage of ammonium nitrate in Forcite, it was assumed that the 'effectiveness' of 40% Forcite was that of 40% Ammonia dynamite.

As both the RWS and RBS of Amex, which is basically an ANFO explosive, are 99 (given that ANFO has an assigned RWS and RBS of 100), it was assumed that the 'effectiveness' of the U.S. Ammonium Nitrate cratering charge (which was further assumed to be straight ANFO) from Table B-4, could be applied to the Amex charges. This produced a slight discrepancy in the comparative effectiveness of the converted Forcite and Amex charges. The 'effectiveness' of Forcite was assumed to be 0.41 (for 40% Ammonia dynamite), which was only slightly less than the 0.42 assumed for Amex. The RWS of Forcite, however, is only 80% of that given by CIL for Amex. Thus while CIL states that Forcite is not as strong as Amex, it has been assumed herein, using the 'effectiveness' figures quoted, that Forcite is virtually as strong as Amex.

Hydromex is an ammonium nitrate and TNT slurry (CIL, 1968). As no information is given by CIL as to the exact composition of the mix, the strength parameters reported by CIL had to be used in the equivalency calculation. This was carried out by first computing the equivalent Amex charge weight for the Hydromex charges using the reported RWS (RWS was used as explosive weights were involved), then convert-

ing to TNT using the 'effectiveness' ratio assumed for Amex.

The number of shots of Forcite, Amex and Hydromex which were converted in the above manner were 8, 5 and 5 respectively. Given that the final set of normalized data included 177 shots, the error in equivalent TNT charge weights introduced by the gross assumptions indicated above, for 10% of the data set, was considered negligible.

Adding the converted Chilcotin data to that already converted, and analysing by regression in the manner previously outlined, gave the following statistical parameters for the analysis.

	All Terms	Reduced Terms
Mean	2.1810	2.1810
Standard Error of Estimate	0.6070	0.6101
Multiple Correlation Coefficient	0.6214	0.6102
Multiple r^2	0.3862	0.3724
F Statistic	11.67	14.32
Degrees of Freedom	167	169
Number of Parameters	9	7

The resulting regression equation, for the case of reduced terms in the regression model, was:

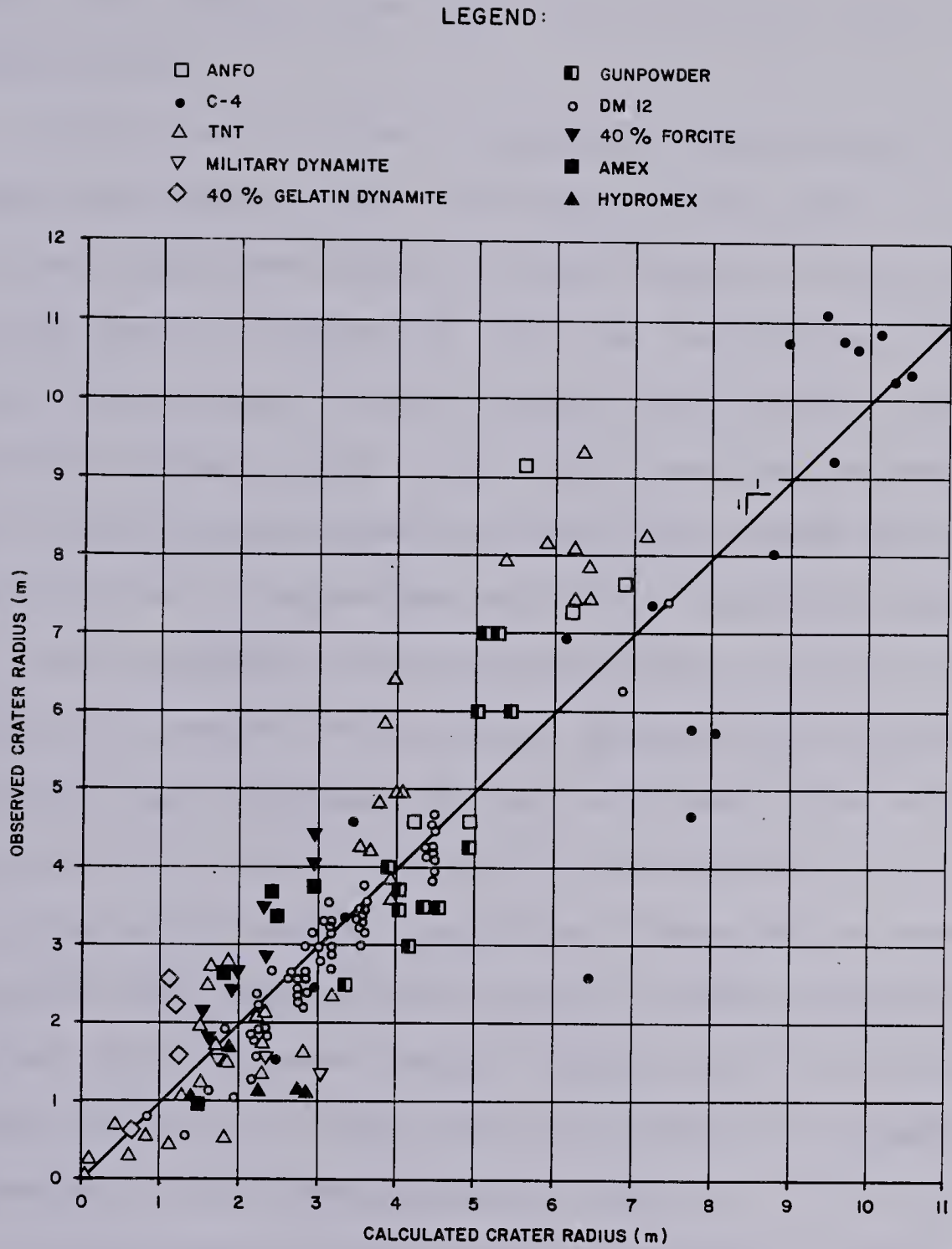
$$\begin{aligned}
 Y = & 2.458 - 1.392(X_2) - 0.430(X_1^2) + 7.576(X_2^2) \\
 & + 0.159(X_1^3) - 0.820(X_1^2X_2) + 2.352(X_1X_2^2) \\
 & - 8.779(X_2^3) \quad \dots (16)
 \end{aligned}$$

As was found earlier in the analysis of the data analysed by Mellor, converted to equivalent TNT charges, there is a decrease in the multiple correlation coefficient from the analyses using straight charge weight.

Two other regression analyses were conducted, with the equivalent TNT weights of the Forcite charges computed in the same manner as the Hydromex had been, ie converting Forcite to Amex, then to TNT. The resulting multiple correlation coefficients, however, were less than those given above. It was therefore decided to keep the regression where the Forcite charge weights had been converted using the 'effectiveness' ratio of 40% Ammonia dynamite.

The comparison between crater radius computed using the converted data and Equation 16, and observed crater radius is shown in Figure 24. Though all charge weights used in the analysis had been converted to energy equivalent TNT charges, different symbols were used in the figure to show what the explosives were before the conversion. Recall from previous discussion (Section 6.2.2) that the four C-4 shots for which calculated crater radius is greater than observed was due to charge placement conditions, not because of the explosive. These four points are not considered in the following discussion.

For the explosives whose energy release was already greater than that of TNT, ie C-4 and DM-12, converting their charge weights to an energy equivalent weight of TNT had caused the plotted points to fall to the right of where they



had been in Figure 22. This is particularly noticeable for the larger craters created by C-4, which reflects large charges. This suggests that Equation 16 predicts the observed craters better.

For TNT and the other explosives whose energy release was less than that of TNT, the relationship given by Equation 16 has caused the points to fall further to the left of where they were in Figure 22. This is particularly noticeable for the gunpowder shots. Again, the plotting positions of the calculated crater radii for these explosives fell closer to where reason would suggest they should be, if the 'transformation' of explosive weight via specific energy was valid, hence suggesting further that Equation 16 is a better predictor of crater radius than Equation 14. Therefore, Equation 16 was considered to be the 'best' available, in terms of the parameters included in the analysis.

Equation 16 can be seen from Figure 24 to generally underpredict the observed data. This is more noticeable for the larger craters, hence larger charges, but it is true for the whole range of crater radii. For smaller charges, the underprediction is, understandably, less.

The maximum of the surface described by Equation 16 gives a maximum scaled crater radius of $2.68 \text{ m/kg}^{1/3}$ for a scaled ice thickness of $0.549 \text{ m/kg}^{1/3}$, when the scaled depth of placement is $0.461 \text{ m/kg}^{1/3}$. Therefore, with ice thickness measured in metres, the optimum conditions for ice demolition using TNT-energy-equivalent charges are described by:

$$W = 6.03 t_i^3 \quad \dots (17a)$$

$$d = 0.84 t_i \quad \dots (17b)$$

$$\text{to give } R = 4.88 t_i \quad \dots (17c)$$

where W is in kilograms, d and R are in metres.

6.3 The Effects of Gas Venting

In the survey of the literature it was noted that Wade (1966) had taken the precaution of filling the placement holes for his charges with ice chips and snow, and had allowed the slush that formed to freeze over before detonating his charges. He gave no indication as to the reason for this precaution, but it is noteworthy that of all the references, only his tests allowed the placement hole to refreeze before the charges were detonated. None of the references considered whether or not the placement hole would have any effect on the resulting craters.

In the discussion of the background to the problem (Section 1.3), it was noted that the presence of an open placement hole may allow the gaseous products of detonation to vent through the ice before all of the useful work could be obtained from their expansion. As stated previously 'in normal blasting operations the placement hole is effectively stemmed ... so that venting ... is not a problem'. However, the possibility of venting has not been considered in the ice blasting literature.

Because charges should be placed fairly close to the underside of the ice sheet, as suggested by Equations 13b and 17b, it is possible that the maximum bubble radius R_0 would not be obtained before the gas vented to the atmosphere. Figure C1 of Appendix C shows that the radius of the gas bubble for the charge weights used during the experiments would be between 1.07 and 2.4 m if the explosive were TNT. If the gas bubbles from the DM 12 explosive are anywhere near comparable, the gas bubble would not have finished expanding, for the relatively shallow placement depths given in Table 1 for Shots 9 through 40, before it would have reached the upper surface of the ice. A series of shots for Experiment 2 were therefore designed to assess the effect of gas venting on the resulting crater dimensions.

Three open placement hole sizes were incorporated into the first series of the experiment. For a fourth placement hole condition, charges were set through a number of the smallest holes, which were then filled with ice chips and snow and allowed to freeze overnight. Each of these four placement hole conditions were used with the charges set at the lower surface of the ice, and at the optimum depth of placement according to Mellor's preliminary scaled optimum conditions. The data for Shots 9 through 24 of Table 1 document the results for charges being set at the lower surface of the ice sheet, and Shots 25 through 40 of Table 1 for optimum placement.

The data are shown in Figure 25, along with the data

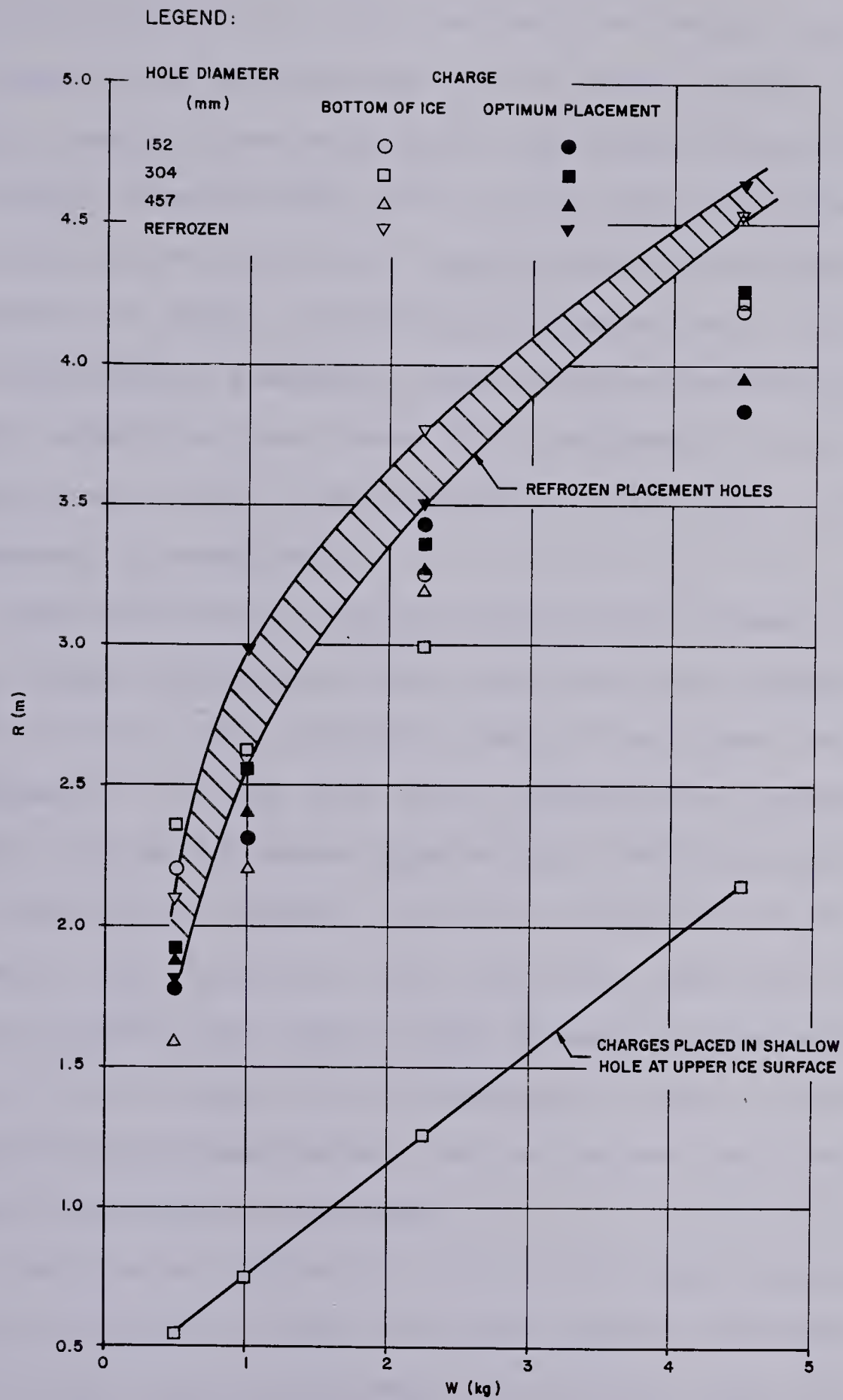


FIGURE 25
EFFECT OF PLACEMENT HOLES
(GAS VENTING)

from Shots 5 through 8, which document the effects of placing charges in a shallow hole at the upper surface of the ice, and tamping them with snow. The figure clearly shows that charges placed under the ice are more effective than charges placed on top of the ice, as would be expected from the results of normal demolitions. Charges which are initially confined by sandbags, earth or water stemming, etc., are more effective than those left unstemmed, as the confinement causes slightly more pressure to be built up before the stemming is demolished.

From Figure 25 it can be seen that the craters formed by the charges whose placement holes had been stemmed and allowed to freeze were generally larger than those for which the placement hole was left open. Although the increase is distinct, it is no means spectacular. The cause of the slight increase in crater radius is considered to be that immediately upon detonation, the expanding gases are confined by the frozen over layer, which causes the gas bubble to flatten slightly while still expanding, so that it stresses a slightly larger portion of the ice before the ice sheet fractures and releases the gases.

There is no indication in Figure 25 that the size of hole has any effect on the resulting crater dimensions, at least for the sizes of placement hole tested. Thus the mere presence of an open water surface, appears to be the important consideration.

A further point indicated by Figure 25 is that there

does not seem to be any noticeable effect on the resulting crater due to the two placement depths. For the smallest and largest charges, the craters resulting from charge placement at the lower surface of the ice appeared to be generally larger than those placed according to Mellor's preliminary optimum scaled depth, while the converse appeared true for the other two charge weights. However, considering the small placement depths required (about 13 cm), and the physical size of the charges (which ranged from 9.5 x 5.8 x 6.2 cm (one block of DM 12) for the 0.5 kg charges, to 19.0 x 11.6 x 11.6 cm (approximately) for the 4.5 kg charges) this scatter is not surprising. A small measurement error before tying the charge off to its suspending stick would have been sufficient to alter the scaled depth of placement. The same is true for the condition of trying to set the charge with its centre of mass at the lower surface of the ice.

6.4 Charges Placed at the Ice Surface

6.4.1 Chilcotin Data

Experiment 3 was designed to document the effect of placing unconfined charges on the surface of the ice as a hasty demolition technique. Two large charges of DM 12 , 9 and 18 kg, were detonated to investigate this. The results are given in Table 1 as Shots 85 and 86. Four other charges, listed in Table 1 as Shots 5 through 8 had been detonated within shallow (7.6 cm) holes cut into the ice surface, and

had been 'confined' by packing them with snow. These charges were close enough to the surface, and the confinement was minimal, such that the shots can be considered in this analysis. For convenience, the data are summarized in Table 4 following.

TABLE 4
Summary of Surface Charge Data
Chilcotin Experiment 3

Shot No.	W (kg)	t_i (m)	R (m)	A_o (m^2)
85	9.00	0.395	1.86	10.87
86	18.00	0.395	2.99	28.09
5	0.50	0.368	0.55	0.98
6	1.00	0.387	0.74	1.72
7	2.25	0.343	1.26	4.99
8	4.50	0.381	2.14	14.39

In the previous section it was shown that charges placed in a shallow hole in the ice surface are far less efficient than charges of the same weight placed under the ice. Referring to Figure 25, it can be seen that the 9 kg charge created a crater of the same order of magnitude as the smallest crater formed with a 0.5 kg charge. Similarly, the 18 kg charge created a crater approximately the same size as both the largest crater from a 1 kg charge, and the smallest from a 2.25 kg charge.

As a means of comparison between the charges placed on the surface and those set in the shallow holes, the crater radius and cratered area were plotted, as a function of

charge weight, in Figure 26. From the figure it can be seen that placing the charges in the shallow holes appears to make a noticeable difference in the resulting crater radii. This finding is comparable to known relationships in standard demolition work, where the quantity of explosive required to destroy a target from within is less than that needed if the charge is placed as an external breaching charge.

All of these craters had upward of 95% ice retention in them. In fact, the crater from the 18 kg charge had so much broken ice in it that the writer was able to stand in the middle of the crater immediately following its formation. The craters for the 9 and 18 kg charges are shown in Photos 15 and 16 respectively. That the craters and the area surrounding them are so dark, is because the ice was stained with the soot from the solid products of the detonation reaction.

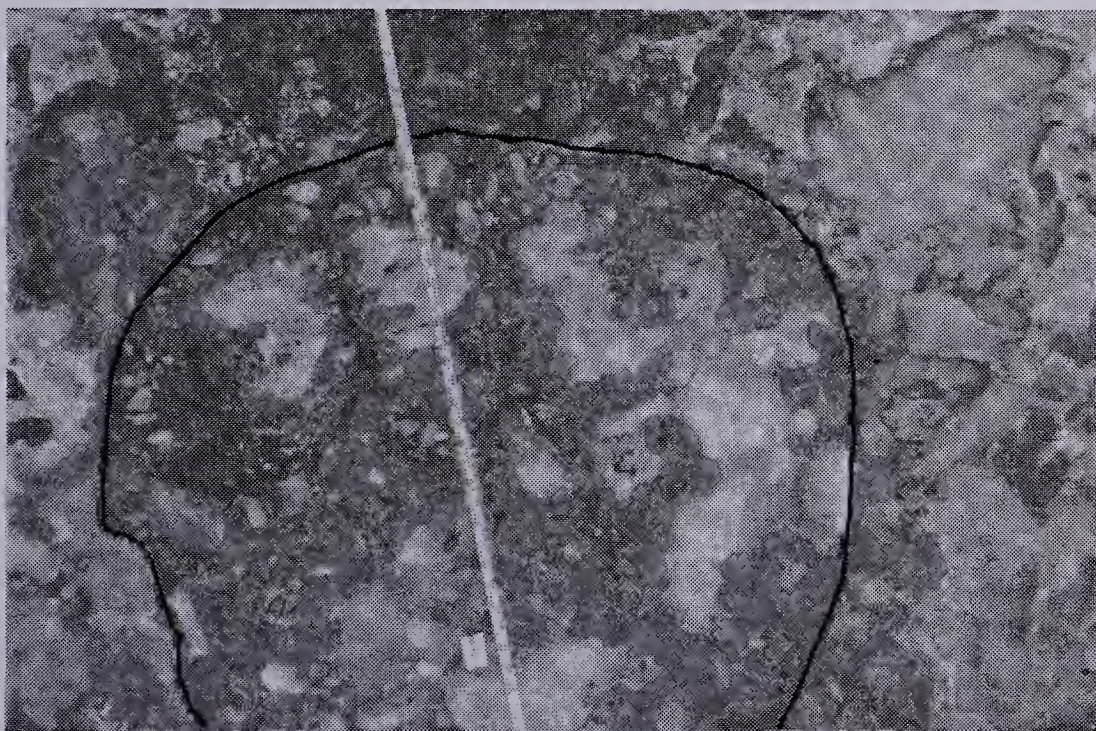


Photo 15: Crater for 9 kg Surface Charge

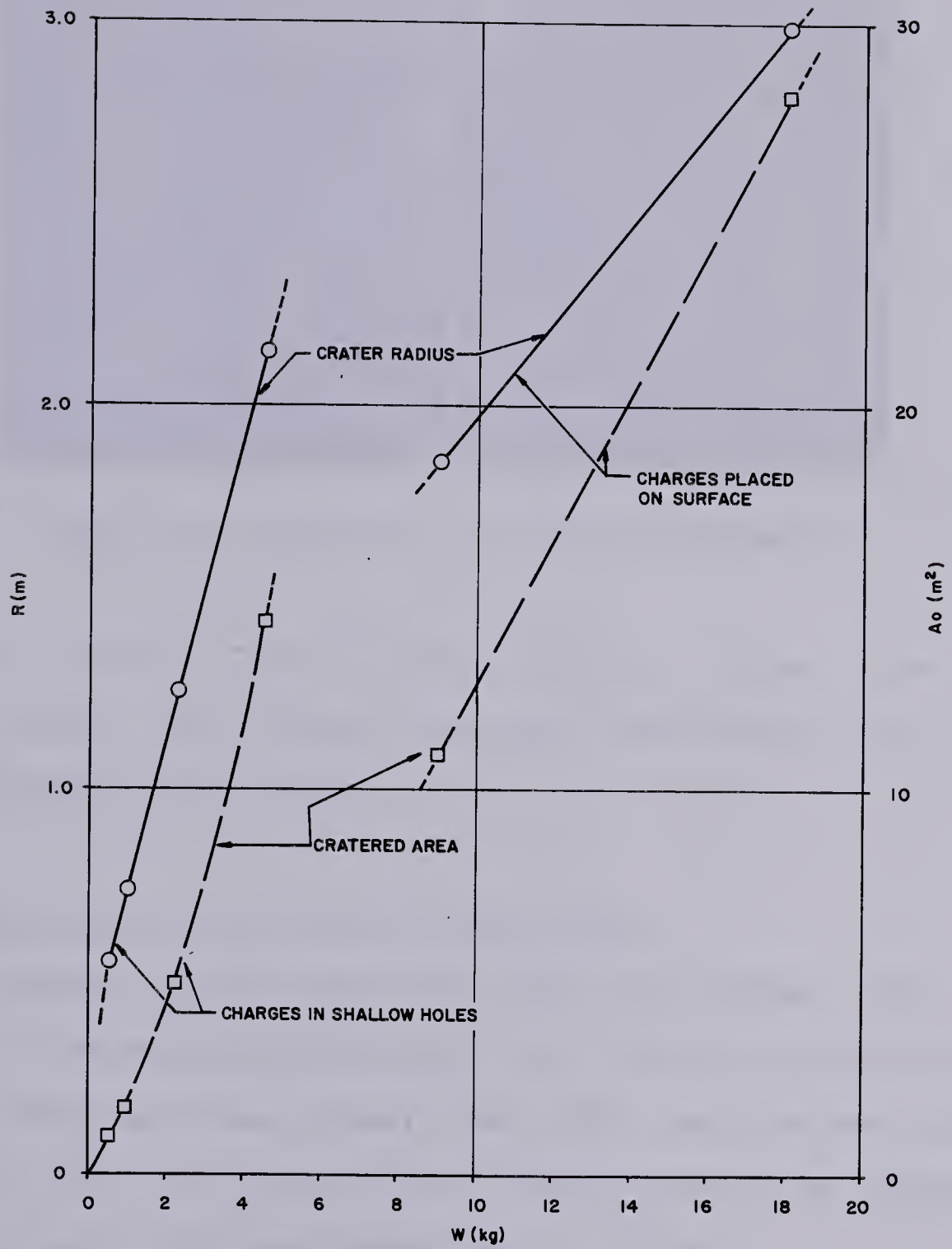


FIGURE 26

SURFACE CHARGE RESULTS

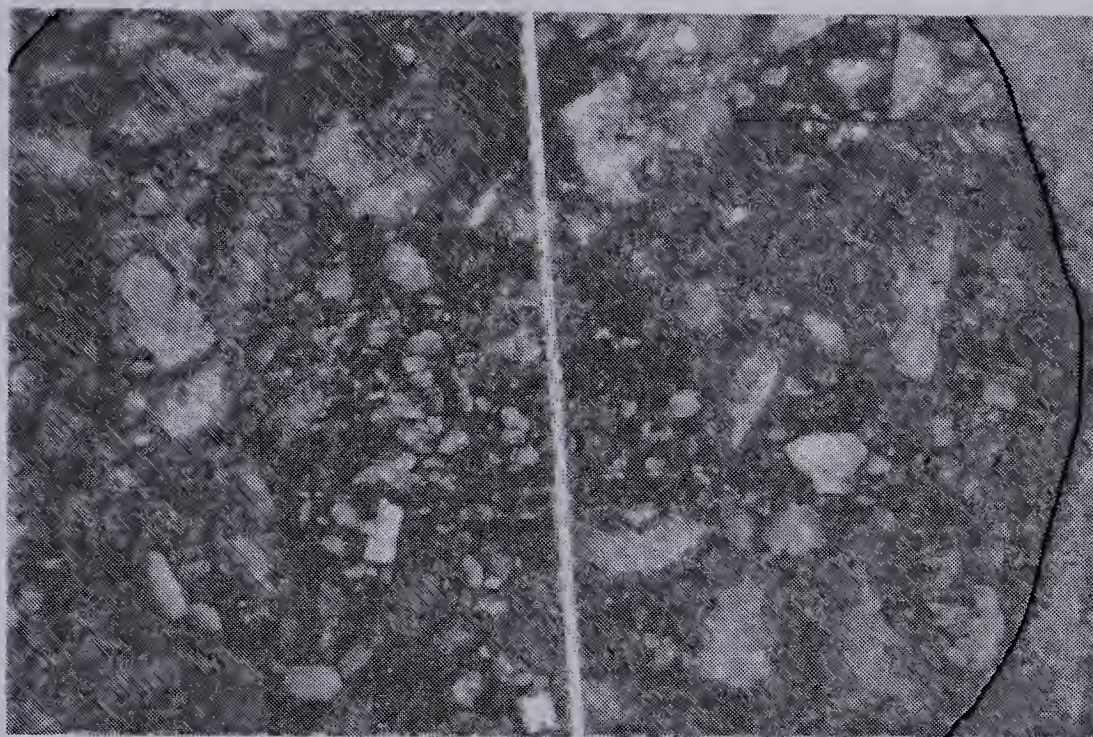


Photo 16: Crater for 18 kg Surface Charge

To quantify the relation between crater size and charge weight for surface charges, additional data was sought from the literature.

6.4.2 Analysis of All Surface Charge Data

Charges placed above the lower ice surface were included in the studies of Van Der Kley (1965), Purple (1965), Barash (1966) and Wade (1966), for which the data are given in Tables A-1, A-3, A-4 and A-5 respectively. For convenience, the data have been summarized in Table 5.

Crater radius for charges with $h=0$ is plotted against charge weight in Figure 27. From this distribution - compared with that of Figure 26 for subsurface placement - it is again evident how inefficient surface-laid charges are.

The line of best fit shown in the figure has the

TABLE 5

Surface Charge Data From the Literature

Reference	Explosive	W	t_i	h^1	R
		(kg)	(m)	(m)	(m)
Van Der Kley	American TNT	0.454	0.120	0.0	0.965
		0.908	0.120	0.0	1.325
		1.362	0.120	0.0	1.250
	Dutch TNT	8.50	0.280	0.0	3.250
		0.25	0.280	0.0	0.300
		0.50	0.280	0.0	0.375
		1.00	0.280	0.0	0.650
		0.25	0.410	0.0	0.0
		0.50	0.410	0.0	0.0
		1.00	0.410	0.0	0.400
		1.00	0.210	0.0	0.200
		1.00	0.210	0.0	0.200
	Unspecified 'Plastic'	0.0625	0.280	0.0	0.200
		0.125	0.280	0.0	0.250
		0.125	0.280	0.0	0.250
Purple	C-4	2.27	0.127	0.0	3.658 ²
Barash	American TNT	3.63	0.584	0.610	0.0
		3.63	0.584	0.305	0.0
		3.63	0.686	0.305	0.0
		3.63	0.686	0.0	0.762
		0.454	0.610	0.0	0.0
		0.454	0.610	-0.305	0.457
		0.454	0.686	-0.343	0.457
Wade	ANFO	72.57	0.508	0.0	4.572

Notes:

1. 'h' is the height above the upper surface of the ice to the centre of the charge, measured positive upwards.
2. Purple's surface charge was confined by sand-bags, hence is not part of the same data population.

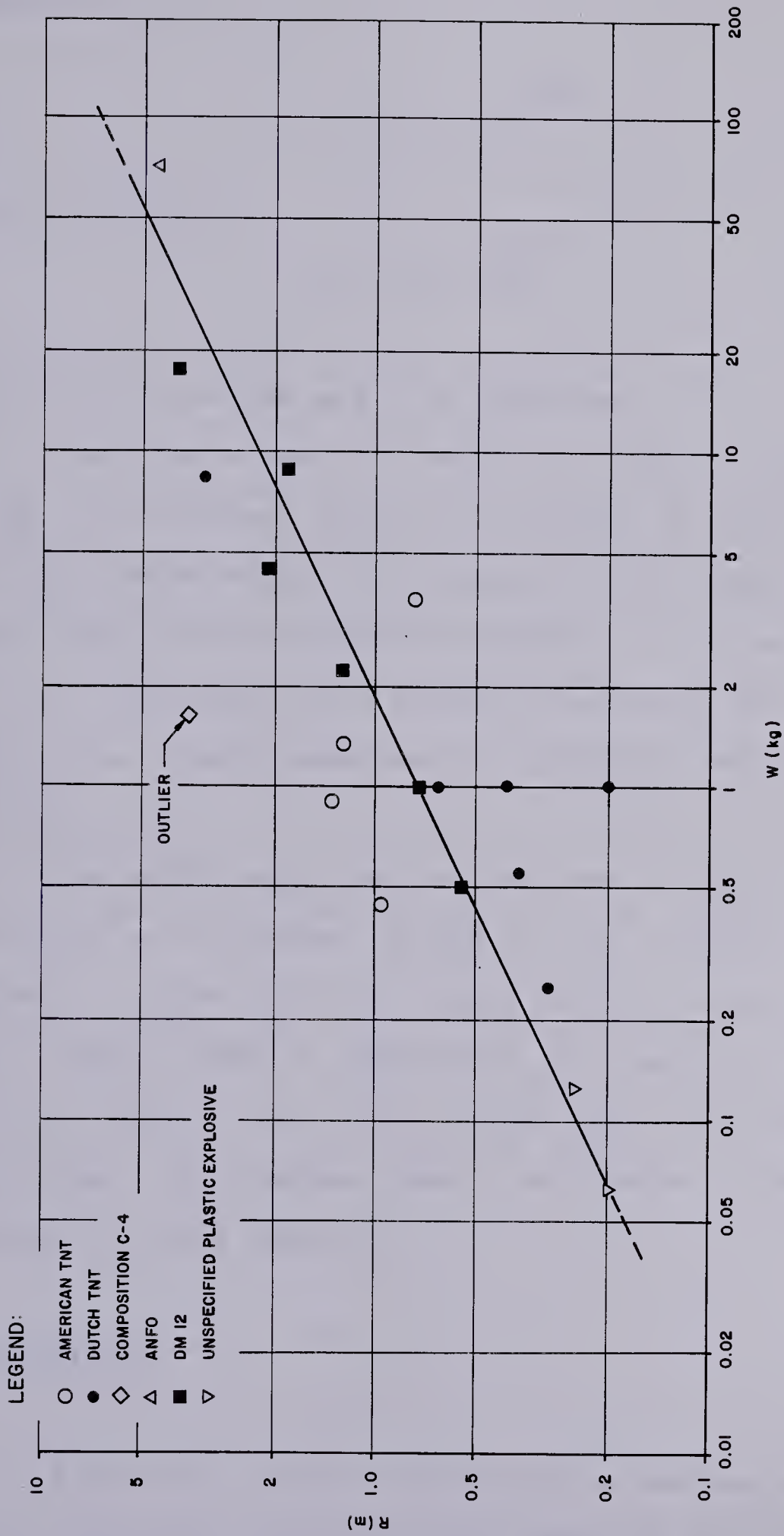


FIGURE 27
CRATER RADIUS FOR SURFACE CHARGES
(ALL DATA)

equation:

$$R = 0.75 (W)^{0.48} \quad \dots (18a)$$

or approximately:

$$R = 0.75 (W)^{0.5} \quad \dots (18b)$$

where R is in metres and W is kilograms.

The single shot of C-4, from Purple (1965), shown in Figure 27, had been initially confined by placing sandbags over the charge while the remainder of the data shown in the figure were for unconfined detonations. This point indicates how much the effect of a surface explosion can be enhanced through the simple expedient of initially confining the explosion.

The above equation may be used to plan a hasty ice demolition with charges placed on the surface of the ice. However, if time permits, every effort should be made to chip a small hole or depression in the ice, in which to place the charge, and, to increase the effectiveness of the explosions, the charges should be tamped (confined) with sandbags or other material.

6.5 Findings

Except for the ice demolition investigation by Mellor (1972), previous investigations reported in the literature

had not included the effect of ice thickness in the overall ice demolition relationship. Each investigation had reported an 'optimum' demolition condition, but these must be considered to be specific for the ice thickness tested and for the particular explosive used. Mellor's analysis generalized the ice demolition relationship by analysing a large number of nondimensional or scaled data. However, he had not included in his investigation the effects of the properties of the explosives used. As the coefficients for his regression model had not been published, and have since become lost, it has been necessary to scale ice demolition parameters from a set of curves that had been published. In order to assess the results of the Chilcotin Experiments in light of other reported ice demolition data, it was necessary to replicate Mellor's analysis.

It was found that Mellor's final regression equation could be reproduced, at least in terms of the statistical parameters associated with the regression analysis which Mellor reported. The results of the replicated analysis showed however that the observed scaled crater radii were skewed with respect to the theoretical best fit relationship with the calculated scaled crater dimensions. It was considered that this skew was due to either an insufficient number of the dimensionless terms of the general relationship having been included in the regression model, or, the combinations of the dimensionless parameters used were not enough to fully explain the inter-relationships between them.

It was found that in spite of the skew in the scaled relationships, the calculated regression equation predicted crater radius fairly well. There was a tendency for the equation underpredict the observed data, thus it could be used as a conservative guide to ice demolitions. The regression equation obtained described a surface which had a maximum, from which the 'optimum' ice demolition parameters could be derived. These criteria were found to be:

$$W = 25 t_i^3 \quad \dots (13a)$$

$$d = 0.4 t_i \quad \dots (13b)$$

$$\text{to give: } R = 8 t_i \quad \dots (13c)$$

where t_i , d and R are in metres, and W is in kilograms of explosive. As the properties of explosives had not been included in the analysis, the relationship may be used for any explosive type, however, there will be a variation in the results obtained for any two explosives, due to the 'strength' properties of the particular explosives used.

A small improvement in the results of the regression analysis was obtained by including one of the dimensionless terms of the general relationship (the gravitational term) in an attempt to reduce the skew of the scaled data. This analysis showed that the effects of gravity on the general ice demolition relationship were negligible. Therefore, the term was not included in subsequent regression analyses.

From this, it has been determined that if the skew of

the data is due to an insufficient number of the dimensionless terms being included in the regression analysis, the terms which should correct this deficiency are one or both of the size of the placement hole or the radius of the gas bubble.

Repeating the regression analysis including the point charge data published since Mellor conducted his investigation (including the data reported herein) did not improve significantly upon the previous findings. The form of the relationship between observed and calculated scaled crater radius determined with the extended data was similar to the initial finding, ie the data was skewed from the theoretical best fit, however, as the number of data points, as well as the number of explosive types had increased, the scatter of the plotted points had also increased. This was observed in spite of the Chilcotin experiments having been designed based upon the preliminary ice demolition relationships derived from Mellor's analysis (Equations 8a, 8b and 8c). As the number of explosive types had increased, and as the gas effectiveness of each explosive is different, it is considered that the increase in the number of explosives may have caused the increased scatter in the data, which was then investigated.

Due to the proliferation of both the methods used to compare explosives, and the performance data reported for these explosives, it was difficult to find one parameter that could be used for this purpose. Meyer (1977) had indi-

cated that the 'comparative' methods (comparing an explosive's performance in terms of a standard weight of a base explosive) were not as good an indicator as single parameter explosive properties, and further, that the measure of specific energy was the "most relevant thermodynamically calculable" parameter which could be used for this purpose. However, specific energy is not reported for the mixtures of explosive compounds reported in the ice demolition literature. It was found that the 'Effectiveness as an External Charge' used by both the CAF and U.S. Forces was a fairly good indicator of the ratio of specific energy of a particular explosive to that of TNT. This parameter was then used to convert the charge weight, for each data set where the explosive could be properly identified and for which an 'effectiveness' was available, into an energy-equivalent charge weight of TNT.

Reanalyzing by regression the data converted in this manner, excluding the Chilcotin data, gave a regression equation whose statistics were comparable to those reported by Mellor. Inclusion of the Chilcotin data converted in this manner caused a decrease in both the multiple correlation coefficient and the standard error of estimate for the scaled data. However, the plotted relationship between observed and calculated crater radius was found to improve. The derived regression equation from this analysis was therefore considered the 'best' available, in terms of the parameters included for consideration, and was used in the investiga-

tion of other phenomena. The 'optimum' ice demolition criteria determined from the maximum of the surface described by the regression equation for equivalent TNT charges were found to be:

$$W = 6.03 t_i^3 \quad \dots (17a)$$

$$d = 0.84 t_i \quad \dots (17b)$$

$$\text{to give: } R = 4.88 t_i \quad \dots (17c)$$

or, approximately:

$$W = 6 t_i^3 \quad \dots (17a')$$

$$d = 0.84 t_i \quad \dots (17b')$$

$$\text{to give: } R = 4.9 t_i \quad \dots (17c')$$

where t_i , d and R are in metres, and W is in kilograms of TNT. These relationships show a significant decrease (approximately 75%) in the amount of explosive required to demolish ice of a given thickness from that determined from Mellor's analysis, though the crater radius obtained is approximately 40% smaller. That the amount of explosive (particularly TNT) required is so much less than if determined from the results of Mellor's analysis is considered to be because the coefficients of Mellor's equation have to make up for the influence of a wide variety of explosive types, which was not considered in his analysis.

The effects of gases venting through the placement

hole before all of the usefull work could be obtained from them were investigated. It was found that if there were no free water surface, ie the placement hole was refrozen, the resulting craters were perceptively larger (15% for a 1 kg charge to 7% for a 4.5 kg charge) than craters formed by the detonation of a charge where the placement hole was left unfrozen. There was no discernable effect, for the placement hole sizes tested, of the size of open placement hole on the resulting crater radius. From this it is concluded that if placement hole size and gas bubble radius are the only two parameters available to remove the skew from the scaled data, then gas bubble radius must be the one which will have the greatest affect.

Finally, the effects of charges placed on the surface of the ice, and those detonated within the ice were investigated. It was shown, quite dramatically, that charges detonated on or near the surface of the ice were far less efficient in demolishing ice than charges detonated under the ice sheet. A preliminary relationship was derived to give crater radius as a function of charge weight for charges detonated on the surface of the ice. The resulting radius was found to be proportional to (approximately) the square root of the charge weight, rather than the cube root as was found for charges detonated below the ice. The derived equation was:

$$R = 0.75 W^{0.5} \dots (18b)$$

The relationship must be considered preliminary, as the effect of the ice thickness and the explosive type was not included in the investigation.

It was shown in this last analysis, from a single data point provided by Purple (1965), that the effectiveness of charges set on the surface of the ice is significantly increased if the explosion from those charges is initially confined or 'stemmed' by packing the charge with some material to prevent the explosion effects from escaping directly to the atmosphere. For his test Purple used sandbags. Thus, for expedient or hasty demolition of an ice sheet, if time does not permit the charges to be set below the ice, the effect of surface charges can be enhanced by confining the explosion with sandbags or other available material. It is considered that the snow used to tamp the four charges set in a shallow hole in the ice surface during the Chilcotin experiments was not an 'effective' means of stemming the explosion, as snow density is so little that it can not confine the buildup of gases from the detonation.

CHAPTER 7

THE EFFECTS OF ROW CHARGES

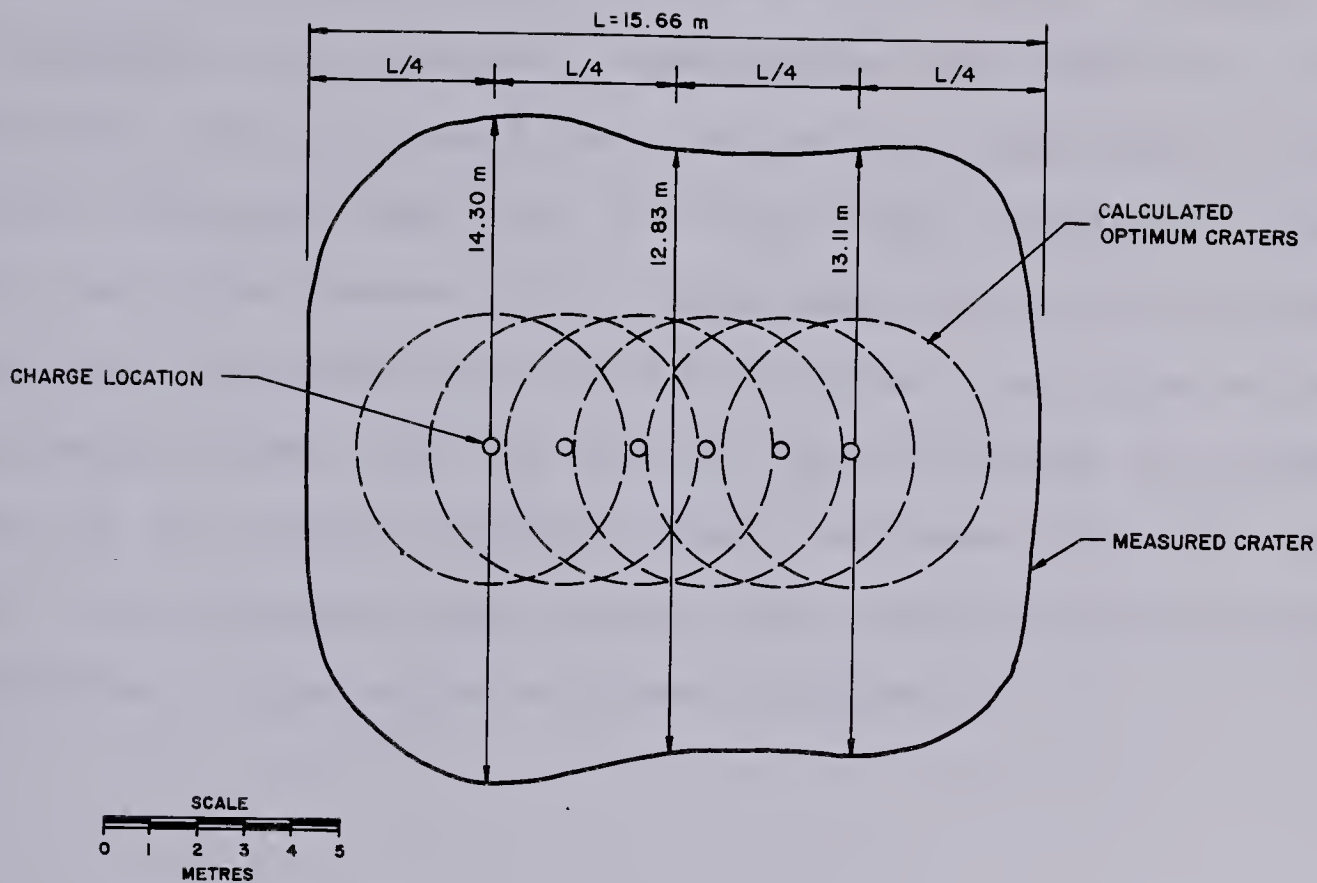
7.1 The Chilcotin Data

The row charge data from the Chilcotin tests included the results of Experiment 1, which tested 1 CER's SOP for ice demolition, and one test with charges placed at a spacing of 1.5 times the calculated optimum crater diameter. The data are given in Table 6, and are shown in Figure 28. The craters from the program extension test did not connect to form one long crater, but remained separate, with a 'bridge' of ice between them, hence the test will be referred to herein as a 'row'. For this reason the data have been included in Table 1 as single shots 61 through 66 inclusive (Addition No. 6 to the program in Table 1). It should be noted that the crater diameters and bridge widths shown in Figure 28 are not the three-measurement average diameters discussed in the section on measurement technique (Section 5.4.3), but are the measured distances along the line of the row.

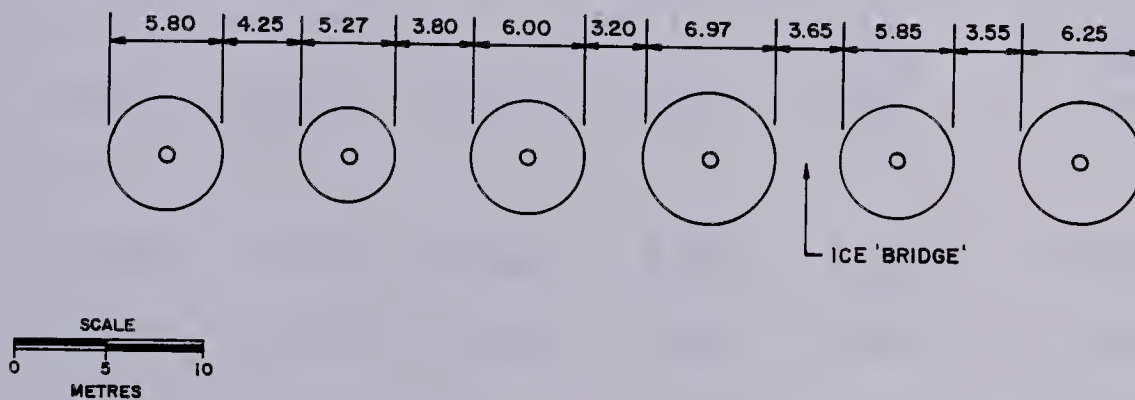
7.2 Analysis of Experiment 1

7.2.1 Single Charge Comparative Data

For Experiment 1 the charge weight, placement depth and spacing were all predetermined by 1 CER's easily remem-



EXPERIMENT I
(1 CER SOP)
SPACING = 1.52 m



ADDITIONAL ROW
ADDITION # 6
SPACING = 1.5 OPTIMUM DIAMETERS

FIGURE 28
CHILCOTIN ROW CRATERS

bered SOP - "5 lbs placed 5 ft below the ice, and spaced 5 ft apart". Ice thickness measurements were made at each placement hole to facilitate analysis of the data in the manner conducted thus far. Two shots were included to measure the effectiveness of the placement criteria as single charges. These have been listed in Table 1 as shots 49 and 50 (Addition No. 3 to the program shown in Table 1). A summary of the charge placement data for these two shots, as well as calculated crater radii, for three of the analyses conducted in Chapter 6, is given in Table 7.

TABLE 7

Single Shot Data for 1 CER's Placement Criteria

W	t_i	d	R	Calculated Crater Radius (R_C)		
				Mellor	All Data	Equivalent TNT
(kg)	(m)	(m)	(m)	(m)	(m)	(m)
2.25	0.406	1.50	3.53	3.01 ¹	2.86 ²	3.15 ³
2.25	0.394	1.54	3.33	2.97	2.83	3.11

Notes:

1. From Equation 12, replication of Mellor's analysis.
2. From Equation 14, analysis of all data, straight charge weight.
3. From Equation 16, analysis of all TNT equivalent data.

It was found that for the average thickness of ice encountered (0.363 m), a charge weight of 2.25 kg for 1 CER's SOP produced a scaled ice thickness of $0.277 \text{ m/kg}^{1/3}$, which was near Mellor's indicated optimum of $0.331 \text{ m/kg}^{1/3}$ (10 in/lb^{1/3}). That this was 'near' Mellor's optimum was due to the small curvature, in the region of optimum ice thickness, of the curves of Figure 7. The depth of placement, however, was excessive according to these curves.

It can be shown that although the 2.25 kg charge weight was near optimum according to Mellor's curves of Figure 7, on a 'demolished area per unit weight' basis, it is more efficient to use smaller charges placed closer to the underside of the ice than 1 CER's SOP dictates. Cratered area is considered herein instead of a crater radius, as there seems to be a convention in the literature that when a circular crater is not being discussed, the relevant parameter to use for comparison is area.

Using the data listed in Table 1 (in order that the explosive is constant, hence variance in explosive energy can be omitted from consideration), to compare the area of ice demolished per unit weight of explosive gives the results shown in Figure 29. This figure clearly shows that while the two single charges using 1 CER's placement criteria gave crater areas comparable to other charges of the same weight, generally, more ice was cleared per unit weight of explosive using smaller charges. The placement depths for these smaller charges was between 0.0 and 0.15 m, ie, less

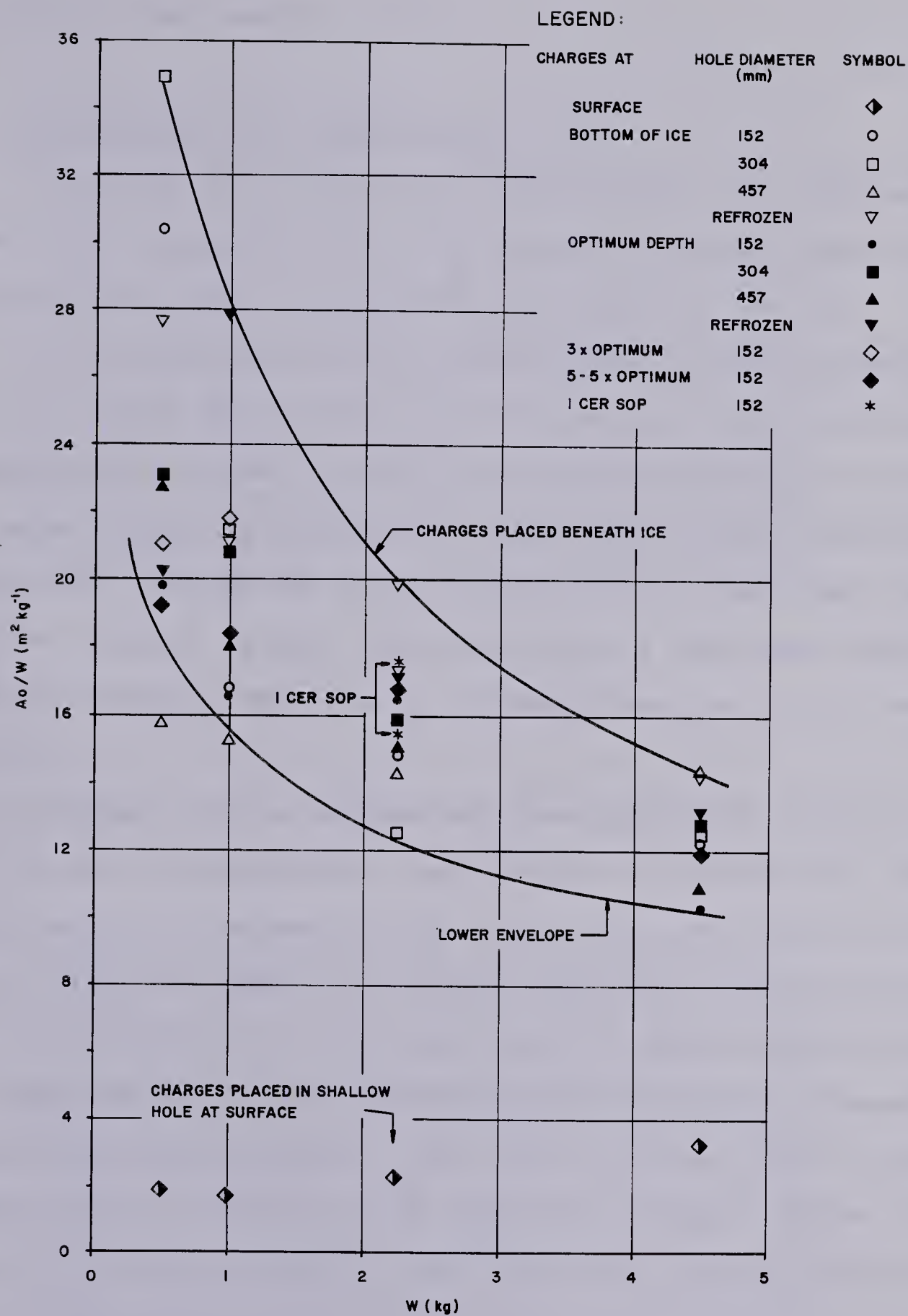


FIGURE 29

AREA DEMOLISHED PER UNIT WEIGHT

than 10% of that used by 1 CER.

7.2.2 Row Charge with 1 CER's SOP

A series of six charges using the SOP of 1 CER were placed and detonated, with the resulting crater shown in Figure 28. The area of ice demolished (A_0) was 193 m^2 .

It has been shown that placing single charges according to 1 CER's SOP is not as efficient as using smaller charges placed nearer the ice. It remained therefore to assess what effect the spacing of charges in a row, according to that SOP, has on the total cratered area. Given that the cratered area of 193 m^2 from Experiment 1 had been formed using six charges, the area of ice demolished per charge was 32.2 m^2 .

However, if the charges had been placed far enough apart to act independantly, and using the equivalent TNT charge weight to determine the crater areas for their particular placement conditions (minor variations in ice thickness) from Equation 16, the total area of destruction would have been 184 m^2 , or 30.7 m^2 per charge. Hence the measured crater area from Experiment 1 was only 5% larger than if the craters had been spread out as individual charges. Hence, in terms of the total area of ice demolished spacing charges using 1 CER's SOP, little is gained.

What was remarkable however was the ejection of ice from the crater. Photo 17 shows the ice remaining in one of the two single shot craters using this placement criteria,

which shows approximately 70% ice retention in the crater.

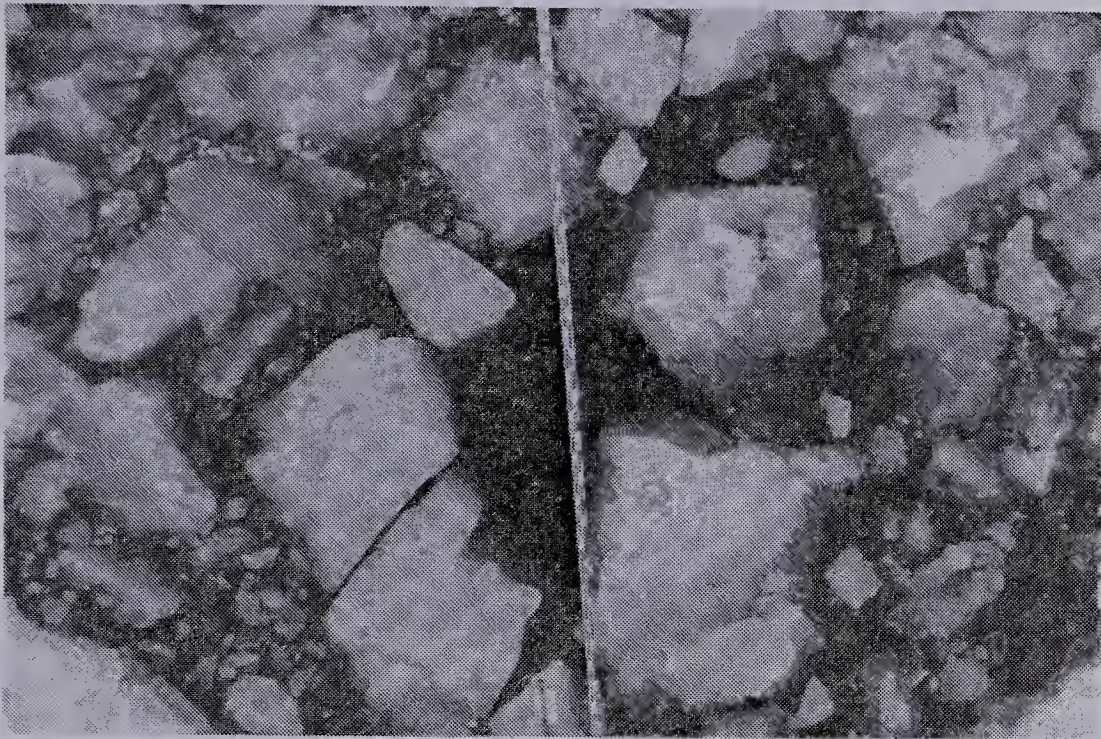


Photo 17: Ice Debris for Single Shot
1 CER Placement Criteria

Photos 18 and 19 show the ice remaining in the crater from Experiment 1, which indicates that far more ice is ejected.

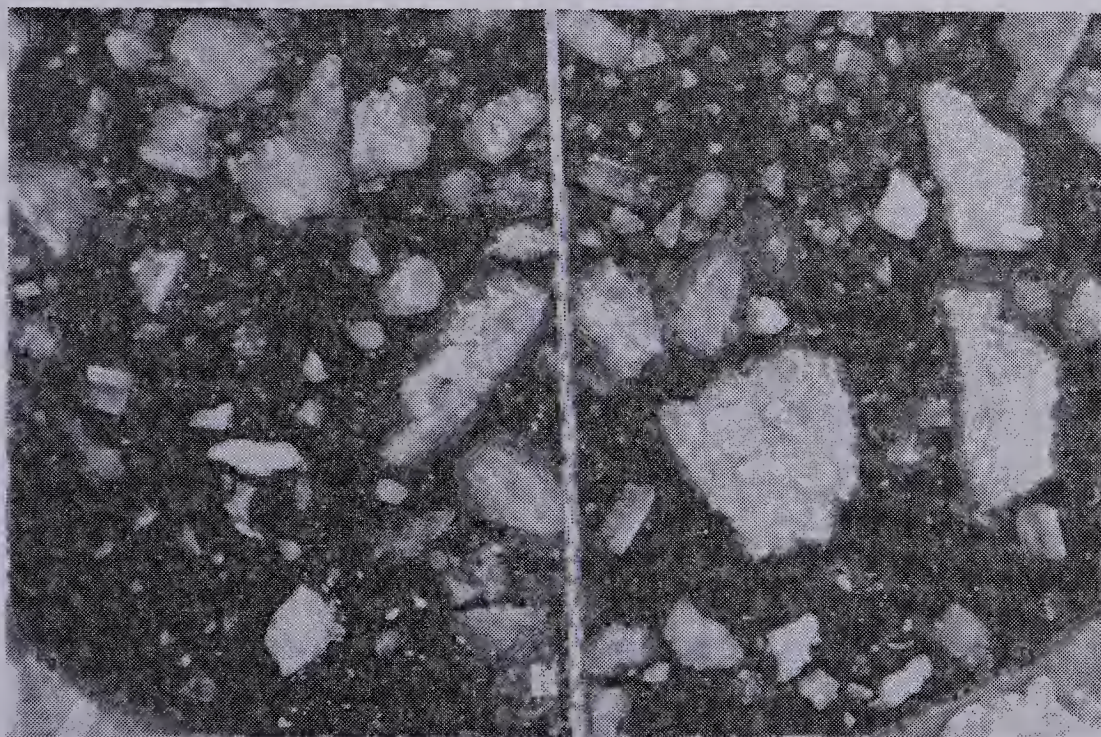


Photo 18: Ice Debris; Experiment 1

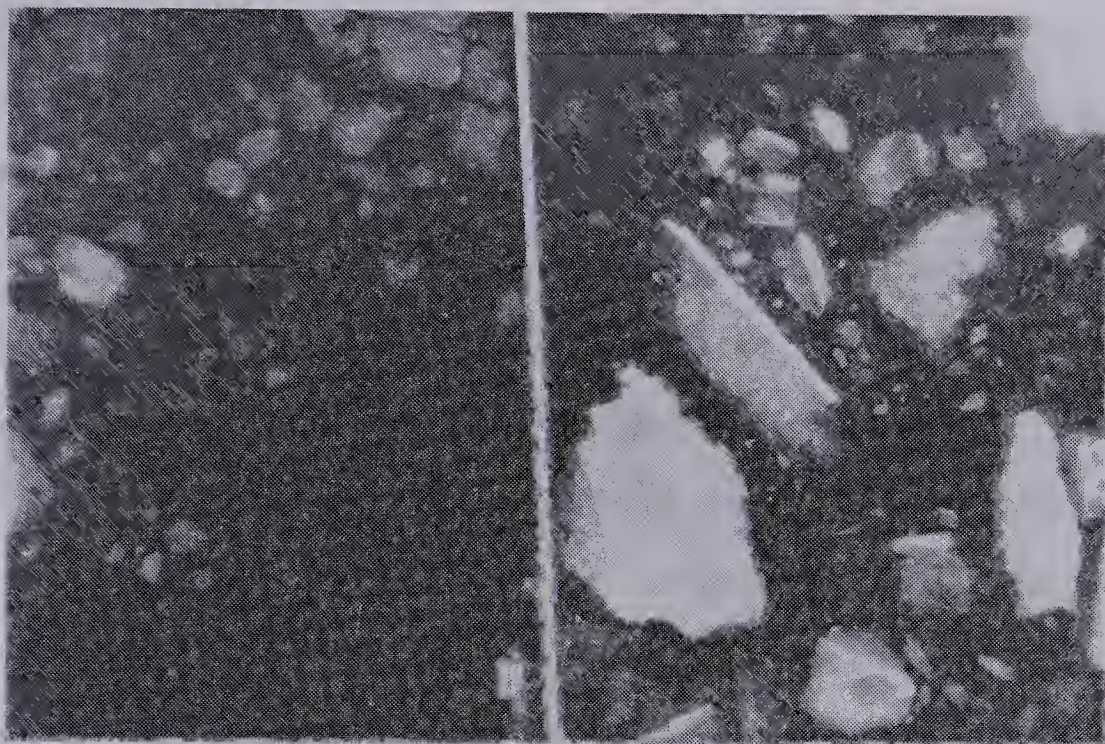


Photo 19: Ice Debris; Experiment 1

7.3 Analysis of the Additional 'Row'

As Kurtz et.al. (1966) had detonated row charges with spacings between the charges of 1, 1.5 and 2 times their optimum crater radius, this addition to the program was included to test the efficacy of spacing optimum charges 3 calculated optimum radii apart. As has been noted, the resulting craters did not connect, as shown in Figure 28.

The average of the observed crater radii (R_O) given in Table 7 is 3.05 m. This compares favourably with the calculated crater radius (R_C) of 3.15 m, determined from Mellor's preliminary relationships, from which the charge spacing was set, as well as with the calculated crater radius of 3.2 m from Equation 16 obtained with the equivalent TNT charge weight.

From the charge spacing, deducting the number of average observed crater radii between the end charges resulted in an average ice bridge width of 3.35 m. Similarly, using the crater radius R_C of 3.20 m determined from Equation 16, the average ice bridge width was 3.06 m. Thus, for this case, spacing the charges three optimum radii apart resulted in ice bridges between the craters which were one optimum radius in width. Thus it may be expected that the maximum spacing between charges to ensure a continuous crater should be close to two crater radii.

In order to pursue the matter, the row crater data from the literature was sought.

7.4 Analysis of All Row Charge Data

The data for the row charges detonated by Kurtz et. al. (1966) are given in Table A-7 of Appendix A. Figure 30 shows the craters resulting from these detonations. The 'necking' of the right end of the crater for Row B was drawn in accordance with a sketch of the crater given by the original authors. Note that at the scale of Figure 30, the crater from Experiment 1 would be about the same size as two of the maximum ice blocks shown adjacent to Row C, placed side by side.

From the discussion of both Experiment 1 and the additional Chilcotin row, and from the row craters created by Kurtz et.al., three questions arose concerning the spacing

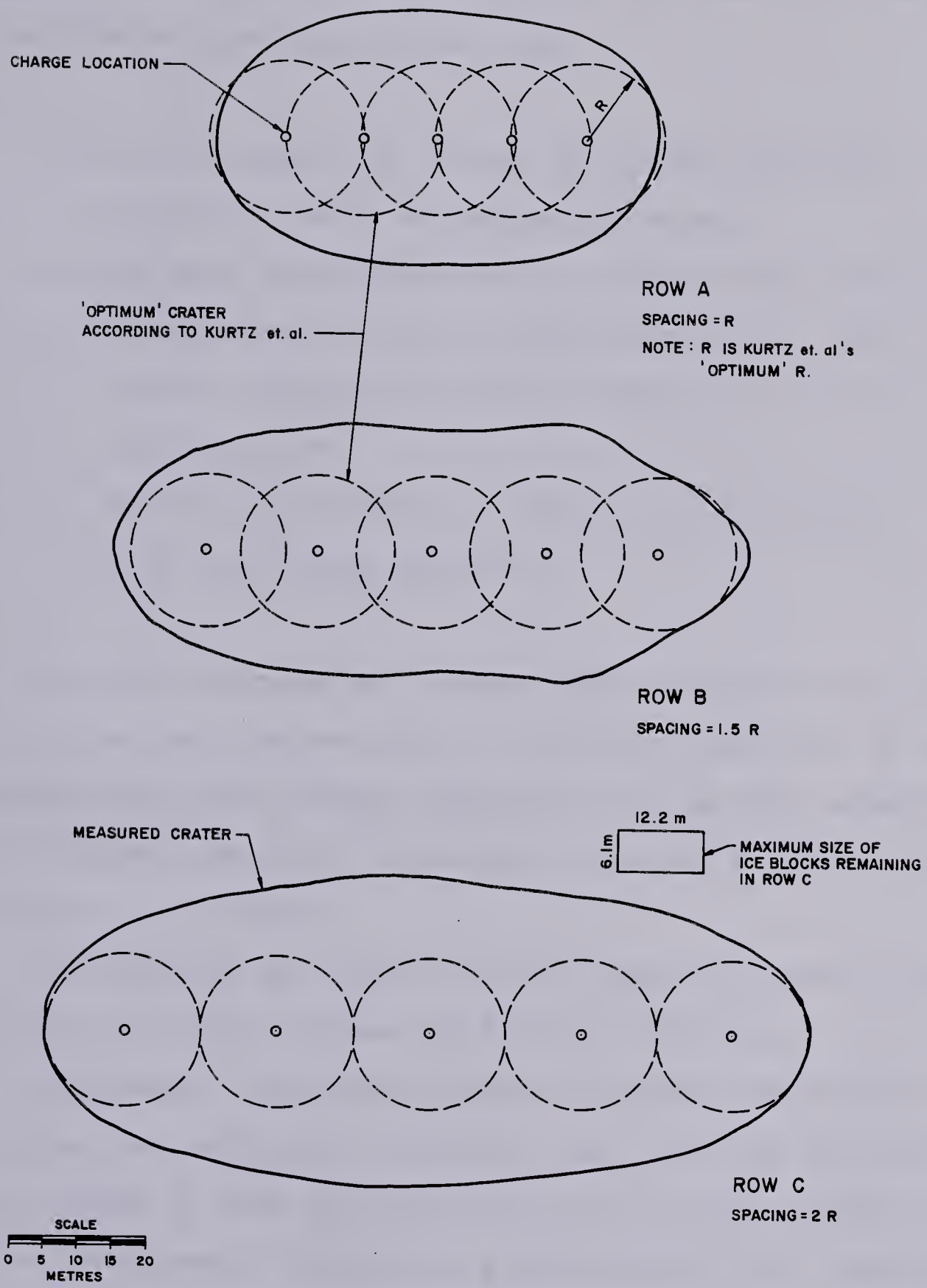


FIGURE 30
ROW CRATERS
AFTER KURTZ et. al. (1966)

of charges in a row, and the area of ice demolished using the row charge technique. These were:

- a. How far apart can charges be placed and still expect to obtain a continuous crater?,
- b. How much of an increase in cratered area can be expected by placing the charges as a 'row charge' rather than spacing them out as individuals?, and
- c. How is this increase in cratered area affected by the charge spacing?.

The data for the row charges were analysed using the equation derived from analysis of the data converted to energy-equivalent TNT charges (Equation 16), as this equation is considered the best available in spite of the lower correlation coefficient.

The craters for Kurtz et.al.'s Rows A, B and C had areas (A_0) of 1954, 2715 and 3932 m² respectively.

Equivalent individual charge weights and placement conditions as originally reported were used to calculate crater radius R_C with the Equation 16 as if the charges had been set separately. From these a theoretical total cratered area A_C was determined as the sum of the calculated individual areas. Table 8 summarizes the results of the calculations and the experiment. The ratios A_0/A_C and S/R_{av} given in the table are referred to herein as the 'area' and 'spac-

TABLE 8

Row Charge Analysis with Equivalent TNT Charges

Row	Charge	Calculated Radius R_C (m)	Calculated Cratered Area A_C (m ²)	Actual Cratered Area A_O (m ²)	$\frac{A_O}{A_C}$ (-)	Spacing S (m)	Average Calculated Radius R_{av} (m)	$\frac{S}{R_{av}}$ (-)
A2	1	9.747						
	2	9.562						
	3	9.850						
	4	9.799	1500.	1954.	1.303	10.973	9.772	1.123
	5	9.901						
B3	1	9.462						
	2	9.704						
	3	9.997						
	4	9.544	1475.	2715.	1.841	16.459	9.687	1.699
	5	9.730						
C4	1	9.715						
	2	9.844						
	3	9.857						
	4	9.623	1495.	3932.	2.630	21.946	9.756	2.249
	5	9.741						

Notes:

1. Sum of areas computed with R_C
2. Row A charges were spaced 1.0 times Kurtz et.al.'s optimum radius (10.97 m).
3. Row B charges were spaced 1.5 times Kurtz et.al.'s optimum radius.
4. Row C charges were spaced 2.0 times Kurtz et.al.'s optimum radius.

TABLE 8
(Continued)

Row Charge Analysis with Equivalent TNT Charges

Row	Charge	Calculated Radius R _C (m)	Calculated ¹ Cratered Area A _C (m ²)	Actual Cratered Area A _O (m ²)	$\frac{A_O}{A_C}$ (-)	Spacing S (m)	Average Calculated Radius R _{av} (m)	$\frac{S}{R_{av}}$ (-)
Expt 5 2	1	3.011						
	2	3.139						
	3	3.124						
	4	3.132	184.3	193.3	1.049	1.524	3.127	0.487
	5	3.163						
	6	3.187						
Add 6	1	3.197						
	2	3.197						
	3	3.197						
	4	3.197	192.6	176.1	0.914	9.449	3.197	2.956
	5	3.197						
	6	3.197						

Notes:

- 5. Experiment 1, 1 CER's SOP.
- 6. Additional 'Row' from Chilcotin Experiments.
- 7. Determined from sum of observed three-measurement-average crater radius.

ing' ratios. The results of this analysis are shown in Figure 31, including an area ratio calculated for the original data reported by Kurtz et.al.

As the spacing ratio goes to zero, the charges in a row can be considered to be one large single charge, therefore the area ratio should go to 1.0 as the calculated and observed areas should be the same. Similarly, when the spacing ratio is increased beyond the point where the resulting craters no longer connect to form one continuous crater, the area ratio should again be 1.0.

The area and spacing ratios for the data of Kurtz et. al. were calculated using their reported 'optimum' crater radius of 10.97 m (36 ft) for the charge weight used, and the total cratered area determined by the writer. Kurtz et.al. did not consider the effects of ice thickness or cratered area in their report. Instead of cratered area, they used the increase in row crater half-width over the individual crater radius (Section 3.2.5). These data have been included in Figure 31 to show how the inclusion (in the writer's analysis) of ice thickness into the overall ice demolition relationship affects the findings of the original authors. As can be seen, the original data do not indicate a significant increase in cratered area for spacing ratios less than 1.0.

The results of the Chilcotin additional row fell below the expected area ratio of 1.0. This was attributed to Equation 16 generally underpredicting the observed radii.

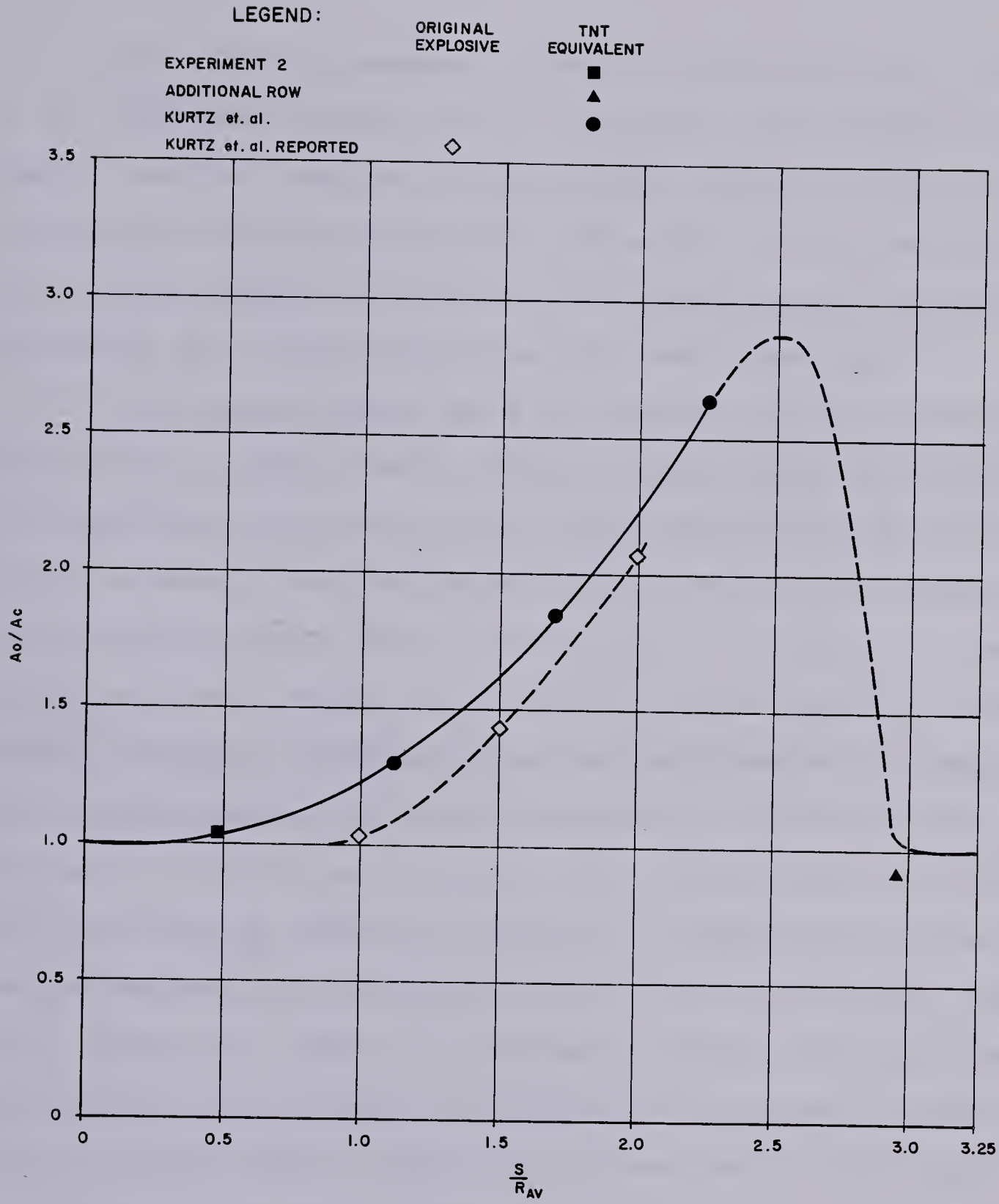


FIGURE 31

ROW CHARGE CRATER AREA FOR VARIOUS CHARGE SPACINGS

DATA CONVERTED TO EQUIVALENT TNT CHARGES

7.5 Findings

For 1 CER's placement criteria it has been shown that on an individual charge basis, more ice is destroyed by placing smaller charges closer to the bottom of the ice sheet than 1 CER's SOP dictates. Placement of smaller charges in this manner would result in a considerable saving in explosives and in the detonating cord used 'down hole'.

For charges placed as a row charge, it was found by Kurtz et.al. (1966) that optimum charges could be placed with spacings up to two optimum crater radii apart and still expect to obtain one continuous crater. This was corroborated by the analysis of the additional row included in the Chilcotin tests, where ice 'bridges' in the order of one crater radius in width remained between craters for which the charge spacing had been increased to 3 optimum radii. Analysis of all of the row data, with the equivalent TNT regression equation derived in Chapter 6, suggested that charge spacing could be increased to about 2.25 crater radii and still expect to obtain a continuous crater. However, the equation used to perform the analyses was observed to underpredict crater radius, hence the maximum spacing ratio might again revert to a value closer to 2.0.

It was determined from the original data of Kurtz et.al. that there was little increase in cratered area by placing the charges one radius apart, over placing the charges separately. As the spacing ratio increased beyond 1.0,

an increase in the cratered area occurred. The maximum increase from Kurtz et.al.'s data was for a spacing ratio of 2.0, and was in the order of 100%.

Analysis of all of the row charge data with the regression equation of Chapter 6 showed that for the case of energy-equivalent TNT charges, the maximum increase in cratered area, over placing the charges as individuals, could be as much as 160% (Figure 31).

CHAPTER 8

MULTIPLE CHARGES

8.1 Introduction

In the context of this thesis, 'multiple charges' denotes two charges placed in close proximity for purposes of modifying the explosive effect of one or both of the charges. Multiple charges are not 'row charges'. Two types of multiple charge blasting have been reported in the literature, the 'decked' or 'percussion' charges reported by Van Der Kley (1965) and Nikolayev (1971), and the multiple charges used in the directed blasting technique reported by Nikolayev (1971). The latter will be referred to herein as 'directed charges'.

8.2 Decked Charges

Decked charges consist of a main and auxiliary charge, with the auxiliary placed vertically over the main. Van Der Kley did not discuss the expected effects of the decked charges he detonated, or the reasons for the choice of main and auxiliary charge weights he used. His data is given in Table A-2 of Appendix A. However, as there was no discussion of his tests, and the data does not show any particular pattern to indicate which of the parameters was being investi-

gated, and as there was no comparable single charge data, Van Der Kley's decked charges were not analysed herein.

Nikolayev (1970) had tested two single charge weights on Antarctic sea ice (Table A-10 of Appendix A). Of these he selected the larger, 30 kg, to conduct experiments with decked charges. This charge weight was broken down into a main charge of 25.2 kg and an auxiliary of 4.8 kg. No reason was given in the reference for dividing up the charge in these proportions, though it transpired from his 1971 paper that 25.2 kg was the weight of one case of TNT. The explosive used in the decked charge experiments was Trotyl, not TNT, however it is assumed that there was a similar reason for proportioning the main and auxiliary charges as he did. The main charge was detonated first, with the auxiliary detonation following 0.025 seconds later. No reason was given in the 1970 paper for the choice of this delay. Nikolayev's decked charge data are given in Table A-11 of Appendix A. Note that the main charge placements for the four decked charges were exactly the same as four of his 30 kg single shots of Table A-10. This allowed a comparative analysis between the decked charge data and that for the same explosive mass detonated as a single charge.

The theory behind detonating the charges in the manner indicated was given in Section 3.2.7, however, to reiterate, as the gas bubble from the main charge was expanding, the auxiliary charge was detonated such that its expanding gas bubble would interfere with the expansion of the former,

causing it to 'flatten out', hence obtaining a larger main charge bubble in plan.

The increase in crater radius obtained through breaking down the 30 kg charge and detonating the two resulting in the manner indicated is shown in Figure 32. For the charges placed at depths of 2.5, 2.9 and 3.4 m below the ice, the increases in crater radius were 7.5, 18.5 and 13.3% respectively. There was no increase for the case of the main charge having been placed at a depth of 2.1 m, which was the 'optimum' depth of placement from his point charge experiments using a 30 kg charge. Nikolayev observed that there was no increase in the fraction of ice ejected from the crater by using the decked technique. It was stated (1971) that for both single and decked charges "the lead produced ... becomes 95 to 100% clogged with ice fragments, ranging from 0.5 to 1.5 m³ in size".

From the figure it can be seen that the increase in crater radius appears to have a fairly sharp peak, with a maximum which occurs - for the charge weight and ice thickness encountered - at a placement depth in the order of 2.9 m.

8.3 Directed Blasting

The theory behind directed blasting, according to Nikolayev (1971), was briefly outlined in Section 3.2.7. To reiterate, a main charge is placed beneath the ice, with a

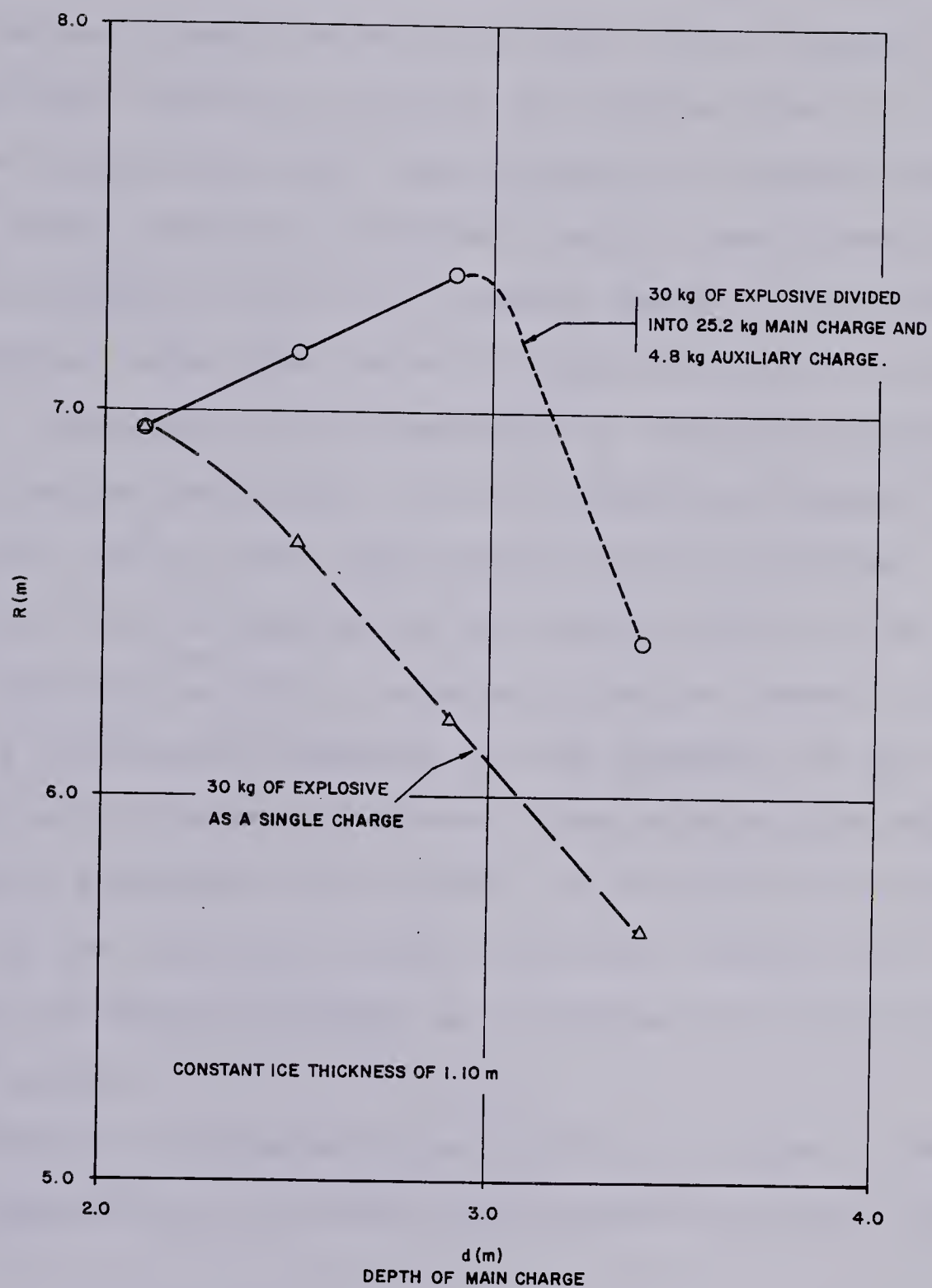


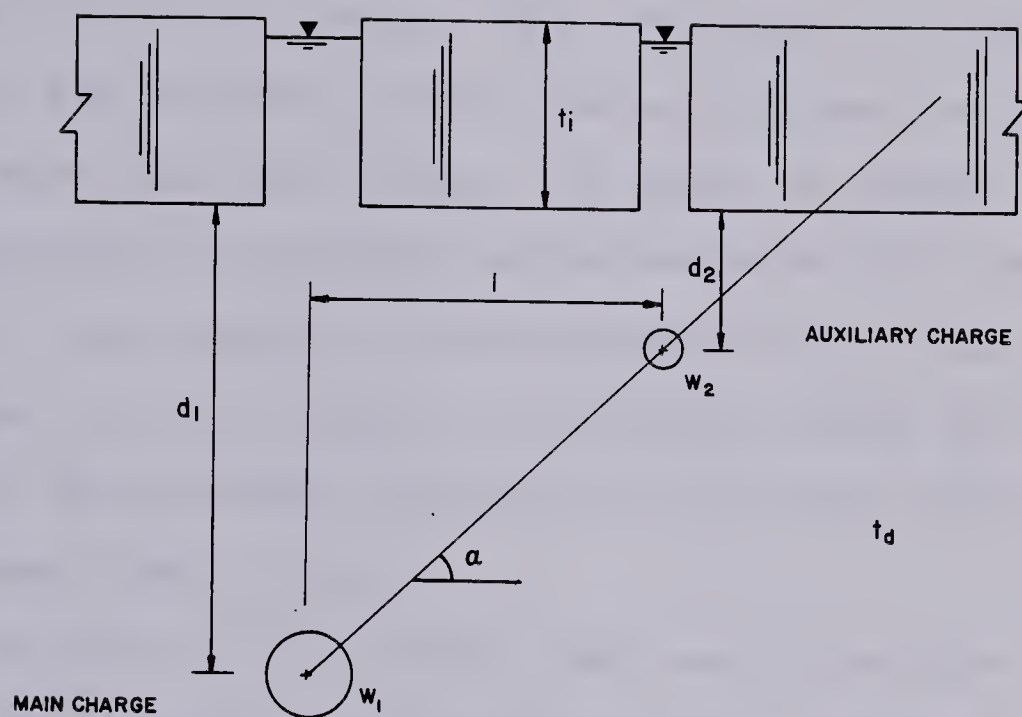
FIGURE 32
EFFECT OF DECKED CHARGES
(DATA FROM NIKOLAYEV , 1970)

smaller auxiliary charge placed above and to one side of the main, as shown in Figure 33, and the auxiliary is detonated first. The main charge is detonated when the gas bubble from the auxiliary charge has reached its maximum size. In this manner an artificial 'free' water surface is created beneath the ice which provides a shorter line of least resistance for the explosive action of the main charge to work with. The expanding gases from the main charge detonation are induced or 'directed', by the presence of the smaller bubble, to vent through the centre of that bubble, and hence vent through the ice at some angle other than the vertical. The purpose of this redirection of the venting plume is to increase the fraction of ice ejected from the crater by imparting a horizontal component to the momentum of the ice and water set in motion, and hence throw or carry ice debris out, and to the side of the crater. In all previous experiments, the gas plume had vented vertically through the ice, carrying the debris straight up, allowing it to fall back into the crater.

Nikolayev's directed blasting data are given in Table A-12 of Appendix A. All tests were carried out on ice 1.10 m thick.

8.3.1 Experiments of Nikolayev

Nikolayev's first experiment was to investigate the influence of the time delay between detonation (t_d) of the auxiliary and main charges. Charge weights, depths of place-



LEGEND:

- t_i = ICE THICKNESS
- w_1 = MAIN CHARGE WEIGHT
- d_1 = MAIN CHARGE PLACEMENT DEPTH
- w_2 = AUXILIARY CHARGE WEIGHT
- d_2 = AUXILIARY CHARGE PLACEMENT DEPTH
- l = HORIZONTAL DISTANCE BETWEEN CHARGES
- α = DIRECTING ANGLE
- t_d = TIME DELAY BETWEEN DETONATIONS

FIGURE 33

FACTORS AFFECTING DIRECTED BLASTING

ment and horizontal spacing (1) between the charges (hence the directing angle) were held constant. The main and auxiliary charge weights were the same as used in his decked charge experiments (25.2 and 4.8 kg), and the directing angle was held at a constant 45° . The results of this experiment for the observed cratered area (A_0) and the percent of ice ejected from the crater are shown in Figure 34. There are pronounced, coincident narrow peaks in both the cratered area and ice ejection relationships. From this Nikolayev concluded that the optimum detonation delay t_d was 0.025 seconds. This probably explains why the delay was chosen for the decked charge tests.

As part of the first experiment Nikolayev detonated two single charges, one being the same weight as the main charge alone (25.2 kg), and the other being equal to the total weight of the main and auxiliary charges (30 kg), and placed them at the 'optimum' depth of placement (2.1 m) determined from his previous study with single charges. The cratered areas for the 25.2 and 30.0 kg charges were 143.1 and 151.7 m^2 respectively. The ejection of ice from the craters was reported to be less than 5%. For the 30 kg single charge Figure 34 shows that directed blasting with the same charge weight broken into two charges increases the cratered area by 47%, and the fraction of ice ejected was as high as 50%.

The second experiment was designed to study the influence of the directing angle (α). The main charge weight

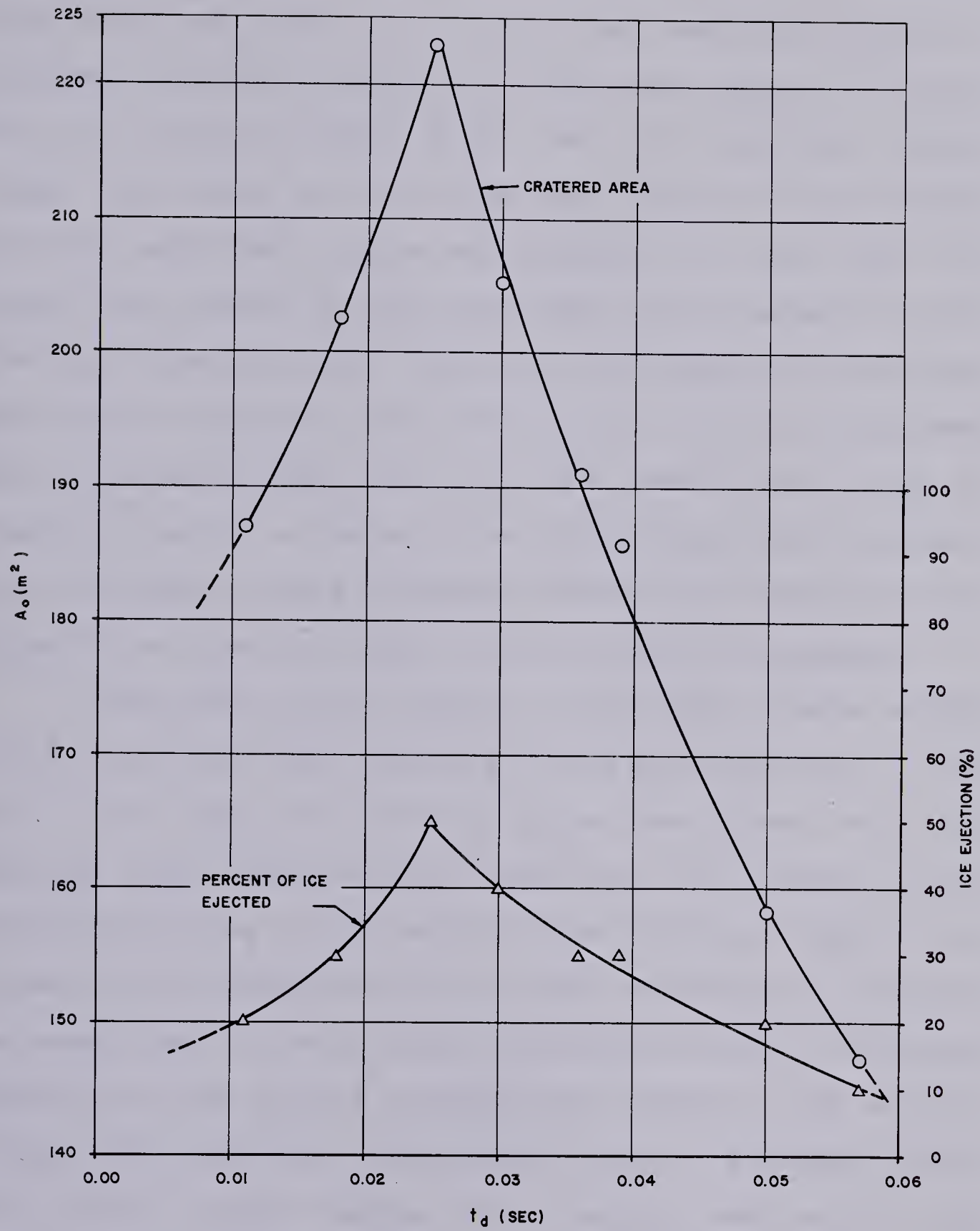


FIGURE 34
EFFECT OF DETONATION DELAY IN DIRECTED BLASTING
(DATA FROM NIKOLAYEV, 1971)

was held constant, as was the detonation delay. The directing angle was varied by setting the auxiliary charge in different locations relative to the main charge. It can be seen in the data (Table A-12), that the auxiliary charge weight was varied as well. Thus the size of the gas bubble from the auxiliary charge was different in each case. As stated, the intent of the experiment was to assess the effect of directing angle. However, the changes in auxiliary gas bubble dimensions make the results of this experiment less conclusive than the first. The results are shown in Figure 35, again in terms of the cratered area and ice ejection. The figure shows coincident maxima for these relationships for a directing angle of 45° as might be expected.

The effect of the change in auxiliary charge weight did not seem to affect the form of the relationships in Figure 35. In fact, the largest crater was formed with the smallest total charge weight. That there is an affect on the relationships due to the weight of the auxiliary charge will be seen in the discussion of the next experiment. It should be noted that the main charge placement depths (indicated adjacent to the plotted cratered area points in the figure) bracket the previously determined 'optimum' placement depth (2.1 m) for single charges of the weight used and for the ice thickness encountered. Placement depth presumably had to vary to allow for the different sizes of auxiliary gas bubble to maintain the desired directing angle. The maximum crater obtained during this experiment occurred with the

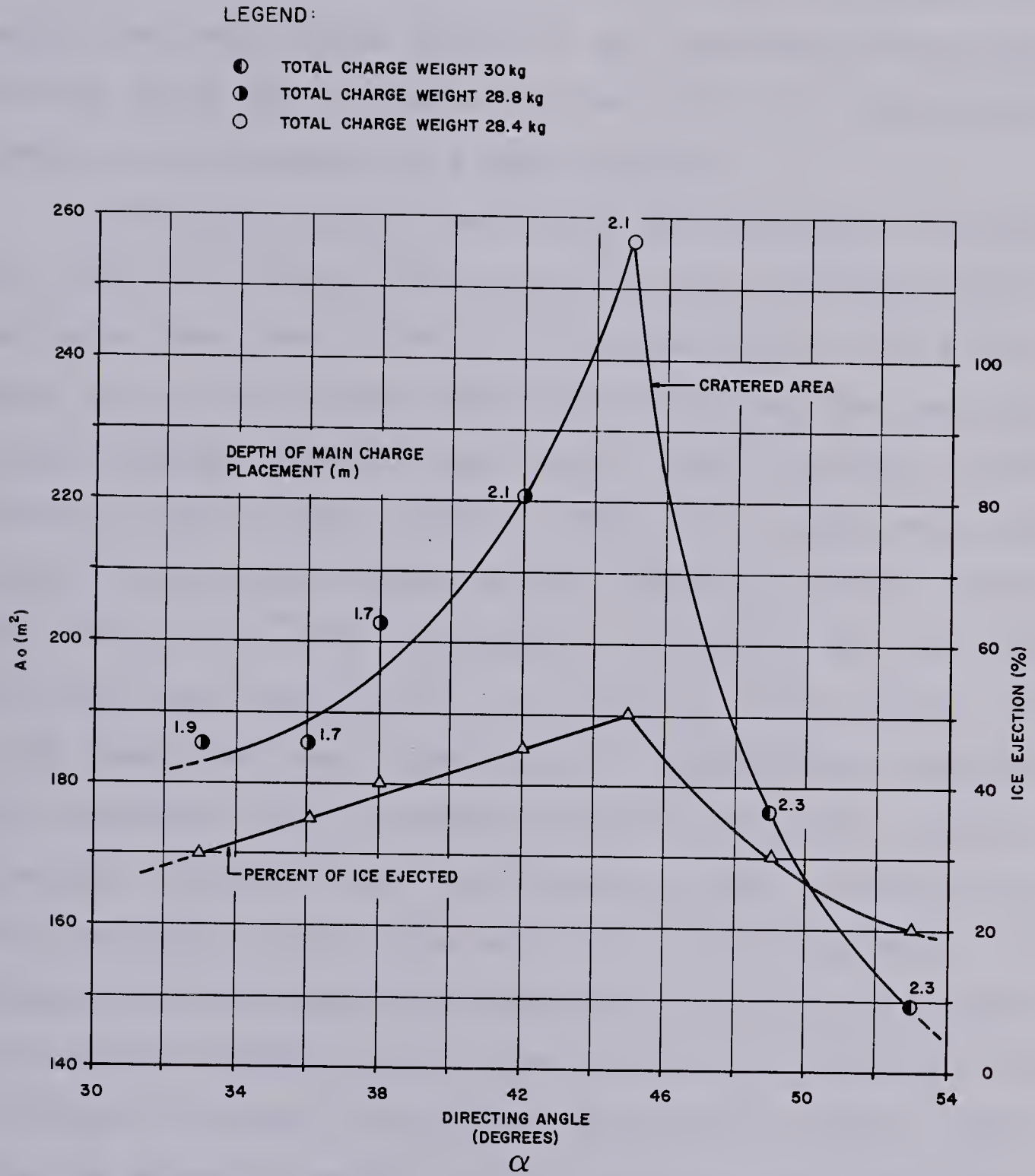


FIGURE 35
EFFECT OF DIRECTING ANGLE IN DIRECTED BLASTING
(DATA FROM NIKOLAYEV , 1971)

main charge placed at the previously determined optimum depth. The influence on the result of this experiment of having the main charge placed at the previously determined optimum depth for a single charge cannot be ascertained, though it is discussed in a later section.

Nikolayev's third experiment was designed to study the effect of varying the weight of the auxiliary charge, and hence the size of the auxiliary gas bubble, for a constant main charge weight. Nikolayev indicated that the auxiliary charge weights used were $1/8$ th (0.125), $1/7$ th (0.143), $1/6$ th (0.167), $1/5$ th (0.200), $1/4$ (0.250) and $1/3$ rd (0.333) of the main charge weight. The data, however, shows that these were only approximate fractions, and the fractions used were 0.127, 0.143, 0.175, 0.190, 0.246, and 0.333 times the main charge weight respectively. The main and auxiliary charge placement depths were held constant. Nikolayev indicated that the directing angle was held constant as well, but the data does not substantiate this. Although the charge placement depths were held constant, hence the distance between them in the vertical was constant, the horizontal distance (1) between the charges varied, therefore the directing angle was not constant. Note 5 of Table A-12 gives the calculated directing angles based on the relative positions of the two charges.

The results of this experiment are shown in Figure 36 again in terms of cratered area and ice ejection. The figure shows a maximum cratered area for an auxiliary charge weight

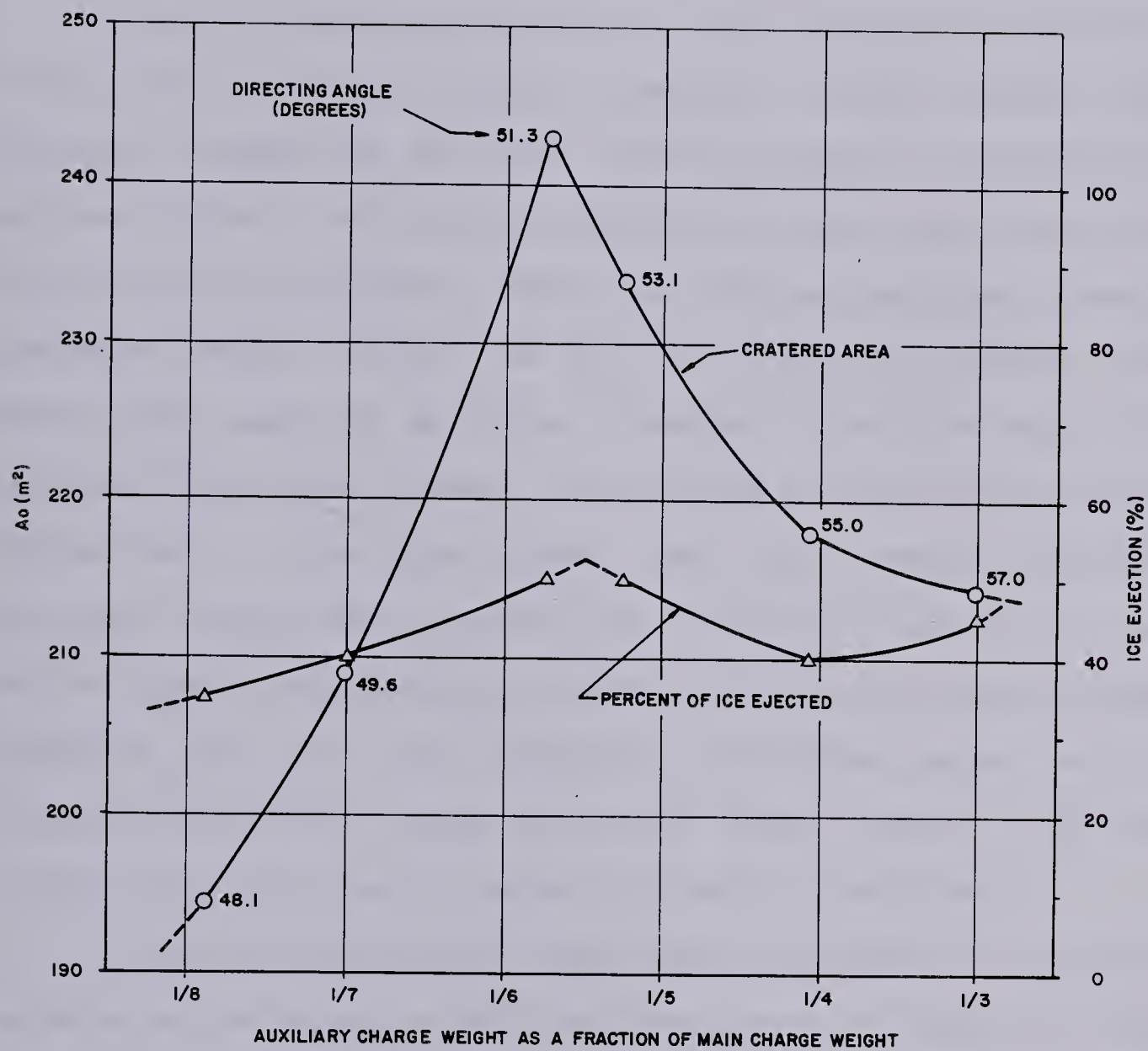


FIGURE 36
EFFECT OF AUXILIARY CHARGE WEIGHT IN DIRECTED BLASTING
(DATA FROM NIKOLAYEV, 1971)

that was 0.175 times the main charge weight (approximately 1/6th). The percent of ice ejected was generally high, hence did not show as sharp a peak as the relationship had shown previously.

For the final experiment it was difficult to tell exactly what was being studied. Constant charge weights were employed, except for one shot (which ultimately produced the maximum crater), and both the directing angle and detonation delay were held constant. Both the main and auxiliary charge placement depths varied, as did the vertical distance between them, hence to maintain a constant directing angle the horizontal distance between the charges had to vary as well. Inspection of the data shows that only three auxiliary placement depths were tested for a total of six shots, and one horizontal and vertical distance between charges was repeated as well. The only parameter which was varied continuously was the main charge placement depth, hence it was believed that this was the parameter being investigated.

The results of this experiment, in terms of the cratered area and ejection of ice, are shown in Figure 37. The figure shows that the maximum cratered area and percent of ice ejection occurred for a main charge placement depth that was equal to the previously determined optimum depth for the total charge weight as a single charge. However, the maximum observed ice ejection was also obtained with a second charge placed 0.2 m deeper, and, the curvature of the ice ejection relationship suggests that a higher fraction of ice might be

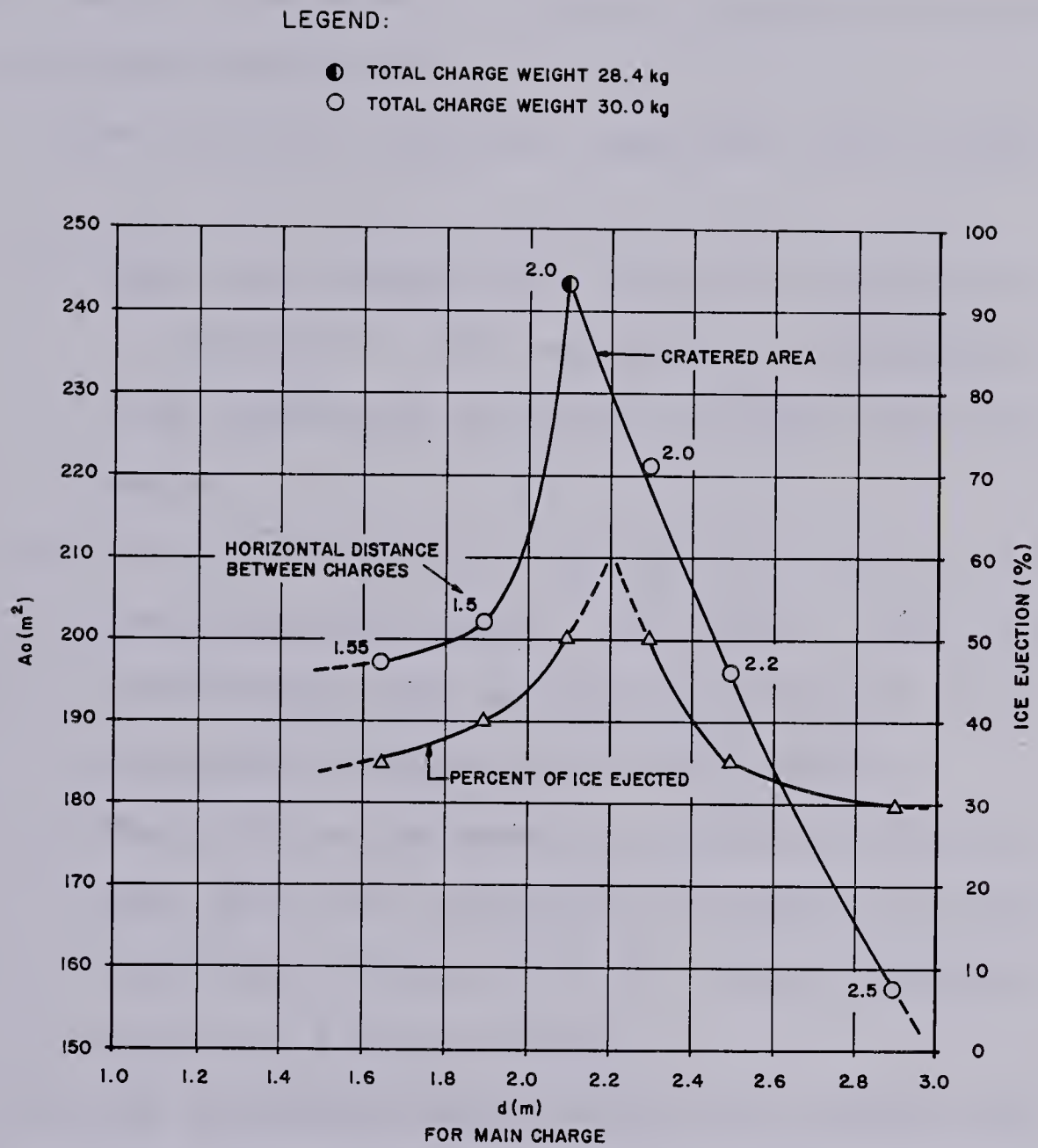


FIGURE 37

EFFECT OF MAIN CHARGE PLACEMENT DEPTH IN DIRECTED BLASTING

ejected if the main charge were to be placed at a depth of 2.2 m instead of the optimum 2.1 m for a 30 kg charge. The pronounced peak in both functions suggests that since the maximum crater was formed with the only different total charge weight, the effect of charge weight may be greater than Nikolayev anticipated.

From the above, Nikolayev concluded (1971) that:

- a. The total charge weight should be computed as a function of the measured ice thickness, from previously determined optimum relationships.
- b. This weight should be broken down into a main and auxiliary charge, the latter being approximately 1/6th of the resulting main charge weight (1/7th of the total weight),
- c. The main charge should be placed in accordance with the previously determined optimum placement criteria for the total explosive weight as a single charge,
- d. The auxiliary charge should be placed such that the resulting directing angle is 45° , and
- e. The auxiliary charge should be detonated 0.025 seconds before the main charge.

Nikolayev did not assess the effect of the placement

depth of the auxiliary charge experimentally, which is the only remaining unknown in the procedure, nor is his data conducive to such an analysis. However, on a theoretical basis, Nikolayev did note:

"The depth of [placement of] the auxiliary charge depends to a considerable extent on its weight, and is assumed to be the distance from the charge's centre to the water surface [static phreatic water surface within the ice] ... [and] ... the value of the maximal radius of gaseous cavity ... [from] the auxiliary charge should be less than this distance."

The explosive used by Nikolayev for his directed blasting experiments was TNT. As the placement of the auxiliary charge and the delay between the auxiliary and main detonations, to allow the gas bubble from the auxiliary to reach maximum size, appears to be the crucial factors in directed blasting, the recommendations made by Nikolayev may not be appropriate for all explosives, as the gas effectiveness of other explosives varies from that of TNT, as shown in Table B-5 of Appendix B.

The directed blasting data was analysed using the regression equation obtained in Chapter 6 for equivalent TNT charges (Equation 16). In order to carry this out, the total charge weight of the main and auxiliary charges was considered to act at the placement depth of the main charge, as Nikolayev had done. Nikolayev's craters were elliptical rather than circular, therefore for this comparison an 'observed' crater radius was determined as that which gave the

observed cratered area for the elliptical crater. The comparison between observed and calculated crater radius is shown in Figure 38, as well as for the two single shots mentioned earlier. As all of the charge weights for Nikolayev's first experiment had been constant, they plot in a vertical line above the computed radius. The effect of the detonation delay in increasing the cratered area can, however, be clearly seen. It is interesting to note the similarities in the 'peaked' relationship between observed and calculated radius for Nikolayev's third and fourth experiments, with that noted previously in Figures 36 and 37. The effect of directed blasting in generally increasing the crater dimensions is also well illustrated in the figure.

8.3.2 Discrepancies in Nikolayev's Observations

A detailed study of Nikolayev's (1971) paper shows that the recommendations for the depth of auxiliary charge placement and the detonation delay are open to speculation. It will be noted from Nikolayev's data (Table A-12) and from the previous portrayals of his results (Figures 34 through 37 inclusive), that where he experimentally determined the optimum detonation delay, his main and auxiliary charge weights were 25.2 and 4.8 kg respectively, the directing angle was 45°, and the depth of placement of the main charge was 2.3 m.

In his second experiment, where directing angle was investigated, the optimum angle was determined to be 45°,

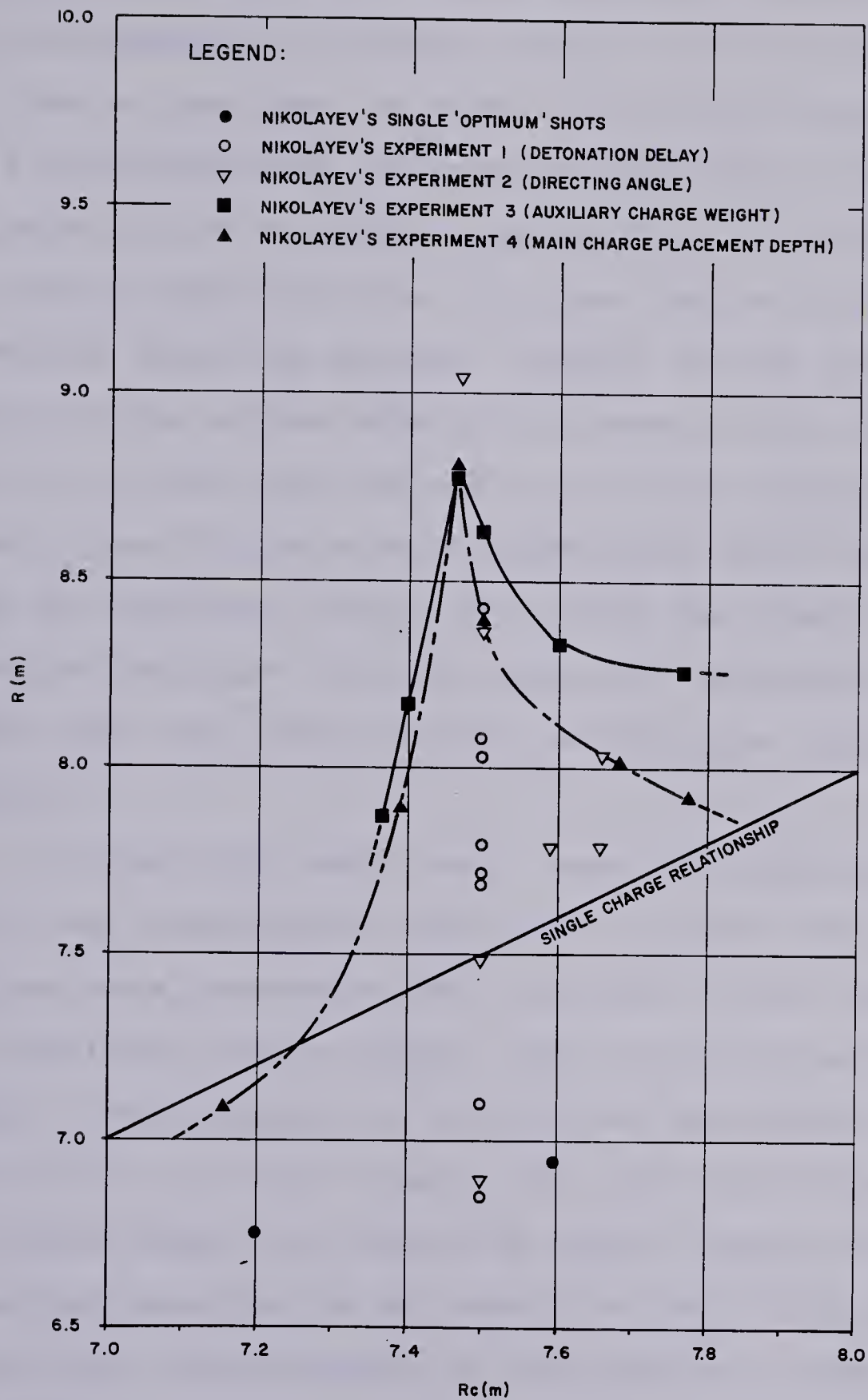


FIGURE 38

NIKOLAYEV'S DIRECTED DATA ANALYSED AS SINGLE TNT CHARGES

however, the auxiliary charge weight was 3.2 kg, and the depth of placement of the main charge was 2.1 m. From Figure 36 it can be seen that the effect of auxiliary charge weight has a pronounced peak (in terms of the crater size), hence the selection of an optimum angle using a different auxiliary charge weight from that which was used to determine the detonation delay was dubious. Further, it was later determined that the optimum depth of placement of the main charge was 2.1 m, which, as the effect of main charge placement depth (Figure 37) has a very strong peak, could have influenced the resulting crater size, with the result that the determined 'optimum' directing angle was determined for conditions that were not as constant as Nikolayev would have us believe.

In the third experiment, where the auxiliary charge weight was investigated, the maximum crater size and ice ejection were determined for conditions which used yet a third auxiliary charge weight, and a directing angle which, though it was reported to be 45° , has been shown (Note 5, Table A-12) to be 51.3° . Again, the influence of the auxiliary charge weight and directing angle, having such strong peaks, may have led to an inaccurate conclusion regarding the ultimate proportioning of the auxiliary charge to the main charge.

Finally, in the last experiment, where the main charge placement depth was investigated, the directing angle and detonation delay were held constant, as were the main and

auxiliary charge weights, for all but the final shot, where the auxiliary charge weight was changed and the maximum crater resulted.

Thus it has been shown from a detailed examination of Nikolayev's data, that for every case of both the maximum crater size and ice ejection obtained, at least one parameter, which was otherwise held constant throughout the remainder of the series, varied where it would not have in a properly designed experimental program. Whether the alteration of a particular variable in a series caused the maxima to occur, or whether it was coincidental, could not be assessed from the data alone. The apparent discrepancies could not be explained in terms of the theory presented by Nikolayev either, as that presentation was somewhat confusing. Presumably, the details of some of the principles involved in directed blasting were lost when Nikolayev's original paper was translated.

8.4 The Chilcotin Data

The directed blasting tests carried out at Drummond Lake were described in Section 5.2.5. In terms of the experimental objectives (Section 5.1), Experiment 4 was for the secondary objective of 'testing' methods of increasing the fraction of ice ejected from the crater. The objective was only to test the method, as the previously discussed discrepancies in Nikolayev's results made a properly planned

experimental design impossible until such time as some of the discrepancies were investigated. Nine directed blasting shots were detonated, the data for which will be presented later. The experiments for the testing of directed blasting were designed in the field, from a dimensional analysis of the factors affecting the gas bubble.

8.4.1 Design of the Directed Shots.

The investigation of directed blasting was centred on an investigation of the detonation delay time t_d , hence was concerned with the expansion of the gas bubble from the auxiliary charge. It was considered that the following parameters would influence the expansion of this bubble (Note: all variables are implied to have the subscript 2, as this discussion is limited to the auxiliary charge.) :

- E , the energy of detonation,
- R_0 , the radius of the expanded bubble,
- d , the detonation depth,
- ρ , fluid density,
- g , gravitational constant, and
- t , the time of bubble expansion
to maximum size (R_0).

A simple dimensional analysis of the above parameters with E , ρ and d as repeating variables will yield:

$$f_1 \left(\frac{\rho R_o^5}{E t^2}, \frac{d}{R_o}, \frac{\rho g R_o^4}{E} \right) = 0 \quad \dots (19)$$

It was initially considered that the weight of water would be small compared to its inertia, hence the third term could be omitted from consideration. It was also considered that the depth of explosion could be omitted as its effect accounted for the governing hydrostatic pressure, which should have gone out when g was eliminated with the previous term. Thus, in its simplest form, the relationship investigated was:

$$f_2 \left(\frac{\rho R_o^5}{E t^2} \right) = 0 \quad \dots (20)$$

Substitution of the weight of explosive W for the energy E , incorporating ρ into the constant implicit in such a function, and rearrangement led to:

$$t = C \frac{R_o^{5/2}}{W^{1/2}} \quad \dots (21)$$

Little data was available to evaluate the constant C . Kurtz et.al. (1966) had presented the vertical ice displacement as a function of time for two of their tests (Shots 3 and 4), which they had obtained from analysis of the high speed photography taken of those shots. It was

assumed for this investigation that the initial displacement of the ice was due to the gas bubble having expanded to the lower surface of the ice, hence that the bubble radius was equal to the depth of placement of the charges. The time elapsed to obtain a small ice surface displacement (0.15 m, 6 in) was taken from Kurtz et.al.'s displacement history as the bubble expansion time t . A third data point to assist in the determination of C was taken as the third shot of Nikolayev's (1971) first directed blasting experiment, from which he had obtained his optimum detonation delay. The gas bubble radius, however, was taken as the distance between the auxiliary and main charge along the directing line. The data used, and the calculation of C , are given in Table 9.

TABLE 9

Determination of 'C'

Source	W	R _O	t	C	W	R _O	t	C
	(kg)	(m)	(sec)	(x10 ³)	(lb)	(ft)	(sec)	(x10 ⁴)
Nikolayev	4.4	2.56	0.025	5.0	9.7	8.4	0.025	3.8
Kurtz #3	58.97	3.05	0.010	4.7	130.0	10.0	0.010	3.6
Kurtz #4	64.18	4.57	0.025	<u>4.5</u>	141.5	15.0	0.025	<u>3.4</u>
Average				4.7	Average 3.6			

The initial calculation of C had been carried out in the field in English units, from which some small rounding off of the numbers resulted in a C value of 3.4×10^{-4} (Eng-

lish dimensions) being used in the design of the test shots. The 6% difference is considered minor. The calculations of the time for the gas bubble for the Chilcotin tests to expand were carried out with charge weight and bubble radius converted to English dimensions.

The design of each series of three shots was based on a rough application of the preliminary ice demolition relationships determined from Mellor's analysis (Equations 8a, 8b and 8c). A placement depth for the main charge was preselected. For this depth, a main charge weight was chosen to yield a certain crater size, though not necessarily the optimum for the thickness of ice. For the first two series of shots, the auxiliary charge weight was taken as 20% of the main charge weight (a rough application of Nikolayev's recommendation for the size of the auxiliary charge), and was rounded off to the nearest half-block (0.5 kg) of DM 12. For the third series, the auxiliary charge weight was taken as 1% of the weight of the main charge, rounded off to the nearest quarter-block (0.125 kg) of DM 12.

For the first series of three shots, the main charge depth was selected such that the auxiliary charge could be placed at the lower surface of the ice sheet and give a 45° directing angle. The auxiliary charges for the second and third series were placed such that they again gave a 45° directing angle, and were equidistant from the centre of the main charge and the lower surface of the ice sheet. With the distances along the directing line between the two charges

being taken as the 'radius' of the expanded gas bubble, the auxiliary charge weight and the constant $C = 3.4 \times 10^{-4}$ were used to compute the time it would take for the bubble to expand to this radius according to the derived Equation 21. The computed bubble expansion time t for the three series were:

Shots	t (m sec)
D1-D3	4.25
D4-D6	3.30
D7-D9	15.60

For each series, this time was assumed to be the desired detonation delay t_d , and a length of det cord was calculated, from the detonation velocity of the explosive filler, which would produce the computed delay. To facilitate the making up of these delays, the length of det cord was rounded off to the nearest 50 or 100 feet (15 to 30 m). One shorter 'delay' and one longer were included to bracket the calculated bubble expansion time. The three delays then comprised a series of three shots for a given main and auxiliary charge weight.

Photo 8, used previously in Chapter 5 to depict the placement of a charge, is actually of a 12 kg main charge being lowered into position. The auxiliary charge had already been placed through the small hole seen below the stick in the photograph, which was supporting the charge.

8.4.2 Observations From Experiment 4

As previously stated, nine directed blasting shots were detonated as Experiment 4. The data for these shots are given in Table 10.

The data were analysed using the observed crater area, as Nikolayev had done, and the cratered area for the whole charge weight set as a single equivalent TNT charge at the placement depth of the main charge. As well, observations were made concerning ice ejection from the crater, from notes made in the field and interpretation of photographs taken of the craters. The cratered area calculations are summarized in Table 11, and the results for the first six shots are shown in Figure 39.

For the first series (Shots D1-D3), the figure shows a weak tendency for the crater radius, indicated by the observed crater area, to decrease with an increase in detonation delay. The three points appear to define a minimum of some functional relationship in the vicinity of the calculated auxiliary bubble expansion time (4.25 m sec), rather than the expected maximum. The source of this discrepancy was traced back to the initial calculations used in designing the series. It was stated that the underlying assumption in determining the delay time was that it would be equal to the auxiliary gas bubble expansion time to reach the main charge. In the initial calculations, however, the expanded 'radius' was not the distance between the two charges, but was the distance between the main charge and the bottom of

TABLE 10
Directed Blasting

Chilcotin Data												
Shot Number	(1)		d ₁ (m)	d ₂ (m)	l (m)	(2)		(3) Area A _O (m ²)	(4) Crater Diameter Measurements			
	t _i (m)	W ₁ (kg)				W ₂ (kg)	t _d (sec)		Angle (°)	a (m)	b (m)	c (m)
D1	0.305	4.0	0.914	0.0	0.914	0.0019	45	61.38	9.14	8.53	8.84	-
D2	0.305	4.0	0.914	0.0	0.914	0.0038	45	57.15	8.53	8.53	8.53	-
D3	0.305	4.0	0.914	0.0	0.914	0.0077	45	59.97	8.84	8.53	8.84	-
D4	0.366	12.0	1.829	1.067	0.762	0.0019	45	109.59	11.58	12.20	11.73	11.73
D5	0.363	12.0	1.829	1.067	0.762	0.0038	45	104.89	11.75	11.41	11.71	11.35
D6	0.365	12.0	1.829	1.067	0.762	0.0077	45	99.54	11.24	11.31	11.23	11.25
D7	0.370	12.0	1.829	1.067	0.762	0.0115	45	98.40	11.13	11.20	10.85	11.58
D8	0.380	12.0	1.829	1.067	0.762	0.0231	45	112.96	11.95	12.08	11.61	12.32
D9	0.350	12.0	1.829	1.067	0.762	0.0462	45	118.01	12.47	12.40	12.33	11.82

Notes:

1. Subscripts 1 and 2 refer to the main and auxiliary charges respectively.
2. Detonation delays were obtained through the use of different lengths of det cord between the auxiliary and main charges.
3. Cratered area was determined as the average calculated area for the crater diameter measurements a through d.
4. For Shots D1, D2 and D3, three equiangular crater diameters were measured. For the remainder, four diameters were measured; (a) along the directing line, (b) perpendicular to the directing line, and (c) and (d) two intermediate measurements between the first two

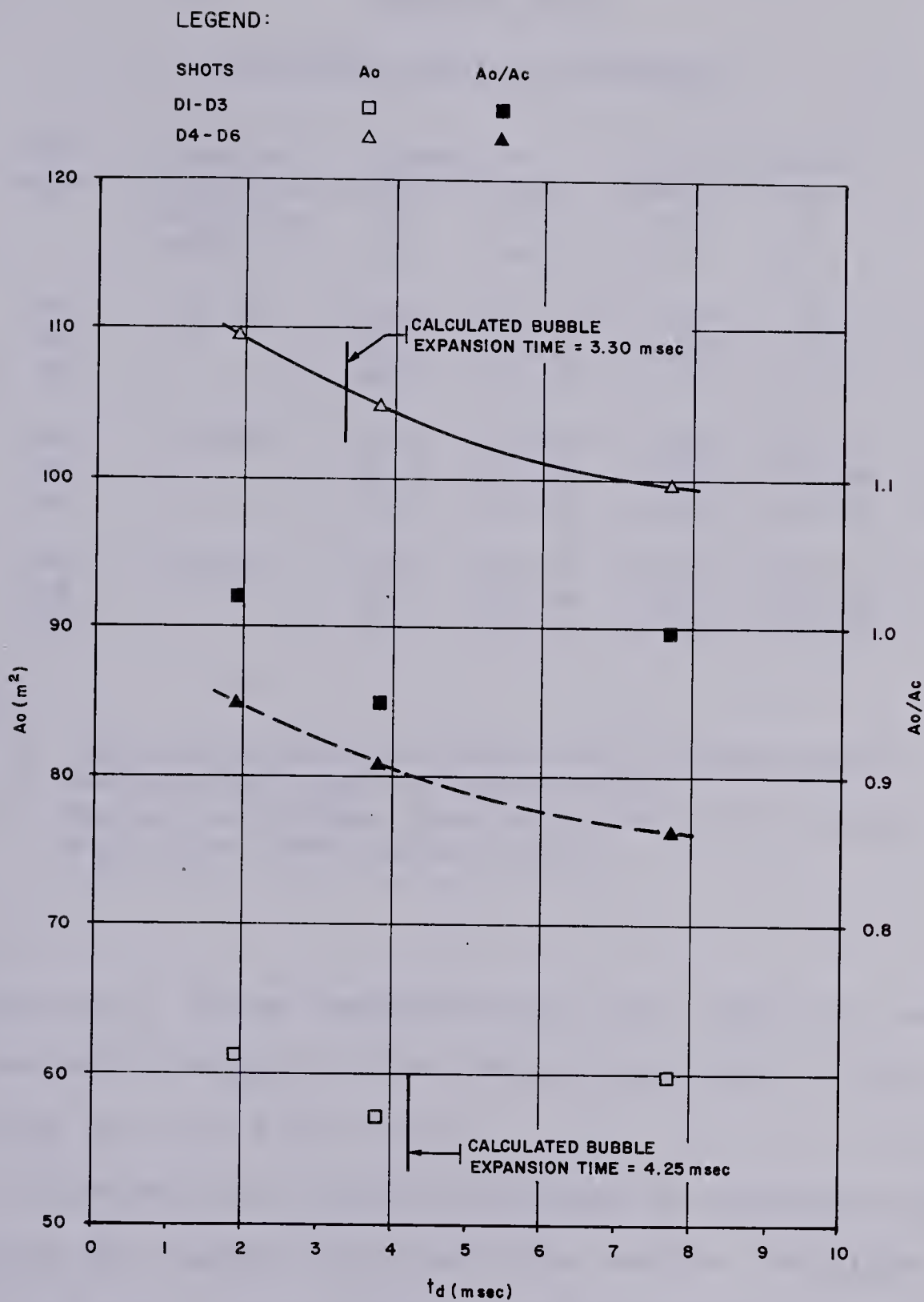


FIGURE 39
DIRECTED BLASTING
CHILCOTIN SHOTS D1-D6

TABLE 11
Cratered Area
Chilcotin Directed Blasting

Shot Number	Design ¹ Detonation Delay t_d (msec)	Observed Radius R (m)	Area A_O (m ²)	Calculated ² Radius R_C (m)	Area A_C (m ²)	$\frac{A_C}{A_O}$
D1	4.25	4.42	61.38	4.375	60.13	1.021
D2		4.27	57.15	4.375	60.13	0.950
D3		4.37	59.97	4.375	60.13	0.997
D4	3.30	5.91	109.59	6.066	115.60	0.948
D5		5.78	104.89	6.065	115.58	0.908
D6		5.63	99.54	6.066	115.60	0.861
D7	15.60	5.60	98.40	5.708	102.37	0.961
D8		6.00	112.96	5.712	102.49	1.102
D9		6.13	118.01	5.703	102.18	1.155

Notes:

1. Calculated delay for auxiliary charge weight and spacing from the main charge.
2. Radius calculated from Equation 16 for energy equivalent TNT charge weight.

the ice sheet. To be comparable with the other two series, the gas bubble expansion time should have been in the order of 10.1 m sec, not 4.25 m sec.

A second point arose concerning the expansion of the auxiliary gas bubble for this first series. Nikolayev had indicated that, theoretically, the placement depth of the auxiliary charge should be such that when the bubble was fully expanded, it should, at most, be tangential to the phreatic surface within the ice. This is not unreasonable,

for if the ice is shattered by the shock wave, or the placement hole is left open and the gas bubble reaches the 'free' water surface before it has fully expanded, the gases will vent through the shattered ice or the placement hole before the desired subsurface cavity is created. As the auxiliary charges for the first series were placed at the lower surface of the ice, the distance from the centre of the charge to the atmosphere would have been about a quarter of the distance to the main charge. The placement holes for all of the directed blasting charges had been left open, hence the gas bubble may have started to vent before the desired cavity had been created under the ice. This is not to say that there was not a small cavity, just that the desired cavity from the lower surface of the ice to the main charge probably did not exist for this series.

That there seems to be a trend in the data opposite to that expected, ie a minimum was observed in the relation of crater size to detonation delay, is considered to be due to a combination of a different bubble 'radius' being inadvertently used in the design of the detonation delay for the first series, and the proximity of the detonation to the atmosphere with regards to gas venting.

At least a partial directing effect was achieved with Shot D3, which had the longest delay of the series. Photo 20 clearly shows a small redirected venting plume, though the vertical plume appears to be the stronger of the two. The delay for this shot was in the order of twice the initially

calculated expansion time, but is about equal to the corrected delay of 10 m sec.

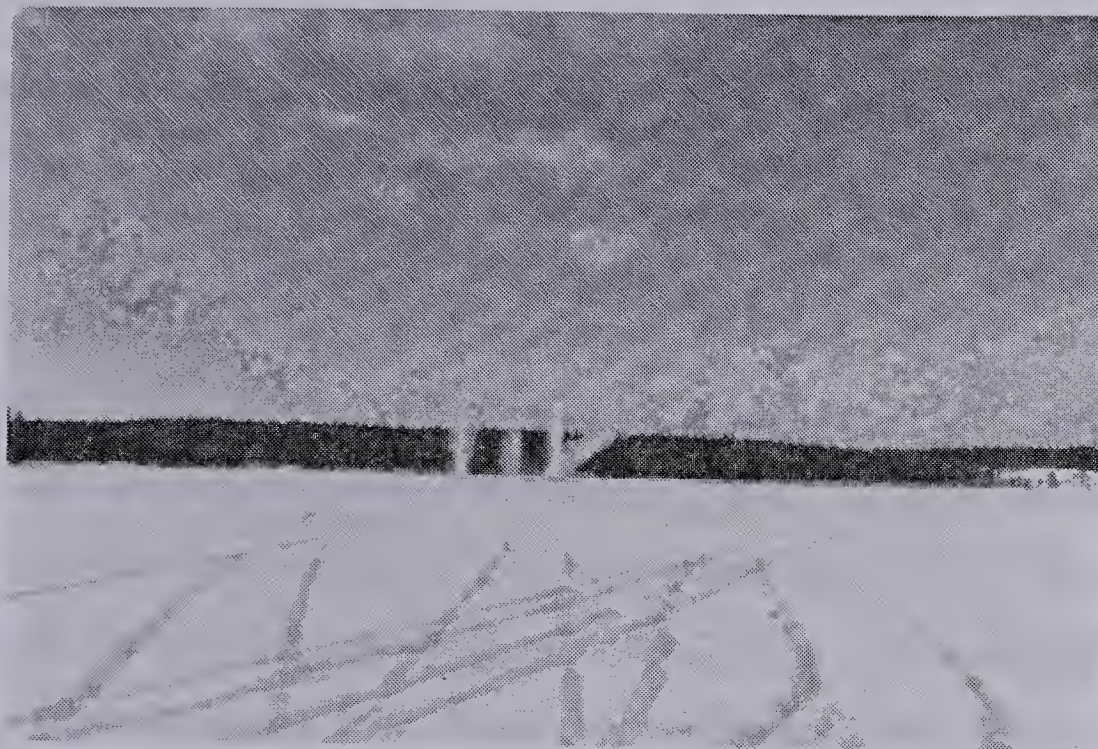


Photo 20: Venting Plume from Directed Blasting
Shots D1 through D3

Despite the appearance of Photo 20, observation of the ice debris in and around the crater indicated that the desired major throwing effect of the debris had not been attained. There was, however, evidence that some smaller ice fragments and a certain amount of water had been carried by the redirected plume.

There was no evidence of the crater having been enlarged in the manner Nikolayev had noted for his shots, as shown by the ratio of observed to calculated area shown in Figure 39. As well, there was little evidence of the crater having been elongated into an elliptical shape, as Nikolayev reported his had been, though one of the three measured di-

ameters (column (a) of Table 10) was longer than the rest. The difference in the three diameter measurements was not outside range of other diameter measurements from Experiment 2, where essentially circular craters were observed.

For Shots D4 through D7 (calculated bubble expansion time of 3.3 m sec), Figure 39 shows a distinct decrease in crater dimensions for an increase in the delay time. In every case, the crater was smaller than was calculated (Table 11) for an equivalent TNT charge. That crater radius increased in the direction of decreasing detonation delay is thought to be an indication that the delay time was overestimated. The size of the auxiliary charge for this series (2.5 kg) is such that its released energy and volume of detonation gases would be far greater than those for the other two series, hence it is not unreasonable to suspect that the bubble expansion time would be shorter, on a relative basis, because of the increased volume of gases occupying a similar initial space (the volume of the unexploded charge), hence under higher pressure. The inclusion of W in Equation 21 should, however, have compensated for this.

The craters from this series are shown as the second row in from the bottom of Photo 21. (Note: the two large craters shown just above this row were not from the directed blasting series, they are the craters for Shots 51 and 52 of Experiment 2).

The craters are, from right to left, D4 through D6 respectively. The photo shows little evidence of the direct-



Photo 21: Directed Blasting Craters; D4 through D9

ing effect for Shot D6. From the surge splash stain around crater D5, the centre crater, there is an indication that the water surge to the far side of the crater was more pronounced, however, the distribution of ice debris in and around the crater indicates that there was a tendency for the ice to be thrown to the near side of the crater. The crater for Shot D4, the right hand crater, shows a pronounced surge stain at the upper right side of the crater, with virtually no surge splash to the lower left side. The ice debris remaining in the crater, however, is on the side where the surge stain is the least. This could be due to either a 'sloshing' action within the crater following the surge, or, by the directing effect the charge was designed for. Unfortunately, no record was kept of the directing direction for this row. The distribution of ice debris around

the outside of crater D4 shows that there was a pronounced ejection of ice to the lower left side of the crater. The total distribution of ice debris therefore shows that a throwing or directing action had occurred, though it is not known if this was in the direction it was supposed to have been thrown. Photo 22 gives a view of the craters D4 through D6, as well as the next series, D7 through D9, from a different angle, which may assist in the observation of the points being noted.

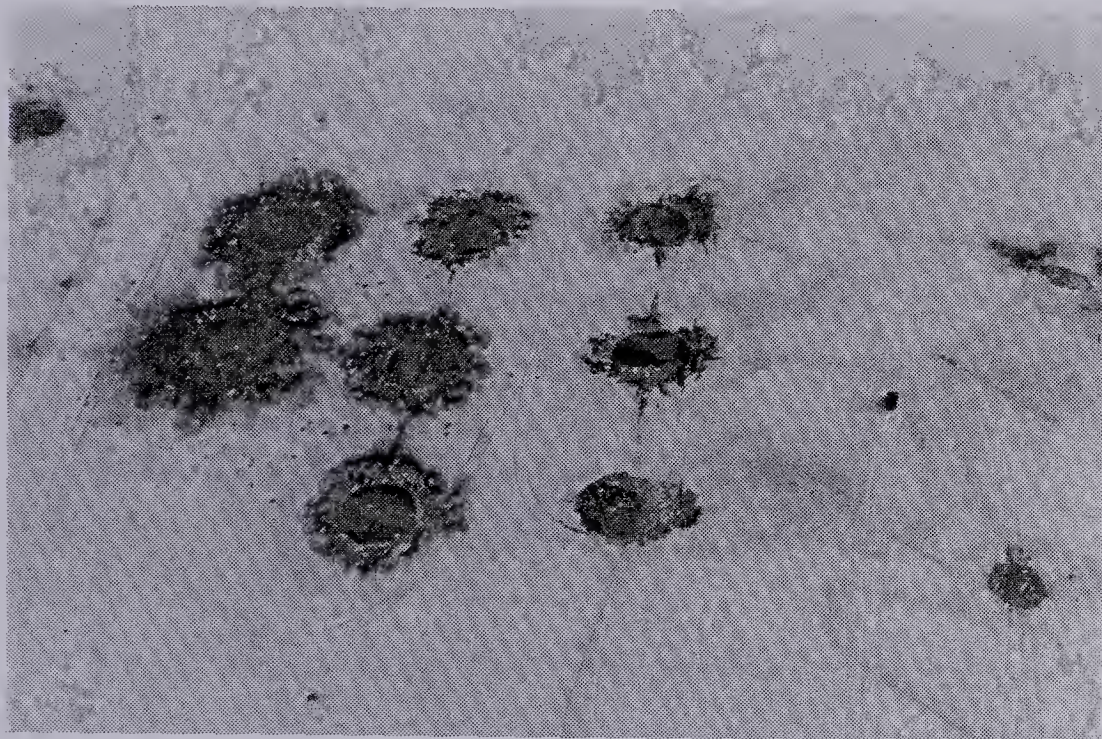


Photo 22: Directed Blasting Craters; D4 through D9

The final series of directed blasts, D7 through D9 are shown from right to left, respectively, as the first row in from the bottom of Photo 21. The data for these three shots has been plotted in Figure 40. The figure shows that a definite increase in cratered area occurred for Shots D8 and D9, and also shows the possibility that the 'optimum' time

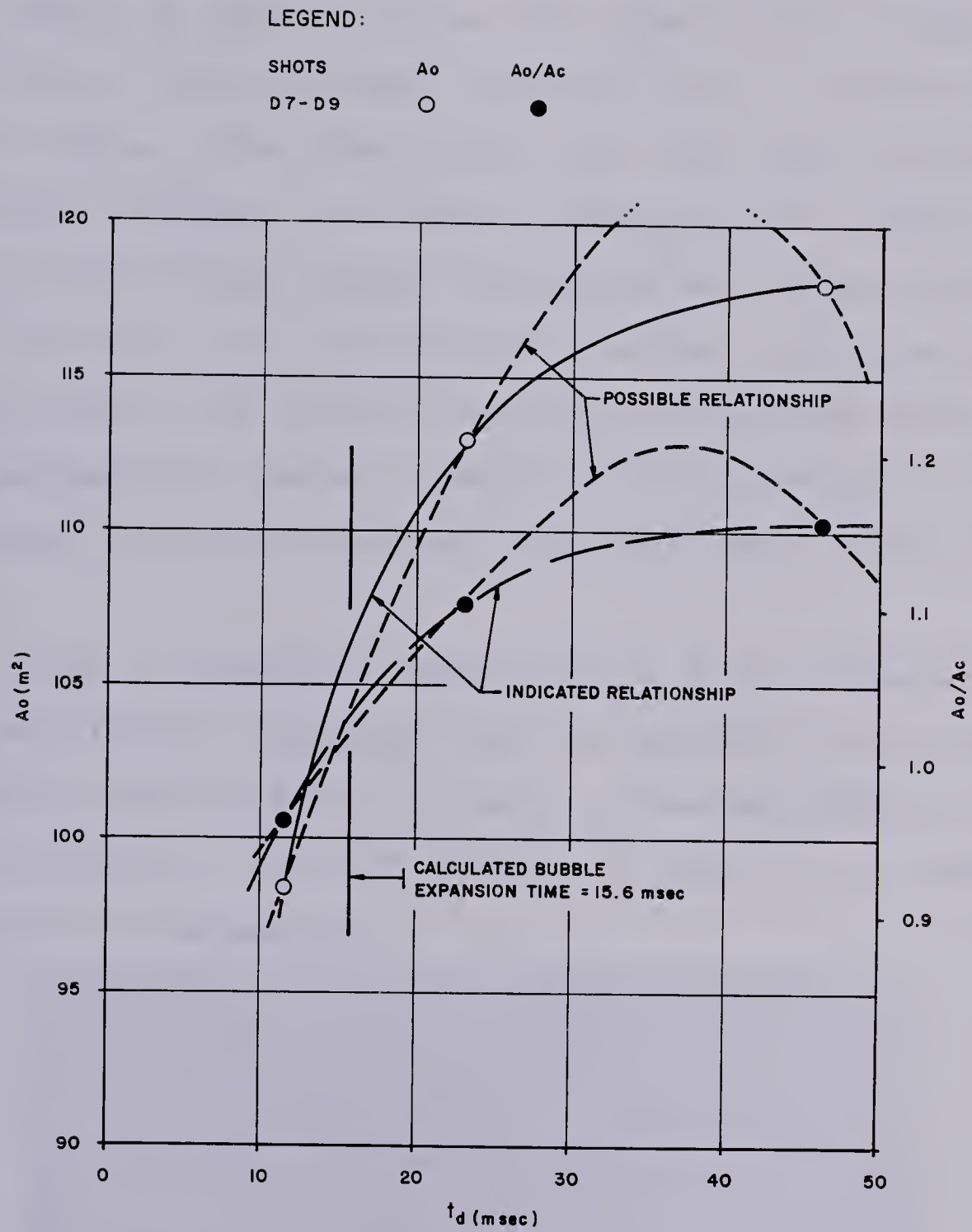


FIGURE 40

DIRECTED BLASTING

CHILCOTIN SHOTS D7 - D9

delay (expansion time of the auxiliary bubble), for the charge weights and placement positions used, has been bracketed. Photo 21 shows that for all three of the craters in this series, the main water surge had been to the near side of the crater in the photograph, and, that there had been a pronounced 'throwing' of debris, especially for charge D9. For this shot, approximately 50% of the ice had been ejected from the crater, and the remaining ice was all concentrated on one side of the crater. The other two craters appear to have had more ice removed, though the distribution of ice in and around the crater does not show where the ice was thrown to.

That a reasonable approximation of the directed effect described by Nikolayev had been achieved in this last series is shown in Photo 23, which is the photograph of the venting plumes of Shots D7 through D9 (near to far respectively in the photograph).

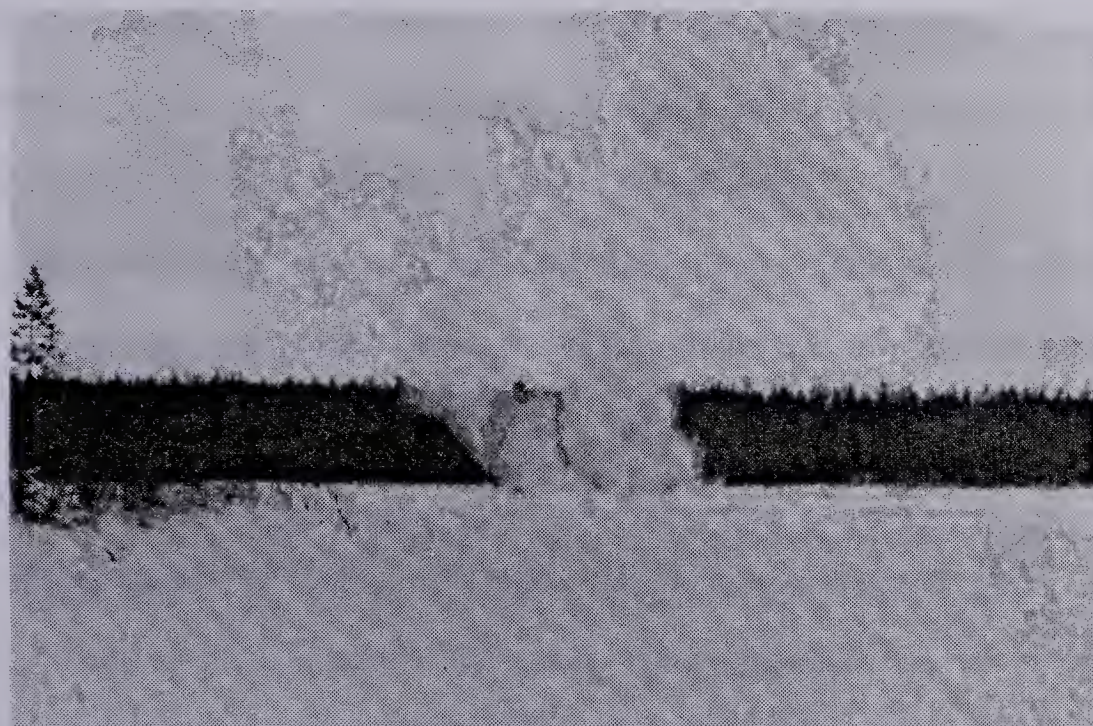


Photo 23: Venting Plume from Directed Blasting
Shots D7 through D9

Some of the directing angle shown by the plumes in the photograph was due to the prevailing wind causing drift of the vapour and smaller ice particles. However, most of the directivity was due to the detonation of the charge alone, shown by the heavier concentration of debris near the ice surface. The direction of venting shown in this photograph is the same as indicated by the debris and surge stain of Photo 21.

8.5 Findings

The objective of Experiment 4 was given as "testing" methods of increasing the fraction of ice ejected from a crater, specifically using the directed blasting technique, as close scrutiny of Nikolayev's data and 'conclusions' opened more questions than his study answered.

It was found that for certain combinations of auxiliary charge weight, placement depth and detonation delay, the redirection of the venting plume, and therefore directed throwing of the ice debris, was evident.

One of the three series of three shots produced little in the way of results, and it was determined that there had been a different 'expanded gas bubble radius' condition assumed inadvertently for the calculation of the detonation delay. For that series, it was also speculated that the auxiliary charges had been placed too close to a free water surface (in the open placement hole), to allow the expansion

of the bubble to the radius assumed before it would have vented through the placement hole into the atmosphere.

The particular shots where the directive aspect of the tests were observed were Shot D3, where a small directed venting plume was caught on film; Shot D4, where the ice ejection to one side of the crater was more pronounced, though where the main water surge appeared to be more pronounced in the opposite direction; and Shots D7 through D9, but notably D9, where both the water surge and ice ejection were coincident and in the direction planned. Of all of these, two shots (D3 and D9) were for detonation delays which were greater than computed. The implication from this is that a more rational method must be determined to compute the optimum delay.

The method used to compute this delay was based on having the auxiliary gas bubble expand all the way to the main charge, thus the main charge would be detonating into a gas sphere that would virtually be at atmospheric pressure, hence the directivity of the blast would be assured to be through the centre of the auxiliary bubble. However, there was nothing in the theory of directed blasting to indicate that the auxiliary bubble must extend all the way to the main charge, merely that it should provide an artificial free surface beneath the ice and hence cause a shorter line of least resistance for the action of the main charge to be attracted to. In point of fact, Nikolayev made a specific point that the distance between the surface of the auxiliary

gas bubble and the centre of the main charge (a distance he called 'W') was the crucial factor. If viewed in this context, the assumptions made for the testing of directed blasting were not quite what Nikolayev had indicated, however, due to the uncertainty of the results of his experiments, the assumptions made herein were at least a starting point from which to test the technique.

In general, it was found that directed blasting has merit as a technique, if the main concern is to maximize the amount of ice ejected from the crater. The theory of directed blasting has to be refined before a serious investigation of the technique can be undertaken.

In terms of application by either the military or by civilian agencies, once the technique has been refined to a reasonable state of simplification, it shows promise as a means of increasing the fraction of ice ejected by a blast. At present, however, because of the apparent sensitivity of the technique to the detonation delay between the two charges, and a marked shortage of detonators (commercial or military) of the delay time apparently required (<30 m sec), the technique is difficult to utilize unless a sufficient quantity of det cord is available to improvise the desired delay in the manner carried out during these experiments.

CHAPTER 9

LINEAR CHARGES

9.1 Introduction

Civilian dynamites are usually packaged as tubular sticks or cartridges with waxed or plasticized paper wrappings, such that they can be placed into boreholes and rammed in with a tamping rod to increase the loading density. However, some of the explosives come packaged in rigid tubular containers which can be screwed together or connected with the use of special cylindrical sleeves. Bulk explosives, such as prills and slurries can also be loaded, pneumatically or by gravity, into boreholes. In effect, the column of explosive produced in this way becomes a linear charge, as the explosive mass cannot be considered to act at a single point. Instead, the column of explosive acts along a line. For the study carried out for this thesis the types of linear charges considered were special explosive devices manufactured for military use.

These charges consist of a tubular casing enclosing an explosive mass. The most common special explosive device of this type is the military Bangalore Torpedo, in which the casing is metal, and the explosive filler can be one of Composition B, Amatol 80/20 (U.S. Department of the Army, (1969)), or 50/50 Pentolite (Hemphill, 1981). A torpedo

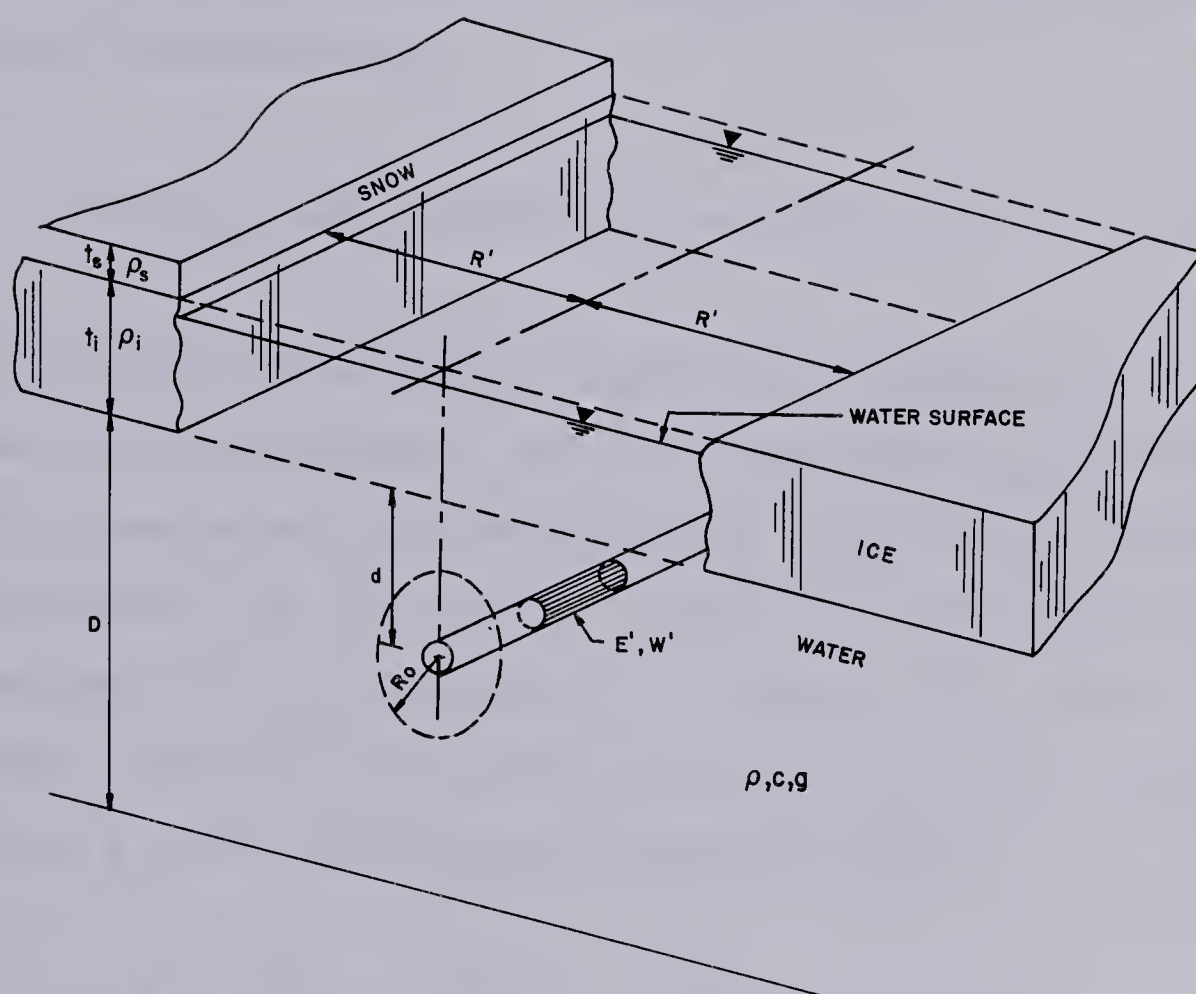
'set' includes a number of explosive-filled tubes and cylindrical sleeve couplers to permit joining tubes together to form one long charge. The primary use of the Bangalore Torpedo has been in clearing barbed wire obstacles, whereby a number of tubes are connected, pushed under the obstacle and detonated. They have also recieved some use in the clearance of footpaths through anti-personnel minefields, by causing sympathetic detonation of the mines from the shock of the exploding Bangalore.

Other types of military linear charges include the explosive-filled plastic hose 'Viper' class of minefield clearing devices. While it had been planned to test these as expedient ice demolition charges during the Chilcotin Experiment 6, Viper charges were not available.

In the strict sense, military det cord or civilian primacord can also be considered as linear charges as defined above.

9.2 Dimensional Analysis

The factors affecting the cratering of ice with linear explosives, shown in Figure 41, are primarily the same as those discussed in Chapter 2 for point charges. As indicated in the figure three variables have been redefined. Three variables previously considered in Chapter 2, E the energy of detonation, W the weight of explosive, and R the crater radius have been redefined to E' and W' , the energy and



NOTE: ALL VARIABLES SHOWN ARE AS OUTLINED IN CHAPTER 2 (FIGURE 1) EXCEPT THE FOLLOWING:

- E' = ENERGY OF DETONATION / UNIT LENGTH (J m^{-1})
- W' = WEIGHT OF EXPLOSIVE / UNIT LENGTH (kg m^{-1})
- R' = HALF WIDTH OF CRATER (m)

FIGURE 41

FACTORS AFFECTING LINEAR EXPLOSIONS

weight per unit length of the charge, and R' the half-width of the resulting crater.

The parameters shown in Figure 41 imply the following functional relationship:

$$f_1(t_i, t_s, D, \rho_i, \rho_s, \rho, E', R_0, c, d, R', g) = 0 \quad \dots (22)$$

As with the previous dimensional analysis for point charges, the relationship may be simplified by removing a number of variables from consideration due to their relative insignificance. In this manner t_s, ρ_s and D can be removed for reasons cited in Section 2.3. Choosing ρ, c and E' as repeating variables, to be consistent with the previous analysis, a simple dimensional analysis yields:

$$f_2 \left(\frac{t_i}{(E'/\rho c^2)^{1/2}}, \frac{\rho_i}{\rho}, \frac{R_0}{(E'/\rho c^2)^{1/2}}, \frac{d}{(E'/\rho c^2)^{1/2}}, \frac{R'}{(E'/\rho c^2)^{1/2}}, \frac{c^2}{g(E'/\rho c^2)^{1/2}} \right) = 0 \quad \dots (23)$$

It is again assumed that ρ, ρ_i and c are constant for most situations encountered, and can be incorporated into the constants implicit in such a function. Recalling that the energy released upon detonation is proportional to the charge weight (Baker et.al, 1973), W' can be substituted for E' to yield:

$$f_3 \left(\frac{t_i}{W'}^{1/2}, \frac{R_O}{W'}^{1/2}, \frac{d}{W'}^{1/2}, \frac{R'}{W'}^{1/2}, \frac{1}{gW'}^{1/2} \right) = 0 \quad \dots (24)$$

The relationship can be further simplified, as was done in Chapter 2, by assuming that gravity effects are small, and that the gas effectiveness of the explosive fillers are comparable. The relationship reduces to:

$$f_4 \left(\frac{t_i}{W'}^{1/2}, \frac{d}{W'}^{1/2}, \frac{R'}{W'}^{1/2} \right) = 0 \quad \dots (25)$$

The only difference from the relation for point charges is that the inclusion of the 'per unit length' parameters has caused the scaling to become 'square root' instead of 'cube root'.

9.3 Experiment 5

9.3.1 Linear Charge Description

Two linear explosives were used during the Chilcotin experiments. They were the Bangalore Torpedo (mark) M1A1, and military Reinforced Detonation Cord C3 (Det Cord).

Each tube of Bangalore Torpedo M1A1 was 1.83 m (6 ft) in length, and 40 mm (1.57 in) in diameter. The explosive filler of this particular mark of torpedo is 3.81 kg (8.40 lb) of Amatol 80/20. When a number of tubes are connected

together, the detonation is initiated from one end only, therefore at each end of the tube there is a small booster charge to pass the detonation wave from tube to tube. In the M1A1, these booster charges are 0.118 kg (0.26 lb) of TNT. Photo 24 shows a Bangalore Torpedo, five tubes (9.14 m, 30 ft) in length.



Photo 24: A Bangalore Torpedo

Table B-4 of Appendix B gives the 'effectiveness as an external charge' of Amatol 80/20 as 1.17, hence allowing the calculation of the equivalent TNT-filled charge. The explosive filler is then 4.01 kg of straight Amatol 80/20 (2.194 kg/m), or 4.69 kg of TNT (2.567 kg/m).

The det cord consisted of a core of explosive wrapped in a reinforced and waterproof plastic coating, having a cord diameter of 5.1 mm. The exact explosive filler was not known to the writer, however, from previous experience with

military explosives, the colour and texture of the filler indicate that the explosive was likely Composition C-4. The charge weight per unit length was given to the writer by one of the DRES advisors as 500 grains/foot, which is equivalent to 0.1063 kg/m (0.0714 lb/ft) of C-4, or 0.1424 kg/m (0.0957 lb/ft) of TNT. During the calculation of charge weight for the tests using these explosive 'density' (weight per unit length) figures, the charge weights seemed excessively high to the writer, based on his experience with military explosives. The explosive density finally chosen for use in this thesis was obtained in an indirect manner, as follows.

In Photo 2 (Chapter 5), the samples of DM 12 shown were resting on a det cord packing crate. Crates containing explosives are painted, hence the crate shown in Photo 2 was not a DM-12 container. That the crate shown in Photo 2 was a det cord crate is confirmed by translation of the labeling of the same crate shown in Photo 4. From the (upside-down) lettering on the side of the crate in Photo 2, it can be seen that the contents of the crate (2 x 1000 ft rolls of det cord) weighed 51 pounds. Ignoring the weight of the spools which the det cord is wound around (Photo 4), and the weight of the reinforced plastic coating of the det cord, the (conservative) weight of explosive can be calculated as 0.0255 lb/ft, roughly one-third of the weight calculated using the 500 grain/ft figure. The explosive density of 0.0255 lb/ft is considered 'more correct' than the previous value of 0.0714 lb/ft, as, only one roll of det cord at the

previous charge density would weigh 71.4 lbs, and there are two rolls packed in a crate. It is known from experience that the labeling of the packing crate is correct.

Using the computed value of 0.0255 lb/ft, the charge weight per unit length is 0.0379 kg/m (0.0255 lb/ft) of C-4, or 0.0509 kg/m (0.0342 lb/ft) of TNT.

9.3.2 Experiment Description

For Experiment 5, three shots were fired using a Bangalore Torpedo as the linear charge, and three were fired using multiple strands of det cord. It was not considered that the det cord tests would prove a viable ice demolition technique, however, the information collected would at least provide a lower limit to the data available in terms of the results obtained for very small charge 'densities'.

Two of the Bangalore detonations were designed to simulate 'hasty' demolition techniques. The first involved detonating a five-tube length of torpedo (9.14 m, 30 ft) laid on the surface of the ice, shown in Photo 25.

The second was designed to simulate the point charges described earlier, by suspending one tube (1.83 m, 5 ft) of Bangalore vertically below the ice, with the top of tube at the lower ice surface. Photo 26 shows the installation of this charge before detonation, indicating the small size of placement hole required to place the charge in this manner.

The third Bangalore shot simulated a deliberate demolition technique. For this shot, a five-tube length of tor-



Photo 25: Surface-laid Bangalore Torpedo



Photo 26: Placement of Vertical Bangalore Tube

pedo was suspended horizontally at the lower surface of the ice by the Shallow Water Divers of 1 CER and the U.S. Navy 'Seals' Diving Team. Two small placement holes were augered 9.14 m apart to receive the torpedo and ring main. The divers entered the water through an entry hole (Photo 27) set 10 m from one of the two placement holes.



Photo 27: Divers at Entry Hole

Swimming under the ice, the divers located the first placement hole and took a cord passed down to them over to the second placement hole. The cord was attached to one end of the torpedo, which was lowered through the first hole already 'primed' with det cord. A second cord was attached to the other end of the torpedo, such that when the torpedo was fully in the water, the two cords could be pulled in to bring the torpedo up against the underside of the ice. The placement process was lengthy, because very little light

diffused through the ice and the divers had difficulty locating the placement holes.

Of the det cord shots, one consisted of 15.24 m (50 ft) of three strands of det cord bundled together as a 'charge', placed in a shallow groove chipped with an axe in the surface of the ice, and covered with snow, shown in Photo 28.



Photo 28: 3-Strand Det Cord Charge on Surface

The other two were also 15.24 m charges, consisting of five and ten strands of det cord bundled together. These were placed against the lower surface of the ice by the divers in the same manner as for the Bangalore Torpedo.

Faster placement times would occur for a charge of this type being placed under the ice of a river, as the charge, with floatation devices such as strips of wood or styrofoam to keep the charge up against the ice, would only

have to be fed into the placement hole, allowing the river current to carry the charge downstream.

Photo 29 shows the detonation of, from left to right, the surface-laid Bangalore, the surface-laid three strand det cord charge, and the single tube of Bangalore set vertically below the ice.

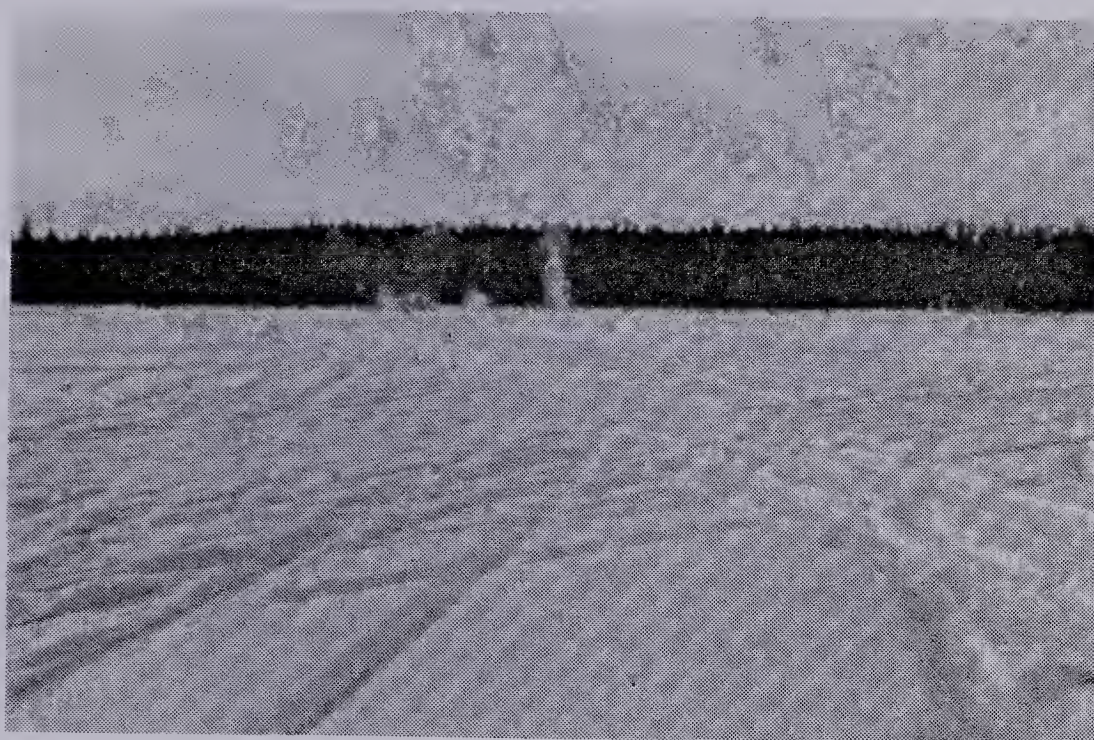


Photo 29: Detonation of Surface Bangalore,
Surface Det Cord and Vertical Bangalore Tube

In the photo it can be seen that a gas venting plume similar to those already seen for point charges occurred for the vertical Bangalore. The explosion action for the other two charges appears to be mainly in the air above the ice.

9.3.3 Discussion of Results; Det Cord Charges

The three-strand charge laid in a shallow groove cut in the surface of the ice did little more than blow the snow

away from it, as shown in Photo 30.



Photo 30: 3-Strand Det Cord Results

The groove shown in the photo was that cut to emplace the charge; there was no evidence that the explosion increased the size of the groove. That this shot did not produce results was not surprising, considering the charge consisted of only 0.11 kg/m of explosive.

The outcome of the two det cord charges fired beneath the ice was only slightly better than that for the surface-laid charge. The charge placement, in elevation, and the resulting 'craters' for the five and ten strand charges are

shown in Figure 42.

As the figure shows, a 'crater' was not formed by either of these charges, though the placement holes had been enlarged. This was thought to be due to the ice shattering from the radiating shock wave and gas bubble from the portions of the charges coming up through the ice, to be connected to the ring main. Thus the enlarged placement holes can be considered a 'boundary condition' to the linear aspect of the explosions being investigated. Therefore, the length over which the expected linear explosion had occurred was taken as the distance between the enlarged placement holes.

For the five-strand charge an area 0.3 m wide, and extending over most of the charge length, occurred where the ice surface had spalled due to the passage of the shock wave, as shown in Photo 31. (Note that the snow was cleared off the line of the charge before detonation).

The majority of the ice spalling was centred between the two placement holes. Presumably this was because the detonation reaction was initiated at both ends of the charge by the ring main, hence the detonation front travelling from each end met in the middle. Where spalling had occurred, approximately 1.5 cm of ice had broken loose from the surface. Cracks running parallel to the charge had occurred down the middle of the spall zone, and were presumably tension cracks caused by the ice heaving from below. These cracks were dry, indicating that they did not extend all the way through the

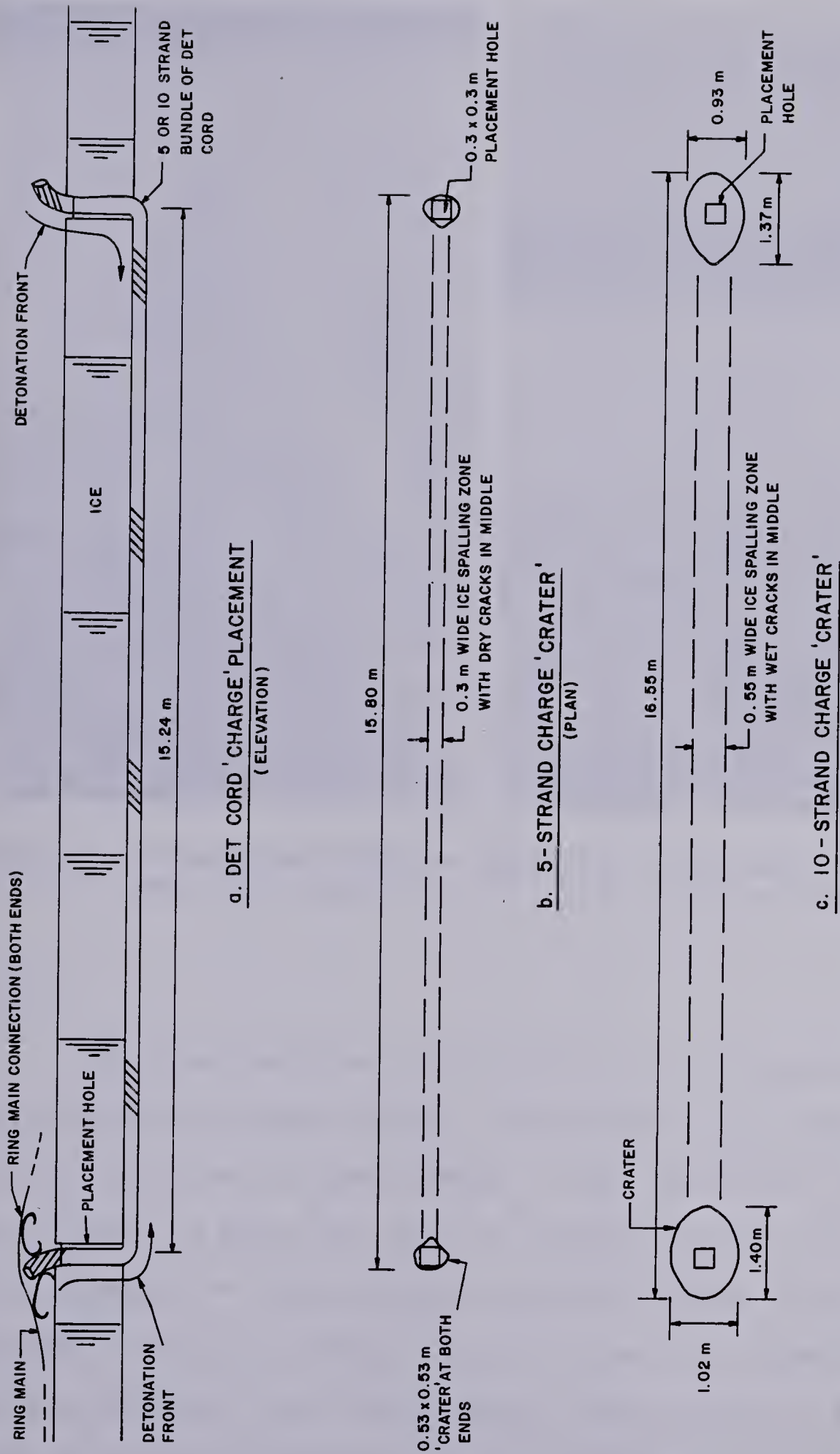


FIGURE 42
LINEAR CHARGE CRATERS FOR DET CORD CHARGES



Photo 31: Subsurface 5-Strand
Det Cord Results



Photo 32: Subsurface 10-Strand
Det Cord Results

ice.

The same features occurred for the ten-strand charge, ie, enlarged placement holes, ice spalling, and cracks parallel to the line of the charge in the middle of the spall zone. Photo 32 shows the line of detonation for this charge, with emphasis on the enlarged placement holes. More ice had spalled from the surface than for the five-strand charge, and the spalling zone was slightly wider, being 0.5 m wide. Some of the longitudinal cracks were wet, hence extended

right through the ice sheet.

The data for the three det cord charges are given below in Table 12.

TABLE 12
Linear Crater Data; Det Cord Charges

Shot	Strands	Placement	W l	W'	t _i	d ²	R'
No			(kg)	(kg/m)	(m)	(m)	(m)
L1	3	Surface	1.56	0.103	0.356	-0.356	0.0
L2	5	Subsurface	2.60	0.171	0.340	0.011	0.0
L3	10	Subsurface	5.21	0.342	0.380	0.016	0.0

- Notes:
- 1. Weights are equivalent weights of TNT.
 - 2. Placement depth to the middle of the charge bundle.

9.3.4 Discussion of Results; Bangalore Torpedos

The craters obtained from detonating the three Bangalore Torpedos are shown in Figure 43, for which the data is given in Table 13.

As the effects of the vertical Bangalore (Shot L4) would not be strictly as presented in the dimensional analysis, the shot was considered in light of previous findings from the point charge analysis. Unscaled criteria were used, as the scaling relationships for the point and linear charges were different. If the equivalent DM-12 explosive weight were considered as a point charge and plotted on Figure 25 (effects of gas venting (Section 6.3)), it would be seen

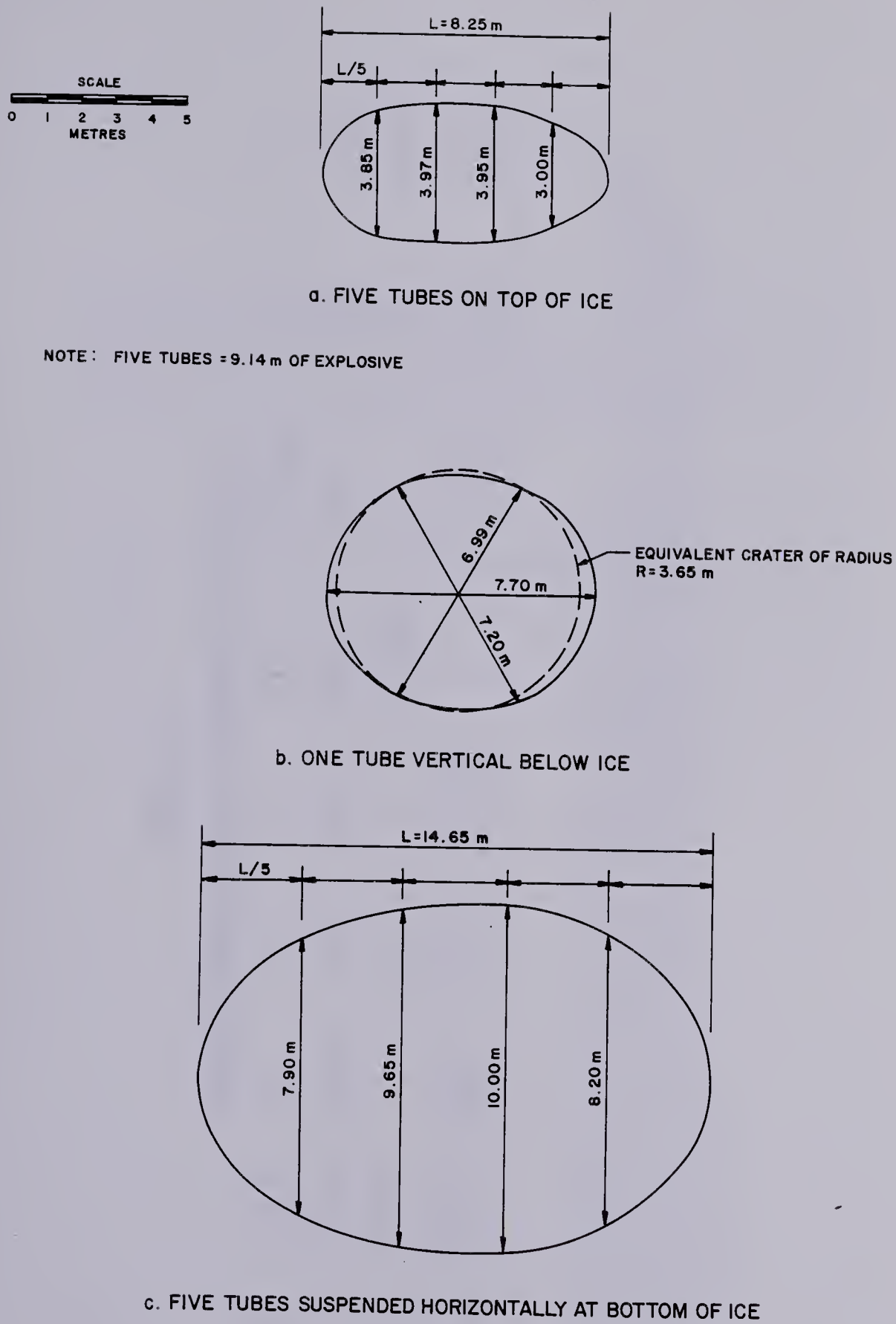


FIGURE 43

LINEAR CHARGE CRATERS FOR BANGALORE TORPEDOS

TABLE 13
Linear Crater Data; Bangalore Torpedos

Shot Placement	W l (kg)	W' (kg/m)	t _i (m)	d (m)	R ² (m)	R' avg (m)	L (m)	A (m ²)
L4 Vertical	4.69	-	0.356	-	3.651	-	-	41.89
L5 Surface	23.47	2.567	0.356	-0.376	-	1.846	8.25	27.47
L6 Subsurface	23.47	2.567	0.370	0.020	-	4.469	14.65	115.72

Notes:

1. The total weight W is the equivalent weight of TNT.
2. Crater radius for the vertical Bangalore was calculated from the average area determined from the three crater diameter measurements, as these had varied more than the diameters from which the point charge radii were averaged from.

that the crater (Photo 33) fell within the envelope of the radii created using point charges. Figure 25, used for this comparison, was drawn using only the data points from Experiment 2 to eliminate the effect of specific energy of the



Photo 33: Vertical Bangalore Crater

explosive from consideration. Hence the use of single Bangalore tubes set in this manner is as effective as placing individual point charges. However, the preparation time for a Bangalore demolition would be far less, as individual charges would not have to be made up. Therefore, as an expedient, or hasty, demolition technique, use of individual Bangalore tubes set in this manner is attractive from a timing point of view.

Of note for this shot was that a larger amount of ice was ejected from the crater by the explosion than for the point charge shots of roughly the same total explosive weight. Photo 34 shows the debris in the crater, in plan.

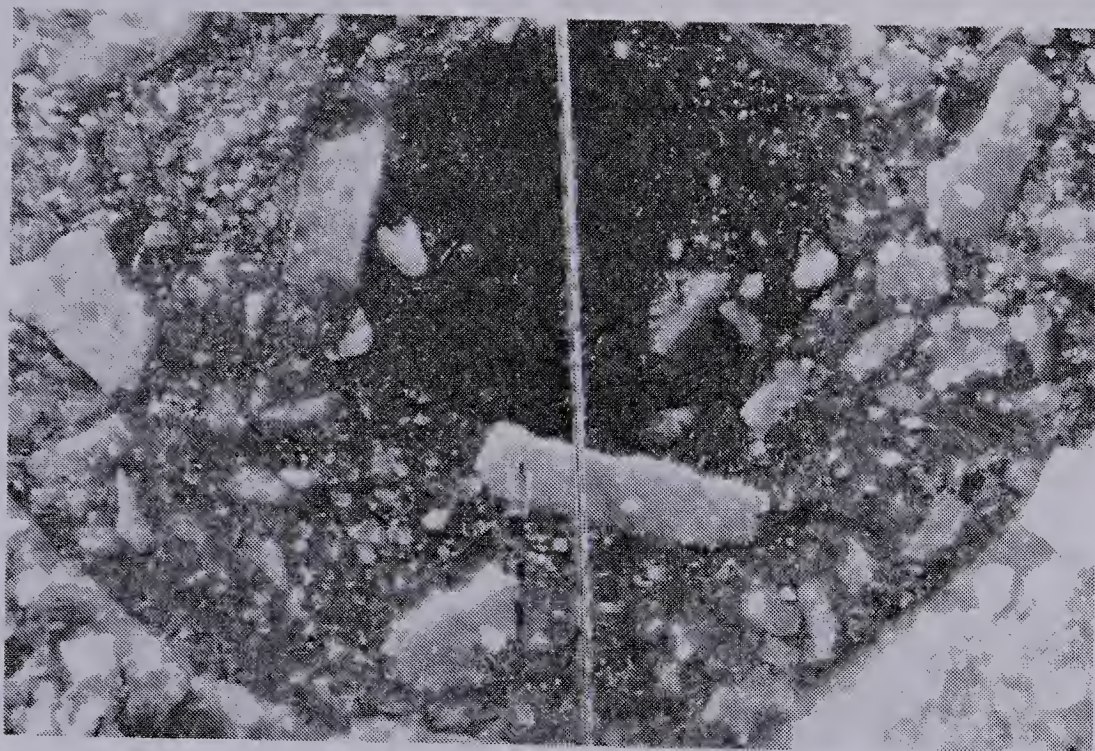


Photo 34: Ice Debris; Vertical Bangalore Crater

It was estimated that the fraction of ice ejected from the crater approached 50%. That so much ice was ejected from the crater was thought to be due to the initial confinement of the explosion by the metal tube. The confinement of the explosion gases, for even a fraction of a second, is considered to be sufficient to cause slightly increased gas pressures, and when the gases are released, the fluid below the ice would have been pushed back further than by the expanding bubble from an unconfined explosion. When the gas bubble subsequently collapsed, the momentum of the masses of water set in motion, meeting at the initial line of the charge, would have caused a larger surge than that from an unconfined explosion, and cleared more ice from the crater.

The data of Table 13 clearly show that the horizontal Bangalore set under the ice was more effective than that

detonated on the surface. The narrow end of the crater from the surface-laid charge (Figure 43 a) is at the end at which the detonation reaction was initiated. Note from the figure that the length of crater (L) was 0.89 m shorter than the length of the charge. Presumably the shorter crater and narrowing of the crater at the initiating end reflect the development of the full effect of the explosion on the ice. Thus, if a longer torpedo had been used in the experiment, it is considered that the crater width would be closer to the average of the remaining crater measurements, or 3.93 m, than the 3.69 m indicated by R' in Table 13, which included the measurement of the narrower width in the calculation of the average R' . Photo 35 shows this crater viewed in a direction opposite to that which the detonation wave had come from.



Photo 35: Surface Bangalore Crater

The crater formed from the detonation of the Bangalore set below the ice (Photo 36), which had been initiated from both ends, did not show this explosion 'buildup' aspect, and in fact was longer than the charge used.



Photo 36: Subsurface Bangalore Crater

This was considered to be due to the confinement of the detonation gases by the ice, whereas Photo 29 shows most of the explosion effect from the surface Bangalore was directed into the atmosphere.

Photo 37 shows the ice remaining in the crater from the surface-laid Bangalore. The Bangalore detonated below the ice cleared a much larger percentage of ice, as shown in Photo 36.

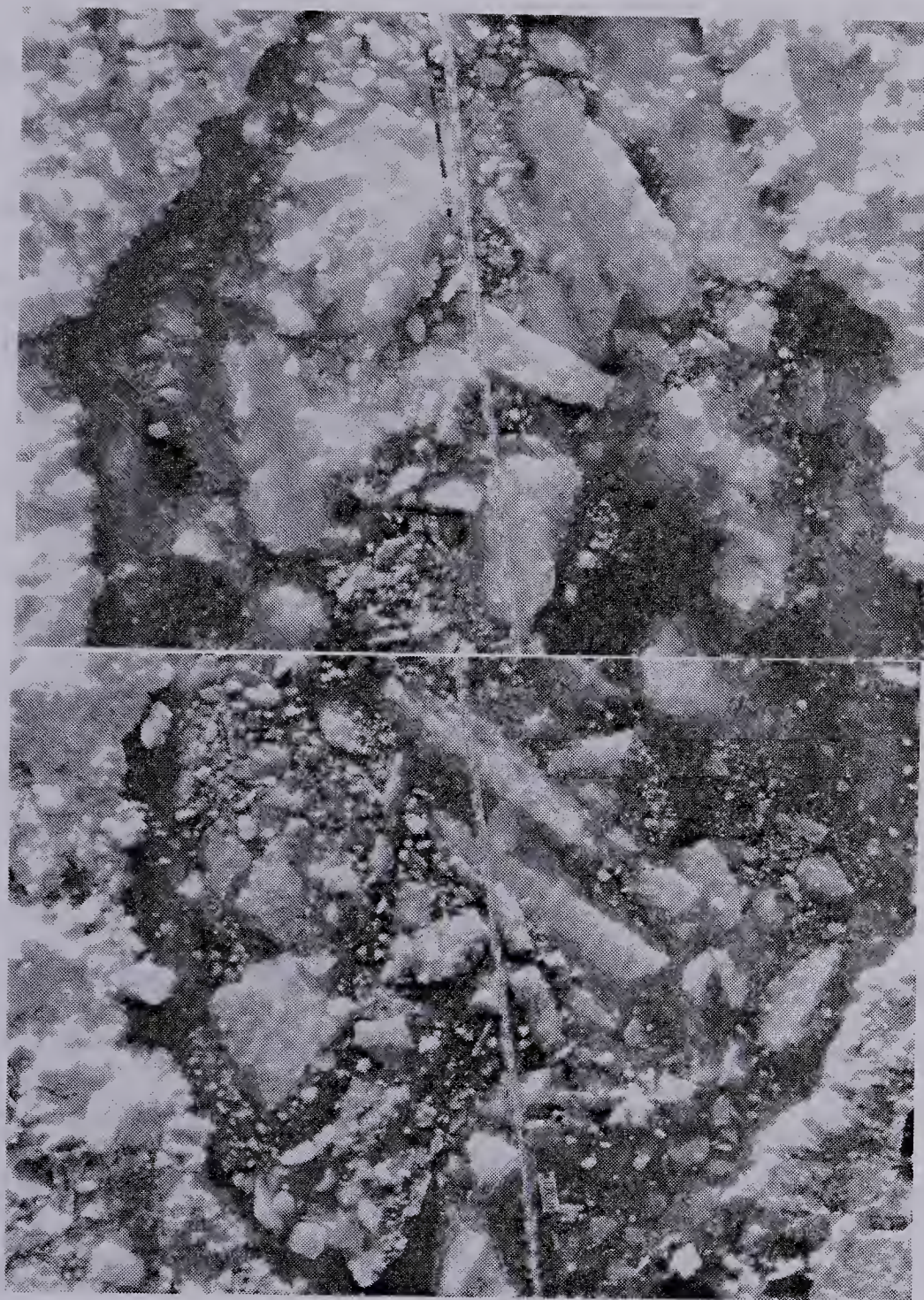


Photo 37: Ice Debris; Surface Bangalore Crater

9.4 Analysis of the Linear Charges

As the effect of the Bangalore tube set vertically through the ice was not strictly similar to the effect of linear charges considered during the dimensional analysis, it is not considered in this section. The effect of that explosion has been dealt with in terms of a special form of point charge (Section 9.3.4).

The scaled parameters for the remaining linear charges are given in Table 14 for the equivalent TNT explosive weight.

Scaled crater half-width has been plotted in Figure 44 as a function of scaled ice thickness, with the corresponding scaled charge depth indicated beside the plotting position. A number of lines have been added to show whether the direct relationship between points is in front of, behind, or crosses the x - y plane. The lines shown are not necessarily functional relationships. They were added only to give an indication of what the functional relationship might look like. With only five points to consider, it is difficult to visualize what the surface these points lie on would look like.

All of the data points for the charges detonated beneath the ice lie forward of the x - y plane, which is not surprising, as the charges were set below the ice and therefore had a positive d . From the relative positions of the data points for the ten strand det cord shot and the surface

TABLE 14
Scaled Parameters for the Linear Charges

Shot	W' (kg/m)	t_i (m)	d (m)	R' (m)	t_i/W' (1)	d/W' (1)	R'/W' (1)
Det Cord							
L1	0.103	0.356	-0.356	0.0	1.109	-1.109	0.0
L2	0.171	0.340	0.011	0.0	0.822	0.027	0.0
L3	0.342	0.380	0.016	0.0	0.650	0.027	0.0
Bangalore							
Torpedo							
L5	2.567	0.356	-0.376	1.846	0.220	-0.235	1.152
L6	2.567	0.370	0.020	4.469	0.231	0.013	2.789

Note: 1. The dimensions of the scaled parameters are $m^{3/2}$ $m^{1/2}$ /kg .

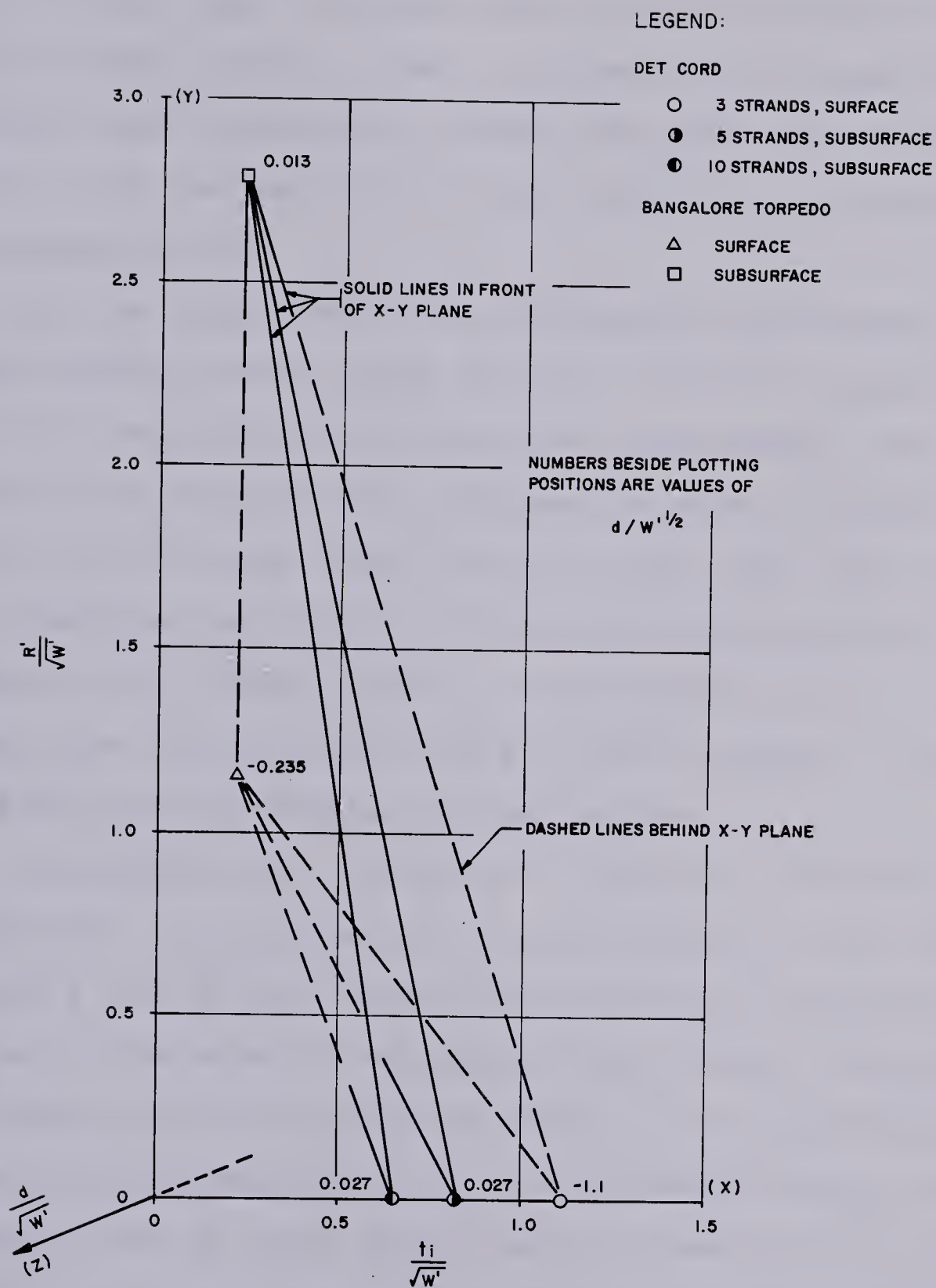


FIGURE 44

SCALED PARAMETERS FOR LINEAR CHARGES
(EQUIVALENT TNT CHARGE WEIGHT)

Bangalore shot, and considering that as the weight per unit length of det cord increased the plotting position moved nearer to the origin in the x - y plane, it is possible to speculate that a subsurface charge that would just create a crater in the ice would occur for a scaled ice thickness of approximately 0.5.

At the upper end of the indicated relationship, the surface appears steep, which is not surprising considering that for a constant ice thickness the charge weight must increase as the square of the thickness in order to reduce the scaled ice thickness. Reason tells us that there must be an upper limit to the size of crater that can be produced by increasing the charge density in this manner, hence it is thought that the surface must end at the y - z plane, as negative scaled ice thicknesses are meaningless.

Considering the scaled half width as a function of scaled depth (y - z plane); for point charges it was shown (Figures 2 and 4) that crater radius reached a maximum as a function of the depth of explosion, then reduced, presumably as a function of the pulsation phase of the migrating gas bubble. If it is considered that the gas bubble from a linear charge fired at great depth does not break up into a number of spherical bubbles, it can be considered that scaled crater half width will reach a similar maximum as a function of scaled depth of burst, then will approach a minimum. It is thought that the relationship in the y - z plane might look something like the curves Mellor presented for point charges

in this plane (Figure 6).

The horizontal linear charge data can be compared to the row charge data as well, as linear charges are a limiting case of a row charge, or vice versa. The data from Experiment 2 and Rows A, B and C from Kurtz et.al. (1966), were calculated as a weight per unit length between the ends of where the single charges had been placed. The data are given in Table 15 and Figure 45.

TABLE 15

Comparison of Linear and Row Charge Craters

Shot	Total Weight W l (kg)	Weight per Unit Length W' (kg/m)	Measured Cratered Area A _o (m ²)	A _o /W (m ² /kg)	A _o /W' (m ² /kg/m)
Det Cord					
L1	1.56	0.103	0.0	0.0	0.0
L2	2.60	0.171	0.0	0.0	0.0
L3	5.21	0.342	0.0	0.0	0.0
Bangalore					
L5	23.47	2.567	27.47	1.17	10.70
L6	23.47	2.567	115.72	4.93	45.08
Experiment 2	19.31	2.533	193.33	10.01	76.31
Row A	416.35	9.486	1954.	4.69	205.99
Row B	408.75	6.209	2715.	6.64	437.30
Row C	415.14	4.729	3932.	9.47	831.44

Note: 1. All charges are equivalent TNT charge weights.

It can be seen in the figure that on both a total weight and weight per unit length basis, there is a distinct

LEGEND:

SHOT	A_o/W	A_o/W'
DET CORD	◇	◇
SURFACE BANGALORE	△	▲
SUBSURFACE BANGALORE	▽	▼
EXPERIMENT 2	○	●
ROW CHARGES OF KURTZ et.al.	□	■

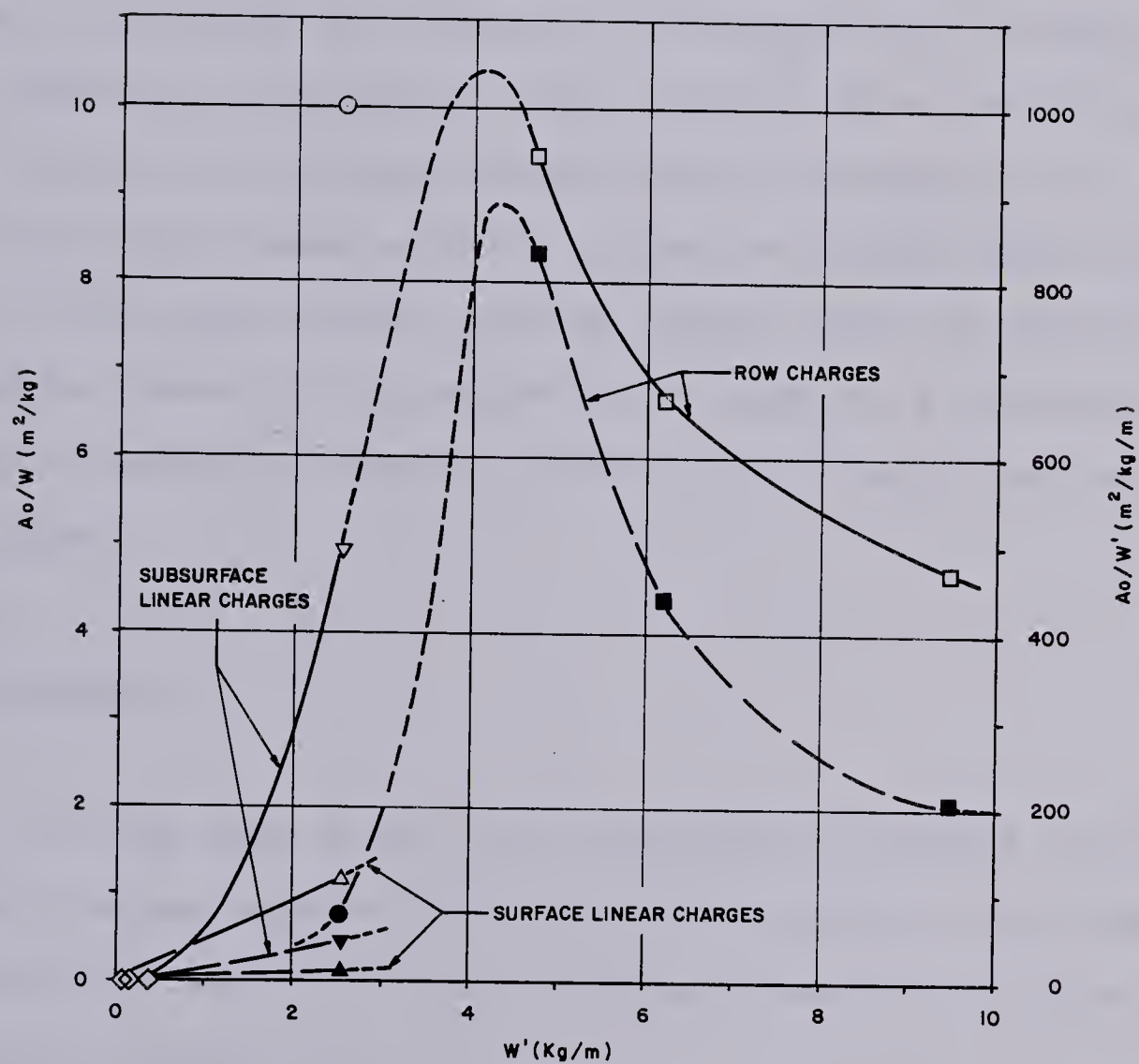


FIGURE 45

CRATERED AREA LINEAR AND ROW CHARGES
(ALL DATA EQUIVALENT TNT WEIGHTS)

advantage to using row charges, in terms of cratered area, when time permits these charges to be set.

From the crater sizes shown in Figure 43, it is apparent that more effective use may be made of the Bangalore Torpedo by placing individual tubes vertically below the ice as in Shot L4. More tests would be required to determine the effect of varying ice thickness on charges set in this manner. However, according to the findings from row charges, for ice of the thickness encountered at Drummond Lake (0.35 m), individual tubes could be placed two crater radii apart and a continuous crater should result. Use of individual Bangalore tubes in this manner would lead to a considerable saving in Bangalore Torpedos expended in a hasty ice demolition task.

9.5 Findings

It has been found that prepackaged standard military linear charges such as the Bangalore Torpedo can be used to demolish ice when the charge is placed both on the ice and suspended beneath it.

As a hasty demolition technique, Bangalore Torpedos laid on the surface of 0.35 m thick ice will produce a gap approximately 3.9 m wide, sufficient to prevent a man crossing without assistance. The gap will have most of the ice from the crater remaining as debris, as most of the explosive force is downward. This should allow the crater to re-

freeze quicker than if there was no debris remaining.

A Bangalore Torpedo detonated at the lower surface of the ice will produce a wider crater, in the order of 9 m, and will clear more of the ice from the gap. However, the problems associated with charge placement prohibit this technique in most operational circumstances, unless the charges are set well in advance as a deliberate demolition. If charges are to be set in this manner and left to sit for long periods of time, some types of Bangalore Torpedo will not be suited to the task unless extra time is spent waterproofing the ends of the torpedo. The explosive filler for some types of Bangalore, notably the Amatol 80/20 of the M1A1 tested during the Chilcotin experiments, does not have any inherent water resistance as shown in Table B-4 of Appendix B. Other types of Bangalore, filled with Composition B, would be better suited to this task.

The Viper class of linear charges, by extension of this analysis, may be utilized effectively as a hasty surface-laid charge in ice demolition. The smaller of the Viper class, the 'Baby Viper', has the same minefield clearance role the Bangalore used to fulfill, thus it should be comparable to the Bangalore in terms of its charge density (weight per unit length), and should therefore be similar in its ice clearing ability. The 'Giant Viper', designed to clear a larger path through a minefield, should be more effective than the Bangalore Torpedo. As the charge densities of these two linear charges were not known to the writer,

their ultimate performance in ice demolition can only be speculated upon.

If there is time available for the preparation of an ice sheet for demolition, yet not enough for a full-scale deliberate demolition, it has been found that more effective use of the Bangalore Torpedo may be made in a hasty demolition by suspending individual tubes through a small placement hole augered in the ice, and detonating them as 'point' charges. For the 0.35 m thick ice of Drummond Lake, it was found that a 7.30 m diameter crater resulted that was cleared of approximately 50% of the ice. The single tubes of Bangalore should be able to be spaced one crater diameter apart and still obtain a continuous crater. This procedure would be less time consuming than setting a row of charges, as little charge preparation time is required.

For 'true' linear charges, as considered in the dimensional analysis, it was found that on an area of ice demolished per unit weight of explosive, and weight per unit length of charge, the Bangalore Torpedo was not as effective in demolishing ice as single charges placed in row.

It was found, however, that a Bangalore Torpedo set under the ice as a linear charge was effective in clearing ice from the crater.

It was speculated after the tests that a single tube of Bangalore set through the ice at a 45° angle, with the top of the tube at the upper ice surface, may be an effective way of clearing ice from a crater. The principle is

much the same as that for directed blasting, where a horizontal component is imparted to the momentum of the ejecta. Also, the gas bubble created in this manner should be lopsided, as the gas radiating from the upper side of the tube should vent through the ice fairly quickly. The water surge from the collapse of a bubble of the type theorized should have a horizontal component in its momentum, in the same direction as the gas vent, and should carry additional ice debris from the crater.

CHAPTER 10

SHAPED CHARGES

10.1 Introduction

Experiment 6 was included to test the effectiveness of using shaped charges with different standoff distances (Figure 8a) in making placement holes in ice. Benert (1957), Section 3.3.3, had shown that cone shaped charges could be used to penetrate ice, with a resulting two-part crater as shown in Figure 9. The parts will be referred to as the 'crater', or upper portion, and the 'penetration hole', or lower portion of Figure 9. Benert's data, given in Table A-14 of Appendix A, showed that the penetration hole would exist through 2.13 m (84 in) of ice, but that it had a small diameter (0.127 m , 5 in), likely too small to place an explosive charge through, except for a tube of Bangalore Torpedo, large enough to demolish the ice. The crater, which ranged in diameter from 0.203 m (8 in) to 1.092 m (43 in), was between 0.203 and 0.762 m deep. These depths were shallower than the ice was thick. The diameter and depth of both the crater and penetration hole dictate the size of explosive charge which can be lowered through the ice. The results of Experiment 6 would give data comparable to that of Benert, but for smaller thicknesses of ice.

10.2 Description of Charges

It had been planned to use the Canadian 'Charge Demolition No.1, 6 inch Mk3 Beehive', a cone shaped charge similar to those tested by Benert. These, however, were not available. In their stead, the Canadian 'Charge Demolition No.14 Mk1, 11 lb Hayrick', a wedge shaped charge was used (Photo 38).



Photo 38: Charge Demolition No 14 Mk1 11 lb 'Hayrick'
with Zero Standoff

The explosive filler of the Hayrick is 5 kg of Pentolite (RDX and TNT mixture), of undisclosed proportions. It was assumed that the explosive was a 50/50 Pentolite, similar to that used as the explosive filler for some types of Bangalore Torpedo (Hemphill, 1981). The charge dimensions were 240 mm long, 135 mm wide and 255 mm high.

10.3 Analysis of Experiment 6

Five standoff distances were used, from zero metres (charge sitting on the ice as in Photo 38), to 1.22 m as shown in Photo 39.

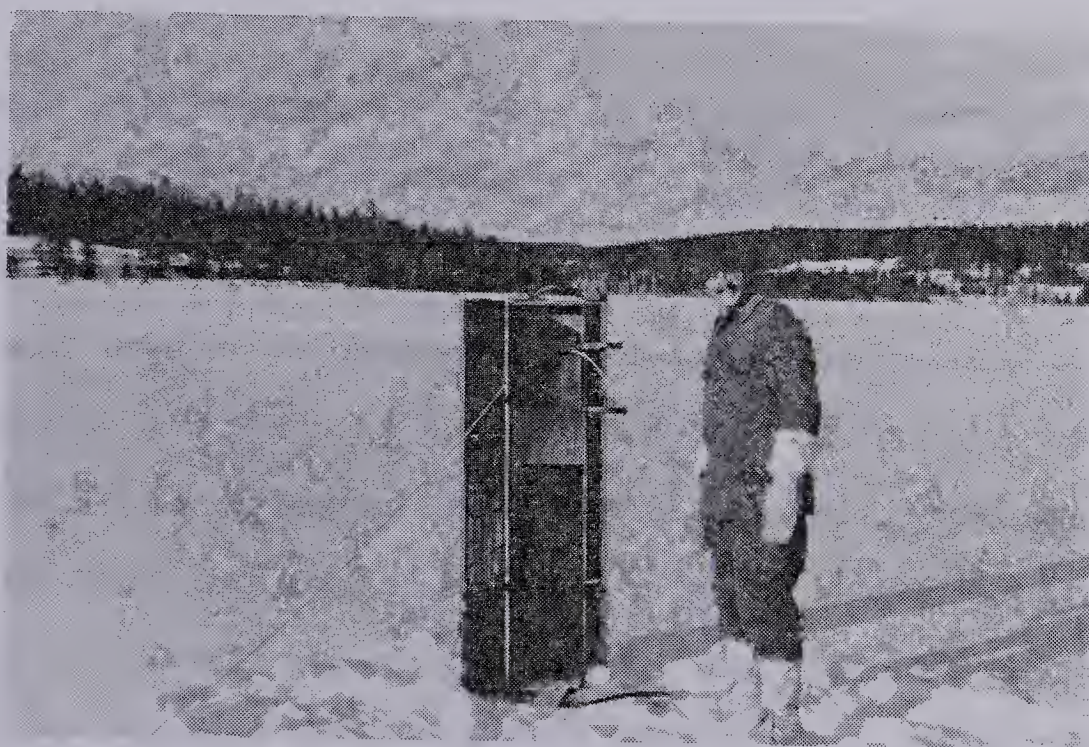


Photo 39: Hayrick Charge with 1.22 m Standoff

Photo 40 shows the detonation of, from left to right, the 'additional row' of Experiment 1, the subsurface Bangalore Torpedo from Experiment 5, and the five shaped charges,

marked by the dark smoke.



Photo 40: Detonation of Shaped Charges

The detonation of Hayrick charges created craters which extended through the full depth of the ice. Thus, it could not be determined if the 'penetration hole' portion of the overall crater is formed in ice from the detonation of a wedge shaped charge. It is considered unlikely, however, that a 'hole' as noted by Benert would result from the penetration of the jet and slug from a wedge shaped charge. If anything, a 'slit' might result, as the primary purpose of the Hayrick charge is to make a line-cut in steel or concrete targets, or more likely, that the crater will taper off like a 'V'. The data for the shaped charge shots is given in Table 16. Figure 46 shows the resulting crater size for the five standoff distances used, as well as the data from Benert.

TABLE 16

Chilcotin Shaped Charge Data

Shot	W (kg)	t _i (m)	Standoff h (m)	Diameter D ₁ (m)	Measurements D ₂ (m)	R (m)	Description ¹	Estimated ² Debris (%)
S1	5.00	0.361	0.00	2.55	2.40	1.238	Regular	85
S2	5.00	0.361	0.305	1.35	1.30	0.663	Regular	80
S3	5.00	0.361	0.610	1.15	1.15	0.575	Irregular	65
S4	5.00	0.361	0.914	0.80	0.92	0.430	Irregular	60
S5	5.00	0.361	1.219	0.85	0.92	0.443	Irregular	55

Notes:

1. Regularity of craters described in terms of approximation of a circle.
2. Debris estimates are percent of ice from crater remaining in the hole.

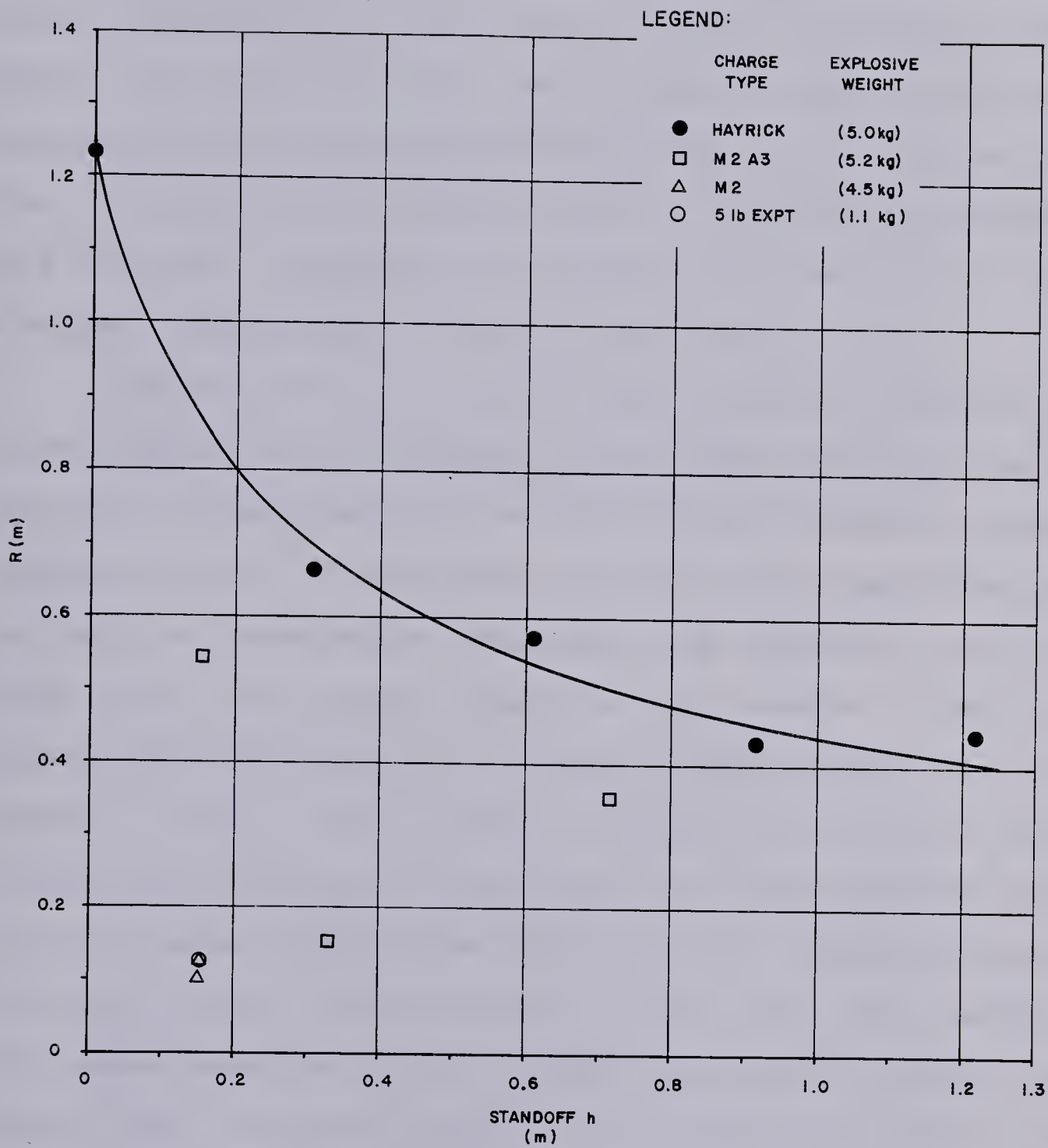


FIGURE 46
CRATER RADIUS FOR SHAPED CHARGES

In terms of the weight of explosive, the Hayricks which were stood-off the ice did not create as large a crater in the ice as the unconfined surface charges detonated during Experiment 3. The largest crater, produced by the charge with zero standoff, had a crater radius which approached the best fit relationship of Figure 27 (crater radius as a function of charge weight for unconfined surface laid charges), however, the remainder fell well below the envelope of data points shown by the figure.

The Chilcotin data in the figure shows a decrease in crater radius for an increase in standoff, which was to be expected. In the discussion of the action of shaped charges (Section 3.3.2), it was noted that for cone shaped charges the depth of penetration increased with standoff, until an upper limit was reached caused by the breakup of the jet produced by the explosion. It was considered that the decrease in crater radius shown in Figure 46 was due in part to the larger distance of the centre of the explosion from the ice, hence reduced peak shock from the overall detonation, and in part to the breakup of the jet. That the Hayrick shots produced larger craters than those measured by Benert, some for approximately the same explosive weight, is thought to be due to the explosive effect of the cone shaped charges being concentrated at a point, while that of the Hayrick is concentrated along a line.

Photos 41 and 42 show the craters which resulted from the detonation of the shaped charges with 0.305 and 1.219 m

standoffs, respectively.

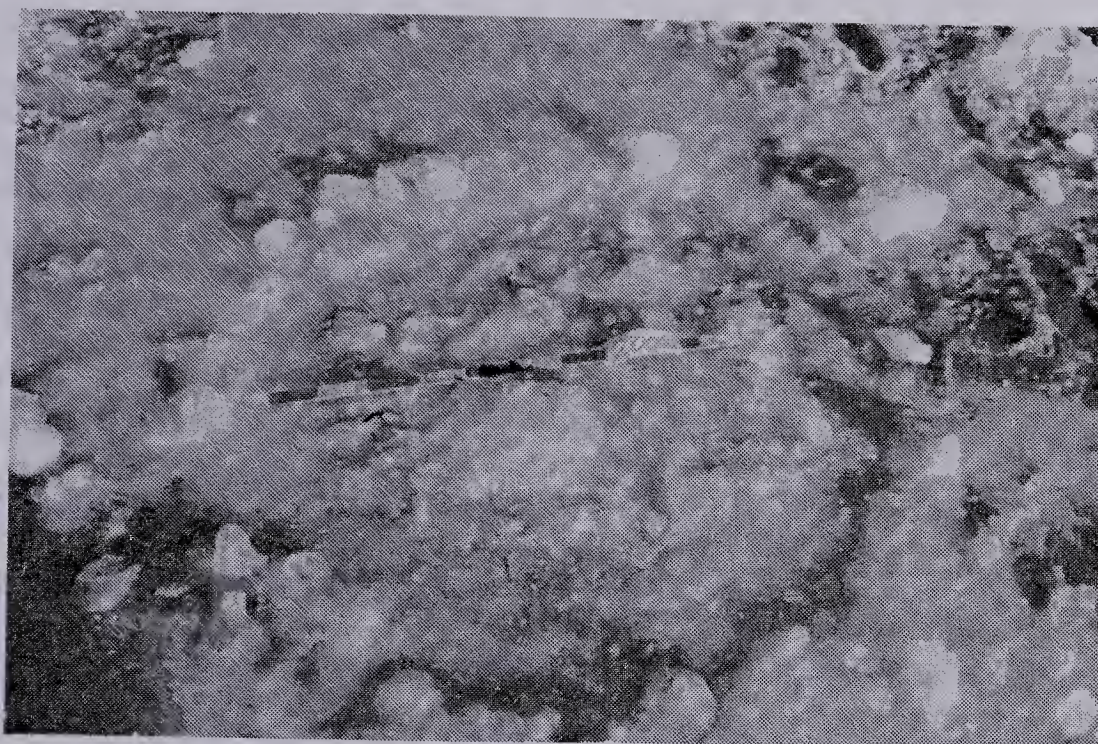


Photo 41: Crater for Hayrick with 0.305 m Standoff



Photo 42: Crater for Hayrick with 1.219 m Standoff

The photographs were taken the morning after the shots were fired, as there was too little light to take the photographs immediately following the detonation, hence the craters were frozen over when the photographs were taken. The photos show that, although the effect of the charges are linear, there was no tendency of the craters to be elongated.

As all of the craters from Experiment 6 extended the full depth of the ice, the ultimate crater depth for the charges fired could not be determined. Benert's data, however, gives the crater depths for the charges he detonated. The relationship between crater depth and standoff is shown in Figure 47. The figure indicates that there may be a difference in the shaped charge explosion effect on saline and freshwater ice. However, there is insufficient data to draw a firm conclusion.

10.4 Findings

The results of Experiment 6 show that Hayrick wedge shaped charges can be used to quickly create a placement hole in ice up to 0.35 m thick. The resulting placement holes vary from 1.24 m in radius for a zero standoff, to 0.44 m for a 1.22 m standoff. All of the craters formed had upwards of 50% ice debris content, which may have to be scooped out or pushed aside in order to lower an ice demolition charge through the hole. The fraction of ice



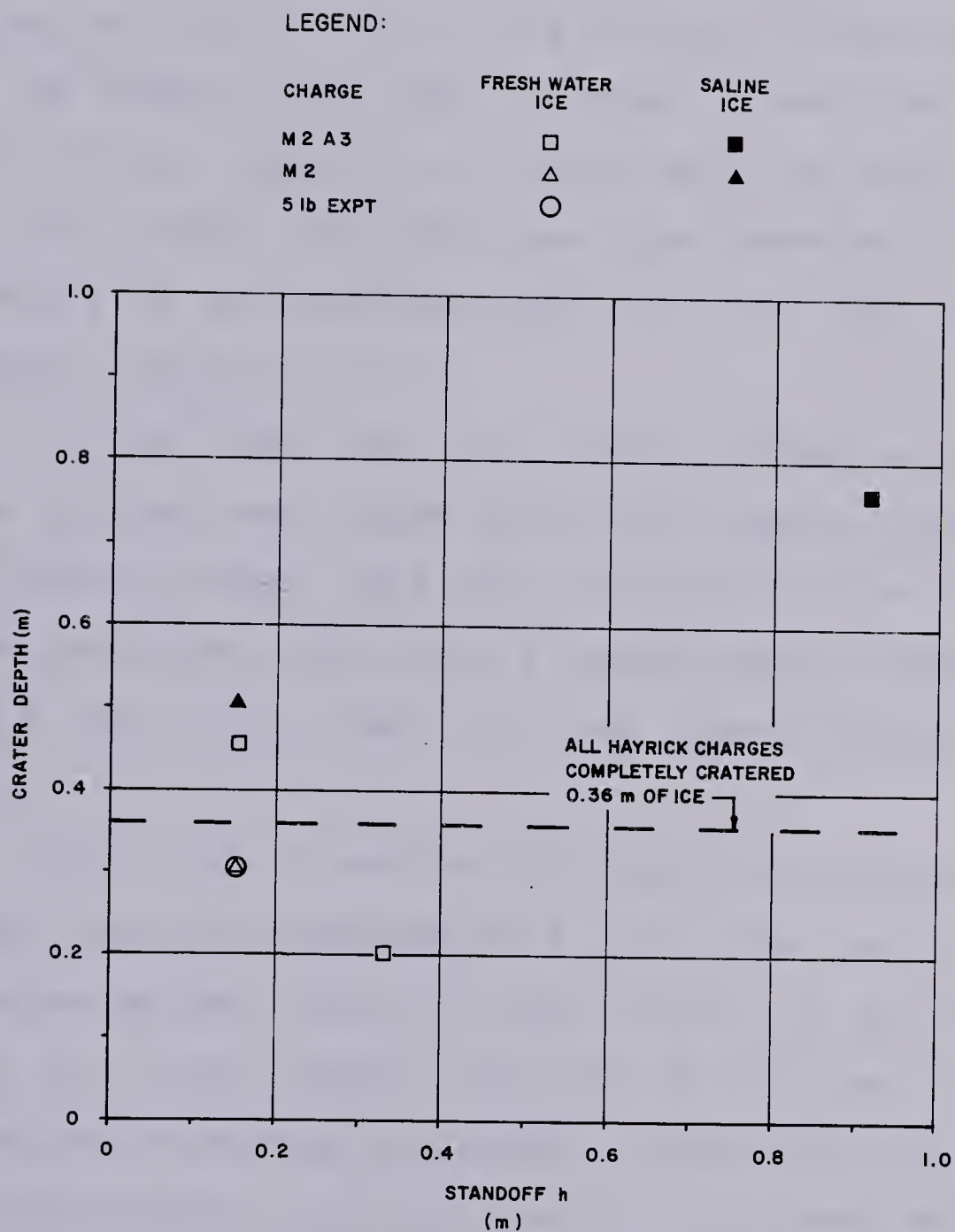


FIGURE 47

CRATER DEPTH FOR SHAPED CHARGES



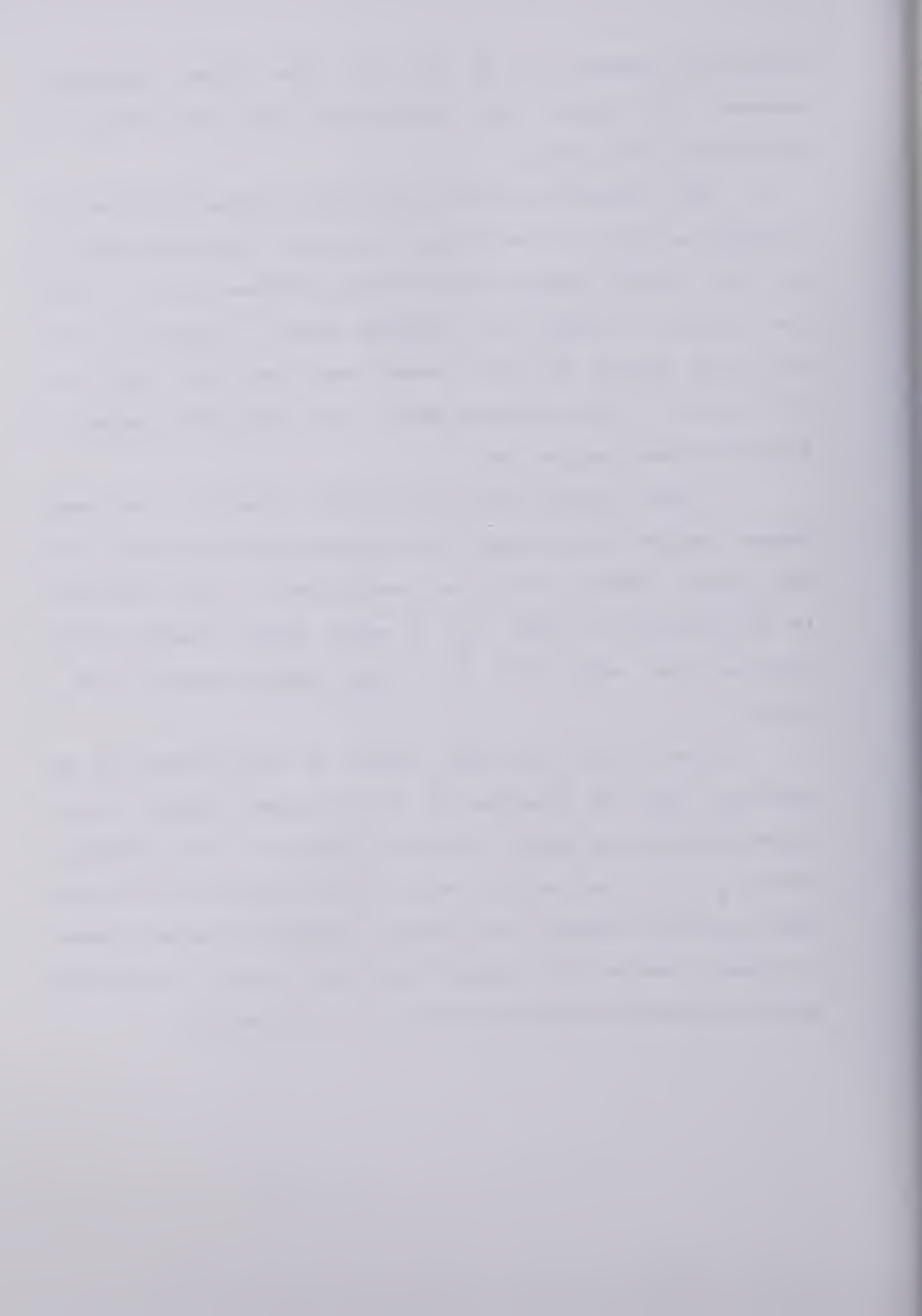
Figure 1 and Figure 2 show the relationship between the concentration of a solution and the measured property. The theoretical curve (Figure 1) and the experimental curve (Figure 2) are plotted for comparison.

remaining appeared to be less for the higher standoffs, however, the craters were smaller and may not accept the main demolition charge.

The ultimate depth of the craters formed could not be assessed as all of the craters extended right through the ice. The shaped charge data of Benert shows that in thick ice (>1.35 m), there is a limiting depth to which the craters will extend. His data shows that there may also be a difference in the cratered depth, for the same charge, in freshwater and saline ice.

It was found that the craters formed by the wedge shaped charges were larger than those Benert measured from cone shaped charges. This was attributed to the difference in the explosion effect for a wedge shaped charge, being along a line, while that of a cone shaped charge is at a point.

Given, from a previous finding in the analysis of gas venting, that the presence of a free water surface allows the expanding gas bubble to vent through to the atmosphere before all of the usefull work can be obtained from them, when explosive charges are lowered through the holes created by shaped charges, the crater should be allowed to refreeze before detonating the main charge, if time permits.



CHAPTER 11

CONCLUSIONS

11.1 General

The investigation carried out for this thesis covered five main areas, and will be concluded as such.

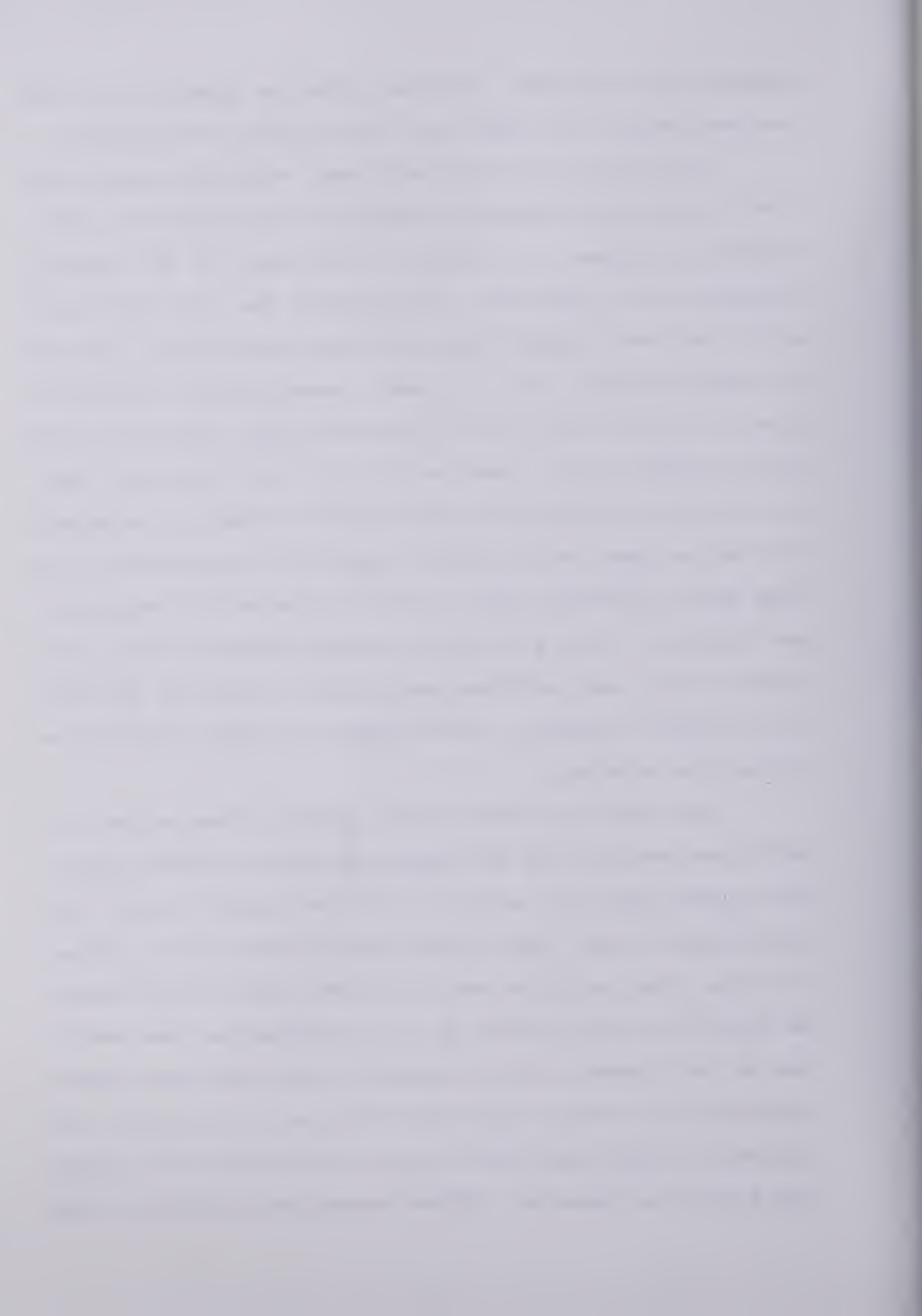
11.2 Point Charges

An analysis of the point charge data contained in the literature, as well as that obtained during the experimental portion of this investigation, independantly confirmed an earlier analysis conducted by Mellor (1972). Therefore, Mellor's contention that the thickness of ice should be included with charge weight and depth of placement in the assessment of optimum ice demolition criteria is supported. Mellor had presented a family of curves defining the overall relationship between crater radius, charge weight, depth of placement and ice thickness in nondimensional form, from which the optimum amount of explosive required to demolish an ice sheet could be determined. Determination of the maximum of the scaled ice demolition relationship obtained by replicating Mellor's analysis led to simplified equations for which the charge weight, depth of placement and resulting crater radius could be determined as a function of the

measured ice thickness. These are given as Equations 13, and are considered to be applicable for any type of explosive.

Because of the relatively poor statistics associated with the multiple regression analysis, two supportive investigations explored the effect of the terms of the general nondimensional functional relationship for ice demolition which had been omitted from the first analysis for reasons of simplification. One of these investigations determined that the term involving the gravitational constant g had little effect on the results of the first analysis, hence its omission was justified. The second investigation showed that while there was an effect caused by the presence of an open charge placement hole in the ice, the effect was minor, and further, for the range of charge placement hole sizes tested, there was no discernable effect caused by the size of the holes. Neither of these factors had been investigated in previous studies.

The remaining factor which could influence the size of crater produced was the radius of the gas bubble generated by the explosion, which in turn is related to the type of explosive used. Other investigators had given an indication that there might be such an effect, but had not analysed what that effect might be. An investigation was carried out in this thesis which considered the explosive charges converted into energy-equivalent weights of a standard explosive, in this case TNT. For this conversion it was determined that the reported 'Effectiveness as an External Char-

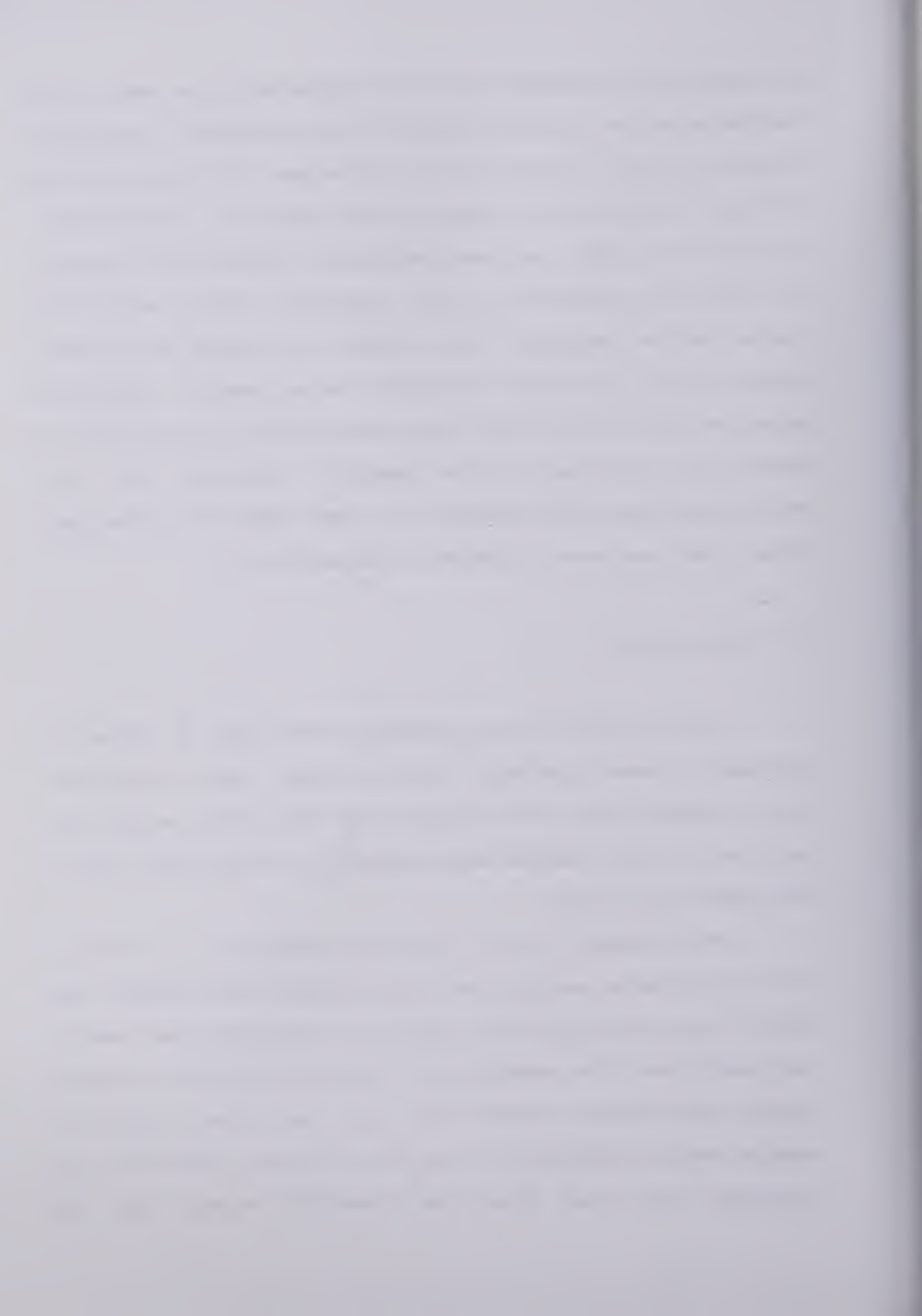


ge' used by the Canadian and U.S. Forces could be used as an indicator of the specific energy of the different explosives reported in the ice demolition literature. The investigation of the ice demolition relationship using the 'normalized' data did not yield improved regression statistics, however, the plotting positions of the observed versus calculated crater radius comparison had changed in a manner which indicated a more reasonable functional relationship. Simplified equations were derived for the determination of optimum ice demolition criteria for the specific explosive TNT, and energy-equivalent TNT charges for other types of explosives. These equations were presented as Equations 17.

11.3 Row Charges

The analysis of row charges showed that a series of uniformly spaced optimum point charges, when detonated, could increase the cratered area over that which would have occurred had the charges been spaced far enough apart not to influence one another.

The spacing of the individual charges, in terms of the crater radius an optimum single charge would create, was found to be the controlling factor in increasing the area of ice demolished. The experiments conducted for this investigation effectively defined the upper and lower limits of charge spacing. Analysis of the data from the Chilcotin experiments plus that from the literature showed that the



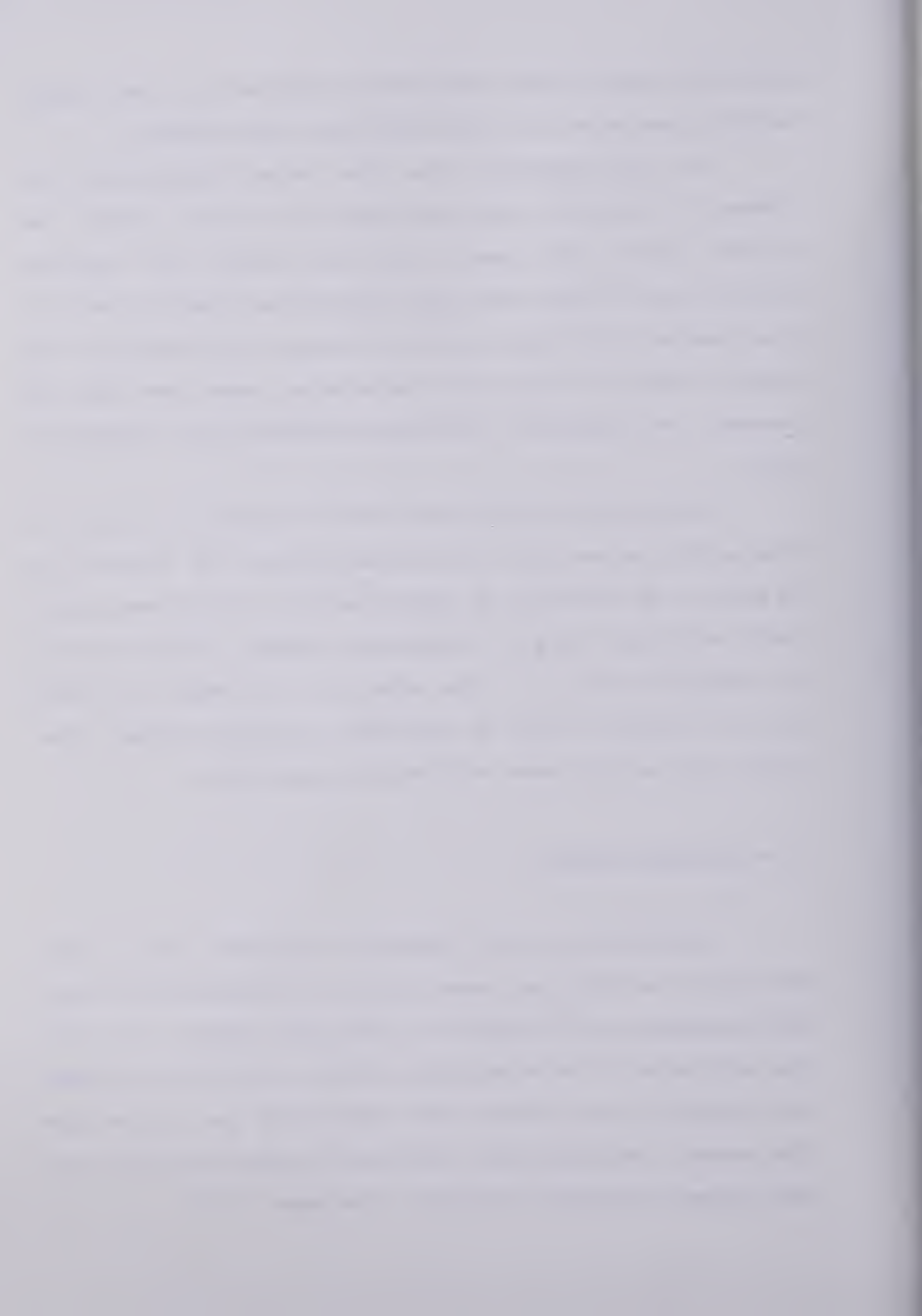
smoothest single-curve relationship occurred with the charge weights considered as energy-equivalent TNT charges.

It was determined that the maximum documented increase in cratered area occurred for charges spaced two optimum crater radii apart. For this spacing, the cratered area was about twice that which would have occurred for single charges placed so as not to enhance one another. The 'bonus' effect in using the row charges comes from the ice between the theoretical individual craters being removed as well.

Preliminary indications from the analysis of the row charge data showed that the spacing between the charges may be able to be increased to approximately 2.25 optimum crater radii and still obtain a continuous crater, whose increase in cratered area is in the order of 2.6 times the summed area of craters formed by individual optimum charges. However, this has not been verified experimentally.

11.4 Multiple Charges

Information in the literature suggested that a small portion of an optimum charge could be detached and placed advantageously with respect to the main charge, such that the detonation of this multiple charge system would increase the cratered area, and also the fraction of ice ejected from the crater. The particular technique for ejecting debris has been termed 'directed blasting' (Nikolayev, 1971).



The theory behind this 'directivity' aspect initially seemed straight forward, though the presentation of the theory was somewhat clouded, probably due to the translation from the original Russian. The application of the theory in the reference was also somewhat distorted, making full comprehension difficult. Therefore, a series of detonations were designed, predicated on the early understanding of the theory, to investigate the technique. The results of the experiments showed that the directional aspect of the technique could be achieved with certain combinations of auxiliary charge weight and detonation delay between the charges, though not to the extent that the original reference had indicated. The experiments showed that the method is highly dependant upon the gas bubble generated by the auxiliary charge, which in turn is dependant upon the weight of that charge. The technique also seems highly dependant upon the detonation delay between the two charges, which must be a function of the distance between the charges and hence the distance between the main charge and the auxiliary gas bubble at the time it reaches its maximum size.

At present, the application of the theory is not sufficiently refined to make the technique useable. Also, commercial delay detonators seem to be manufactured with delays longer than 30 m sec, whereas the detonation delays indicated by this preliminary assessment and the original reference suggest delays of 25 m sec and less. Hence, delays of the magnitude desired have to be improvised using various



lengths of det cord between the charges.

11.5 Linear Charges

The investigation of prepackaged military linear charges carried out for this thesis showed that on an equal weight basis, linear charges were not as effective as a row charge in creating a gap or lane in an ice sheet.

However, from a military denial operation point of view, it has been determined that a linear charge such as the Bangalore Torpedo can be used to create a crater in ice, approximately 0.35 m thick, by detonating the Bangalore on the surface of the ice. It was determined that as with single charges detonated on and below the ice, the Bangalore is more effective if detonated below the ice. The difficulties in placing the charge under the ice, however, makes other ice demolition techniques more attractive.

Nevertheless, it was found that individual tubes of Bangalore Torpedo lowered through a small placement hole and suspended vertically beneath the ice was an effective means of ice demolition, comparable to point charges of the same explosive weight.

As the supply of Bangalore Torpedos may be limited during winter warfare operations, their use in an ice demolition role may have to be limited.

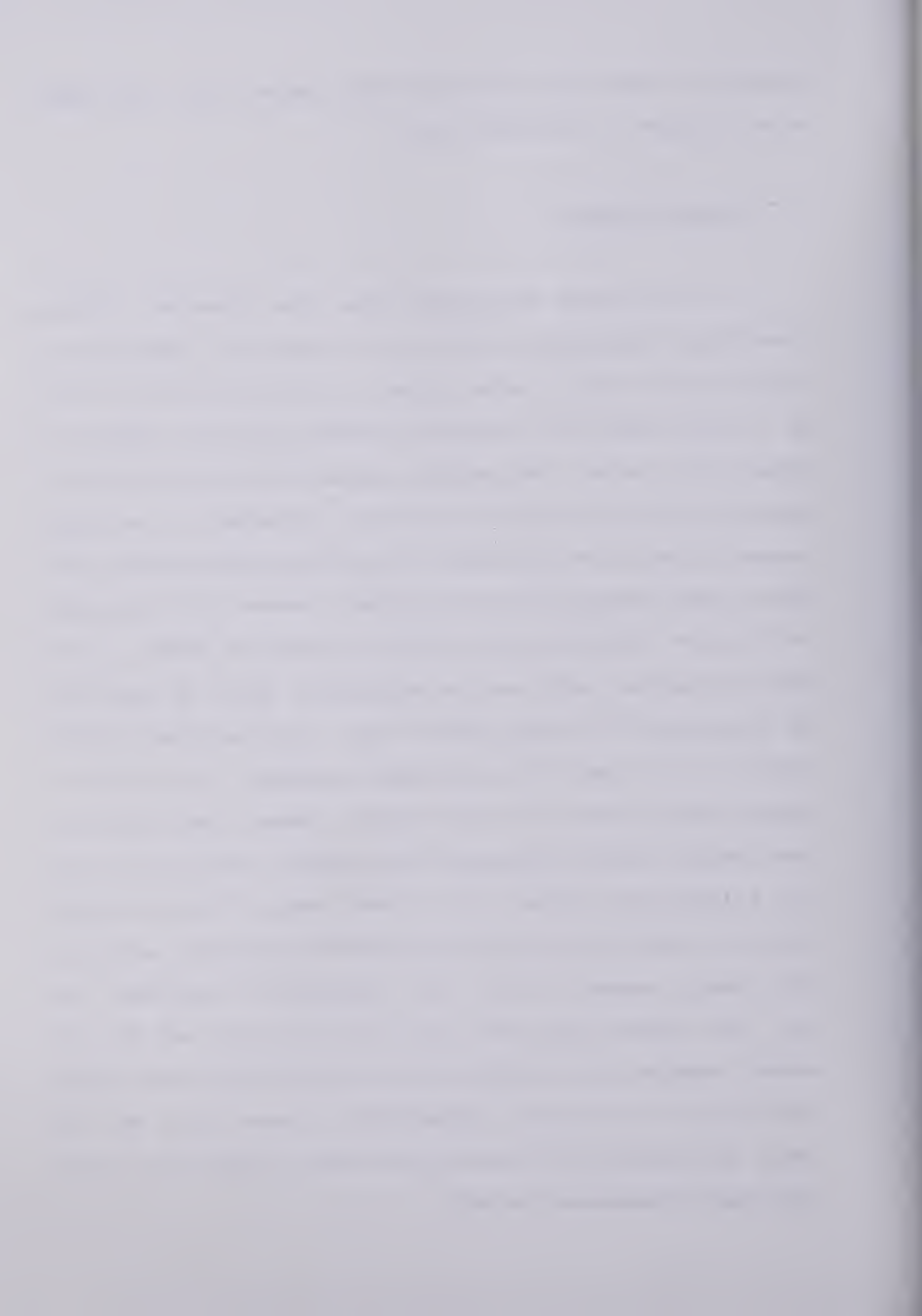
By extension of the findings for Bangalore Torpedos, it is concluded that 'Baby' and 'Giant' Vipers would be com-



parable to, and more effective than, respectively, the Bangalore Torpedo in ice demolition.

11.6 Shaped Charges

It has been determined that the Canadian 'Charge Demolition Shaped No 14 Mk 1 11 lb 'Hayrick'' wedge shaped charge can be used to make craters in ice up to 0.35 m thick as a hasty method of creating placement holes for other ice demolition charges. The maximum crater size was found for a Hayrick with zero standoff, and was comparable to an equal amount of explosive detonated as an unconfined surface charge. As each charge detonated created a crater the full depth of the ice thickness, the maximum cratering depth of the Hayrick charges could not be determined. Also, it could not be determined if a 'penetration hole' (such as Benert (1957) found in his study of cone shaped charges) occurred for a wedge shaped charge. In this respect, Benert found that for cone shaped charges detonated over thick ice (1.12 to 2.13 m), a crater was formed only through part of the ice thickness, but that the jet and slug from the explosive action of the charge caused a hole that completely penetrated the ice. The charges he used were the U.S. M2A3 and M2 cone shaped charges, for which the penetration hole was 100 mm and 127 mm in diameter respectively. These holes are too small to accept an ice demolition charge, except for a single tube of Bangalore Torpedo.



CHAPTER 12

RECOMMENDATIONS FOR FURTHER RESEARCH

12.1 Introduction

A study encompassing as many aspects of ice demolition as this one must leave a certain number of questions unanswered, as well as generate a new set of problems to be investigated. A few of these can be approached without the necessity of requiring further fieldwork, though such fieldwork would be advantageous. The following are a few areas for which the writer considers further investigation is warranted.

12.2 Recommendations Regarding Point Charges

12.2.1 Extension of Tests to Thicker Ice

It has been demonstrated that the thickness of ice must be incorporated into the determination of optimum ice demolition criteria. However, the vast majority of the data used to determine these optimum criteria have been from tests conducted on ice less than one metre thick.

The analysis of scaled data contained herein should allow for the extension of the results, through dynamic similarity criteria, to ice thicknesses greater than those from which the equations were derived. However, given that



the number of 'thick ice' data points used in the present analysis was so small, there is a need to collect point charge data for ice thicknesses greater than one metre, to confirm the present analysis and the extension thereof.

It is therefore recommended that a series of tests be conducted on ice with thickness greater than one metre. It would be advantageous if some of these tests were to be conducted in the Arctic, where ice thicknesses in the order of two metres or greater might be found.

12.2.2 Confirmation of the Recommendations With Respect to Energy Equivalent Charges

The analysis conducted herein used the specific energy of explosives as the method of comparing the performance of explosives in ice demolition. It was shown that the 'Effectiveness as an External Charge' was a fairly good indicator of specific energy. However, the method used to compute the specific energy of mixtures of explosive compounds may have been somewhat inaccurate as it did not account for the energy producing ability of the additives in an explosive's formulation. Further, while the comparison using specific energy showed some improvement in the results of the analysis, the finding that the size of the gas bubble may play an important role indicates that a parameter such as the specific volume of detonation gases may be a more appropriate method of comparison. Meyer's (1977) data on explosive properties (Table B-5) shows that there is no particular rela-



tionship between specific energy and volume of detonation gases, therefore the use of the latter may improve the findings of the regression analyses.

Irrespective of the possibility that a better comparator might be available, a series of experiments using a minimum of three different explosives with known different specific energies should be able to determine if the comparison of explosives based on specific energy was valid. If the specific energy of three explosives cannot be obtained from the references or from the manufacturer, the 'Effectiveness as an External Charge' may be used as a guideline. Selection of three explosives should cover a wide range of 'effectiveness'. Possible explosives for consideration would be ANFO or Black Powder, whose effectivenesses are less than that of TNT, TNT itself as the second explosive, and one of Amatol 80/20, Pentolite 50/50 or Composition C-4, whose effectivenesses are greater than that of TNT.

Using the effectiveness to determine equivalent charge weights of each explosive type, a series of detonations with these charges fired at identical placement conditions should reveal if there is a substantial difference in the resulting crater radii obtained.

12.2.3 Investigation of the Influence of the Gas Bubble

If the gas effectiveness of the various explosives used in the ice demolition literature can be ascertained, its use in computing the initial radius of the gas bubble,

in a manner similar to that outlined in Appendix C if the temperature of the explosion could be determined, for the charges reported in the literature, and hence an investigation into the effect of the bubble radius would be advantageous.

As a second step, the gas bubble must be investigated with respect to not only its initial radius (at the detonation depth), but also the pulsation period of the bubble, its migration rate toward the surface and the effect of the change in hydrostatic pressure on the expanding bubble as it pulsates must be investigated, such that the particular phase of the pulsation when the bubble vents through to the atmosphere may be ascertained. This will help to quantify the observed maximum, minimum and increasing crater radii noted by Barash (Figure 2).

The above, plus an analysis of the velocity of bubble expansion would be of use in the further consideration of the directed blasting technique as well, where one of the controlling unknowns is the detonation delay, which is linked to the time of auxiliary bubble expansion.

12.2.4 Investigation of Simpler Regression Models

Throughout this thesis the regression model proposed by Mellor (1972) was accepted and used exclusively. Mellor, however, gave no reason why a third order polynomial model was used in his initial study. One plausible reason is that a cubic term was required to explain the increase in crater

radius noted by Barash for explosions occurring deeper than some scaled depth for the particular charge weight used. However, there seems to be little reason for the inclusion of a cubic term for the scaled ice thickness.

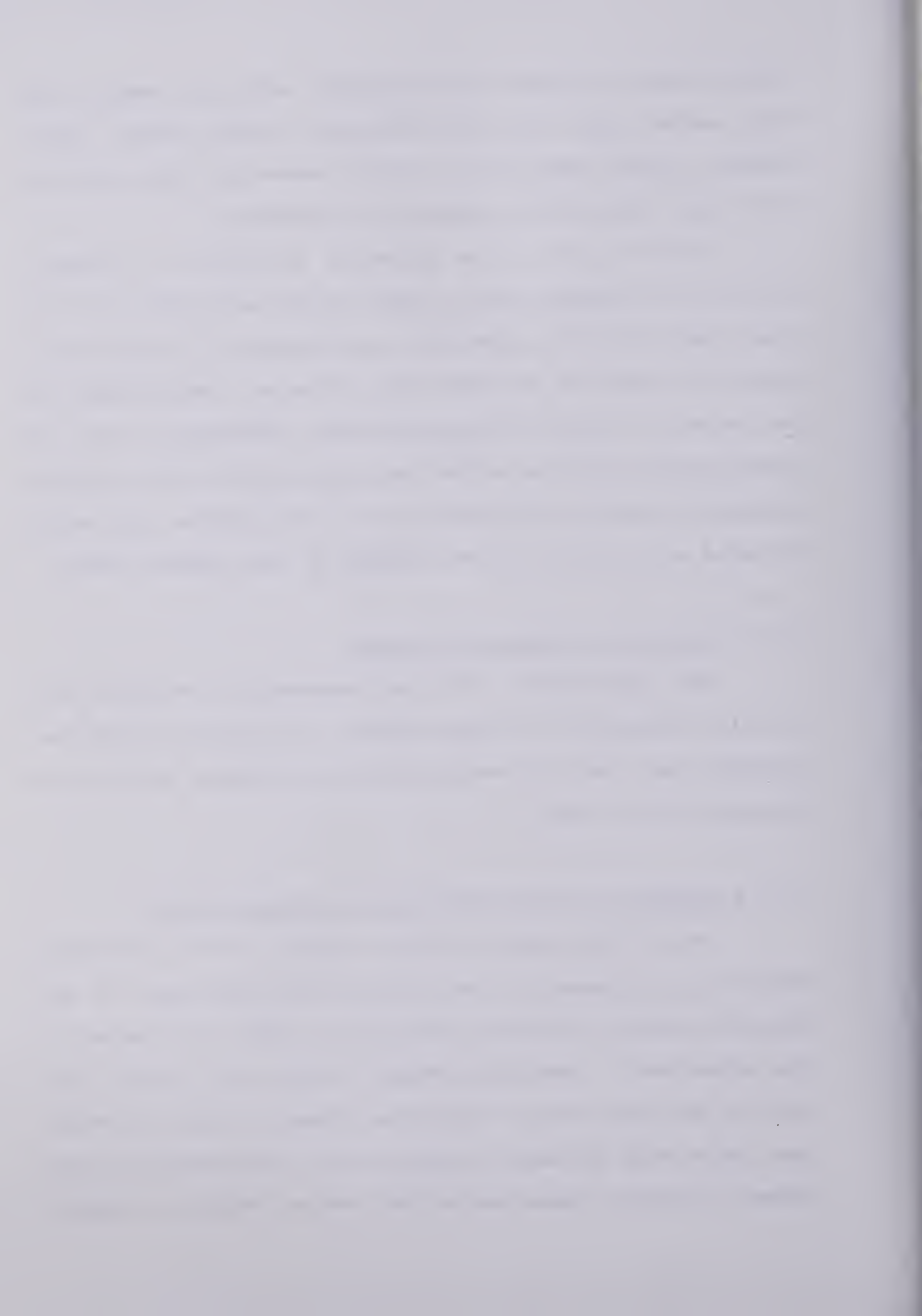
With only the data presently available, or supplemented with findings from a study of the gas bubble, an office study could be undertaken to determine if better correlations could be obtained with different combinations of the terms in Mellor's regression model (Equation 7). Or, an investigation could be undertaken starting with the simplest regression models and working up to more complex with terms included as a result of the findings of the simpler models.

12.2.5 Extension to Other Ice Forms

The application of the recommended criteria for blasting floating ice sheets should be tested on both reinforced ice, such as occurs with ice bridges, and to the phenomena of ice jams.

12.2.6 Methods of Determining the Ice Debris Content

One of the aspects of the results of ice cratering which is of interest to the Forces is the life span of the obstacle created in ice by cratering it. This is governed by the atmospheric conditions which control ice growth, and also by how much new ice has to be formed to make the refrozen crater safe to walk on. This is in turn governed by the amount of debris remaining in the crater. Methods of deter-



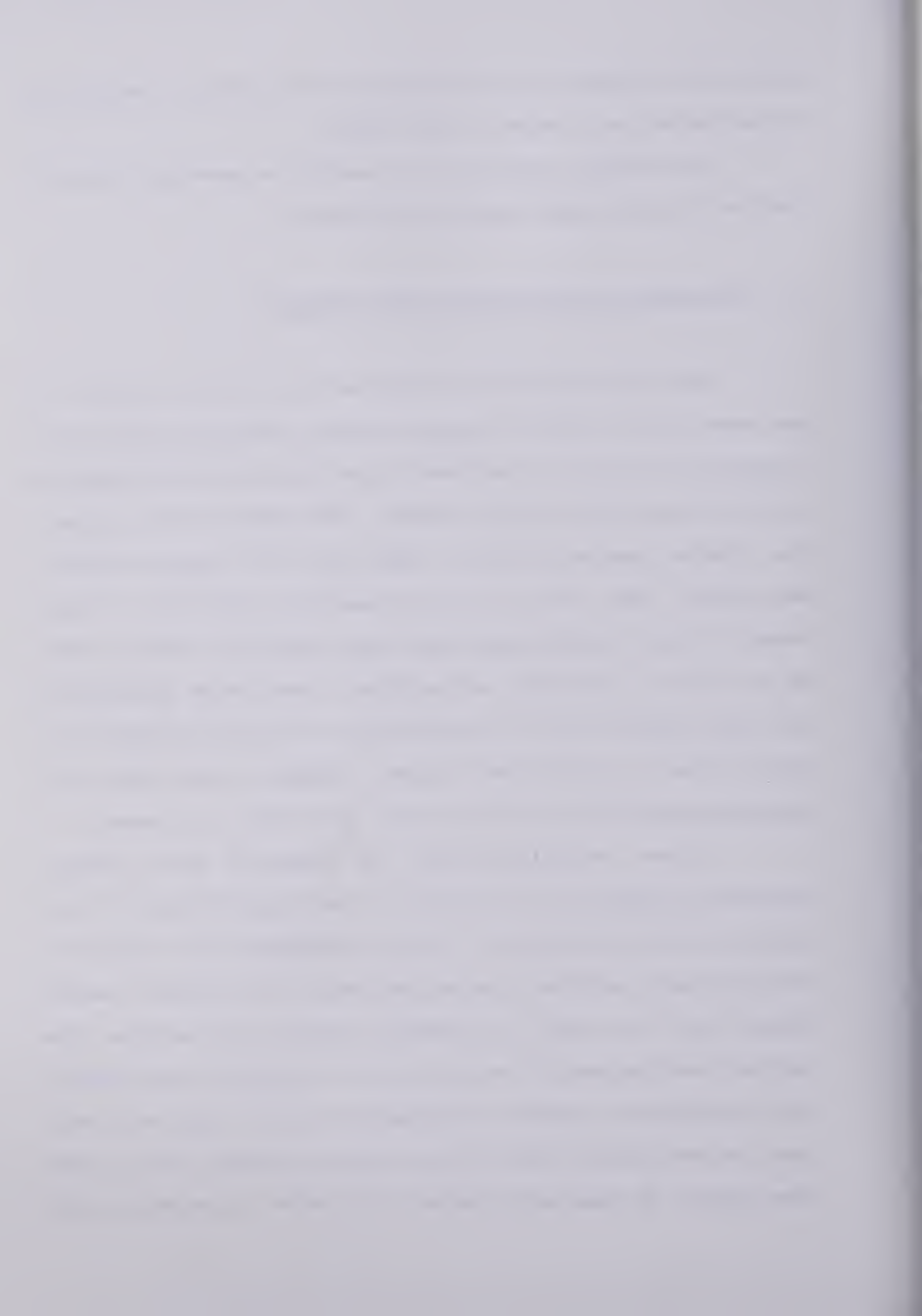
mining the volume of ice ejected by the explosion should be investigated and tested in the field.

This aspect would also be useful in assessing the effect of the directed blasting technique.

12.3 Recommendations Regarding Row Charges

From the investigation carried out for this thesis it was shown that a row of optimum charges could be placed with a spacing of up to two optimum crater radii between them and a continuous crater would result. The area of that crater, for charge spacings greater than about 0.5 optimum radii, was larger than the sum of the computed individual crater areas for the charges had they been spaced far enough apart so as not to influence one another. There were indications that the spacing might be able to be increased slightly and still obtain a continuous crater, though it was shown that charges spaced three optimum radii apart did not connect.

Further experimentation is required with optimum charges to define the maximum of the relationship for row charges shown in Figure 31. It is recommended that rows of a minimum number of five charges be used. It is further recommended that in order to properly assess the maximum, the initial spacing should be set at 1.8 optimum crater radii, with subsequent spacings incremented by 0.1 optimum radii until a continuous crater is no longer attained. One or two rows should be detonated beyond this point to determine the



resulting ice 'bridge' width in relation to the optimum radius.

The relationship shown in Figure 31 was derived from an energy equivalent charge basis, and that analysis technique has yet to be experimentally verified. The ice thickness as well as the type of explosive used was different for the two data sets used to determine the form of the relationship shown in the figure. Therefore, it would be advantageous to conduct experiments with one explosive type, on a constant thickness of ice, that covers the whole range of charge spacings. The spacings should begin with a 0.5 optimum radius spacing, and increment by 0.5 radii up to two optimum radii. The spacings should then be incremented by 0.1 optimum radii until the crater formed is no longer continuous. If possible, this series of experiments should be conducted on at least two ice thicknesses to determine if scaled parameters in a figure such as Figure 31 would better define the row charge relationship.

12.4 Recommendations Regarding Linear Charges.

Although the analysis conducted for this thesis showed that row charges were more efficient than linear charges, there is still a requirement for the Armed Forces to investigate the effects of linear charges further. This need arises from a hypothetical tactical situation where the efficiency of row charges is not required as much as the speed



with which linear charges can be emplaced and detonated.

It is recommended that further testing be conducted with Bangalore Torpedos laid on the surface of a range of ice thicknesses to determine the maximum amount of ice the torpedo can breach, as well as the size of gap created. A similar series of experiments should be conducted with 'multiple torpedos', that is two or more lying side by side or stacked, in order to determine the effects of increased charge density (weight per unit length) on the relationship.

It is also recommended that because of their rapid deployment capability, tests be conducted with the Viper class of linear charges to determine their effectiveness in this role over a range of ice thicknesses.

Finally, it is recommended that further research be conducted into the use of single tubes of Bangalore Torpedo as expedient 'point' charges, especially since the one shot fired during the Chilcotin tests exhibited such high ice clearance characteristics. These tests should include shots for a wide range of ice thickness for tubes suspended vertically below the ice. As well, setting the charges through the ice at an angle should be investigated in order to ascertain the ice clearance characteristics of the resulting explosion. Experiments should also be conducted using rows of single tubes of Bangalore Torpedo, spaced in accordance with the findings of this thesis for row charges, and the results of the recommended tests with vertical tubes detonated under a wide range of ice thicknesses.

12.5 Recommendations Regarding Shaped Charges

Because of their rapid deployment capability, the use of shaped charges in creating placement holes in ice should be investigated further. Such an investigation should test both the cone shaped 'Beehive' and wedge shaped 'Hayrick' charges in ice of various thicknesses in order to determine their ultimate cratering depths for various standoff distances. The existence of a 'penetration hole' from Hayrick charges should be investigated and documented, as well as the penetration depth for both types of shaped charge.

12.6 Recommendations Regarding Directed Blasting

Nikolayev's (1971) presentation of the theory of directed blasting should be studied in greater detail to sort out what is relevant, or the factors should be reassessed from first principles.

As mentioned in the recommendations for research into the influence of the gas bubble, an investigation into the size, expansion time and pulsation period of this bubble is mandatory for the further investigation of directed blasting. Once the characteristics of the auxiliary gas bubble are determinable through consideration of the type of explosive, charge weight and placement depth, then other aspects of directed blasting can be investigated. An experimental design such as first used by Nikolayev, but without the dis-

crepancies, would be beneficial in studying the technique.

BIBLIOGRAPHY

BIBLIOGRAPHY

- Anderson, G.D., (1968), 'The Equation of State of Ice and Composite Frozen Soil Material', Research Report 257, U.S. Army Cold Regions Research and Engineering Laboratory (CRREL), Hanover New Hampshire.
- Andres, D.D. and M.E. Quazi, (1975), 'Ice Breakup Observations and Mitigation at the Town of Peace River, April 1975', Alberta Environment Report, Technical Services Division, River Engineering Branch, Edmonton.
- Baker, W.E., P.S. Westine and F.T. Dodge, (1973), 'Similarity Methods in Engineering Dynamics', Spartan Books, Hayden Book Co. Inc., Rochelle Park, New Jersey.
- Barash, R.M., (1966), 'Ice Breaking By Explosives', NOLTR 66-229, U.S. Naval Ordnance Laboratory, White Oak, Maryland. (Extracts from a CONFIDENTIAL report by Barash, 1962, 'Underwater Explosions Beneath Ice', NOLTR 62-96, U.S. Naval Ordnance Laboratory, White Oak, Maryland.)
- Barnes, H.T., (1928), 'Ice Engineering', Renouf Publishing Co, Montreal, Quebec.
- Bauer, A. and J.L. Workman, (1973), 'Explosives for Controlling Ice Jams', Proc. "Seminar on Ice Jams in Canada", Technical Memorandum No. 107, Snow and Ice Subcommittee, Associate Committee on Geotechnical Research, National Research Council of Canada, Ottawa, pp 102 - 121.
-
- and W.A. Crosby, (1980), 'Cratering and Ditching in Frozen Ground', Paper presented at the Department of National Defence Technology Transfer Workshop on Northern Geotechnical Engineering, Held at the University of Alberta, February, 1980, Unpublished.
- Benert, R., (1957), 'Penetration of Shaped Charges into Frozen Ground', Technical Report No. 45, U.S. Army, Snow Ice and Permafrost Research Establishment, Corps of Engineers, Wilmette, Illinois.

BIBLIOGRAPHY

- Benson, M.A., (1965), 'Spurious Correlation in Hydraulics and Hydrology', Proc. ASCE, Jour of Hydraulics Div., Vol 91, No HY-4, pp 35-42, New York, N.Y.
- Bolsenga, S.J., (1968), 'River Ice Jams', Research Report 5-5, U.S. Army Corps of Engineers, Lake Survey, Rock Island District
- Buckley, Maj. R., (1963), 'Report on Ice Jam Demolition Carried out at Whitecourt Alberta from 18 April 1963 to 23 April 1963', Canadian Armed Forces Report, Headquarters, Alberta District.
- Canadian Industries Limited, (1968), 'Blaster's Handbook', 6 th Ed. (Printed 1976), Montreal, Quebec.
- _____, (1980), 'Quick Facts', CIL Inc., Montreal.
- Cole, R.H., (1948), 'Underwater Explosions', Princeton University Press.
- Cook, M.A., (1958), 'The Science of High Explosives', American Chemical Society Monograph No. 139, Reinhold Publishing Corp., New York.
- Daugherty, R.L. and J.B. Franzini, (1977), 'Fluid Mechanics with Engineering Applications' 7th Ed., McGraw-Hill Book Company, New York, N.Y.
- Davies, L.B., R.K. Deeprose and H.M. Hunt, (1976), Observations and Report on River Ice Conditions and Breakup at the Town of Peace River, Alberta, 1974-1975', Joint Task Force Report to Deputy Ministers of Alberta and British Columbia Departments of the Environment.
- DenHartog, S.L., (?), 'Ice Jam Removal', CRREL Internal Report, U.S. Army CRREL, Hanover, New Hampshire.
- _____, and G.C. Appel Jr., (1977), 'Use and Destruction of Ice Covers', CRREL Technical Note, U.S. Army CRREL, Hanover, New Hampshire.

BIBLIOGRAPHY

- Deugo, D., (1973), 'Ice Control on the Rideau River, Ottawa', Proc. "Seminar on Ice Jams in Canada", Technical Memorandum No. 107, Snow and Ice Subcommittee, Associate Committee on Geotechnical Research, National Research Council of Canada, Ottawa, pp 102 - 121.
- Dixon, W.J. and M.B. Brown (Ed), (1979), 'BMDP-79 Biomedical Computer Programs, P-Series', Health Sciences Computing Facility, University of California at Los Angeles, University of California Press, Berkely.
- Doyle, P.F., (1977), '1977 Breakup and Subsequent Ice Jam at Fort McMurray', Report SWE-77/01, Transportation and Surface Water Engineering Division, Alberta Research Council, Edmonton.
- _____, and D.D. Andres, (1978), '1978 Breakup in the Vicinity of Fort McMurray and Investigation of Two Athabasca River Ice Jams', Report SWE-78/05, Transportation and Surface Water Engineering Division, Alberta Research Council, Edmonton.
- _____, and D.D. Andres, (1979), '1979 Spring Breakup and Ice Jamming on the Athabasca River near Fort McMurray', Report SWE-79/05, Transportation and Surface Water Engineering Division, Alberta Research Council, Edmonton.
- Draper, N.R. and H. Smith, (1966), 'Applied Regression Analysis', John Wiley & Sons Inc. New York.
- Fonstad, G.D., R. Gerard and B. Stimpson, (1980), 'The Explosive Demolition of Ice Sheets', Interim Report to 1 Combat Engineer Regiment and the Defence Research Establishment - Suffield, Unpublished, The University of Alberta, Edmonton.
- Frankenstein, G.E. and N. Smith, (1966), 'Operation Breakup FY 1966, Engineering Properties and Crater Hole Measurements', Internal Technical Note U.S. Army CRREL, Hanover, New Hampshire.

BIBLIOGRAPHY

- Frankenstein, G.E. and N. Smith, (1970,a), The Use of Explosives in Removing Ice Jams', Proc. International Association for Hydraulic Research, "Symposium on Ice and its Action on Hydraulic Structures", Reykjavik, Iceland, September, 1970.
- _____, (1970,b), 'The Use of Explosives for Ice Cratering', Internal Report, U.S. Army CRREL, Hanover, New Hampshire, December, 1970.
- Froehle, Lt. H.A., (1966), 'ANFO in the Arctic', The Military Engineer, Jan.-Feb. 1966, pp 16 -18.
- Hemphill, G.B., (1981), 'Blasting Operations', McGraw-Hill Book Co., New York.
- Jordaan, J.M. Jr., (1969), 'Simulation of Waves by an Underwater Explosion', Proc. ASCE, Jour of Waterways and Harbours Div., Vol 95, No WW-3, pp 355-377, New York, N.Y.
- Kennedy, J.B. and A.M. Nevill, (1976), 'Basic Statistical Methods for Engineers and Scientists', 2nd Edition, Thomas Y. Crowell Company, New York, N.Y.
- Kurtz, M.K., R.H. Benfer, W.G. Christopher, G.E. Frankenstein, G. Van Wyhe and E.A. Roguski, (1966), 'Consolidated Report, Operation Breakup, FY 66 , Ice Cratering Experiments, Blair Lake Alaska', NCG/TM 66-7, U.S. Army Nuclear Cratering Group, Lawrence Radiation Laboratory, Livermore, California.
- Livingston, C.W., (1960), 'Explosions in Ice', Technical Report No. 75, U.S. Army, Snow Ice and Permafrost Research Establishment, Corps of Engineers, Wilmette, Illinois.
- Mellor, M. and A. Kovacs, (1972), 'Breakage of Floating Ice by Compressed Gas Blasting', Special Report (SR-184) for U.S. Coastguard, U.S. Army CRREL, Hanover, New Hampshire.
- Mellor, M., (1972), 'Data for Ice Blasting', CRREL Technical Note, U.S. Army, CRREL, Hanover, New Hampshire.

BIBLIOGRAPHY

- Mellor, M., (1975), 'Controlled Perimeter Blasting in Cold Regions' Technical Report 267, U.S. Army CRREL, Hanover, New Hampshire.
- _____, A. Kovacs and J. Hnatiuk, (1977), 'Destruction of Ice Islands with Explosives', Proc. Fourth International Conference on Port and Ocean Engineering Under Arctic Conditions (POAC - 77), Memorial University of Newfoundland, September 1977 (Preprint).
- Meyer, R., (1977), 'Explosives', Verlag Chemie, Essen, Germany, Distributed in North America by Weinheim, New York, N.Y.
- Moor, J.H. and C.R. Watson, (1971), 'Field Tests of Ice Jam Prevention Techniques', Proc. ASCE, Jour. of Hydraulics Div., Vol 97, No HY-6, pp 777 - 789, New York, N.Y.
- Nikolayev, S.Ye., (1970), 'Blasting Fast Ice in the Antarctic' 'Sovetskaia Antarkticheskaia Ekspeditsiia, Informatsionnyi Biulleten', (Soviet Antarctic Expedition, Information Bulletin, Translation February 1973.)
- _____, (1971), 'Cutting Sea Ice by Directed Blasting', 'Trudy Arkticheskogo i Antarkticheskogo Nauchno - Issledovatel'skogo Instituta', Transactions of Arctic and Antarctic Scientific Research Institute, No. 300, Leningrad), U.S. Army CRREL Draft Translation No. 396, August, 1973, Hanover, New Hampshire.
- Nuttall, J.B., (1974), 'Report on Ice Breakup at Peace River, Alberta, 1974', Unpublished Consultant's Report to Alberta Environment, Edmonton.
- Purple, Maj. R.A., (1965), 'Crossing Frozen Rivers in Korea', 'The Military Engineer', Sept.-Oct. 1965, pp 331 - 333.
- Riddoch, Capt. R.G., (1979), 'Cratering and Ditching in Frozen Soils', M.Eng. Thesis, Department of Civil Engineering, The Royal Military College of Canada, Kingston, Ontario.

BIBLIOGRAPHY

- Sinotin, V.I., et.al., (1970), 'Recommended Practice for Combatting Ice Jams', Draft Translation 400, U.S. Army, CRREL, Hanover, New Hampshire, (1973).
- Szabon, W. and M.E. Quazi, (1976), 'Ice Breakup Observations and Mitigation at the Town of Peace River, April 1976', Alberta Environment Report, Technical Services Division, River Engineering Branch, Edmonton.
- Thalimer, R.H. and F.R. Burfoot Jr., (1960), 'Ice Jam on French Creek', The Military Engineer, Nov.-Dec. 1960, pp 479 - 481.
- U.S. Department of the Army, (1969), 'Engineer Field Data', Department of the Army Field Manual FM 5-34.
- Wade, M.D. Jr., (1966), 'Operation Peggy', Corps of Engineers U.S. Army, Alaska District, Anchorage, Alaska.
- Westine, P.S., (1970), 'Explosive Cratering', Journal of Terramechanics, Vol. 7, No. 2, pp 9-19, Pergamon Press, Great Britain.
- Williams, G.P., (1970), 'Breakup and Control of River Ice', Proc. International Association for Hydraulic Research, "Symposium on Ice and its Action on Hydraulic Structures", Reykjavik, Iceland, September 1970.
- Van Der Kley, J., (1965), 'The Use of Explosives for Clearing Ice', Rijkswaterstaat Communications No. 7, The Hague, Netherlands.
- Van Wylen, G.J. and R.E. Sonntag, (1965), 'Fundamentals of Classical Thermodynamics', John Wylie and Sons Inc., New York, N.Y.

APPENDIX A

DATA ON ICE BLASTING

FROM THE LITERATURE

TABLE A-1

Data from Van Der Kley (1965)

(Single Charges)

Explosive	No. of Tests	W (kg)	t _i (mm)	d (m)	R (m)
Gunpowder	5	7.00	250.0	1.25	2.50
	5	12.00	250.0	1.75	4.00
	5	12.00	350.0	1.65	3.50
	5	15.00	350.0	2.15	3.75
	5	25.00	350.0	2.15	6.00
	5	12.00	450.0	1.55	3.00
	5	25.00	450.0	2.05	7.00
	5	12.00	550.0	1.45	3.50
	5	25.00	550.0	1.95	7.00
	5	12.00	650.0	1.35	3.50
	3	25.00	650.0	1.85	6.00
	3	25.00	1900.0	0.60	4.25
Dynamite	4	2.50	150.0	0.85	3.75
	4	2.50	250.0	0.25	3.50
	8	5.00	250.0	0.25	3.75
	12	5.00	250.0	1.75	4.25
	30	2.50	350.0	0.65	4.00
	3	5.00	350.0	1.65	4.50
	16	2.50	450.0	0.55	4.00
	12	2.50	550.0	0.45	3.25
	7	2.50	650.0	0.35	3.50
	5	2.50	850.0	0.15	2.625
Guncotton	6	0.28	630.0	0.32	1.20
	1	0.28	520.0	0.43	1.25
	4	0.28	470.0	0.48	1.425
	6	0.28	950.0	0.00	1.105
	3	0.56	630.0	0.32	2.00
	2	0.56	520.0	0.43	1.90
	6	0.56	470.0	0.48	1.79
	3	0.84	630.0	0.47	2.00
	1	0.84	520.0	0.58	2.50
	2	0.84	470.0	0.63	2.50
American TNT	1	0.454	90.0	0.00	1.525
	1	0.454	110.0	0.50	1.70
	1	0.908	100.0	0.00	2.11
	1	0.908	140.0	0.50	2.10
	1	0.908	130.0	2.00	1.25

(Continued)

TABLE A-1

(Continued)

Explosive	No. of Tests	W (kg)	t _i (mm)	d (m)	R (m)
Dutch TNT	1	0.25	400.0	1.00	0.575
	1	0.25	350.0	0.00	1.25
	1	0.50	360.0	0.00	1.725
	1	1.00	390.0	0.00	2.30
	1	2.00	350.0	0.00	3.075
	1	0.25	300.0	0.00	1.20
	1	0.50	300.0	0.00	1.95
	1	1.00	300.0	0.00	2.65
	1	8.50	400.0	2.70	4.75
	1	0.50	400.0	2.00	0.40
	1	1.00	400.0	2.00	0.50
	1	2.00	400.0	2.00	3.00
	1	3.00	400.0	2.00	3.50
	1	8.50	300.0	1.50	5.25
	1	0.50	400.0	1.00	2.10
	1	1.00	400.0	1.00	3.15
	1	2.00	400.0	1.00	3.50
	1	3.00	400.0	1.00	4.625
	1	0.50	300.0	0.50	1.95
	1	1.00	300.0	0.50	2.45
	1	2.00	300.0	0.50	3.00
American TNT	1	0.454	120.0	-0.12	0.965
	1	0.908	120.0	-0.12	1.325
	1	1.362	120.0	-0.12	1.25
Dutch TNT	1	8.50	280.0	-0.28	3.25
	1	0.25	280.0	-0.28	0.30
	1	0.50	280.0	-0.28	0.375
	1	1.00	280.0	-0.28	0.65
	1	0.25	410.0	-0.41	0.00
	1	0.50	410.0	-0.41	0.00
	1	1.00	410.0	-0.41	0.40
	1	1.00	210.0	-0.21	0.20
	1	1.00	210.0	-0.21	0.20
'Plastic' Explosive	1	0.0625	280.0	-0.28	0.20
	1	0.125	280.0	-0.28	0.25
	1	0.125	280.0	-0.28	0.25



TABLE A-2

Data from Van Der Kley (1965)

('Percussion' or Decked Charges)

Explosive	No. of Tests	(1) W_1	(2) W_2	t_i	d_1	d_2	R
		(kg)	(kg)	(mm)	(m)	(m)	(m)
Dutch TNT	1	2.00	1.00	280.0	1.22	0.22	3.825
	1	8.50	3.00	400.0	1.50	0.50	6.00
	1	8.50	3.00	400.0	2.00	1.30	6.50
	1	3.00	1.00	500.0	2.00	0.60	4.60
	1	3.00	1.00	530.0	1.97	1.27	3.50
	1	3.00	0.50	400.0	2.00	2.00	3.875
	1	3.00	1.00	400.0	1.60	1.50	3.75
	1	3.00	1.00	450.0	1.55	1.45	4.425
	1	3.00	1.00	550.0	0.45	0.15	3.50
	1	8.50	3.00	550.0	1.45	1.15	6.00
	1	8.50	1.00	550.0	1.45	1.15	5.25
	1	8.50	0.125	550.0	1.45	1.45	4.50
	1	8.50	1.00	500.0	2.30	2.00	5.375
	1	8.50	1.00	450.0	2.45	2.15	5.625
Ammonal	(3) 1	3.00	1.00	500.0	1.50	0.50	3.25
	1	3.00	1.00	450.0	0.95	0.20	4.125
	1	6.00	2.00	500.0	1.50	0.50	5.00
	1	3.00	3.00	500.0	0.95	0.45	4.50

Notes:

1. Subscript 1 refers to the main charge.
2. Subscript 2 refers to the auxiliary charge.
3. Ammonal charges were in tins.

TABLE A-3Data from Purple (1965)

Explosive	W	t _i	d	R
	(lb)	(in)	(ft)	(ft)
Composition C-4	5.00	5.00	10.0	5.00
	5.00	5.00	5.0	8.00
	5.00	5.00	2.0	11.00
	5.00	5.00	0.0	15.00
	5.00	5.00	-0.42	12.00

TABLE A-4

Data from Barash (1966)

Explosive	W (lb)	t _i (in)	(1) d (ft)	(2) R (ft)	(1) D (ft)
TNT	42.0	24.5	2.50	24.50	46.0
	42.0	28.0	3.75	25.75	48.0
	42.0	24.0	5.00	24.50	34.5
	42.0	29.5	5.00	30.50	28.5
	42.0	30.0	6.00	26.50	23.3
	42.0	29.5	8.00	26.75	43.5
	42.0	25.0	10.00	26.00	48.5
	42.0	25.0	17.22	21.00	55.8
TNT	8.0	23.0	(3) -3.92	0.00	22.8
	8.0	23.0	-2.92	0.00	22.8
	8.0	27.0	-3.25	0.00	14.5
	8.0	27.0	-2.25	2.25	16.1
	8.0	25.0	0.00	12.50	31.8
	8.0	26.0	0.27	11.75	13.2
	8.0	25.0	1.45	16.25	31.8
	8.0	26.0	1.45	16.25	15.0
	8.0	22.5	2.90	17.00	38.1
	8.0	24.5	4.00	15.75	25.3
	8.0	23.0	5.00	14.00	30.3
	8.0	25.5	5.00	13.75	22.7
	8.0	29.0	7.50	7.625	25.4
	8.0	20.0	10.00	7.625	31.2
	8.0	20.0	10.00	9.00	31.3
	8.0	29.0	13.00	9.00	32.8
	8.0	28.0	16.00	8.875	30.2
	8.0	27.0	20.00	5.25	57.75
HBX-3	8.0	29.0	2.90	20.50	25.4
	8.0	29.0	20.00	11.875	63.9
HBX-3	1.0	30.0	1.45	3.50	15.5
	1.0	29.0	2.50	3.00	16.8
	1.0	23.0	5.00	4.00	29.1

(Continued)

Notes on next page.

TABLE A-4

(Continued)

Explosive	W (lb)	t _i (in)	(1) d (ft)	(2) R (ft)	(1) D (ft)
TNT	1.0	24.0	-2.00	0.00	21.8
	1.0	24.0	-1.00	1.50	24.0
	1.0	27.0	-1.125	1.50	13.8
	1.0	22.5	0.00	6.50	24.9
	1.0	25.0	1.45	8.00	22.1
	1.0	22.0	2.50	1.75	41.5
	1.0	30.0	4.00	1.875	64.8
	1.0	23.0	5.00	3.50	33.1
	1.0	26.0	5.00	1.50	18.1
	1.0	30.0	5.00	0.875	64.8
	1.0	30.0	6.00	2.25	62.3
	1.0	29.0	7.50	0.75	28.4
	1.0	27.0	10.00	0.00	30.3
	1.0	29.0	11.00	0.00	62.9

Notes:

1. Barash gave depth below top of ice. However to be consistent with our definition, the depth given in Table A-4 is below the bottom of the ice sheet.
2. Barash gave crater diameter, herein presented as radius.
3. Negative values of d indicate the charge was placed above the bottom of the ice.

TABLE A-5

Data from Wade 'Operation Peggy' (1966)

Explosive	(1) W (lb)	(2) t _i (in)	(3) d (ft)	R (ft)	(3) D (ft)
ANFO	80.0	19.0	30.33	25.00	30.33
	80.0	24.0	12.83	15.00	18.8
	80.0	20.0	5.33	30.00	17.3
	80.0	20.0	9.33	15.00	18.3
	80.0	20.0	9.33	15.00	18.3
	80.0	20.0	9.33	15.00	18.3
	(4) 160.0	20.0	-1.67	15.00	18.3

- Notes:
1. Charge weight does not include 7.5 lb of C-4 booster charge.
 2. Ice thickness is composite of main ice layer then a thin layer of water, and a top layer of ice.
 3. Depth measured to top of snow for first three shots, top of ice for second three. Herein converted to depth below bottom of ice.
 4. The 'double' charge was placed on the ice surface. Neither t_i nor d were measured. Values given here are assumed from data for 80 lb shots.

TABLE A-6

Data from Kurtz et.al. 'Operation Breakup' (1966)

(Single Charges)

Explosive	W (lb)	t _i (in)	(1) d (ft)	R (ft)	(1) D (ft)
Composition 4 (C-4)	(2)				
	136.5	34.4	0.00	33.90	38.00
	135.0	33.5	5.00	33.60	43.75
	130.0	35.8	10.00	36.40	33.75
	141.5	29.8	15.00	35.30	36.00
	130.0	31.6	20.00	19.00	46.50
	142.0	30.9	25.00	24.20	48.75
	138.0	33.0	7.50	35.70	42.33
	127.5	31.9	35.00	22.80	51.67
(3) C-4					
	130.5	31.6	10.00	30.20	10.00
	140.0	32.8	10.00	35.00	21.00
	134.5	31.0	15.00	26.30	20.00
	130.5	32.2	20.00	15.40	20.00
	135.0	31.4	10.00	35.40	30.00
	142.5	31.3	20.00	18.80	29.00
	140.5	36.1	30.00	8.50	30.00
(4) C-4	940.0	34.5	19.00	83.60	46.50
(5) TNT	150.0	29.0	20.00	27.00	51.50
(5) ANFO	160.0	27.9	35.00	23.70	51.50

- Notes:
1. All depths are refered to the bottom of the ice.
 2. Cratering Calibration Series.
 3. Bottom Refelection Series.
 4. Yield Scaling Shot.
 5. Field Fabricated Charges.

TABLE A-7

Data from Kurtz et.al. 'Operation Breakup' (1966)

(Row Shots)

Row	(1)						(2)	
	W (lb)	t _i (in)	d (ft)	D (ft)	Width (ft)		Length (ft)	
(3)								
A	136.0	33.3	10.0	51.0	97.6			
					109.8			
	129.0				116.8			
					122.7			
	140.0				121.6		210.0	
					119.4			
	138.0				115.0			
					110.2			
	142.0				98.4			
	Avg. 137.0				Avg. 116.5			
(4)								
B	126.0	32.4	10.0	49.5	93.0			
					110.0			
	135.0				117.0			
					118.9			
	146.5				117.5		301.5	
					116.5			
	129.0				120.9			
					113.7			
	136.0				79.6			
	Avg. 134.5				Avg. 116.4			
(5)								
C	135.0	33.0	10.0	49.5	98.4			
					119.6			
	140.0				136.7			
					145.2			
	140.5				147.6		362.1	
					141.0			
	131.5				132.5			
					122.6			
	136.0				93.9			
	Avg. 136.6				Avg. 135.0			

Notes: 1. All charges were C-4. Averages are reported in the summary table in the reference.

2. Widths taken at charge locations and between-charge locations. Averages reported in the reference omit measured widths at end charges in computation of averages.

(Continued next Page)

TABLE A-7

(Continued)

Notes: (Continued)

3. Charge spacing 36 ft. ($1.0 \times R$ optimum)
4. Charge spacing 54 ft. ($1.5 \times R$ optimum)
5. Charge Spacing 72 ft. ($2.0 \times R$ optimum)

TABLE A-8

Data from Kurtz et.al. 'Operation Breakup' (1966)

Scaled Single Charge Crater Radii and Depths of Burst
Converted (Scaled) to Standard 136 lb of C-4

t_i (in)	W (lb)	(1) W' (lb)	d (ft)	d' (ft)	R (ft)	R' (ft)
(2)						
34.2	136.5	136.0	0.0	0.00	33.9	33.87
33.5	135.0	136.0	5.0	5.01	33.6	33.67
35.8	130.0	136.0	10.0	10.15	36.4	36.95
29.8	141.5	136.0	15.0	14.81	35.3	34.85
31.6	130.0	136.0	20.0	20.30	19.0	19.29
30.9	142.0	136.0	25.0	24.65	24.2	23.87
33.0	138.0	136.0	7.5	7.46	35.7	35.52
31.9	127.5	136.0	30.0	35.75	22.8	23.29
(3)						
31.6	130.5	136.0	10.0	10.14	30.2	30.63
32.8	140.0	136.0	10.0	9.90	35.0	34.65
31.0	134.5	136.0	15.0	15.06	26.3	26.41
32.2	130.5	136.0	20.0	20.28	15.4	15.62
31.4	135.0	136.0	10.0	10.02	35.4	35.47
31.3	142.5	136.0	20.0	19.69	18.8	18.50
36.1	140.5	136.0	30.0	29.67	8.5	8.41

Notes:

1. Primed variables, ie W', d' and R', refer to data scaled or normalized by Kurtz et.al. to dimensions equivalent to W, d and R for a standard 136 lb charge of C-4.
2. Data from Cratering Calibration Series.
3. Data from Bottom Reflection Series.

TABLE A-9Data from Frankenstein and Smith (1966)

(Data from Mississippi River Tests)

Explosive	(1)	(2)			
	W (lb)	t _i (in)	d (ft)	R (ft)	D (ft)
C-4	50.0	19.5	11.0	21.2	14.0
	50.0	19.5	10.5	20.05	13.0
	33.3	18.0	1.0	16.0	11.0

Notes:

1. Explosive type not given in the reference. As the data was presented with data from Kurtz et.al., who used C-4, it is assumed that the explosive used by Frankenstein and Smith was C-4 as well, or they would not have made the comparative presentation they did.
2. The ice was described as "partially deteriorated" and "much weaker ice than occurred in 'Operation Breakup'".

TABLE A-10
Data from Nikolayev (1970)
(Single Charges)

Explosive	W (kg)	t _i (mm)	(1) d (m)	R (m)
			(2)	
Trotyl	25.2	1070.0	1.33	6.30
	25.2	1070.0	1.73	6.40
	25.2	1070.0	2.13	6.75
	25.2	1070.0	2.43	6.60
	25.2	1070.0	2.93	6.45
	25.2	1070.0	3.43	5.25
	30.0	1100.0	1.70	6.55
	30.0	1100.0	2.10	6.95
	30.0	1100.0	2.50	6.65
	30.0	1100.0	2.90	6.20
	30.0	1100.0	3.40	5.65
Trotyl	(3)			
	25.0	1100.0	1.75	7.10
	30.0	1100.0	1.90	7.55

Notes:

1. Depths of placement given in the reference as 'below top of ice', herein converted to 'below bottom of ice'.
2. Antarctic Ice.
3. Ice in "other bodies of water", not specified.

TABLE A-11Data from Nikolayev (1970)

(Decked Charges)

Explosive	(1)		t_i (mm)	(2)		R (m)
	W_1 (kg)	W_2 (kg)		d_1 (m)	d_2 (m)	
Trotyl	25.2	4.8	1100.0	2.10	0.10	6.95
	25.2	4.8	1100.0	2.50	0.30	7.15
	25.2	4.8	1100.0	2.90	0.15	7.35
	25.2	4.8	1100.0	3.40	0.10	6.40

Notes:

1. Subscripts 1 and 2 refer to the main and auxiliary charges respectively.
2. Delay in detonating auxiliary charge was 0.025 seconds.
3. Depths of placement given in the reference as 'below top of ice', herein converted to 'below bottom of ice'.

TABLE A-12

Data from Nikolayev (1971)

Experiment Number	t _i (mm)	(Directed Blasting)												
		(1)		(2)			(3)			Area Cratered (m ²)	Percentage of Ice Clearance (%)			
		W ₁ (kg)	W ₂ (kg)	d ₁ (m)	d ₂ (m)	l (m)	Delay Time (sec)	Directing Angle (Degrees)	Crater Size (m x m)					
1	1100.0	(4)												
		25.2	4.8	2.3	0.3	2.0	0.011	45	16.1 x 14.8	187.0	20			
		25.2	4.8	2.3	0.3	2.0	0.018	45	17.2 x 15.0	202.5	30			
		25.2	4.8	2.3	0.3	2.0	0.025	45	18.2 x 15.7	223.0	50			
		25.2	4.8	2.3	0.3	2.0	0.030	45	17.2 x 15.2	205.2	40			
		25.2	4.8	2.3	0.3	2.0	0.036	45	15.8 x 15.3	191.0	30			
		25.2	4.8	2.3	0.3	2.0	0.039	45	16.1 x 14.7	185.8	30			
		25.2	4.8	2.3	0.3	2.0	0.050	45	14.5 x 14.0	158.3	20			
		25.2	4.8	2.3	0.3	2.0	0.057	45	13.8 x 13.6	147.3	10			
		25.2	-	2.1	-	-	-	-	13.5	143.1	<5			
2	1100.0	30.0	-	2.1	-	-	-	-	13.9	151.7	<5			
		(5)												
		25.2	3.6	1.9	0.3	2.4	0.025	33	16.1 x 14.7	185.4	30			
		25.2	3.6	1.7	0.1	2.2	0.025	36	16.2 x 14.6	185.6	35			
		25.2	3.6	1.7	0.1	2.0	0.025	38	16.9 x 15.2	202.8	40			
		25.2	3.6	2.1	0.3	2.0	0.025	42	17.9 x 15.7	220.4	45			
		25.2	3.2	2.1	0.1	2.0	0.025	45	18.8 x 17.3	256.8	50			
		25.2	4.8	2.3	0.3	1.75	0.025	49	16.9 x 13.2	176.2	30			
		25.2	4.8	2.3	0.3	1.5	0.025	53	14.6 x 13.1	149.0	20			
		25.2	-	-	-	-	-	-	-	-	-			
3	1100.0	25.2	3.2	2.3	0.3	1.8	0.025	45	17.2 x 14.5	194.4	35			
		25.2	3.6	2.3	0.3	1.7	0.025	45	17.7 x 15.0	209.6	40			
		25.2	4.4	2.3	0.3	1.6	0.025	45	17.9 x 17.3	243.0	50			
		25.2	4.8	2.3	0.3	1.5	0.025	45	18.4 x 16.2	234.0	50			
		25.2	6.2	2.3	0.3	1.4	0.025	45	17.7 x 15.6	218.0	40			
		25.2	8.4	2.3	0.3	1.3	0.025	45	18.3 x 15.0	214.3	45			

TABLE A-12

(Directed Blasting)

(Continued)

Experiment Number	t _i (mm)	(1)		d ₁ (m)	d ₂ (m)	(2) l (m)	Delay Time (sec)	Directing Angle (Degrees)	Crater Size (m x m)	(3)	
		W ₁ (kg)	W ₂ (kg)							Area Cratered (m ²)	Percentage of Ice Clearance (%)
4	1100.0	(4)									
		25.2	4.8	1.65	0.1	1.55	0.025	45	17.2 x 14.5	197.0	35
		25.2	4.8	1.9	0.4	1.5	0.025	45	17.3 x 14.8	202.0	40
		25.2	4.8	2.3	0.3	2.0	0.025	45	18.2 x 15.7	221.1	50
		25.2	4.8	2.5	0.3	2.2	0.025	45	16.7 x 14.8	196.0	35
		25.2	4.8	2.9	0.4	2.5	0.025	45	17.2 x 13.2	157.5	30
		25.2	3.2	2.1	0.1	2.0	0.025	45	18.8 x 16.3	243.1	50

Notes:

1. Subscripts 1 and 2 refer to the main and auxiliary charges respectively.
2. 'l' is the horizontal distance between the charges.
3. Craters were elliptical, Nikolayev gave major and minor axes as dimensions.
4. All charges were TNT.
5. For Experiment 3, Nikolayev gave the directing angle as 45° for all six shots, however it can be shown from:

$$\text{Angle} = \text{Tan}^{-1}((d_1 - d_2) / l)$$

49.6, 51.3, 53.1, 55.0 and 57.0 degrees, respectively. : that the directing angles for the shots were 48.0,

TABLE A-13

Data from Mellor and Kovacs (1972)

Explosive	W	t _i	d	R
	(lb)	(in)	(ft)	(ft)
40% Gelatin	1.0	16.0	0.00	5.25
Dynamite	1.0	19.0	1.50	7.75
	1.0	17.0	3.00	8.50
	1.0	19.0	4.50	2.05
(1)				
Military	2.0	32.5	2.00	5.00
Dynamite	4.0	32.5	2.50	4.50
	3.5	32.5	0.00	5.00

Note:

1. U.S. Military Dynamite "is equivalent in Specific Energy to 60% Commercial Dynamite" (Mellor and Kovacs, 1972), but the type of commercial dynamite, eg straight, gelatin, ammonia, etc. was not specified in the reference.

TABLE A-14

Data from Benert (1957)

Shaped Charge Penetration of Ice

Type of Charge	Standoff (in)	Ice Thickness (in)	Ice Type	Penetration (in)	Hole Diameter (in)	Crater Diameter (in)	Crater Depth (in)
M2A3	6	44	Fresh	Complete	4	43	18
M2A3	36	84	Saline	Complete	4	28	30
M2A3	13 ¹	45	Fresh	Complete	5	12	8
M2	6	84	Saline	Complete	5	10	20
M2	6	53	Fresh	Complete	5	8	12
5 lb ²	6	53	Fresh	32	0.5 - 2	10	12
5 lb ²	15	53	Fresh	44	0.5 - 2	-	-
2.75 oz ³	4	53	Fresh	23	0.5 - 1.5	-	-

Notes: 1. Standoff was 13 in of snow.

2. Experimental Charges.

3. Jet Tapper Charge.

APPENDIX B

SOME CHARACTERISTICS AND PROPERTIES OF EXPLOSIVES

FROM THE LITERATURE

TABLE B-1

Characteristics of Shaped Charges used by Benert

Charge			Explosive		Cone			Container	
Type	Total Weight (lb)	Weight (lb)	Type	Material	Angle (Deg)	Thickness (in)	Outer Diameter (in)	Weight (lb)	Material
M3	40.0	30.0	Composition B or Pentolite	Steel	60	0.150	9.5	5.6	Sheet metal
20 lb Expt.	28.8	16.8	Composition B	Copper	45	0.190	6.0	4.9	Fiber
M2A3	15.0	11.5	Composition B or Pentolite	Glass	60	0.350	6.0	1.7	Fiber
M2	13.0	10.0	Pentolite	Glass	60	0.350	6.0	1.7	Cloth and Cardboard
5 lb	5.2	2.4	Composition B	Copper	42.5	0.110	3.5	0.8	Fiber
Jet Tapper	0.28	0.14	RDX	Copper	80	0.033	1.75	0.03	Plastic

TABLE B-2

Common Explosives and Ingredients Used
in the U.S. Explosives Industry

MilitaryCommercial

Primary High Explosives

Mercury Fulminate	Mercury Fulminate
Lead Azide	Lead Azide
Diazodinitrophenol	Diazodinitrophenol
Lead Styphnate	Lead Styphnate
Nitromannite	Nitromannite

Secondary High Explosives

TNT (Trinitrotoluene)	NG (Nitroglycerine)
Tetryl (Trinitrophenyl-methylnitramine)	AN (Ammonium Nitrate)
RDX (Cyclotrimethyl-enetrinitramine)	TNT
PETN (Pentaerythritol Tetranitrate)	DNT
Ammonium Picrate	Nitrostarch
Piric Acid	PETN
Ammonium Nitrate	Tetryl
DNT (Dinitrotoluene)	
EDNA (Ethylenediamine-dinitrate)	

Low Explosives

NG	NG
Black powder (Potassium nitrate, sulfur, charcoal)	DNT
DNT (Dinitrotoluene ingredient)	Black powder

Nonexplosive Ingredients

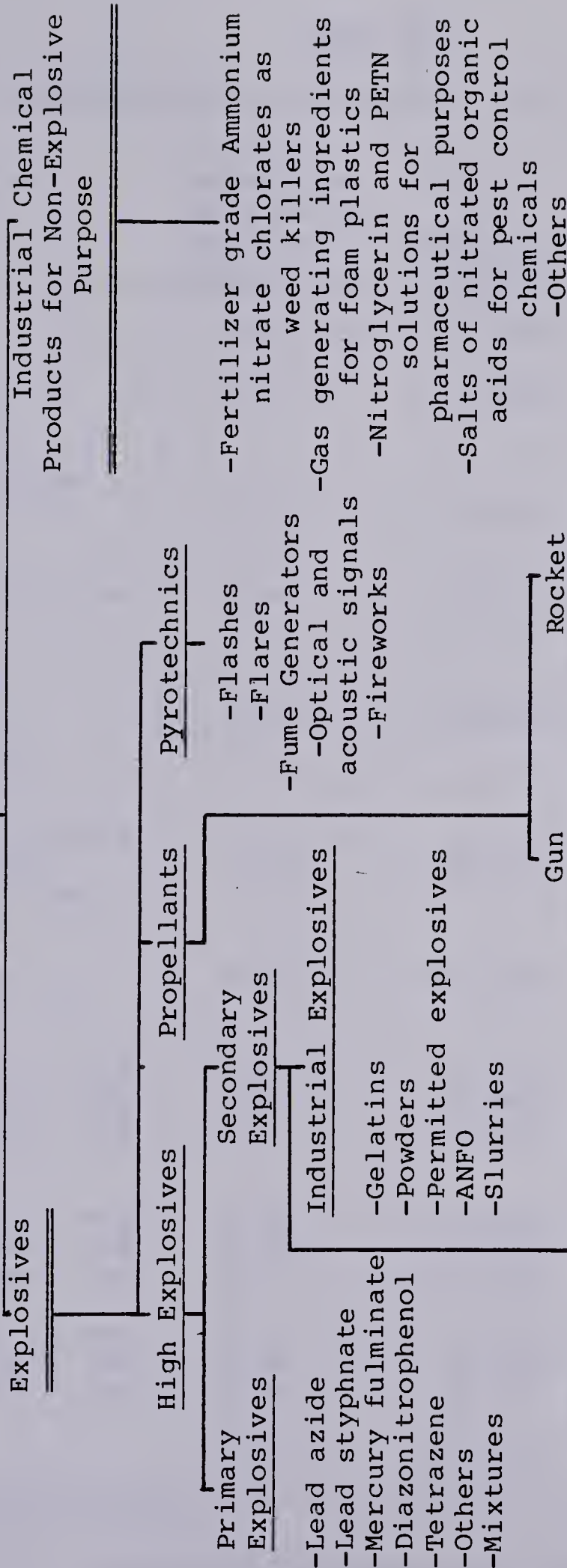
Aluminum	Metal Nitrates
Waxes	Metals (Aluminum, Ferro-silicon)
Diphenylamine	Wood pulps, meals, other combustibles
Metal Nitrates	Paraffin, other hydrocarbons
Mononitrotoluene	Chalk, diphenylamine, Wax, sulfur, carbon

(From Cook, 1958)

TABLE B-3

The Explosives Family

Explosive Matter



- Explosive Compounds eg:
 - TNT
 - RDX (Hexogen)
 - PETN (Nitropenta)
 - Tetryl, and others
- Mixtures eg:
 - Composition B
 - Torpex
 - RDX-based plastics
 - others
- Explosive Compounds eg:
 - Single base
 - Double base
 - Multiple- (picrite-) based prop.
 - Black powder
- Double base
- Composites
- Liquid fuels and oxidizers

(From Meyer, 1977)

TABLE B-4

Characteristics of Principal U.S. Explosives

Explosive Name	Relative Effective- ness as an External Charge	Velocity of Detonation (ft/sec)	Water Resistance
TNT	1.00	23,000.	Excellent
Tetrytol, M1, M2	1.20	23,000.	Excellent
Compositions C-3, M3, M5	1.34	25,000.	Good
M5A1 Composition C-4 M112	1.34	26,000.	Excellent
Ammonium Nitrate (cratering charge)	0.42	14,800.	Poor
Sheet Explosive M186, M118 (charge, demo- lition)	1.14	24,000.	Excellent
Military dynamite M1	0.92	20,000.	Good
Straight 40% (commercial) 50% dynamite 60%	0.65 0.79 0.83	15,000. 18,000. 19,000.	Poor Good Excellent
Ammonia 40% (commercial) 50% dynamite 60%	0.41 0.46 0.53	8,900. 11,000. 12,700.	Good Good Good
Gelatin 40% dynamite 50% 60%	0.42 0.47 0.76	8,000. 9,000. 16,000.	Good Very Good Very Good
PETN	1.66	20,000.- 24,000.	Good

Continued next Page

From U.S. Army FM 5-34 (1969)

TABLE B-4Characteristics of Principal U.S. Explosives

(Continued)

Explosive Name	Relative Effective- ness as an External Charge	Velocity of Detonation (ft/sec)	Water Resistance
Tetryl	1.25	23,400.	Excellent
Composition B	1.35	25,000.	Excellent
Amatol 80/20	1.17	16,000.	Poor
Black Powder	0.55	1,310.	Poor
Nitrostarch	0.80	15,000.	Satisfactory

From U.S. Army FM 5-34 (1969)

TABLE B-5

PROPERTIES OF SOME EXPLOSIVES

(From Meyer, 1977)

Explosive Name	Volume of Detonation Gases l/kg	Detonation Velocity m/sec	Heat of Explosion kcal/kg	Heat of Explosion kJ/kg	Specific Energy mT/kg	Specific Energy kJ/kg	Lead Block cm ³ /10gm
Ammonium Nitrate	980	2700	385	1601			180
Ammonium Perchlorate			266	1114			195
Ammonium Picrate	685	7150	1021	4275			280
ANFO (Ammonium Nitrate and Fuel Oil)							316
Blasting Gelatin							100
Butanetriol Trinitrate			1420	5946			370
Butyleneglycol Dinitrate							
Compositions A, A2, A3		8100					
Compositions B, B2		7800					
Cyanuric Triazide							415
Cyclotrimethylene Trinitrosamine	854	7300	1297	5427			
Diazodinitrophenol		7000					326
Diethyleneglycol Dinitrate	886	6600	1160	4852	116.6	1143	410
Diglycerol Tetranitrate			1262	5284			470
Dinitrochlorobenzene		7100					225
Dinitrodimethylloxamide							360
Dinitrodiethylenamine	546		902	4650	50.2	728	
Dinitronaphthalene	488		1007	4207	50.5	495	
Dinitroorthocresol	603		958	4012	63.3	621	
Dinitrophenoxiethylnitrate		6800					280
Dinitrosobenzene							138

TABLE B-5

PROPERTIES OF SOME EXPLOSIVES

(Continued)

Explosive Name	Volume of Detonation Gases l/kg	Detonation Velocity m/sec	Heat of Explosion kcal/kg	Specific Energy mT/kg	Specific Energy kJ/kg	Lead Block cm ³ /10gm
Dinitrotoluene (DNT)	602		1070	4485	65.8	240
Dioxyethylnitramine Dinitrate	865	7580	1256	5249	130.0	
Dipentaerythrol Hexanitrate	789	7400	1323	5540	123.0	
Erythrol Tetranitrate	704		1443	6041	129.4	
Ethanolamine Dinitrate	914		1123	4700	120.6	410
Ethriol Trinitrate	882	6440	1236	5172		415
Ethylene Diamine Dinitrate	946	6800	937	3923		350
Ethylene Dinitramine		7750	1276	5343		410
Ethyl Nitrate	1032	5800	1038	4425		420
Ethylpicrate	664	6800	1120	4689	83.9	
Ethyltetryl	667		1276	5343	97.9	
Glycerol Acetate Dinitrate			657	2751		200
Glycerol Chloride Dinitrate		6750	1053	4406		475
Glycerol Dinitrate			1201	5029		450
Guanidine Nitrate	967		647	2709	78.5	240
Guanidine Perchlorate		6000				400
Hexamethylenetetramine Dinitrate			788	3297		220
Hexamethylenetriperoxide Diamine	813	4500	1214	5080	91.5	330
2,4,6,2',4',6'-Hexanitro- diphenylamine	624	7200	1237	5179	98.8	325

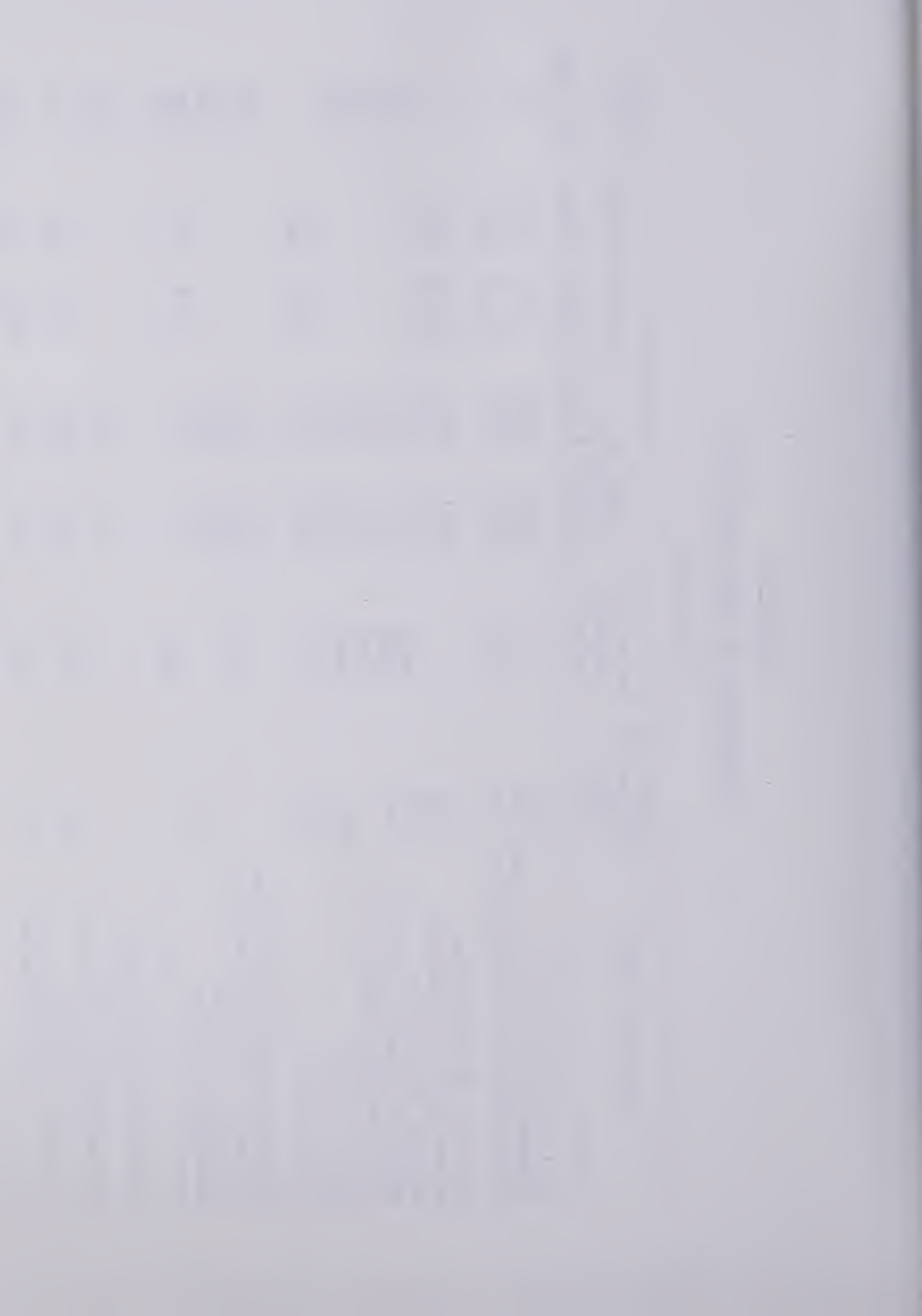


TABLE B-5
PROPERTIES OF SOME EXPLOSIVES

(Continued)

Explosive Name	Volume of Detonation Gases l/kg	Detonation Velocity m/sec	Heat of Explosion kcal/kg	kJ/kg	Specific Energy mT/kg	kJ/kg	Lead Block cm ³ /10gm
Hexanitrodiphenylglycerol Mononitrate							355
2,4,6,2',4',6'-Hexanitro- diphenyloxide		7180					373
2,4,6,2',4',6'-Hexanitro- diphenylsulfide		7000					320
Hexanitroethane	672		743	3111	87.1	854	245
Hexogen (RDX, or, Cyclo- 1,3,5-Trimethylene-2,4,6- Trinitramine)		8750	1439	6025	138.1	1354	480
Hydrazine Nitrate	1001	8690	924	3869	109.4	1073	408
Hydrazine Perchlorate	1000		780	3266			362
Lead Azide (Density 3.8 gm cm ⁻³)	231	4500					110
Lead Azide (Density 4.6 gm cm ⁻³)		5300					
Lead Styphnate		5050	370	1549			130
Mannitol Hexanitrate	694	8260	1420	5945	127.9	1254	510
Mercury Fulminate			355	1486			
Metadininitrobenzene	601		1101	4605	74.2	728	242
Methylamine Nitrate	1027		887	3715	97.6	957	325
Methylnitrate	873	6300	1462	6121	144.8	1420	610
Metriol Trinitrate	853		1236	5175	122.7	1203	400

TABLE B-5

PROPERTIES OF SOME EXPLOSIVES

(Continued)

Explosive Name	Volume of Detonation Gases l/kg	Detonation Velocity m/sec	Heat of Explosion kcal/kg	Heat of Explosion kJ/kg	Specific Energy mT/kg	Specific Energy kJ/kg	Lead Block cm ³ /10gm
Nitrocellulose (13% N)	841		968	4052			420
Nitroethane			926	3889	94.1	923	
Nitroethylpropanediol							
Dinitrate	952		1071	4470	123.0	1206	
Nitroglycerine	715	7600	1510	6322	134.4	1318	520
Nitroglycide			745	3157			310
Nitroglycol	737	7300	1630	6826	143.3	1405	620
Nitroguanidine (Picrite)	895	8200	889	3724	97.0	951	305
Nitroisobutylglycerol							
Trinitrate		7600	1707	7147			540
Nitromethane	1092	6290	1085	4544	136.0	1334	400
Nitromethylpropanediol							
Dinitrate	845	4970	1249	5339	128.3	1258	
Nitrostarch							356
Nitrourea	853		789	3304	93.0	912	
Octogen (Cyclotetra- methylene Tetranitramine)	782	9100	1435	6092	135.4	1328	480
pETN (Pentaerythrol Tetranitrate)	780	8400	1408	5895	136.4	1338	523
Picramic Acid (Dinitroaminophenol)	615		989	4141	70.1	687	166
Picric Acid (2,4,6-Trinitrophenol)	610	7350	1200	5025	92.6	908	315

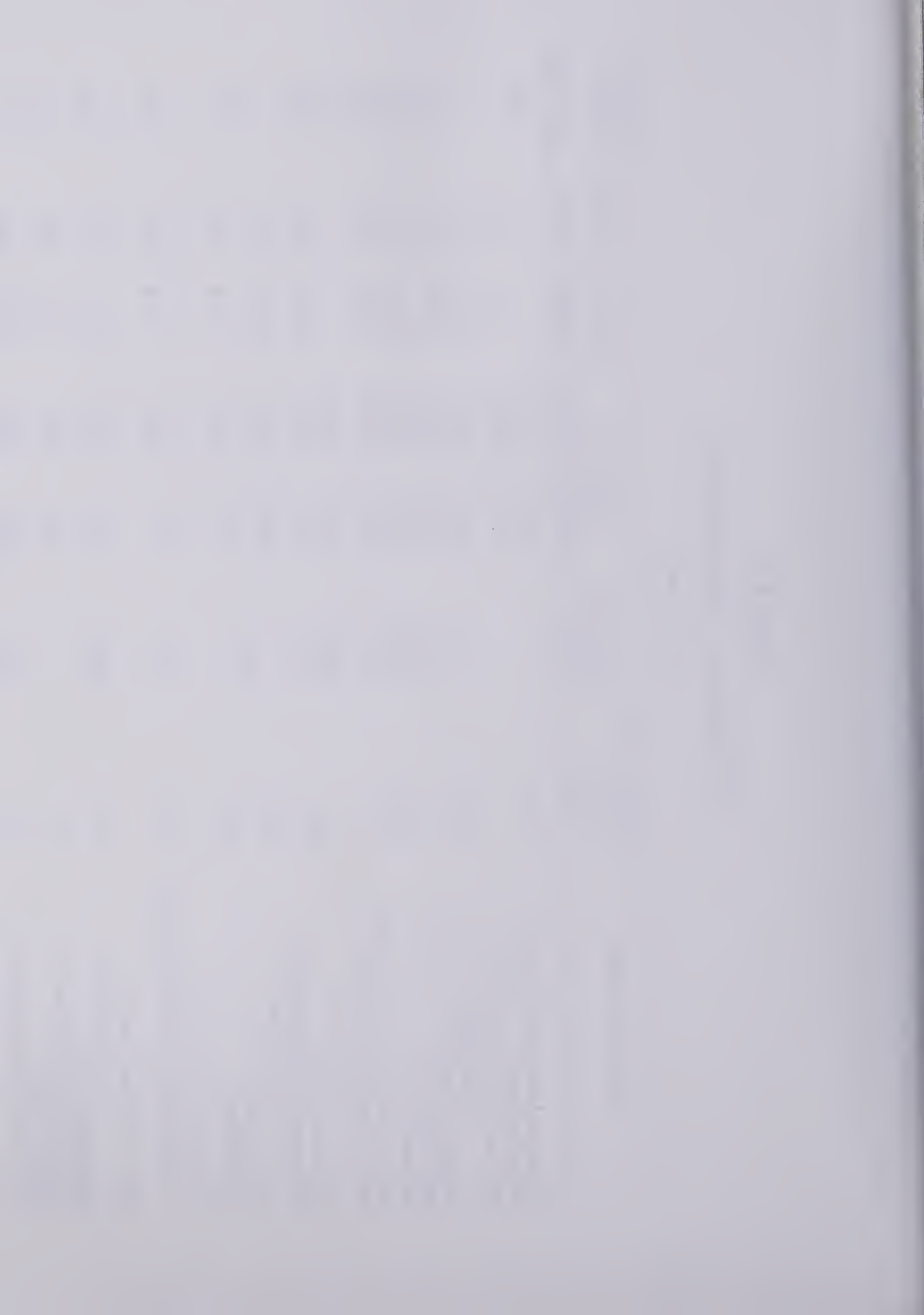


TABLE B-5
PROPERTIES OF SOME EXPLOSIVES

(Continued)

Explosive Name	Volume of Detonation Gases l/kg	Detonation Velocity m/sec	Heat of Explosion kcal/kg	Heat of Explosion kJ/kg	Specific Energy mT/kg	Specific Energy kJ/kg	Lead Block cm ³ /10gm
Polyvinyl Nitrate	955	7000	1180	4941	138.3	1356	
Propyleneglycol Dinitrate			1109	4643			540
Silver Azide	224						115
Styphnic Acid (2,4,6-Tri- nitro-1,3-Dioxymethylene)	608		1117	4681	88.6	869	284
2,3,4,6-Tetranitroaniline	640		1433	5999	120.0	1177	
Tetranitromethane	685	6360	540	2259	70.1	687	
Tetryl (Trinitro-2,4,6- Phenylmethylnitramine)	672	7570	1320	5527	109.0	1069	410
TNT (2,4,6-Trinitrotoluene)	620	6900	1210	5066	85.5	838	300
Triaminoguanidine Nitrate	1206		830	3475			350
Trimethylamine Nitrate	1102		834	3492	86.2	845	
Trimethyleneglycol Dinitrate			1138	4765			540
Trinitroaniline	630		1191	4986			296
Trinitroanisol	701	6800	1104	4622	95.2	934	295
Trinitrobenzene	600	7300	1275	5338	93.4	916	325
Trinitrobenzoic Acid	589		1077	4515	82.1	805	283
Trinitrochlorobenzene		7200					315
Trinitrocresol	624	6850	1139	4769			285
Trinitronaphthalene	581	6000	1058	4433	67.4	661	
TrinitrophenoxthylNitrate	665		1268	5308	103.0	1010	350
Trinitroxylene	649		1125	4711	79.7	782	

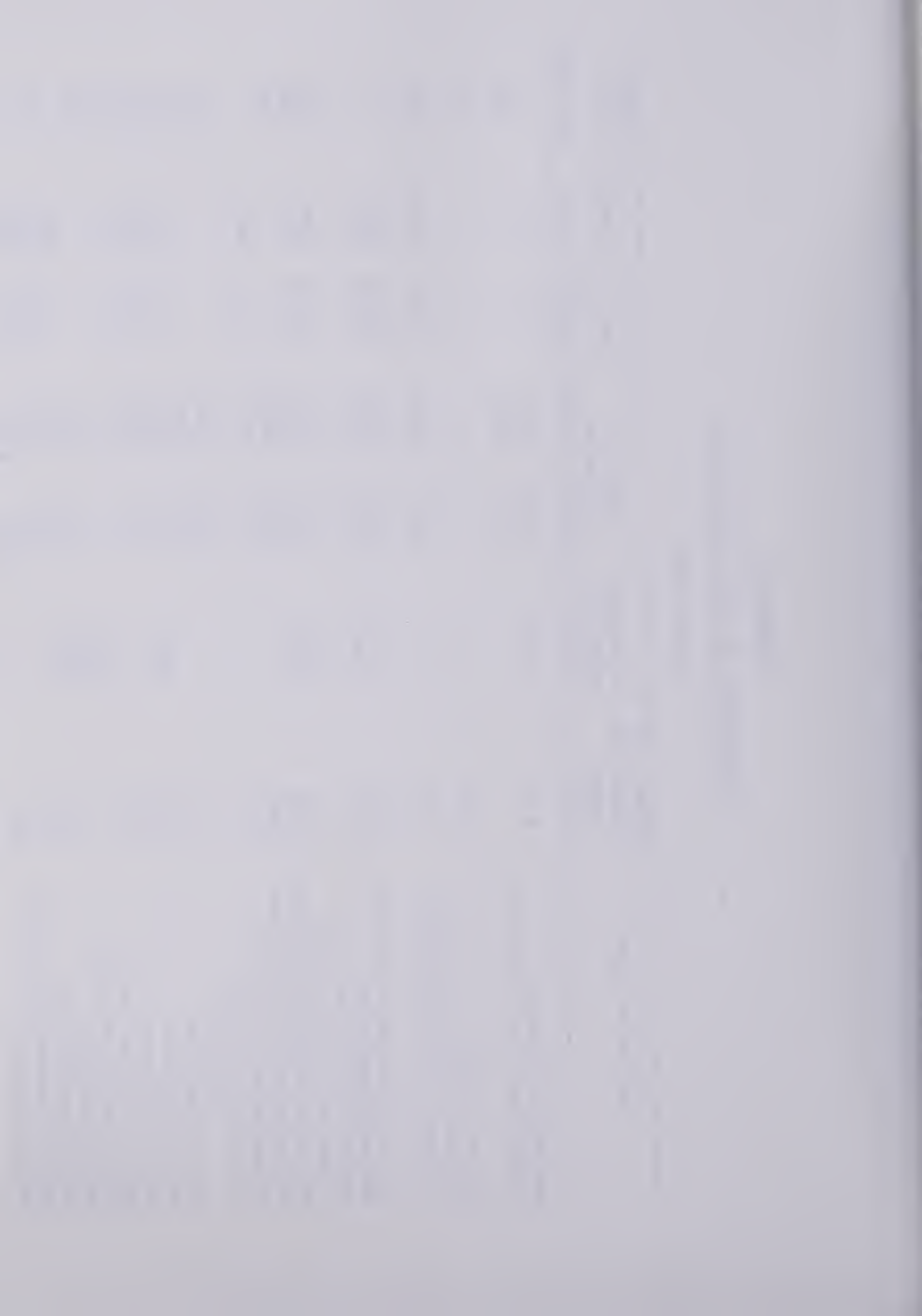


TABLE B-5

PROPERTIES OF SOME EXPLOSIVES

(Concluded)

Explosive Name	Volume of Detonation Gases l/kg	Detonation Velocity m/sec	Heat of Explosion kcal/kg	kJ/kg	mT/kg	Specific Energy kJ/kg	Lead Block cm ³ /10gm
Urea Nitrate	896		639	2675	77.0	755	270

- NOTES:
1. Volume of Detonation Gases, Detonation Velocity and Heat of Explosion are defined in Section 4.4.
 2. Specific Energy is discussed in Section 4.3.7.
 3. Lead Block excavation values are discussed in Section 4.3.

TABLE B-6

Strengths of Explosives Compared to ANFO

Explosive	Relative Weight Strength (% ANFO)	Relative Bulk Strength (% ANFO)	Specific Gravity (gm/cm ³)
'Ajax'	71	135	1.50
ANFO (Gravity loaded)	100	100	0.82
ANFO (Pressure loaded)	100	109	0.92
AN Gelatine Dynamite '75'	114	195	1.40
AN Gelignite '60'	95	174	1.50
AN 'Ligdyn 40'	85	149	1.43
AN 'Ligdyn 25'	68	119	1.42
'Anzite' Blue	114	193	1.40
'Anzite' Red	114	193	1.40
'Anzite' Yellow	97	165	1.43
'Aquamex'	100	170	1.39
Blasting Gelatine	127	233	1.50
'Dynagex'	57	84	1.39
'Dynobel' No. 2	81	109	1.10
'Exactex'	90	107	0.96
'Geophex'	85	163	1.55
'Hydrogel'	111	205	1.50
'Hydromex' M1	95	124	1.50
'Hydromex' M2	127	233	1.50
'Hydromex' M4	152	279	1.50
'Molonal' A	82	140	1.3 - 1.4
'Molonal' D	114	195	1.3 - 1.4
'Molonal' DQ	114	195	1.3 - 1.4
'Monograin'	90	107	0.90
'Morcol'	80	116	1.20
'Plastergel'	95	174	1.50
'Polar' A3			
'Monobel'	71	86	0.98
'Quarigel'	101	186	1.50
Quarry 'Monobel'	100	121	0.98
'Rollex' 60	97	174	1.45
'Roxite'	63	121	1.65
'Seismex'	101	174	1.10
'Seismex' (Aluminised)	113	151	1.10
SN Gelignite 50%	89	163	1.50
Semigel	106	226	1.20
Semigel No. 2	99	135	1.12
'Sunderite'	113	156	1.13

Adapted from ICI Handbook of Blasting Tables



TABLE B-7

Properties of CIL Explosives

Product	Average Density (gm/cm ³)	Velocity of Detonation (m/sec)	Water Resistance	RWS ¹ (%ANFO)	RBS ² (%ANFO)
<u>A. High Explosives</u>					
Belite 60%	1.12	3500	Good	98	129
Cigel 70%	1.28	3600	Good	96	146
Forcite 40%	1.55	4500	Good	79	135
Forcite 75%	1.40	4500	Good	103	171
Powerfrac 75	1.40	5500	Excellent	110	183
Xactex	1.30	2800	Fair	70	108
<u>B. Blasting Agents</u>					
(1) Pneumatically Loaded					
Amex II	1.00	3300	Nil	99	118
Anfomet 120	1.05	3200	Nil	117	146
Anfomet 135	1.05	3200	Nil	133	166
(2) Gravity Loaded					
Amex II	0.84	2700	Nil	99	99
Anfomet 120	0.87	2700	Nil	117	121
Anfomet 135	0.87	3000	Nil	133	138
(3) Packaged Dry Blasting Agents					
Amite II	1.11	3400	Excellent ³	100	132
Metamite 5	1.11	3400	"	120	159
Metamite 10	1.11	3400	"	134	180
<u>C. Cap Sensitive Slurries</u>					
Powermex 500	1.20	4000	Good	112	160
Powermex 300	1.20	4000	Good	89	127
Pillow-Pak	1.15	4000	N/A	89	122
<u>D. Packaged Slurry Explosives</u>					
Aquamex	1.56	4600	Excellent ⁴	96	178
Hydromex T3	1.46	4600	"	89	155
Hydromex M-105	1.50	4600	"	104	186
Hydromex M-210	1.52	4600	"	117	212
Hydromex M-415	1.52	4600	"	129	233

Notes:

1. Relative Weight Strength
2. Relative Bulk Strength
3. If package not damaged
4. In static water

Adapted from 'Quick Facts'
(CIL, 1980)



TABLE B-7

Properties of CIL Explosives
(Continued)

Product	Average Density (gm/cm ³)	Velocity of Detonation (m/sec)	Water Resistance	RWS ¹ (%ANFO)	RBS ² (%ANFO)
<u>E. Bulk Slurry Explosives</u>					
Hydromex T3	1.48	4600	Excellent ⁴	88	155
Hydromex M-103	1.50	4600	"	96	171
Hydromex M-105	1.50	4600	"	104	186
Hydromex M-108	1.50	4600	"	111	198
Hydromex M-210	1.50	4600	"	118	211
Hydromex M-415	1.50	4600	"	130	232
Powergel A	1.25	4500	Excellent ⁴	82	122
Powergel B	1.25	4500	"	93	138
Powergel C	1.25	4500	"	112	167
Powergel D	1.25	4500	"	120	179
Powergel E	1.25	4500	"	131	195

Notes:

1. Relative Weight Strength
2. Relative Bulk Strength
4. In static water

Adapted from 'Quick Facts' (CIL, 1980)

APPENDIX C

INVESTIGATION OF THE GAS BUBBLE RADIUS R_0

Investigation of the Gas Bubble Radius R_0

It has been shown (Cole, 1948) that upon detonation of an explosive charge under water, a gas bubble will result. This bubble reaches a maximum size, given by R_0 , utilizing some of the energy released upon detonation E . The gas bubble pulsates under the influence of hydrostatic pressure at the explosion depth d , as described in Section 3.2.3, and migrates toward the water surface due to its buoyancy. Cole first gave the equation for the initial, maximum gas bubble radius in terms of the volume of a sphere of gas under the hydrostatic pressure at the explosion depth, and the fraction of the total energy associated with the radial flow of fluid caused by the expanding bubble. The equation was:

$$Y = \frac{4 \pi}{3} P_0 R_m^3 \quad \dots (C1)$$

where Y = total energy associated with
the radial flow,

P_0 = hydrostatic pressure at the
explosion depth, and

$R_m = R_0$ = maximum bubble radius.

Cole had indicated that after the emission of the shock wave following detonation, approximately 40% of the energy of detonation remained to be associated with the ra-

dial flow of fluid surrounding the bubble. Jordaan (1969), indicated that:

"... about 40% of the available energy is used to displace the water around the explosion bubble during its expansion to maximum size. (The remainder is divided, about equally, between the shock wave and thermal radiation ...)"

Hence:

$$Y = 0.4 E \quad \dots (C2)$$

where Cole gave E as the heat of detonation (Q), for which he cited a value of 1060 cal/gm for TNT.

Other equations for the maximum bubble radius which have been given in the literature include:

a. Kurtz et.al.(1966)

$$R_O = 12.8 \left[\frac{W}{Z + 34} \right]^{1/3} \quad \dots (C3)$$

where Z is the depth of explosion below the surface of the ice, and the constant '34' arises from atmospheric pressure (1 Atmosphere) being equivalent to a 33.89 foot column of water.

b. Jordaan (1969)

$$Y = 0.4 E = \frac{4 \pi}{3} R_O^3 \rho g (R_O + P) \quad \dots (C4)$$

where the explosion depth was taken as being the maximum bubble radius to obtain maximum wave generation on the surface of the water, and P was the barometric pressure in feet of water.

Jordaan (1969), cited a table of maximum gas bubble radii for TNT charges from 1 oz to 2000 tons detonated in air, and gave extrapolated values for 20, 200, 2000, and 20,000 kilotons (10^3 tons) of TNT. The relationship, except for the extrapolation into the kiloton range, is shown in Figure C1. The best fit line had the equation:

$$R_O = 3.95 (W)^{0.291} \quad \dots (C5)$$

where English dimensions are used.

c. Nikolayev (1971)

$$R_O = \left[\frac{3}{4 \pi} \frac{W Q}{P_O} \right]^{1/3} \quad \dots (C6)$$

where Q was the heat of detonation, given approximately as 1000 cal/gm, and P_O is the pressure in atmospheres at the detonation depth.

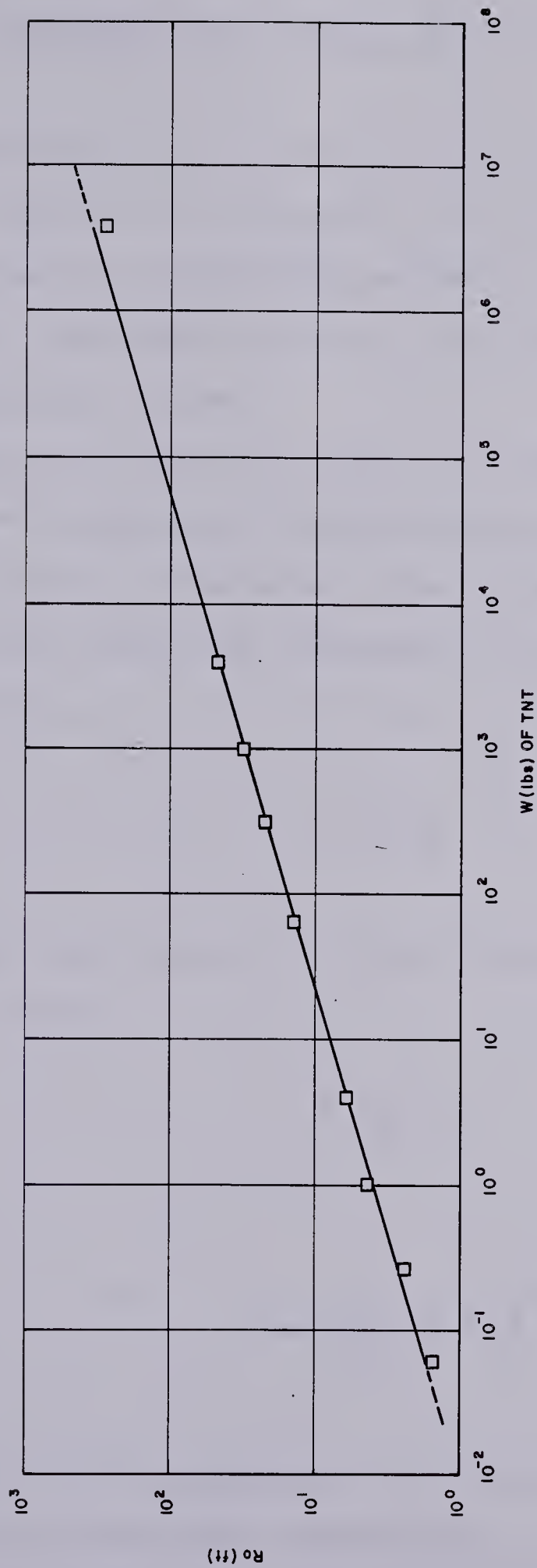


FIGURE C1
GAS-BUBBLE RADIUS FOR TNT CHARGES
(DATA FROM JORDAAN , 1969)



Derivation of a Bubble Radius Relationship

Consider that following the initial expansion of the gaseous products of detonation, the effect of the hydrostatic pressure distribution around the outside of the bubble is not sufficient to cause the bubble to be distorted from a spherical shape.

Using the specific volume of detonation gases (v_g) at 0°C and one atmosphere pressure given by Meyer (1977), reproduced herein in Table B-5, the volume of gases (V) produced by the explosive decomposition reaction of a charge weight W is:

$$V = W v_g \quad \dots (C7)$$

Thus the radius of the gas sphere can be determined from its volume:

$$V = \frac{4\pi}{3} R_o^3 \quad \dots (C8)$$

as:

$$R_o = \left(\frac{3}{4\pi} W v_g \right)^{1/3} \quad \dots (C9)$$

where the internal temperature and pressure of the 'bubble' are 0°C and 1 atmosphere respectively.

Assuming the gases can be considered 'ideal', the effect of the gas temperature (equal to the explosion temperature, derived from the heat of explosion) and pressure, on the volume of the sphere can be assessed from:

$$\frac{P_1 V_1}{T_1} = \frac{P_2 V_2}{T_2}$$

as:

$$V_2 = V_1 \frac{P_1 T_2}{P_2 T_1}$$

where T is temperature in $^{\circ}\text{K}$, the subscript 1 implies conditions at 273.15 $^{\circ}\text{K}$ (0°C) and 1 atmosphere pressure, and subscript 2 implies conditions at the explosion depth (for pressure) and temperature.

Thus:

$$R_O = \left[\frac{3}{4\pi} W v_g \frac{P_1 T_2}{P_2 T_1} \right]^{1/3} \dots (C10)$$

P_1 is the internal pressure of the bubble if the detonation had occurred in air, hence must be the atmospheric pressure (P_O), which can be expressed in terms of an equivalent water column (33.89 ft, 10.33 m) to keep dimensional homogeneity in later expressions. P_2 is the internal pressure of the submerged gas bubble, which will be taken as the hydrostatic pressure at the detonation depth d . The

pressure at this depth can again be expressed as an equivalent water column extending from the phreatic surface within the ice to the detonation depth, hence, as an absolute pressure:

$$P_2 = P_0 + (\rho_i / \rho) t_i + d$$

Therefore:

$$R_0 = \left[\frac{3}{4\pi} W v_g \frac{P_0}{(P_0 + (\rho_i / \rho) t_i + d)} \frac{T_2}{T_1} \right]^{1/3} \dots (C11)$$

Taking (ρ_i / ρ) to be approximately 0.90, substituting 10.33 m for P_0 and 273.15 °K for T_1 , Equation C11 becomes:

$$R_0 = \left[\frac{3}{4\pi} W v_g \frac{10.33}{(10.33 + 0.9 t_i + d)} \frac{T}{273.15} \right]^{1/3}$$

or:

$$R_0 = 20.82 \times 10^{-2} \left[\frac{W v_g T}{(10.33 + 0.9 t_i + d)} \right]^{1/3} \dots (C12)$$

where T is the explosion temperature.

For TNT Meyer (1977) gives the specific volume of detonation gases as 620 l/kg (0.62 m³/kg). The explosion temperature for TNT was not known to the writer, however,



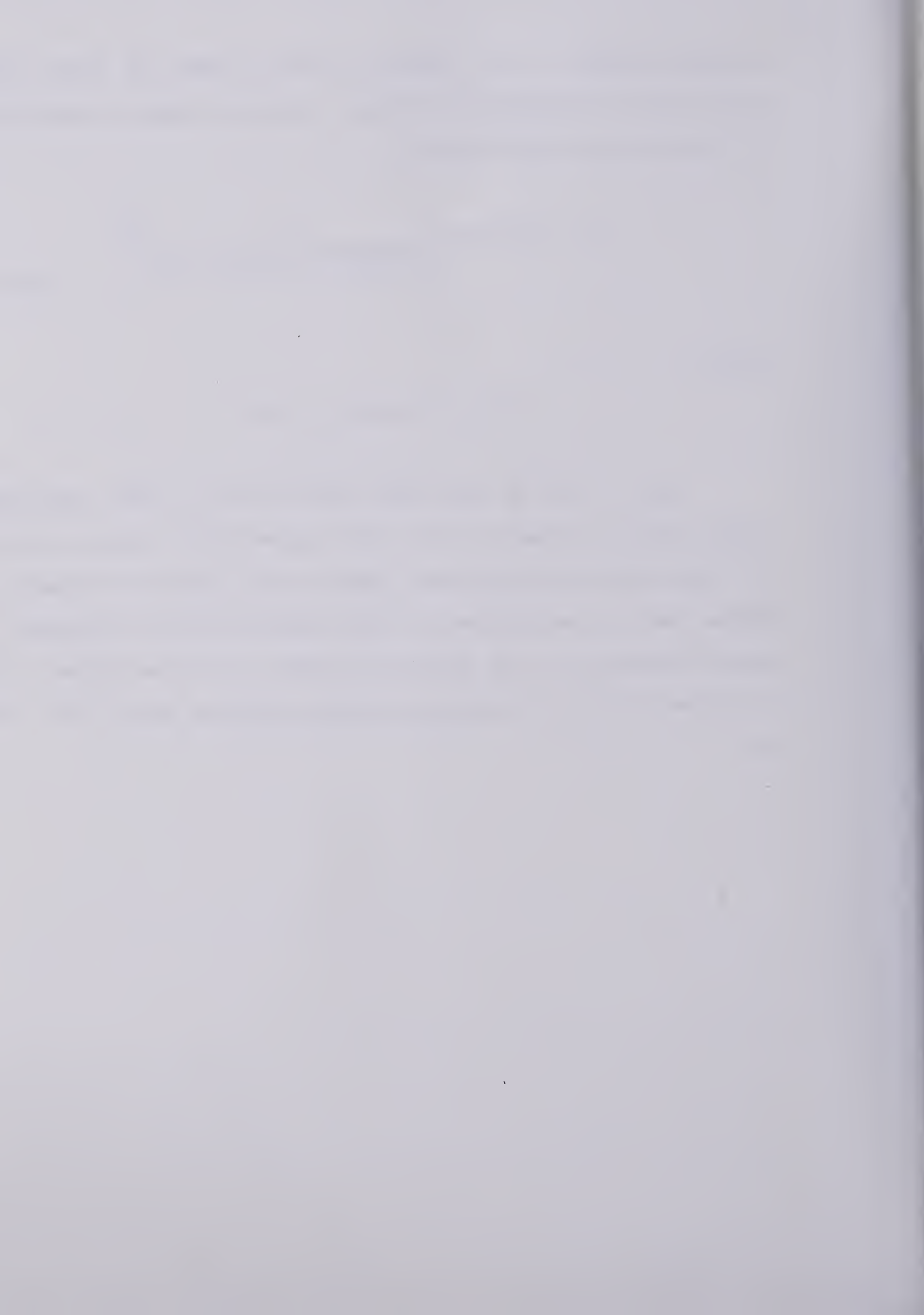
assuming $3000^{\circ}\text{K} \leq T \leq 5000^{\circ}\text{K}$, from a table of heats of formation of detonation products given by Meyer, Equation C12 becomes, for TNT charges:

$$R_0 = \text{Constant} \left[\frac{W}{(10.33 + 0.9 t_i + d)} \right]^{1/3} \dots (\text{C13})$$

where:

$$2.56 \leq \text{Constant} \leq 3.04$$

Here it can be seen where Kurtz et.al. (1966) derived their equation (Equation C3), with appropriate consideration for the system of dimensions. Kurtz et.al. used the experimental heat of detonation in their derivation, and considered the pressure at the detonation depth to be equivalent to a column of water extending from the surface of the ice (Z m).



B30299